



Flood Risk Mapping for All: A Generic Flood Risk Assessment Methodology for the Small Island Developing States

Hanne Glas

Doctoral dissertation submitted to obtain the academic degree of
Doctor of Engineering Technology

Supervisors

Prof. Greet Deruyter, PhD* - Prof. Em. Philippe De Maeyer, PhD**

* Department of Civil Engineering
Faculty of Engineering and Architecture, Ghent University

** Department of Geography
Faculty of Sciences, Ghent University

May 2021



Flood Risk Mapping for All: A Generic Flood Risk Assessment Methodology for the Small Island Developing States

Hanne Glas

Doctoral dissertation submitted to obtain the academic degree of
Doctor of Engineering Technology

Supervisors

Prof. Greet Deruyter, PhD* - Prof. Em. Philippe De Maeyer, PhD**

* Department of Civil Engineering
Faculty of Engineering and Architecture, Ghent University

** Department of Geography
Faculty of Sciences, Ghent University

May 2021

ISBN 978-94-6355-487-9

NUR 905

Wettelijk depot: D/2021/10.500/35

Members of the Examination Board

Chair

Prof. Em. Luc Taerwe, PhD, Ghent University

Other members entitled to vote

Prof. Luuk Boelens, PhD, Ghent University

Prof. Renaat De Sutter, PhD, Ghent University

Prof. Amaury Frankl, PhD, Ghent University

Prof. Stefan Van Damme, PhD, Universiteit Antwerpen

Katrien Van Eerdenbrugh, PhD, Witteveen+Bos Belgium

Supervisors

Prof. Greet Deruyter, PhD, Ghent University

Prof. Em. Philippe De Maeyer, PhD, Ghent University

WORD OF GRATITUDE

As it has been more than a year now, working from home with little to no social contact, I cherish the amazing adventures and moments that have defined my PhD path even more. These moments could not have existed without the wonderful people that have guided me, professional as well as personal, these past seven years and helped me to get where I am today.

There is no other person I could start this word of gratitude with than you, Greet. You were there from the very beginning, believing in me. You've been my biggest support, advising me and guiding me through these past seven years as true mentor. We've had some amazing experiences together, from working in the beautiful snowy landscape of Juuka to enjoying the sun at the Bulgarian seaside. Our biggest and most intense adventure was without a doubt the fieldwork in Haiti, and I'm so grateful that I could share this experience with you. What I've loved most in every single one of our adventures, were our endless talks. Sitting in the train station of Stockholm, we were so wrapped up in all our talking that we've even missed our train. Thank you for being there, always. I can't imagine a better mentor or a better friend. As crucial as Greet has been, this doctoral dissertation would have never existed without the help of Philippe. You've given me a solid research foundation and handed me the tools and contacts to get off to a flying start. In the following years, you let me set my own course, supporting me from the sidelines in the best possible way. Thank you for always sharing your ideas, your feedback and unlimited knowledge.

During the course of this PhD, I got the opportunity to do fieldwork in amazing environments. These fieldwork missions could not have happened without the aid of a multitude of people. As the first fieldwork in Jamaica was performed in 2014, right at the beginning of this PhD research, I was still very new in the flood risk research field and the world of academia in general. I'm grateful to Maxine for accompanying me during the fieldwork mission and assisting me in the research. I'm proud of the work we've done together. Arpita and Sherene, we would have been lost in Jamaica without you. Thank you for showing us your country and the study area, sharing your contacts and aiding us in the data collection. The second fieldwork, in Haiti, was a lot more complicated to organize. It took us a few tries (and a few years), but it was definitely worth the trouble. Katrien and Johan, and all the colleagues at Join for Water, thank you for your assistance in the preparation of the fieldwork, for arranging the journey and providing us with the necessary contacts. Once we've arrived in Haiti, we were received so well by Ann and

the local employees of Join for Water, who were our local guides and support system during the trip. Bruce and Deb, I will never forget your warmth and hospitality. Together with Sadrack and the rest of the staff members of ODRINO, you were an immense help in assisting us on the field. It was truly an unforgettable experience and I hope we can meet each other again someday.

Thank you to Ivan, Steven, Danitza and everyone else at Antea Group that have helped in the development of the flood risk assessment toolbox. Thank you for the brainstorm sessions, for listening to my ideas and theories, and for adapting them into a useable toolbox. I hope that we can keep working together in the future to further develop the methodology and create a toolbox that makes a real difference. A special word of thanks to Tom, for introducing me at Antea Group and for supporting me at the World Water Week in Stockholm.

After over a year of working from home, I would almost forget that there was a time that we spent our days at the office. I miss the Schoonmeersen coffee breaks, the small talk and the banter. Frank, Dirk, Tom, Kathleen, Wouter, Marijke, Veerle, Hilde, Ignaas, Marc, Ben, Dieter, Inge, Lucas and Sam, I can't wait to meet you all again in the coffee corner and catch up. A special thanks to my office boys, Gieljan, Anthony, Jordi and Ticho, for being my 'background noise' in the office. If anyone still thinks women talk a lot, I'm happy to invite them for a day at our office. So many of my coworkers have become friends, and have stayed friends, even when their career path took them to other places. Kizzy, Sara, Charlotte, Koos, Arne, Leo, Peter and Sven, I can't wait for more dinners, drinks and celebrations in our near future. Koos, as my friend who became my coworker and then again just my friend, I'm grateful you've been there for the entire trip, having my back. Greet and I have missed you at work, but I'm sure we will see each other again soon. Charlotte, my art hero, thank you for painting my cover illustration. As your biggest fan, I can't wait to see what you create next! I was lucky enough to not have just one UGent home. Although I spent too little time at AMRP during my PhD, I really want to thank Luuk, Maja, Jurgen and the other colleagues and researchers of the AMRP group for welcoming me with open arms in your team. I always enjoyed the strategic meetings and team buildings and I'm looking forward to seeing you all again soon, even if we have to cycle during it. A special word of gratitude to the research meeting, with Tim, Annelies, Peter, Karim, Isabelle, Hanne, Amir, Noaman, Mustafa, Tristan and Loren for listening to my test defense, giving me tips and advice and helping me in these last important steps of the PhD road.

While every single one of these colleagues and coworkers has been crucial in this adventure, I could not even have started it without the support from my family. Mom and dad, I'm so proud that I'm your daughter. Thank you for your support and your interest in my professional career, but an even bigger thanks for being there in my personal life. I can't wait for summer dinners in the garden at Ellezelles. Diète en Dieter, I have enjoyed watching your boys grow up these past years, and I can't wait for more walks in the Gavers, or exploring a new zoo. Diète, you are an amazing big sister, looking out for me, asking the right questions, always interested in how I'm really doing. Chantal, Geert, Joren, Tatjana, Eva and Jelle, I look forward to many more long dinners with too much food and too many drinks – hopefully one day in the castle

of Lede, that is rightfully yours – because no one does the Burgundian lifestyle better than the Debruyne family. Hanne and Brecht, friends that became family, there are no cooler people to drink wine with on a French terrace in 40°C and to play Rummikub with. Thank you for being my friends, and for being the best godparents for Renée I could have wished for.

The last person I like – or better: need – to thank is Arne. You've been there, every step of the way. You've given me a push when I needed one, you've calmed me down when I went into full stress mode, you've listened to my troubles and my joys and always let me blow off some necessary steam. You've kept me strong through this whole adventure, and I would not have been where I am today without you and your support. Thank you for being my safe home base, for making me laugh and for challenging me. I can't wait to see what life has in store for us.

SUMMARY

The Small Island Developing States (SIDS) group 52 countries and territories located in the regions of Latin-America, the Caribbean, East Asia and the Pacific, characterized by low-lying, densely populated coastal areas and development challenges due to an unstable economy and political situation. According to the IPCC, the SIDS have a disproportionately higher vulnerability and lower resilience to natural hazards than other countries. While flood risk assessments have been researched and developed extensively in many studies over the past few decades, governments and policy makers in vulnerable developing regions such as the SIDS still struggle to take correct measures to protect their communities and minimize disaster consequences. On the International Day for Disaster Risk Reduction 2017, the United Nations Secretary-General António Guterres described this as: *“The challenge is to move from managing disasters themselves to managing disaster risk.”* In several developed countries, research has led to successful flood risk tools. These tools, however, are based on large amounts of detailed, location-specific input data, making it impossible to apply these tools on data-poor regions such as the SIDS. Moreover, most flood risk assessments remain academic studies and are not or cannot be used by governments or local decision makers. Therefore, the proposed dissertation provides a methodology to create a generic, user-friendly and low-cost toolbox to calculate flood damages and risk in developing regions such as the SIDS.

The first chapter serves as general background on the need for adequate flood risk assessment worldwide. First, an introduction on climate change and the growing impact of natural hazards is given. Of all natural disasters, weather-related events take the lead in economic losses, with floods being the costliest hazard. River flooding is the flood type with the largest impact, costing society up to USD 96 billion in Gross Domestic Product (GDP) and affecting 21 million people worldwide each year. As material and human losses caused by flood events continue to increase year by year due to climate change, population growth and poor land use practices, so does the importance of an adequate estimation of these losses. The approach of flood risk assessments focuses on minimizing the consequences and the corresponding costs rather than minimizing the flood event itself by predicting the potential consequences of flooding and indicating the high-risk areas. Most of the existing flood risk assessment tools follow the conventional notation of risk: $\text{Risk} = \text{Hazard} \times \text{Vulnerability}$. This flood risk methodology has been applied in several region-specific tools, which all use water depth as the main determining parameter for direct damage estimations. An example of such a tool

is LATIS, a uniform risk analysis approach for the different hydrological catchments of Flanders, Belgium, that guides decision makers to allocate their resources. The LATIS risk assessment calculates economic and social risk, not only in the present situation, but also for the future. This allows to visualize the impact of future decisions and changes in land use on the overall risk. Like LATIS, all flood risk tools designed for developed regions, are characterized by their dependence on large quantities of high-quality input data. Therefore, data scarcity remains a hurdle for the development of global models as well as for flood risk assessment in developing countries and the SIDS, which lack the funds to acquire reliable and detailed input data.

Chapter 2 presents a first case study, carried out for the coastal town of Annotto Bay in Jamaica. Although island wide damage and risk assessments have been carried out for major flood events in Jamaica, few studies have been conducted for the creation of damage and risk maps for vulnerable areas and micro-scale study areas. In this study, a risk-based methodology was developed by transferring and adapting the LATIS methodology to Annotto Bay, an area with limited data resources. The created model uses input parameters such as land use, social and economic data to estimate the damage for one flood event in 2001, caused by tropical storm Michelle. The produced map shows the spatial variation of the damage costs, which correlates with the flood depths. Although validation of the exact damage costs was not possible, the damage spread and number of affected elements were accurate. The potential number of people who would be killed as a result of the event was calculated at only 2 casualties. Since in reality no one died, this low estimate can be considered accurate as well. This case study was carried out with a lot less data than existing flood risk tools. However, there was still more region-specific data available compared to other regions in the SIDS. Therefore, the importance of all input data needed to be determined. This has led to the development of a methodology to test the sensitivity of the created flood model towards its input data in order to determine a minimum set of indispensable data, presented in Chapter 3. The economic damage map for the 2001 flood in Annotto Bay was used as benchmark. Three damage types were taken into account: building, road and crop damage. Then, eleven different scenarios were generated, each with another combination of input data, thus testing the result for its sensitivity towards each damage type. This analysis allowed the delineation of a minimum set of input data, indispensable to perform a flood risk assessment using the adapted methodology. An important conclusion was that population density data, which is mostly available, even for data-poor regions, in combination with an average number of people per household is a good parameter in determining the building damage where exact building locations are unknown. Furthermore, the importance of a complete road dataset for an accurate visual result was proven. For crop damage calculations, however, no conclusions could be made since Annotto Bay is a primarily urban community and crop damage has an extremely low impact on the overall result.

An apparent need for more research, data and information on rural areas has led to a second case study in the floodplain of the river Moustiques, in the northeast of Haiti. As there were less data available for this rural region than is minimally required for an adequate flood risk assessment, new input data needed to be acquired. Especially historic flood data, for which existing acquisition methods are inaccessible or

insufficient, are lacking. Therefore, a new method for generating flood input data based on the knowledge of the inhabitants of the area was developed in Chapter 4, by using the memory of people affected by past floods on the damages they suffered. For this purpose, a questionnaire was drawn up and all 294 households in the study area were questioned about the most recent and the most severe flood in their memory. Flood damage factors were generated from the questionnaires, in which the inhabitants indicated how much damage was caused by each inundation to their houses and crops. As the average damage percentage for houses depends on the flood height, a region-specific depth-damage function was created. For crops, however, this relation was not visible due to the fact that the agricultural fields are not located in the same area as the houses of which the coordinates and flood height are used. Therefore, only an overall crop damage degree for the entire study area could be calculated. Although the data gathered in such way have a degree of subjectivity, as the memory of a person is not always an accurate recollection of the event, this low-cost and fast acquisition method provided information on past floods that is otherwise inexistent. By critically analyzing the results, the risk of systematic bias was minimized. Chapter 5 presents the flood risk assessment executed for the floodplain of the river Moustiques, based on the input from the questionnaires, supplemented with existing data, literature, field data, and open source data. The resulting risk maps show an extremely high risk for the region, with nearly 2 million USD and potentially 60 casualties every year. Although the assessment was performed as a quantitative analysis, the results are best interpreted qualitatively, as the exact values cannot be validated.

In a final step, the methodologies for both case studies were adapted in Chapter 6 to create a generic and flexible methodology for mapping flood hazard, vulnerability and risk in study areas worldwide. Although, the methodology was developed and customized for freely available data with global coverage, the default workflow can also be enriched with region-specific information when available. The practical application is assured by a modular toolbox developed on GDAL and PCRASTER. This toolbox was tested for the entire catchment of the river Moustiques, Haiti. After creating hazard, vulnerability and risk maps with the default data, more detailed information, gathered during field work, was added to verify the results of the basic workflow. These first tests show that the generic workflow is a robust algorithm that can be applied to any case study.

The final chapter investigates to what degree the dissertation chapters have succeeded in answering the research questions and the general research objective. The two case studies discussed in the dissertation have directly led to addressing this research objective in Chapter 6. However, a few hurdles still need to be overcome in order to achieve the same level of knowledge and expertise on flood risk in developing countries, which often have a high flood vulnerability, as in developed countries. The lack of adequate input data remains the main restriction for mapping flood risk in developing regions. Throughout this research, however, it has become apparent that there is often more – sometimes indirect – data available for a study area than initially anticipated. Therefore, sharing data and knowledge has to be encouraged more in order to create an open research climate. A second hurdle is finding suitable new case studies to test the developed methodology. As the characteristics of these study areas must be

well-known to the researchers, input data must often be acquired through field work. A final hurdle are prognoses on the effects of climate change in the SIDS. In order to take adequate future-proof measures, decision makers should not only take into account current hazards and their consequences, but also the effects of climate change and its interaction with the social, ecological and economic systems. Therefore, a tool to evaluate the climate resilience of the study area is indispensable and must contain an integrated multi-disciplinary approach that combines the knowledge of experts from different disciplines with spatial data in order to adequately evaluate the climate resilience and identify the opportunities and risks of the study area and new projects. The author took a first step in the development of such a climate resilience test, by delineating a straight-forward, clear and easy-to-use methodology to identify the areas at future risk.

SAMENVATTING

De *Small Island Developing States* (SIDS) zijn een groep van 52 landen en gebieden, gelegen in Latijns Amerika, de Caraïben, Oost-Azië en in de Stille Oceaan. Deze worden gekenmerkt door laaggelegen, dichtbevolkte kustgebieden en ontwikkelingsuitdagingen veroorzaakt door een onstabiele economie en politieke situatie. Volgens het IPCC hebben de SIDS een disproportioneel hogere kwetsbaarheid en lagere weerbaarheid voor natuurrampen dan andere landen. Ook al werden overstromingsrisicobeoordelingen de voorbije decennia reeds uitgebreid onderzocht en ontwikkeld in verschillende onderzoeksprojecten, toch worstelen overheden en beleidsmakers in kwetsbare ontwikkelingsgebieden zoals de SIDS nog vaak om gepaste maatregelen te nemen die hun gemeenschap beschermen en de gevolgen van natuurrampen beperken. Op de *International Day for Disaster Risk Reduction 2017* verwoorde António Guterres, de secretaris-generaal van de Verenigde Naties, dit als volgt: “*The challenge is to move from managing disasters themselves to managing disaster risk.*” In verschillende ontwikkelde landen heeft onderzoek geleid tot succesvolle tools om het overstromingsrisico te berekenen. Deze tools zijn echter gebaseerd op grote hoeveelheden gedetailleerde, locatie-specifieke input data, wat het onmogelijk maakt om deze tools te gebruiken in data-arme gebieden zoals de SIDS. Bovendien blijven de meeste overstromingsrisicobeoordelingen academisch onderzoek en worden ze niet gebruikt door overheden en lokale beleidsmakers. Daarom stelt dit proefschrift een methode voor om een generische, gebruiksvriendelijke en betaalbare toolbox te ontwikkelen die overstromingsschade en -risico berekent in ontwikkelingsgebieden zoals de SIDS.

Het eerste hoofdstuk beschrijft het algemene achtergrondonderzoek naar het adequaat beoordelen van het overstromingsrisico wereldwijd. Eerst wordt een inleiding gegeven over klimaatverandering en de groeiende impact van natuurgevaren (*hazards*). Van alle natuurrampen worden de grootste economische verliezen veroorzaakt door rampen gerelateerd aan het weer, waarvan overstromingen de kostelijkste zijn. Rivieroverstromingen zijn het type overstroming met de grootste impact en kosten de maatschappij elk jaar 96 miljard dollar in Bruto Nationaal Product (BNP) en treffen jaarlijks 21 miljoen mensen wereldwijd. Door klimaatverandering, bevolkingsgroei en slechte ruimtelijke planning nemen de materiële en menselijke verliezen veroorzaakt door overstromingen jaarlijks toe, en daarmee ook het belang van een correcte inschatting van deze verliezen. In dit hoofdstuk wordt een theoretisch kader gegeven van risico, kwetsbaarheid en *hazard*. Er wordt ingegaan op *disaster risk management* en de actoren in het algemeen, waarna

gefocusd wordt op *disaster risk reduction* en hoe risicobeoordelingen hier een rol kunnen in spelen. Tenslotte bespreekt het theoretisch kader ook het management van overstromingsrisico en hoe dit proefschrift overstromingsrisicobeoordeling benadert. De aanpak van overstromingsrisicobeoordelingen focust op het minimaliseren van de gevolgen en de bijhorende kosten in de plaats van op het minimaliseren van de overstroming zelf, dit door middel van het voorspellen van de mogelijke gevolgen en het bepalen van de hoge-risicogebieden. In het methodologisch kader wordt dieper ingegaan op de reeds bestaande overstromingsrisicotools, die meestal de conventionele notatie van risico volgen: $\text{Risico} = \text{Gevaar (hazard)} \times \text{Kwetsbaarheid}$. Al deze bestaande tools maken gebruik van waterdiepte als belangrijkste parameter voor de directe schadebepalingen. Een voorbeeld van zo'n tool is LATIS, een uniforme aanpak voor risico-analyse voor de verschillende hydrologische stroombekkens van Vlaanderen, in België, die beleidsmakers begeleidt in de toewijzing van hun middelen. De LATIS risicobeoordeling berekent economisch en sociaal risico voor zowel de huidige situatie als voor de toekomst. Dit laat de visualisatie toe van de impact van zowel toekomstige beslissingen als veranderingen in het landgebruik op het algemene risico. Alle overstromingsrisicotools die ontworpen zijn voor ontwikkelde gebieden, rekenen op grote hoeveelheden van gedetailleerde en kwalitatieve input data. Daarom blijft het gebrek aan data een belangrijke beperking in de ontwikkeling van globale modellen en van overstromingsrisicobeoordelingen in ontwikkelingslanden en de SIDS, die geen budget hebben om betrouwbare en gedetailleerde input data te verzamelen.

In Hoofdstuk 2 wordt een eerste gevalsstudie voorgesteld, uitgevoerd in de kuststad Annotto Bay in Jamaica. Er werden reeds schade- en risicoanalyses uitgevoerd op landelijke schaal voor de belangrijkste overstromingen in Jamaica, maar slechts zeer weinig onderzoeken hebben schade- en risicokaarten geproduceerd voor kwetsbare gebieden en onderzoeksgebieden met een kleinere schaal. In dit onderzoek werd een methodologie voor overstromingsrisicobeoordeling ontwikkeld door de methodes van LATIS en andere tools voor overstromingsrisicobeoordeling aan te passen naar Annotto Bay, een gebied dat zeer kwetsbaar is voor overstromingen maar slechts over beperkte geografische en numerieke data beschikt. De ontwikkelde methodologie laat toe om aan de hand van overstromingskaarten met verschillende *Annual Exceedance Probabilities* (AEPs) het economisch en sociaal overstromingsrisico te bepalen. Aangezien er onvoldoende data beschikbaar was om deze overstromingskaarten te produceren, werd de methode enkel voor één overstroming uit 2001, veroorzaakt door de tropische storm Michelle, uitgevoerd, waarvoor een overstromingskaart met waterdieptes beschikbaar was. De laatste stap van de methodologie, het produceren van de risicokaarten, kon hierdoor niet uitgevoerd worden, maar het model kon wel gebruikt worden om de economische en sociale schade veroorzaakt door deze ene overstroming in te schatten. Het model maakt hiervoor gebruik van input parameters zoals landgebruik en socio-economische data. De geproduceerde economische schadekaart toont de ruimtelijke variatie van de schadekosten, verbonden met de overstromingsdieptes. Ook al was de validatie van de exacte schadekosten niet mogelijk, de spreiding van de schade en het aantal getroffen elementen waren wel accuraat. De sociale schade, het aantal potentiële dodelijke slachtoffers door de overstroming, werd berekend op slechts 2. Aangezien er in realiteit niemand stierf, kon dit lage aantal ook als accuraat worden gezien. Ook al kon de methodologie voor overstromingsrisicobeoordeling niet

volledig uitgevoerd worden, door het gebrek aan meer overstromingsdata, toch was deze eerste gevalstudie belangrijk om alle stappen die voorafgaan aan het creëren van de risicokaarten in de methodologie te testen.

Deze gevalsstudie werd uitgevoerd met veel minder data dan reeds bestaande overstromingsrisicobeoordelingen. Nochtans was er nog steeds meer regio-specifieke data voorhanden dan in andere gebieden in de SIDS. Daarom moest het belang van alle input data zoals deze in de gevalstudie uit Hoofdstuk 2 gebruikt werden, bepaald worden. Dit heeft geleid tot de ontwikkeling van een methode om de gevoeligheid van het gecreëerde model voor overstromingsrisicobeoordeling ten opzichte van de input data te testen om een minimum set van onmisbare input data te bepalen, voorgesteld in Hoofdstuk 3. De economische schadekaart voor de overstroming uit 2001 in Annotto Bay werd als benchmark gebruikt. Drie schadetypes werden in rekening gebracht: schade aan gebouwen, schade aan wegen en schade aan gewassen. Daarna werden elf verschillende scenario's gegenereerd om zo het resultaat te testen op de gevoeligheid naar elk schadetype toe. Bij het bepalen van deze scenario's werd rekening gehouden met welke data gratis beschikbaar is op wereldwijde schaal, om zo het generiek karakter van de uiteindelijke toolbox te vrijwaren. Dit werd gedaan door telkens een andere combinatie van input data te gebruiken en door deze data te vereenvoudigen en veralgemenen om zo de gratis beschikbare data na te bootsen. Deze gevoeligheidsanalyse liet toe om een minimum set van input data af te bakenen die onmisbaar is om een overstromingsrisicobeoordeling aan de hand van de aangepaste methodologie uit te voeren. Een belangrijke conclusie was dat data over bevolkingsdichtheid, die globaal beschikbaar is, ook voor data-arme gebieden, in combinatie met een gemiddeld aantal mensen per huishouden een goede parameter is om de schade aan gebouwen te bepalen als de exacte gebouwenlocaties niet gekend zijn. Ook werd het belang van een complete dataset van wegen voor een accuraat visueel resultaat bewezen. Voor de berekening van schade aan gewassen kon echter niets geconcludeerd worden aangezien Annotto Bay vooral een stedelijke gemeenschap is en de schade aan gewassen een extreem lage impact had op het algemeen resultaat.

Er was een duidelijke nood aan meer onderzoek naar en data en informatie over rurale gebieden. Dit heeft geleid naar een tweede gevalsstudie in de overstromingsvlakte van de rivier Moustiques, in het noordwesten van Haïti. Aangezien er minder data beschikbaar was voor deze landelijke regio dan minimaal nodig is voor een adequate overstromingsrisicobeoordeling, moest er nieuwe input data verzameld worden. In het bijzonder historische overstromingsdata ontbrak, waarvoor bestaande acquisitietechnieken, zoals veldwerk tijdens een overstroming of satellietbeelden en luchtfotografie met hoge resolutie, niet konden toegepast worden. Daarom werd een nieuwe methode ontwikkeld in Hoofdstuk 4 om overstromingsdata te genereren op basis van de kennis van de inwoners van een gebied. Zij zijn namelijk de mensen die getroffen zijn door voorbijgevoerde overstromingen en dus herinneringen hebben over de geleden schade. Om deze informatie te verzamelen, werd een enquête opgesteld en alle 294 huishoudens in het studiegebied werden bevraagd over de meest recente en de hevigste overstroming die ze zich herinneren. In totaal werd op deze wijze informatie verzameld over 19 verschillende historische overstromingen, beschreven in 347 beantwoorde enquêtes. Overstromingsschadefactoren werden gegenereerd op basis van de antwoorden waarin

de respondenten aangaven hoeveel schade aan hun huizen en gewassen veroorzaakt werd door elke overstroming. Door het gemiddelde schadepercentage voor huizen aan de overstromingsdiepte te linken, werd een regio-specifieke schadefunctie gecreëerd. In deze functie is duidelijk te zien hoe het schadepercentage voor huizen stijgt bij een grotere waterdiepte. Voor gewassen was deze relatie echter niet zichtbaar, aangezien de agrarische velden niet gelegen zijn in hetzelfde gebied als de huizen waarvoor de coördinaten en overstromingsdieptes gebruikt werden. Daarom kon enkel een algemene schadefactor voor gewassen voor het hele studiegebied berekend worden. Ook al heeft data die op deze manier verzameld wordt een zekere graad van subjectiviteit, aangezien de herinneringen van een persoon niet altijd een accurate weergave zijn van de gebeurtenis, toch voorziet deze betaalbare en snelle acquisitie-techniek informatie over historische overstromingen die anders onbestaande zou zijn. Door de resultaten kritisch te analyseren, werd het risico op systematische vooringenomenheid geminimaliseerd.

In Hoofdstuk 5 wordt de overstromingsrisicobeoordeling voorgesteld die werd uitgevoerd voor de overstromingsvlakte van de rivier Moustiques, gebaseerd op de input van de enquêtes, aangevuld met bestaande data, literatuur, velddata en open source data. Voor het studiegebied waren drie overstromingskaarten beschikbaar, met AEPs van 50%, 10% en 2%. De methodologie voor risicobeoordeling, zoals bepaald in Hoofdstuk 2, kon dus volledig toegepast worden en zowel een economische als een sociale overstromingsrisicokaart werden geproduceerd. De resulterende kaarten tonen een extreem hoog risico voor overstromingsschade in de regio, met jaarlijks risico op bijna 2 miljoen USD economische schade en potentieel 60 dodelijke slachtoffers. In deze gevalsstudie werd duidelijk dat het risico op schade aan gewassen in rurale gebieden zeker niet verwaarloosbaar is in de methodologie. Het jaarlijkse risico op schade aan gewassen was van een vergelijkbare grootteorde als het risico op gebouwschade, met respectievelijk 30% en 33% van het totale economische risico. Ook al werd de beoordeling uitgevoerd als een kwantitatieve analyse, toch worden de resultaten beter kwalitatief geïnterpreteerd, aangezien de exacte waarden niet konden gevalideerd worden.

In een laatste stap in Hoofdstuk 6 werden de methodologie van beide gevalsstudies aangepast om een generische en flexibele methodologie te creëren om overstromingsgevaar, kwetsbaarheid en risico in kaart te brengen voor studiegebieden, niet alleen in de SIDS maar wereldwijd. De methodologie werd ontwikkeld en op maat gemaakt voor gratis beschikbare data met globale dekking, maar deze standaard workflow kan ook aangevuld worden met regio-specifieke informatie als deze beschikbaar is. De praktische applicatie is verzekerd door een modulaire toolbox die ontwikkeld werd met GDAL en PCRASTER. De toolbox bestaat uit drie onafhankelijke modules: de *hazard* module, de *vulnerability* module en de *risk* module. De eerste module laat toe om overstromingskaarten te genereren met verschillende AEPs voor het studiegebied. De *vulnerability* module produceert drie kaarten die de economische, de fysische en de sociale kwetsbaarheid weergeven. Deze kwetsbaarheid is onafhankelijk van de *hazard*. In de laatste module worden de kaarten uit de voorgaande modules gecombineerd aan de hand van schadefuncties om op deze manier overstromingsrisicokaarten te produceren. De gebruiker kan zelf kiezen welke modules uitgevoerd moeten worden,

met welke data dit gebeurt en hoe de output gevisualiseerd moet worden. De toolbox werd getest voor het volledige stroombekken van de rivier Moustiques in Haïti. Nadat de kaarten voor overstromingsgevaar (*hazard*), kwetsbaarheid en risico gecreëerd werden met de standaard beschikbare data, werd meer gedetailleerde informatie, verzameld tijdens veldwerk, toegevoegd om de resultaten van de standaard workflow te verifiëren. Deze eerste testen tonen dat de generieke workflow een robuust algoritme is dat op elk studiegebied kan toegepast worden.

Het laatste hoofdstuk, de conclusie, onderzoekt in welke graad de hoofdstukken van dit proefschrift erin geslaagd zijn om een antwoord te bieden op de onderzoeksvragen en het algemene onderzoeksdoel. De twee gevalsstudies die in dit proefschrift besproken werden, hebben rechtstreeks geleid tot het beantwoorden van het onderzoeksdoel in Hoofdstuk 6. De ontwikkelde generieke methodologie laat toe om het overstromingsrisico te beoordelen, niet alleen in de SIDS, maar ook in andere data-arme gebieden. Tijdens het doctoraatsonderzoek werden deze methodologie en de bijhorende berekeningen, net als de input data, steeds zo grondig mogelijk gevalideerd. Het was echter vaak onmogelijk om ook de output van de methodologie te valideren. Er moeten dus zeker nog enkele hindernissen overwonnen worden om hetzelfde kennisniveau en dezelfde expertise over overstromingsrisico als in ontwikkelde landen te bereiken in ontwikkelingslanden, die vaak een hoge kwetsbaarheid hebben tot overstromingen. Het gebrek aan adequate input data blijft de belangrijkste beperking bij het in kaart brengen van overstromingsrisico in ontwikkelingsregio's. Tijdens dit onderzoek werd echter duidelijk dat er vaak – soms indirect – meer data voorhanden is voor een studiegebied dan oorspronkelijk verwacht. Daarom moet het delen van data en kennis meer aangemoedigd worden om een open klimaat voor onderzoek te creëren. In dit proefschrift werd een methode voorgesteld om de input data die wel onbestaand is op een snelle en goedkope manier te verzamelen. Bovendien laten enquêtes toe om regio-specifieke informatie te verzamelen, zoals bijvoorbeeld de schadefuncties, om zo het gebruik van algemene functies of functies die gemaakt werden voor andere gebieden te elimineren. Een laatste belangrijke conclusie omtrent de input data gaat over het datatype. In beide gevalsstudies werd gebruik gemaakt van hoofdzakelijk vector data. Om het generieke karakter van de toolbox te bewaren, werd hier echter gekozen om over te schakelen naar raster data. Toch blijft vector data een belangrijke meerwaarde, en moet deze waar mogelijk omgezet worden naar rasterformaat, in de vorm van percentages per pixel, om niet aan nauwkeurigheid en kwaliteit in te boeten. Een tweede hindernis is het vinden van geschikte nieuwe gevalsstudies om de ontwikkelde methodologie verder te testen. Aangezien de karakteristieken van deze studiegebieden goed gekend moeten zijn door de onderzoekers moet de nodige input data vaak verzameld worden door veldwerk. Dit vraagt echter tijd en middelen en is daarom niet altijd eenvoudig te organiseren. Bovendien focust dit onderzoek op onstabiele gebieden, die geregeld worden getroffen door natuurrampen en politieke instabiliteit. Hierdoor kan veldwerk niet altijd plaatsvinden. De keuze van een geschikte gevalstudie is niet altijd evident. Deze keuze hangt niet enkel af van de karakteristieken van de gevalsstudie, maar ook van welke elementen getest moeten worden in de methodologie. Een laatste belangrijke hindernis is de prognoses van de effecten van klimaatverandering in de SIDS. Om toekomstbestendige maatregelen te nemen, moeten beleidsmakers niet enkel de huidige natuurgevaren en hun gevolgen in rekening brengen, maar ook de

effecten van klimaatverandering en de interactie hiervan met de sociale, ecologische en economische systemen. Daarom is een tool die de klimaatbestendigheid van een studiegebied evalueert onmisbaar en moet deze tool een geïntegreerde multidisciplinaire aanpak bevatten die de kennis van experts uit verschillende kennisvelden combineert met ruimtelijke data om de klimaatbestendigheid adequaat te evalueren en de opportuniteiten en risico's van een studiegebied en nieuwe projecten te identificeren. De auteur nam een eerste stap in de ontwikkeling van zo'n klimaatbestendigheidstest door een eenvoudige, duidelijke en gemakkelijk te gebruiken methodologie te bepalen die de gebieden identificeert die in de toekomst risico zullen lopen.

CONTENT

Summary	V
Samenvatting	IX
Content	XV
List of Figures	XIX
List of Tables	XXIII
1 INTRODUCTION	1
1.1 Background	2
1.1.1 Climate change and natural hazards	2
1.1.2 The SIDS	4
1.2 Theoretical framework	5
1.2.1 Risk	5
1.2.2 Disaster risk management	6
1.2.2.1 Actors	7
1.2.2.2 Disaster risk reduction	8
1.2.2.3 Disaster risk assessment	8
1.2.3 Flood risk management	10
1.2.3.1 Flood risk assessment	12
1.3 Methodological framework	13
1.3.1 LATIS methodology	17
1.3.2 Flood risk assessments in developing regions	19
1.4 Research objective	20
References	24
2 THE URBAN CASE STUDY: ANNOTTO BAY, JAMAICA	31
Abstract	32
2.1 Introduction	33
2.2 Study Area	34
2.3 Methodology and Data	36
2.3.1 Input data	37
2.3.2 Economic damage calculations	41
2.3.2.1 Building damage	41
2.3.2.2 Crop damage	43
2.3.2.3 Road damage	44
2.3.3 Social damage calculations	44

2.3.4 Risk calculations	45
2.4 Results	45
2.4.1 Economic damage map	45
2.4.2 Social damage map	47
2.5 Discussion	48
2.6 Conclusions	50
Acknowledgments	51
References	51

3 ANALYZING THE SENSITIVITY OF THE FLOOD RISK ASSESSMENT MODEL TOWARDS ITS INPUT DATA

Abstract	56
3.1 Introduction	57
3.1.1 Sensitivity analysis	57
3.1.2 Study area	58
3.2 Methods and results	60
3.2.1 Benchmark map	62
3.2.1.1 Method	62
3.2.1.2 Results	63
3.2.2 Building damage sensitivity	64
3.2.2.1 Methods	64
3.2.2.2 Results	65
3.2.3 Road damage sensitivity	66
3.2.3.1 Methods	66
3.2.3.2 Results	66
3.2.4 Crops damage sensitivity	68
3.2.4.1 Methods	68
3.2.4.2 Results	68
3.2.5 Data type sensitivity	69
3.2.5.1 Methods	69
3.2.5.2 Results	70
3.3 Discussion	71
3.4 Conclusion	73
References	75

4 COLLECTING HISTORIC FLOOD DATA IN DATA-POOR REGIONS – A CITIZEN APPROACH

Abstract	78
4.1 Introduction	79
4.2 Study area	79
4.3 Methodology	80
4.4 Results	83
4.5 Discussion and conclusions	86
Acknowledgments	88
References	88

5	THE RURAL CASE STUDY: THE FLOODPLAIN OF THE RIVER MOUSTIQUES, HAITI	91
	Abstract	92
	5.1 Introduction	93
	5.2 Flood risk methodology	95
	5.3 Study area	95
	5.4 Input data	96
	5.4.1 Land use data	97
	5.4.2 Economic data	98
	5.4.3 Population data	100
	5.4.4 Flood hazard maps	101
	5.4.5 Damage and mortality factors	102
	5.5 Results	103
	5.5.1 Economic risk calculations	103
	5.5.2 Social risk calculations	107
	5.6 Discussion	109
	5.7 Conclusions	110
	Acknowledgments	112
	References	112
6	FLOOD RISK MAPPING WORLDWIDE – A FLEXIBLE METHODOLOGY AND TOOLBOX	117
	Abstract	118
	6.1 Introduction	119
	6.1.1 Definitions	119
	6.2 Materials and methods	120
	6.2.1 Methodology workflow	120
	6.2.1.1 Hazard Module	121
	6.2.1.2 Vulnerability module	123
	6.2.1.3 Risk module	125
	6.2.2 Toolbox	126
	6.2.3 Study Area	128
	6.3 Results	128
	6.3.1 Results Default Modules	128
	6.3.2 Comparison with Results Obtained with Optional Data	132
	6.4 Discussion	134
	6.5 Conclusions	136
	References	137
7	DISCUSSION AND CONCLUSION	139
	7.1 General discussion	140
	7.1.1 Research overview	140
	7.1.2 Addressing the research questions	142
	7.1.3 Discussion	146
	7.2 Critical reflections and future developments	149
	7.2.1 The input data	149
	7.2.2 The case study choice	150

7.2.3 The climate change consequences	151
7.2.3.1 Identifying areas at future risk	152
7.2.3.2 Future development	154
References	155
8 APPENDIX	159

LIST OF FIGURES

Figure 1	Top row: Globally averaged mole fraction (measure of concentration) from 1984 to 2017 of CO ₂ (ppm; left), CH ₄ (ppb; center) and N ₂ O (ppb; right). The red line is the monthly mean mole fraction with the seasonal variations removed (using global observation data and statistical methods); the blue dots and line show the monthly averages. Bottom row: Growth rates representing increases in successive annual means of mole fractions for CO ₂ (ppm per year; left), CH ₄ (ppb per year; center) and N ₂ O (ppb per year; right) (WMO, 2020).	2
Figure 2	Distribution of total economic loss in USD in 83 countries by hazard, 2005–2015 (UNDRR, 2019).	3
Figure 3	Geographic location of the Small Island Developing States (marked in blue).	4
Figure 4	Disaster Risk Management Framework FAO (Baas et al., 2008).	000
Figure 5	Economic optimum in a cost benefit analysis for water infrastructure (Vanneuville et al., 2005).	6
Figure 6	Examples of direct and indirect losses as well as quantifiable and non-quantifiable losses (University of South Carolina, 2014).	13
Figure 7	Framework for economic risk mapping (Kellens et al., 2013).	17
Figure 8	Positioning of the doctoral dissertation chapters in the research framework.	22
Figure 9	Situation map of Annotto Bay, St. Mary, Jamaica, with the drainage network (data source: WRA), DEM (data source: NSDMD, resolution of 6,18m), buildings and parishes (data source: ODPEM).	35
Figure 10	Risk assessment methodology flowchart used in the study of Annotto Bay, Jamaica (based on Glas et al. (2015)).	36
Figure 11	Measured extent of the 2001 flood caused by tropical storm Michelle (DEM source: NSDMD, resolution of 6,18 m).	40
Figure 12	Visual comparison between building damage calculations without buffers (left) and with buffers (right).	43
Figure 13	Economic damage maps for the 2001 flood in Annotto Bay, Jamaica, per damage type (top left: building damage, to right: road damage, bottom: crop damage).	46
Figure 14	Economic damage map for the 2001 flood in Annotto Bay.	47
Figure 15	Social damage maps for Annotto Bay, Jamaica.	48
Figure 16	Situation map Annotto Bay (Glas et al., 2015).	58

Figure 17 Flood extent of 2001 inundations caused by Tropical Storm Michelle in Annotto Bay, Jamaica (Glas et al., 2015)	59
Figure 18 Calculation of the spatial difference (SD) of three center pixels with $SD = \text{number of neighboring pixels with different value} / \text{number of neighboring pixels}$	62
Figure 19 Scenario 1 (S1): Benchmark damage map of Annotto Bay, using all available input data.	64
Figure 20 Damage maps for Annotto Bay for S2, S3, S4 and S5. (Top left: (S2) Building materials and number of floors unknown, Top right: (S3) Building locations, materials and number of floors unknown, Bottom left: (S4) Building density is calculated based on population density, Bottom right: (S5) Building density is calculated based on number of people in study area.)	65
Figure 21 Damage maps for Annotto Bay for S6, S7, S8 and S9. (Top left: (S6) Road classes are unknown, Top right: (S7) All roads are unknown and not taken into account, Bottom left: (S8) All roads are unknown but taken into account as a percentage of land use, Bottom right: (S9) Roads are only used to divide land use polygons – no road damage.)	67
Figure 22 Damage map for Annotto Bay for S10. (Difference between banana plants and other crops is unknown.)	69
Figure 23 Damage maps for Annotto Bay for S11 and S12. (Left: (S11) Raster approach (10x10) based on population density, Right: (S12) Raster approach (30x30) based on population density.)	70
Figure 24 Deviation of total damage of all scenarios in relation to S1 (=0).	71
Figure 25 Deviation of total damaged area of all scenarios in relation to S1 (=0).	72
Figure 26 Deviation of spatial difference of all scenarios in relation to S1 (=0).	72
Figure 27 Overview of the floodplain of the catchment of the river Moustiques, located in the northwest of Haiti.	80
Figure 28 Aerial photo of Ti Charles and Baie des Moustiques (left) and residents of a fishermen dwelling in Baie des Moustiques (right). (Photographs taken during the fieldwork in 2018).	81
Figure 29 Figure from questionnaire to indicate flood height with an example water level reaching to the thigh (Glas & Deruyter, 2018).	83
Figure 30 Location of residential buildings in the floodplain of the catchment of the river Moustiques, Haiti, based on the coordinates acquired by questionnaires, conducted in January 2018 (Glas & Deruyter, 2018).	84
Figure 31 Depth-damage function for residential buildings in the floodplain of the catchment of the river Moustiques, Haiti. The vertical axis shows the degree of damage to the building, while the horizontal axis displays the water level.	85
Figure 32 Study area: floodplain of the river Moustiques in the northwest of Haiti (based on Glas et al. (2018)).	96
Figure 33 Land use map showing the land use taken into account in the economic flood risk assessment of the floodplain of the river Moustiques, Haiti (data source: OpenStreetMap, Join For Water and own data).	98
Figure 34 Population density map for the floodplain of the river Moustiques, Haiti.	100

Figure 35 Flood hazard maps with AEP of 50% (top), AEP of 10% (bottom left) and AEP of 2% (bottom right) for the floodplain of the river Moustiques, Haiti (based on Antea Group 2018).	101
Figure 36 Depth-damage function for residential buildings in the floodplain the river Moustiques, Haiti. The vertical axis shows the degree of damage to the building in percentages; the horizontal axis displays the water level (Glas et al., 2018).	102
Figure 37 Depth-damage functions for buildings, roads and crops in percentages for water heights from 0.00m up to 2.00m for the floodplain of the river Moustiques, Haiti, based on Glas et al. (2018) and Vanneuville et al. (2003).	103
Figure 38 Maximum damage map for the floodplain of the river Moustiques, Haiti.	104
Figure 39 Economic damage maps for floods with AEP of 50% (top), AEP of 10% (bottom left) and AEP of 2% (bottom right) for the floodplain of the river Moustiques, Haiti.	105
Figure 40 Economic flood risk map for the floodplain of the river Moustiques, Haiti.	106
Figure 41 Vulnerability maps for a 50% AEP flood (left), 10% AEP flood (middle) and 2% AEP flood (right) for the villages of Baie des Moustiques and Nan Ti Charles, Haiti.	107
Figure 42 Vulnerability maps for a 50% AEP flood (left), 10% AEP flood (middle) and 2% AEP flood (right) for the village of Augustin, Haiti.	107
Figure 43 Social risk map for the villages Baie des Moustiques and Nan Ti Charles (left), and for the village Augustin (right) in the floodplain of the river Moustiques, Haiti.	108
Figure 44 Workflow of flood risk mapping, as followed in the developed toolbox.	120
Figure 45 Workflow of the hazard module for floods as followed in the developed toolbox (preprocessing steps) and the OpenLISEM model.	122
Figure 46 Workflow of the vulnerability module for social vulnerability (top), physical vulnerability (middle) and economic vulnerability (bottom), as followed in the developed toolbox.	123
Figure 47 Workflow of the risk module for social risk (top), physical risk (middle) and economic risk (bottom), as followed in the developed toolbox.	125
Figure 48 Flood risk mapping toolbox software schema.	127
Figure 49 Composite storms for AEPs of 50% (T2), 10% (T10) and 2% (T50) according to IDF-relationships in West Puerto Rico (NOAA).	129
Figure 50 Flood hazard maps for three AEPs of the catchment of the river Moustiques, Haiti, as created by the toolbox.	129
Figure 51 Social, Economic and physical vulnerability map of the catchment of the river Moustiques, Haiti, as created by the toolbox.	130
Figure 52 Social, Economic and physical risk map of the catchment of the river Moustiques, Haiti, as created by the toolbox.	132
Figure 53 Comparison of the social risk map that was created using detailed input data and the optional modules (left) and the social risk map created using the default modules of the toolbox (right) for the floodplain of the catchment of the river Moustiques, Haiti.	133

Figure 54 Comparison of the economic risk map that was created using detailed input data and the optional modules (left) and the economic risk map created using the default modules of the toolbox (right) for the floodplain of the catchment of the river Moustiques, Haiti.133

Figure 55 Risk of a potential sea level rise of 1m by 2100 for the floodplain of the river Moustiques in Haiti (left) and Annotto Bay in Jamaica (right) (Glas et al., 2019). 153

Figure 56 Drought risk for the floodplain of the river Moustiques in Haiti (left) and Annotto Bay in Jamaica (right) (Glas et al., 2019). 154

LIST OF TABLES

Table 1	Qualitative properties of several flood risk assessment models, relating to their calculation of losses to residential, commercial and industrial units. (adapted from Jongman et al. (2012)).	14
Table 2	Overview of the data used in the methodology of the flood risk assessment.	38
Table 3	Sources of replacement values and depth-damage functions per damage category.	39
Table 4	Replacement values for crops.	40
Table 5	Flood damage factors (%) for wooden and concrete structures and their content, based on Dutta et al. (2003).	42
Table 6	Flood damage factors for crops for a two-day flood, based on Dutta et al. (2003).	43
Table 7	Overview of the damage cost and damaged area per damage type.	46
Table 8	Overview of the estimated number of casualties for Annotto Bay, Jamaica.	48
Table 9	Overview of investigated scenarios in the sensitivity analysis.	60
Table 10	Overview of the input data used per scenario.	61
Table 11	Calculated total damage, total damaged area and spatial difference for S1.	64
Table 12	Calculated total damage, total damaged area and spatial difference for S2, S3, S4 and S5 in comparison to S1.	66
Table 13	Calculated total damage, total damaged area and spatial difference for S6, S7, S8 and S9 in comparison to S1.	67
Table 14	Calculated total damage, total damaged area and spatial difference for S10 in comparison to S1.	69
Table 15	Calculated total damage, total damaged area and spatial difference for S11 and S12 in comparison to S1.	70
Table 16	Overview of the number of descriptions given per historic inundation by the respondents of the questionnaire in the floodplain of the river Moustiques, Haiti (Glas & Deruyter, 2018).	82
Table 17	Overview of the number of people in the floodplain of the river Moustiques, Haiti, for the villages Nan Ti Charles, Baie des Moustiques and Augustin (Glas & Deruyter, 2018).	84
Table 18	Overview of the damage percentages for the crops in the floodplain of the river Moustiques, Haiti, after the flooding in January 2018. The second column shows the number of households that own farmland with this type of crop (Glas & Deruyter, 2018).	86

Table 19	Overview data types and sources for the flood risk assessment of the floodplain of the river Moustiques, Haiti.	97
Table 20	Distribution percentages and replacement values for buildings in the catchment of the river Moustiques, Haiti, based on reports from the UCLBP (2016) and the IHSI (2003).	99
Table 21	Replacement values for crops in the catchment of the river Moustiques, Haiti, based on data from FAOSTAT (2017).	100
Table 22	Overview of the maximum damage values for the floodplain of the river Moustiques, Haiti.	104
Table 23	Overview of the estimated damage values for a 50% AEP flood, a 10% AEP flood and a 2% AEP flood for the floodplain of the river Moustiques, Haiti.	105
Table 24	Overview of the total risk values for the floodplain of the river Moustiques, Haiti.	106
Table 25	Overview of the potential casualties for a 50% AEP flood, a 10% AEP flood and a 2% AEP flood for the villages in the floodplain of the river Moustiques, Haiti.	108
Table 26	Overview of the total number of potential casualties per year for the floodplain of the river Moustiques, Haiti.	108
Table 27	Parameter maps used in the hydrological model openLISEM.	121
Table 28	Overview of default depth-damage functions available in the toolbox. ..	126
Table 29	Overview of the input data for the three modules.	127
Table 30	Flooded area and numerical comparison for the three AEPs in the catchment of the river Moustiques, Haiti.	130
Table 31	Minimum and maximum values of vulnerability levels for social, economic and physical vulnerability in the catchment of the river Moustiques, Haiti.	131
Table 32	Vulnerable area and numerical information on social, economic and physical vulnerability in the catchment of the river Moustiques, Haiti.	131
Table 33	Minimum and maximum values of risk levels for social, economic and physical risk in the catchment of the river Moustiques, Haiti.	132
Table 34	Area at risk area and numerical information on social, economic and physical risk in the catchment of the river Moustiques, Haiti.	132
Table 35	Area at risk and numerical information on the economic risk calculated by the optional modules using detailed input and the toolbox using the default modules and default input data for the floodplain of the catchment of the river Moustiques, Haiti.	134

1

INTRODUCTION

1.1 Background

1.1.1 Climate change and natural hazards

Worldwide, the climate is changing rapidly. One of the key drivers of this evolution is the increasing levels of greenhouse gasses (GHGs) in the atmosphere (WMO, 2020). In 2018, the GHG concentrations reached new highs, with globally averaged mole fractions of CO_2 at 407.8 ± 0.1 parts per million (ppm), methane (CH_4) at 1869.0 ± 2.0 parts per billion (ppb) and nitrous oxide (N_2O) at 331.1 ± 0.1 ppb (WMO, 2019b). These fractions constitute, respectively, 147%, 259% and 123% of the pre-industrial (1750) levels. The global average data for 2019 are not yet available, but local data from Mauna Lao in Hawaii and Cape Grim in Tasmania indicate that these values will most likely fit in the sharp upward trend of the past decades, displayed in Figure 1 (WMO, 2020). In the figure, seasonal variations are removed using global observational data to allow a better comparison of the concentrations over time. These variations are mainly dominated by the land biosphere and are characterized by rapid decreases with 5-20 ppm in the period June-August and large returns of similar magnitude in the period September-December.

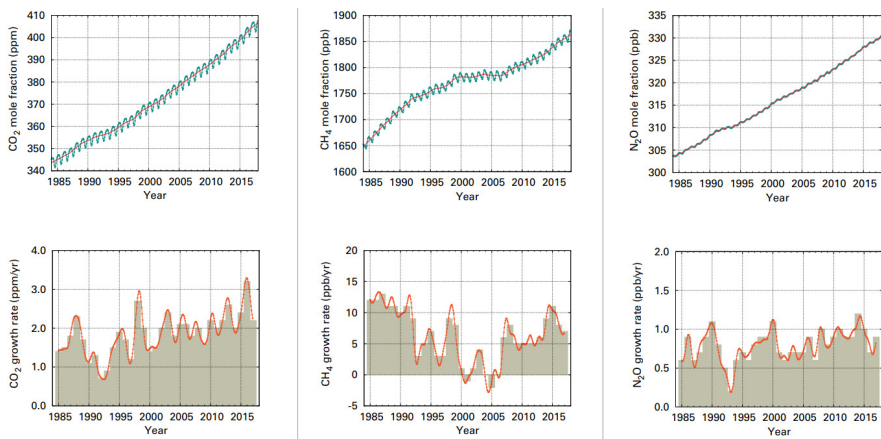


Figure 1 Top row: Globally averaged mole fraction (measure of concentration) from 1984 to 2017 of CO_2 (ppm; left), CH_4 (ppb; center) and N_2O (ppb; right). The red line is the monthly mean mole fraction with the seasonal variations removed (using global observation data and statistical methods); the blue dots and line show the monthly averages. Bottom row: Growth rates representing increases in successive annual means of mole fractions for CO_2 (ppm per year; left), CH_4 (ppb per year; center) and N_2O (ppb per year; right) (WMO, 2020).

If the emission of GHGs continues at this rate, a global warming of 1.5°C will be reached between 2030 and 2052 (IPCC, 2018). This temperature rise will have a devastating impact on the world. In the Fifth Assessment Report, the International Panel on Climate Change (IPCC) states with very high confidence that urban areas will suffer from increasing heat stress, extreme precipitation, air pollution, drought, water scarcity and sea level rise. In rural areas, climate change will additionally impact the water and

food availability and supply, as well as the production of certain crops (IPCC, 2014). Furthermore, due to climate change, the frequency and intensity of natural hazards will drastically increase over the next few decades. Extreme events in the present will thus become more common under future climate conditions. Moreover, the higher occurrence rate of two unrelated hazards will lead to a higher probability of the interaction between these phenomena, resulting in more disastrous events. For example, an extreme spring tide combined with more frequent and serious storm surges will lead to a higher chance of these events coinciding, causing severe flooding (Lavell et al., 2012). The reported losses of extreme weather events have already shown an increase of 151 percent in the past two decades. Between 1998 and 2017, climate-related disasters accounted for 77% of total global economic losses worldwide, with economic damages leading up to USD 2,245 billion. Furthermore, due to these disasters, 1.3 million lives were lost and 4.4 billion people were affected (Wallemacq et al., 2018). Worldwide, more than three times as much people are displaced due to disasters stemming from natural hazards than due to conflict and violence, with disasters displacing an average of 23.9 million people every year in the last decade (UNDRR, 2019). Every year, meteorological, hydrological and climate-related hazards thus already result in disasters that cause significant loss of life and set back economic and social development by years, if not decades (WMO, 2019a).

Although limiting the global warming to 1.5°C or even lower, and thus limiting the devastating corresponding impacts, is possible within the laws of chemistry and physics, it would require unprecedented transitions in all aspects of society (IPCC, 2018). At the UN General Assembly in 2018, Secretary-General António Guterres worded this message as: *“Climate change is moving faster than we are.”*

91 percent of all registered disasters were caused by floods, storms, droughts, heatwaves and other extreme weather events (Wallemacq et al., 2018). Figure 2 shows that these weather-related events take the lead in economic losses, with floods being the costliest hazard (UNDRR, 2019). In Jamaica, the economic damages due to flooding ran up to 1.5 billion USD over a period of four years (ODPEM, 2013b). Inundations in Myanmar and Laos cause damages equal to the countries’ capital stock every year (UNDRR, 2015a). However, not only developing countries suffer from severe flooding and corresponding losses. In the United Kingdom, for example, annual damages due to inundations are estimated at USD 250 million (Penning-Rowsell, 2015).

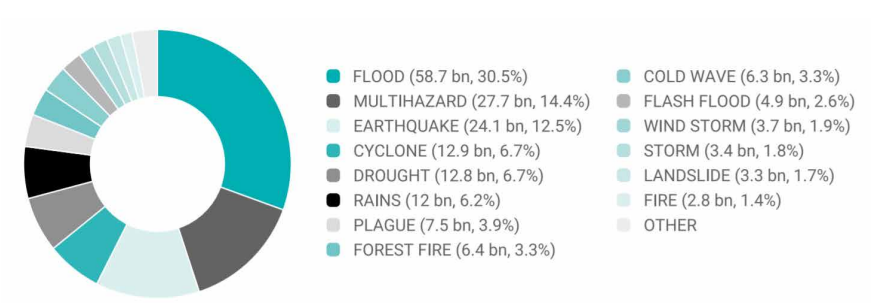


Figure 2 Distribution of total economic loss in USD in 83 countries by hazard, 2005–2015 (UNDRR, 2019).

1.1.2 The SIDS

The Small Island Developing States (SIDS) group 52 countries and territories that are located in the regions of Latin America, the Caribbean, East Asia and the Pacific, as presented in Figure 3. Each of the SIDS is characterized by low-lying, densely populated coastal areas and share similar development challenges due to an unstable economy and political situation (UN-OHRLLS, 2011).



Figure 3 Geographic location of the Small Island Developing States (marked in blue).

According to the IPCC, the SIDS have a disproportionately higher vulnerability and lower resilience to natural hazards than other countries as they are expected to lose 20 times more of their capital stock in disasters each year than Europe and Central Asia (UNDRR, 2015a). Without tropical cyclones, for example, Jamaica's economy would be expected to grow by as much as 4 percent annually, according to calculations of the World Bank. Over the past 40 years, however, it has grown a mere 0.8 percent per year (UNDRR, 2019). In five SIDS, the average annual loss (AAL) is equivalent to over 100 percent of what these countries spend on education, health and social protection (UNDRR, 2015a). The average annual loss (AAL) due to natural hazards of Puerto Rico is estimated at respectively 4,723 million USD (UNDRR, 2015a). Moreover, while disasters in non-SIDS countries affect on average 6 percent of the population, this share rises to 18 percent for disasters in the SIDS (Baas et al., 2018).

A regional breakdown of disaster types reveals that floods and storms are the primary detrimental disasters in the Caribbean SIDS, accounting for more than three fourths of all natural hazards in the region (Collymore, 2011). Droughts take up the largest part of disaster damages in African SIDS, while loss by disaster in Pacific SIDS is mainly caused by storms, earthquakes and tsunamis (Baas et al., 2018). In total, more than 75 percent of all registered disasters in all SIDS relate to rain and flash floods (UNDRR, 2015c). Moreover, the number of registered water- and climate related disasters in the SIDS rose from 212 (1978 – 1997) to 377 events (1998 – 2018), which is an increase of almost 78 percent, while the number of disasters worldwide only rose with 51 percent (Gheuens et al., 2019). Each of these single disaster events has devastating consequences. For example, Hurricane Tomas in 2010 caused losses up to USD 71.1 million in the Saint Lucia housing sector. In Georgetown in Guyana, the 2005 flood had a total damage cost of 59 percent of the country's GDP, impacted 72 percent of the city's population and claimed 34 lives (Mycoo & Donovan, 2017).

1.2 Theoretical framework

1.2.1 Risk

As it is a central issue for policy in areas as diverse as health, environment, technology, finance and security, the term ‘risk’ has a wide variety of interpretations (Eiser et al., 2012). For example, health risk is defined as “something that could cause harm to people’s health” (Dovjak & Kukec, 2019). In the field of finance, risk is often defined as the “quantifiable likelihood of loss” or “less than expected return” (Rajendran, 2012). A widely used definition in physical sciences and engineering considers risk as “the product of the probability of an event and its consequences”, determined by measurement and calculation (Jonkman, 2007). Social scientists, however, often claim that there is no such thing as real risk or objective risk, arguing that risk quantification is a subjective activity which can lead to misleading results (Slovic, 2000). Therefore, in social sciences, risk is seen as a contextual notion that will depend on several underlying determinants of perception. A few formal risk definitions in social sciences are “the probability of undesired consequence”, “the lack of perceived controllability” and “fear of loss” (Vlek, 1996).

In this dissertation, the quantitative approach of risk which is used in the domain of physical sciences and engineering, is adopted. This approach is objectified by relying on rules and assumptions laid down beforehand, as such allowing a rational presentation of risk, but it also estimates and quantifies observable characteristics of risk, for example the frequency of occurrence of events and their consequences. In the research on natural hazards, the former characteristic is described as hazard, while the latter is referred to as vulnerability, leading to the conventional notation in natural sciences of risk, as used in this dissertation: **Risk = Hazard x Vulnerability** (Wisner et al, 2003). Hazard is a broad term, described as a process, phenomenon or human activity that may cause loss of life, injury or other health impacts, property damage, social and economic disruption or environmental degradation. Vulnerability is defined by the UNDRR as a set of conditions and processes resulting from physical, social and economic factors, which increase the susceptibility of a community to the impact of the hazard (UNDRR, 2009). The term vulnerability is often combined with the exposure of an element, as exposure is described as people, property, systems or other elements in hazard zones that are thereby subject to potential losses. The concept of exposure is incorporated in the more elaborate description of risk, defined by the UNDRR as the combination of the probability of a hazardous event and its negative consequences which result from interactions between natural or man-made hazard(s), vulnerability, exposure and capacity. In this definition, capacity is described as the combination of all the strengths, attributes and resources available within the system to manage and reduce disaster risks and strengthen resilience, which is the ability of a system, community or society exposed to hazards to resist, absorb, accommodate to and recover from the effects of a hazard in a timely and efficient manner, including through the preservation and restoration of its essential basic structures and functions (UNDRR, 2009). While incorporating capacity can offer valuable and interesting insights, quantifying this correctly requires a large amount of location-specific input data. As this doctoral

research aims to create a generic toolbox for data-poor regions, capacity is left aside in this dissertation.

1.2.2 Disaster risk management

Disaster risk management can be defined as “the totality of all activities, programs and measures which can be taken up before, during and after a disaster event with the purpose to avoid the event, reduce its impact or recover from its losses” (Khan et al., 2008). According to Warfield (2008), disaster management has three main goals: (i) reducing – or avoiding – the potential losses from hazards, (ii) assuring prompt and appropriate assistance to victims of disaster and (iii) achieving rapid and effective recovery. In general, three key stages are distinguished in disaster risk management frameworks (Figure 4): pre-disaster, response and post-disaster. By consequently adopting disaster risk management into development planning, the current impact of rising disaster impact can be reversed. By rebuilding stronger, faster and more inclusively after disasters, countries can reduce the impact on people’s wellbeing and livelihoods (Hallegatte et al., 2018).

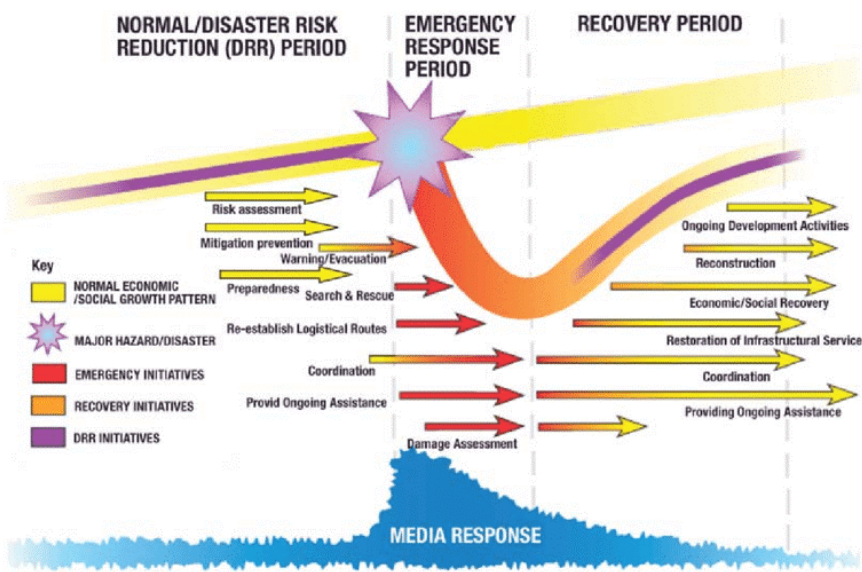


Figure 4 Disaster Risk Management Framework FAO (Baas et al., 2008).

In the first stage of disaster risk management, pre-disaster activities can be taken to strengthen the resilience of the community and reduce losses caused by a potential hazard. Risk-reducing measures can be mitigation or prevention activities such as carrying out awareness campaigns, setting up building codes and zoning, preparing of the disaster management plans or strengthening weak structures. In the second phase, emergency response measures are taken to minimize suffering and save lives and properties. In the post-disaster phase, the focus is on recovery and rehabilitation

of the affected communities (Baas et al., 2008; Khan et al., 2008). Important to note is that disaster risk management frameworks are generally designed for relatively sudden onset disasters, such as floods, earthquakes, bushfires, tsunamis and cyclones. For slow onset disasters, such as droughts, the framework is less representative as there is no recognizable single disaster event that differentiates the stages (Khan et al., 2008).

1.2.2.1 *Actors*

Effective disaster risk management, and risk assessment in specific, is set up with engagement and contributions from a wide range of actors: governments, civil defense, the private sector, civil society, the scientific community and the general public (UNDRR, 2017a). However, the large variety of actors involved in the different stages of the disaster risk management framework complicates the coordination between policies and actors (Pratzler-Wanczura et al, 2012). Nonetheless, appropriate actions at all points in the disaster risk management framework lead to greater preparedness, better warnings, reduced vulnerability or the prevention of disasters in the future (Khan, 2008).

The first stakeholder group in disaster risk management is the authorities. Public administrations play a prominent role in all phases of the risk management cycle, as they often have the ultimate responsibility to make top-level decisions (Akgungor et al., 2019). In the mitigation and preparedness phase, developmental considerations play a key role to effectively confront a future disaster (Khan, 2008). As a disaster occurs, local authorities are often overwhelmed due to limited resources, leadership and skills to cope with the disaster consequences. Combined with a lack of available support, these constraints impact the effectiveness of response and recovery operations. Therefore, governments need to work with other actors, such as the military, inter-governmental agencies and social and community leadership structures (IMC Worldwide Ltd, 2019).

In some countries, civil defense or civil protection departments, which can be controlled by armed forces personnel, manage the response to disasters (Akgungor et al., 2019). Their tasks often consist of operational and logistical support to civilian teams (Lopez-Carresi et al., 2013). This second stakeholder group often consists of a highly diverse range of social actors whose voluntary work saves and rehabilitates people in a disaster. Furthermore, these teams can include emergency services such as fire, rescue and rescue services as the first institutional response. Together with other emergency responders, they tackle the emergency on site, warning, evacuation and communication in the response phase (Akgungor et al., 2019). In this phase of the disaster management framework, humanitarian organizations become involved as well, as they provide emergency and transitional settlement, shelter, water and sanitation (Akgungor et al., 2019; Khan, 2008). Local, national and international NGOs are not only involved in disaster response, as they are often engaged as well in disaster risk reduction, preparedness and mitigation (UNDRR, 2017a).

A final important actor is the private sector, who offer critical commodities – both goods and services – to the community, in all phases of the disaster risk management framework (IMC Worldwide Ltd, 2019).

1.2.2.2 *Disaster risk reduction*

As an integral part of the total disaster risk management framework, disaster risk reduction refers to “the conceptual framework of elements considered with the possibilities to minimize vulnerabilities and disaster risks throughout a society, to avoid or limit the adverse impacts of hazards, within the broad context of sustainable development” (Baas et al., 2008). Investing in risk reduction and building resilience directly saves lives and livelihoods (Marwah, 2020). Moreover, according to the UN, every USD invested in risk reduction and prevention can save up to 15 USD in post-disaster recovery, while every USD invested in making infrastructure disaster-resilient saves no less than 4 USD in reconstruction (UNDRR, 2020).

In order to stimulate the disaster risk reduction worldwide, the United Nations presented the Sendai Framework for Disaster Risk Reduction 2015–2030 at the 3rd UN World Conference on Disaster Risk Reduction. This framework focuses on the substantial reduction of disaster risk and losses in lives, livelihoods and health and in the economic, physical, social, cultural and environmental assets of persons, businesses, communities and countries (UNDRR, 2015b). To achieve the goal of the framework by 2030, seven targets have been agreed upon: (i) Substantially reduce global disaster mortality by 2030, aiming to lower the average per 100,000 global mortality rate in the decade 2020–2030 compared to the period 2005–2015; (ii) substantially reduce the number of affected people globally by 2030, aiming to lower the average global figure per 100,000 in the decade 2020–2030 compared to the period 2005–2015; (iii) reduce direct disaster economic loss in relation to global gross domestic product (GDP) by 2030; (iv) substantially reduce disaster damage to critical infrastructure and disruption of basic services, among them health and educational facilities, including through developing their resilience by 2030; (v) substantially increase the number of countries with national and local disaster risk reduction strategies by 2020; (vi) substantially enhance international cooperation to developing countries through adequate and sustainable support to complement their national actions for implementation of the present Framework by 2030 and (vii) substantially increase the availability of and access to multi-hazard early warning systems and disaster risk information and assessments to people by 2030.

Four priority actions were distinguished to achieve the seven targets as efficient and rapidly as possible: (i) understanding disaster risk, (ii) strengthening disaster risk governance to manage disaster risk, (iii) investing in disaster risk reduction for resilience and (iv) enhancing disaster preparedness for effective response and to “Build Back Better” in recovery, rehabilitation and reconstruction.

1.2.2.3 *Disaster risk assessment*

The first priority action of the Sendai Framework, understanding disaster risk, consists of a set of recommendations for countries ensuring that policies, measures and investments use risk information properly targeted towards reducing risk effectively (UNDRR, 2015b). These recommendations are set up to allow governments to facilitate risk assessment and make risk information understandable and readily available. The aim is a national system for understanding disaster risk, integrated with related policy and planning mechanisms (UNDRR, 2017a).

The international standard on risk assessment ISO 31010:2019 is the most commonly used worldwide. The risk assessment process flow outlined in this standard consists of three steps: risk identification, risk analysis and risk evaluation. In the first step, a very high-level scoping of hazard, exposure and vulnerabilities defines the direction for the rest of the assessment process, based on knowledge and experience of stakeholders and data on past disasters and risk information. In the risk analysis step, a more detailed understanding of disaster risk is obtained by analyzing the interaction of a hazard with the exposure and vulnerability dimensions. In the final step, risk is prioritized for the purpose of managing risk, based on an understanding of capacities, risk perception and risk acceptance of a country's society by the availability and level of resources to manage the risks (ISO, 2019).

The available methods and tools for analyzing risk range from qualitative to semi-quantitative and quantitative methods (UNDRR, 2017a). The methodology choice depends on the purpose the results should serve, the resources it requires and the significance of the risk and level of investment for managing the risk. Moreover, the nature of the hazards a region faces, as well as the relation between these different hazards, must be considered. Methods can analyze the risk of a single hazard, aggregate and compare risk from all hazards or determine the sequential, simultaneous, cascading and interrelated effects of some selected hazards (Curt, 2021; UNDRR, 2017a). Although there is a wide variety of methods and tools available for single hazard assessment, methods for aggregation and comparison of hazards, and cascading and interrelated hazards and vulnerabilities are far more limited (Celano & Dolsek, 2021; Curt, 2021; Daniell, 2011; Kappes et al., 2012).

The risk of a single hazard can be assessed using many different methods, depending on the specifics and characteristics of the study area and the available data. Probabilistic risk analysis is the most rigorous method for single hazard assessment as it considers a large number of possible scenario's, their likelihood and associated impacts (UNDRR, 2017a). This method relies on a significant amount of data on hazard, exposure and vulnerabilities, as well as on information on historical loss and damage data (Clemen & Winkler, 1999; Rozer et al., 2019). When the frequency of occurrence of events cannot fully be assessed in a probabilistic manner, a deterministic analysis, characterizing possible events in terms of size and location of events rather than quantifying the likelihood of occurrence, can be performed (Apel et al., 2004; UNDRR, 2017a). For frequent events, a historical analysis can be performed when a database on damage and loss from past disasters, collected over a reasonably long time, is available (Edmonds & Noy, 2018). For infrequent hazards such as earthquakes, or high-intensity events with low probability such as a flood with a 1% annual probability, a historical analysis can be misleading (UNDRR, 2017a). When there is no information available on likelihood and impacts of events or on historic events, expert judgement can be applied to conduct a risk analysis, which will more commonly be a qualitative analysis (Brooks et al., 2005; UNDRR, 2017a). As this method has a high risk of potential bias, multiple experts should be consulted to provide reliable results.

When performing a multi-hazard assessment, several single-hazard assessments are usually carried out first after which the outputs of these assessments are used as input in

the aggregation and comparison methodology that provides a complete understanding of the risk of all hazards (UNDRR, 2017a). The aggregation of risks can only be carried out if the outputs of all single hazards are presented in a common standard metric. While this is often possible for probabilistic risk analysis outputs, other single hazard approaches are harder to combine. The ISO guideline on risk assessment provides three valuable methods to compare the risks from different hazards: (i) probabilistic analysis, (ii) multi-criteria impact and likelihood scenario analysis and (iii) the index-based approach (ISO, 2019). The probabilistic risk analyses for single-hazard assessment provides a uniform and common output criteria, enabling the straight-forward comparison of different hazard risks (Oberndorfer et al., 2020; UNDRR, 2017a). The second method, multi-criteria impact and likelihood scenario analysis, is based on a set of stress test scenarios, selected as broad as possible based on impact and likelihood. This approach is often used for emergency preparedness and recovery planning for which the worst case scenario is of interest (Caroleo et al., 2018; Ghauami, 2019). The last approach simplifies all available information on hazard, exposure and vulnerability to index scores, which are then combined to one index score per risk (ISO, 2019). The index-based approach does not only offer a comparison of risk levels from various hazards, but between different regions of interest as well. A well-known example of the index-based approach is the index for risk management INFORM, which assigns risks across various countries an overall score out of 10 by combining 53 indicators (IASC, 2020).

The most complex phenomena to model are the sequential, cascading effects of several hazards. These cascading risks have serious implications and the potential to disrupt the functioning of society and the economy (Pescaroli & Kelman, 2016). Understanding these cascades can aid in creating the necessary know how to stop and prevent them from escalating. However, these types of analyses require significant amounts of data and complex modelling tools, making it impossible to conduct a quantitative in-depth assessment. A complementary approach, focusing on identifying triggers and nodes that generate secondary events, is valuable in quantifying the possible extent (UNDRR, 2017a).

This dissertation focuses on a probabilistic single hazard risk assessment of the hazard with the highest frequency and widest distribution in the world, flooding. Although most floods are small events, monster floods are not infrequent (UNDRR, 2017b).

1.2.3 Flood risk management

Flooding is most commonly caused by heavy rainfall, but can result from other phenomena such as storm surges, tropical cyclones, tsunamis or high tide as well. Furthermore, non-natural hazards such as dam failure can also cause intense flooding. These various causes result in a series of different flood types, such as river floods, flash floods, urban floods and floods from the sea in coastal areas (*the assessment and management of flood risks*, Directive 2007/60/EC). Of these types, river flooding has the largest impact, affecting 21 million people with a cost to society of USD 96 billion in Gross Domestic Product (GDP) each year. By 2030, these numbers could grow

up to 54 million people and USD 521 billion in GDP annually (Deltares, 2015). This rise in flood risk can be attributed to population growth, urbanization and poor land use practices in flood prone areas (Keating et al., 2014). Climate change and socio-economic development will further modify the frequency, intensity and regularity of floods and other hazards, especially in already vulnerable regions (UNDRR, 2019).

In the past, decision makers have tried to prevent flooding completely. By implementing technocratic interventions such as dikes and levees, the rainfall was sent downstream as quickly as possible. This approach requires a very high economic investment and does not assure a complete protection against inundations (Vanneuville et al., 2005). Therefore, the focus of flood risk management needed to shift to protecting as much people and infrastructure as possible for a reasonable cost (Vanneuville, et al., 2003). When the investments in flood defense infrastructure no longer lead to a proportional decrease in expected damages, the economic optimum has passed and the total cost of damages and investments increases (De Nocker et al., 2004). This is shown in Figure 5.

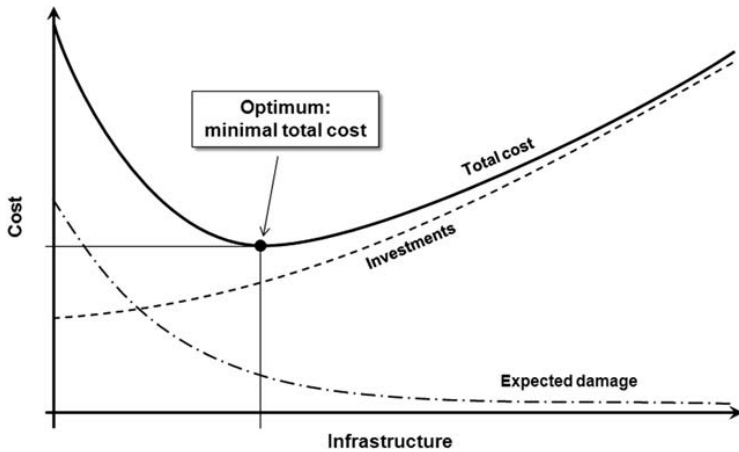


Figure 5 Economic optimum in a cost benefit analysis for water infrastructure (Vanneuville et al., 2005).

A complete flood risk management focuses not only on this optimal protection and prevention, but on preparedness as well. This approach was set forward by the European Flood Risk Directive of 2007 as the 3 P's. Measures that prevent and reduce damage to human health, the environment, cultural heritage and economic activity are combined with giving rivers more space and maintaining and restoring natural floodplains (*the assessment and management of flood risks*, Directive 2007/60/EC). As such, by considering the water system at large, this approach acknowledges that water is a resource before being a threat (UNDRR, 2017b). In more recent literature, this concept is often described as a multi-layer safety system or multi-level flood governance (Dieperink et al., 2016; Kaufmann et al., 2016; Kolen & van Gelder, 2018; Lopez, 2009). In the Netherlands, for example, flood measures are classified in three safety layers: (i) measures for the prevention of flooding such as dykes and storm-surge barriers; (ii) sustainable spatial solutions for the mitigation of losses such as flood proofing or the relocation of buildings to safer places; and (iii) disaster management and emergency management measures such as evacuation (Tsimopoulou et al., 2013).

1.2.3.1 Flood risk assessment

In this dissertation, flood risk is defined through the lenses of the main terms of the risk equation: hazard and vulnerability. When applying the risk definition to flood risk assessment, the term hazard is commonly limited to the probability of flooding as a single event in the study area (Deckers et al., 2009). The types of vulnerability taken into account in flood risk assessment can differ, depending on the available data and the specific aim of the assessment.

In the same manner as other natural hazards, flood hazard assessment models the initiation event – usually rainfall – and its evolution physically and statistically (UNDRR, 2017b). In the case of fluvial flooding, the evolution is modelled using a hydrological model to assess the routing of precipitation from rainfall to runoff and a hydraulic model to evaluate the spatial extent of floodable areas (Arseni et al., 2020). The result of this model is a set of flood hazard maps that cover the geographical areas which could be flooded according to preset scenarios (*the assessment and management of flood risks*, Directive 2007/60/EC). For each scenario, following elements are commonly shown on the flood hazard map: (i) the flood extent; (ii) water depth; and, where appropriate, (iii) the flow velocity.

In comparison to other types of risk, flood suffers from a very strong imbalance in the level of maturity in assessing the different elements of the risk: whereas hazard modelling is well advanced, vulnerability analysis is underdeveloped, and therefore, the weakest link (UNDRR, 2017b). Especially when a quantitative vulnerability assessment for floods is wanted, data availability and the level of accuracy remains a challenge. The type of vulnerability assessment depends on the type of vulnerability under investigation. Flood vulnerability can be defined as the sensitivity of a community or people to flooding considering the social, economic, environmental, physical and cultural components (Munyai et al., 2019). When a flood event occurs, each of these vulnerabilities can result in losses. Losses are quantifiable measures, often expressed in either monetary terms for physical assets or counts such as number of fatalities (GFDRR, 2014). Other losses, for example the destruction of culturally significant sites or ecosystems or psychological consequences, are more difficult to quantify. Such losses are often described as ‘intangible losses’ and are rarely taken into account in disaster risk assessments (GFDRR, 2014). Direct losses refer to the immediate physical and structural impact caused by a flood, such as the destruction of infrastructure. Indirect losses are the secondary results of the initial destruction, such as business interruption losses (University of South Carolina, 2014). Figure 6 gives some examples of direct and indirect as well as quantifiable and non-quantifiable losses. While losses are described as a measure of the damage or destruction caused by a disaster, a flood can have a much further reaching impact, including longer-term social and economic effects in education, health, productivity or in the macro economy. The impact does not only cause losses, which are by definition negative effects, but can also generate gains for some people and economies, for example the construction industry (UNDRR, 2015a).

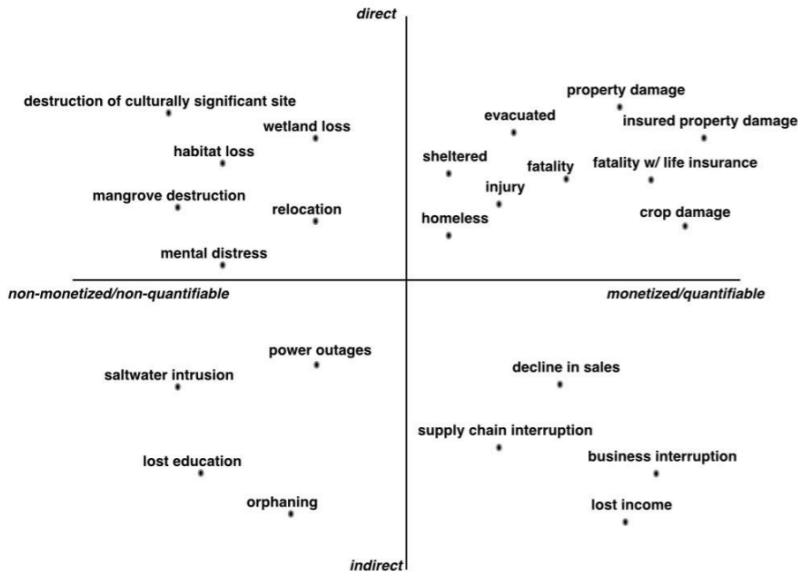


Figure 6 Examples of direct and indirect losses as well as quantifiable and non-quantifiable losses (University of South Carolina, 2014).

By combining flood hazard and vulnerability, flood risk is calculated and visualized in flood risk maps. These maps show the potential adverse consequences associated with the flood scenarios – shown in the flood hazard maps – and are most commonly expressed in the number of people affected or killed and the economic consequences. Other information, such as the pollution potential, is sometimes shown as well if it is an added value for the area under study (*the assessment and management of flood risks*, Directive 2007/60/EC).

1.3 Methodological framework

The theoretical approach of flood risk assessments has been applied in several region-specific tools. Examples of such flood risk tools are HAZUS-MH Flood model in the United States (Tate et al., 2015), Damage Scanner in the Netherlands (Klijn et al., 2007), FLEMO in Germany (Apel et al., 2009), Multi-Coloured Manual in the United Kingdom (Penning-Rowsell et al., 2005), Rhine Atlas in the Rhine Basin (ICPR, 1998), the JRC (Joint Research Centre) Model designed by the European Commission (Huizinga, 2007) and LATIS and FLIAT in Flanders, Belgium (Deckers et al., 2009; Van Ackere et al., 2019). These flood damage models all use water depth as the main determining parameter for direct damage estimations and are developed and applied by governments and academic institutions (Jongman et al., 2012). Table 1 provides an overview of the properties of each of these models. The data method refers to the method used to collect the input data. This can be empirical when based on data from historic events, or synthetic when derived from computer simulations for future events.

Table 1 Qualitative properties of several flood risk assessment models, relating to their calculation of losses to residential, commercial and industrial units. (adapted from Jongman et al. (2012)).

MODEL	SCALE OF APPLICATION	REGIONAL DIFFERENTIATION	UNITS OF ANALYSIS	HYDROLOGICAL CHARACTERISTICS	DATA METHOD	COST BASE
FLEMO	Local Regional National	Local asset values	Surface area	Depth Contamination	Empirical	Replacement values
Damage scanner	Regional National	No	Surface area	Depth	Synthetic	Replacement values
LATIS	Regional National	No	Surface area	Depth	Synthetic	Replacement values
FLIAT	Regional National	No	Surface area	Depth	Synthetic	Replacement values
HAZUS-MH	Local Regional	Local asset values	Individual objects / Surface area	Depth Duration Velocity Debris Rate of rise Timing	Empirical- Synthetic	Replacement values Depreciated values (user's choice)
MCM	Local Regional	No	Individual objects	Depth	Synthetic	Depreciated values
Rhine Atlas	Local Regional	No	Surface area	Depth	Empirical Synthetic	Depreciated values
JRC Model	Regional National European	GDP – normalization	Surface area	Depth	Empirical Synthetic (Statistical)	Replacement values Depreciated values (averaged values)

The FLEMO model has been developed for scientific flood risk analyses from the local to national scale in Germany (Apel et al., 2009). The model contains the rule-based multi-factorial Flood Loss Estimation MOdel for the private sector (FLEMOps) that estimates the direct tangible damage to residential buildings (Thieken et al., 2008) and the rule-based multi-factorial Flood Loss Estimation MOdel for the commercial sector (FLEMOcs) that estimates the direct tangible damage to buildings, equipment and goods of companies (Kreibich et al., 2010). Both models have a similar structure, calculating flood damage using five classes of inundation depth and three classes of contamination, based on empirical damage data from historic floods in the Elbe and Danube catchments (Kreibich et al., 2010; Thieken et al., 2008). On local scale, the models are applicable on the building level, while the models have been adapted using census, geo-marketing and land use data for application on regional and national scale (Jongman et al., 2012). The models have been thoroughly validated using different data sets of repair costs at the scale of single buildings as well as at the scale of whole municipalities (Thieken et al., 2008).

The Damage Scanner Model for the Netherlands is based on the economic values and depth-damage curves of the HIS-SSM module, which estimates potential flood damage on a regional or national scale but requires highly detailed data on individual buildings, industries and infrastructures (Kok et al., 2005). Since this information is not always available, the Damage Scanner Model works with aggregated land use data instead of individual units (Klijn et al., 2007). As local variations are averaged out, the model is specifically designed for application on the regional scale (Jongman et al., 2012). The model only takes into account water depth, as velocity is not added as an influencing factor. The calculations are executed for direct losses, based on rebuilding values for buildings, replacement values for contents and market values for agriculture. Indirect losses are added as a percentage (5%) of the direct losses (Briene et al., 2002).

The HAZUS Multi-Hazard software allows the estimation of the potential economic, financial and societal effects of water, wind and earthquake induced hazards within the United States (FEMA, 2009). The tool consists of different single-hazard models, of which the HAZUS-MH Flood Model spatially assesses potential flood risk on city, county or state scale (Tate et al., 2015). The calculations are based on building data on census block level, infrastructure data and nationally applicable depth-damage functions based on empirical damage data, modelling and expert opinion for direct damages and a separate module for the estimation of indirect costs with functions based on user-defined economic variables, such as unemployment figures or the size of the economy (Jongman et al., 2012). Velocity is only applied as influencing factor to areas subject to significant wave action associated with 100-year storm events (Tate et al., 2015). The HAZUS software is adapted to three levels of user input: (i) “level 1” allows a basic analysis using default input data; (ii) “level 2” analysis uses default data supplemented with regionally specified information; and (iii) “level 3” requires extensive additional economic and engineering studies by the user (FEMA, 2009).

The Multi-Coloured Manual (MCM) for the United Kingdom presents the most advanced method for flood damage estimation within Europe (Jongman et al., 2012). Contrary to most other models, the developed depth-damage curves are absolute, defining potential damage in British Pounds with water depth, rather than using percentages and maximum damage values (Penning-Rowsell et al., 2015). These curves were developed based on synthetic analysis and expert judgment. As the calculation of indirect losses is described as problematic in the MCM, only direct losses are taken into account in this model (Penning-Rowsell et al., 2015). The MCM is an object-based model, similar to HAZUS-MH (Jongman et al., 2012). As such, calculated damages per square meter only reflect on the building and not on the surrounding land.

After serious floods in the Rhine basin in 1995, an Action Plan on Floods was drafted to identify flood risk performance targets within the Rhine area (ICPR, 1998). In order to meet these targets, the Rhine Atlas damage Model was developed (ICPR, 2001). This model is based on empirically based depth-damage functions and maximum damage values for five land use classes (Jongman et al., 2012). Only direct economic costs are taken into account, calculated based on depreciated values. Indirect losses are not included (ICPR, 2001).

The European Commission's Joint Research Centre has developed a pan-European damage model and damage-functions on a global level. The European damage model comprises differentiated depth-damage functions and maximum damage values for 27 countries in Europe (Huizinga, 2007). For nine countries, the depth-damage functions were acquired from existing studies. For other countries where national studies were not available, an average of all existing functions was applied. Maximum damage values were collected in all countries where these data were available. Then, an average of these values was applied to all countries of the study, scaled to the GDP per capita (Huizinga, 2007). As some of the maximum damage values include a percentage for indirect damage, while others do not, the averaging of these values introduces a inconsistency between values across countries (Jongman et al., 2012).

The Flemish model LATIS is designed for assessments on regional and national scale using aggregated land use data, in a similar manner as the Damage Scanner in the Netherlands (Jongman et al., 2012). The methodology computes direct socio-economic impact of floods based on land use information, socio-economic data and depth-damage functions (Deckers et al., 2009). Maximum damage values are based on national averages of housing prices, surface areas and market values. Indirect damage is calculated as a percentage of direct damage (Vanneuville et al., 2003). In a later stage, the raster approach of LATIS was converted into an object-based approach, similar to HAZUS-MH and the MCM, named FLIAT. The FLIAT approach takes into account direct economic and social losses in the same manner as LATIS (Van Ackere et al., 2019).

In their comparison, Jongman et al. (2012) have shown that important differences between the models are translated in the outcomes as well. The main causes of these significant deviations are the input land use data and the uncertainty in depth-damage curves. This shows the need for a regional variation in land use data, asset values and damage factors (Jongman et al., 2012). Nonetheless, there is a considerable homogeneity among the methodologies as well, as each of them approaches the flood risk definition in a similar manner using depth-damage curves (Merz et al., 2010). Furthermore, all methodologies focus on direct tangible damages. While evidence at the country level indicates that indirect losses can surpass the direct costs (UNDRR, 2015a), it is difficult to anticipate and quantify the potential for indirect losses despite their size (GFDRR, 2014). While some models incorporate indirect damages, mostly as a – limited – percentage of direct damages, these values are difficult to validate and are, therefore, rarely accounted for.

As a direct intangible cost, the number of casualties is not incorporated in every model discussed. While the Damage Scanner in the Netherlands translates the number of casualties into a monetary value, based on the age of the victims (Klijn et al., 2007), other models such as LATIS and HAZUS-MH (Deckers et al., 2009; FEMA, 2009), approach the calculations of the number of casualties separately. As there are many elements – time of day, possible warning system, evacuation possibilities, ... – that influence the eventual number of casualties, a simplified approach is needed. In most flood risk models that incorporate a social risk module, a distribution-based approach that distributes the population of an area over different buildings and locations as a function of time is applied (Lentz & Rackwitz, 2004). Due to the fact that warning and

evacuating the people at night is more challenging, high-fatality flood events occur often by night (Jonkman, 2007; Spitalar et al., 2020). As flood risk models tend to use the most cautious approach in their risk estimation, the models that incorporate a loss of life module, calculate the number of casualties based on a nighttime regime for the population distribution (Deckers et al., 2009; EC, 2015; FEMA, 2009). In this nighttime regime, people are assumed to be in their houses. In this dissertation, the same assumption is applied in the social risk calculations.

In order to better grasp the application of the risk definition in these methodologies, the LATIS methodology is discussed in detail. LATIS is the starting point for this dissertation research, but some of the methodologies and calculations of the other existing flood risk tools together with own methodologies are incorporated in the research as well and used to create a new flood risk toolbox, applicable in the SIDS and beyond.

1.3.1 LATIS methodology

LATIS is a flood risk tool developed for Flanders, the low-lying northern part of Belgium, located at the North Sea. This region is vulnerable to long-lasting precipitation, causing overflow of river dikes that results regularly in severe inundations (Deckers et al., 2009). A uniform risk analysis approach in the different hydrological catchments of Flanders, guides decision makers to allocate their resources. The LATIS risk assessment calculates economic and social risk, not only in the present situation, but also for the future. This allows to visualize the impact of future decisions and changes in land use on the overall risk (Vanneuille et al., 2003). In a later stage, the development of a social, ecologic and cultural impact assessment was added (Van Ackere et al., 2019).

Although the economic risk and the social risk are calculated separately and result in two different risk maps, the overall methodology consists of three similar steps for both types of risk. Figure 7 presents the economic risk framework.

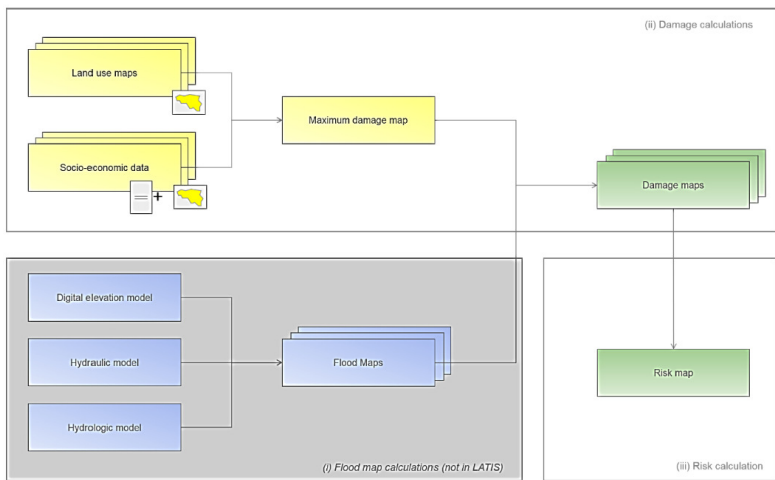


Figure 7 Framework for economic risk mapping (Kellens et al., 2013).

First, a set of flood maps is generated outside of LATIS, each with a certain return period. Then, the maximum economic damage and the maximum social damage are calculated. The former is measured by combining land use maps with socio-economic data, for example the type of housing most present in a statistical sector, and replacement values in order to represent the total cost if a flood would destroy 100 percent of the elements at risk, while the latter is based on the available population data. These maximum damage maps are combined with the flood maps, respectively using damage and mortality factors. The resulting economic damage maps are then joined into a single economic risk map, showing the risk in € m⁻² per year. The social damage maps are combined into one social risk map that visualizes the number of casualties per m² per year (Vanneuville et al., 2005).

As many studies use different definitions of economic damage, it is important to highlight which type of damage is taken into account in the LATIS risk calculations. The methodology considers monetary and internal damage. This includes damage that can be expressed as a financial value and that occurs in the flood zone. The calculations take into account direct damages, such as damage to buildings, furniture and crops, as well as indirect damages, for example cleaning costs or production losses, which are expressed as a fraction of the direct damage (Deckers et al., 2009; Grigg et al., 1976). LATIS' economic damage calculations take into account damage to housing, industry, arable farming, pasture, recreation, infrastructure, roads, railroads, airports and cars (Vanneuville et al., 2005). Average damage values, as given by insurance companies or the government, are given to each element at risk. To increase the accuracy of these values, every element at risk is divided into classes. For example, the houses are divided into classes based on their building density. Furthermore, every element at risk has a matching depth-damage function that determines the percentage of damage for a certain water height. By combining the damage factor with the maximum damage value, the economic damage value is calculated. Mathematically, this can be described as (Vanneuville et al., 2003):

$$(1) D_r = \sum_{\text{unique entities}} \alpha \times D_{\max} \times N$$

with D_r as the real damage in the flood zone, D_{\max} as the maximum damage, α as the damage factor and N as the number of entities.

As the LATIS methodology does not put a monetary value on a human life, the social risk is calculated separate from the economic risk. The social damage is expressed as a number of casualties, mortal victims. Two drowning factors are taken into account that can be combined into one mortality factor, as expressed in Equation (2) (Vrisou van Eck et al., 1999):

$$(2) N = f_d \times f_w \times P$$

with N the number of victims, f_d a drowning factor as a function of the water depth, f_w a drowning factor as a function of the incremental rate of the water level and P the number of people per m².

When the real economic and social damage is calculated for each return period, the two risk maps are developed. The damages are combined by assuming a linear interpolation between two known return periods, as expressed in (Vanneuille et al., 2003):

$$(3) \quad R = \sum_{i=x_i} \left[\left(\frac{\frac{1}{x_{i-1}+1} + \frac{1}{x_{i-1}+2} + \dots + \frac{1}{x_{i-1}+(x_i-x_{i-1})}}{x_i-x_{i-1}} \right) \times (D_{x_i} - D_{x_{i-1}}) \right]$$

where R is the total risk and D_{x_i} is the real damage corresponding to a certain return period x . With these calculated risk values, the final risk maps are generated.

While the LATIS methodology is based on flood hazard maps with return periods, this dissertation classifies a flood hazard map with an Annual Exceedance Probability (AEP). The Annual Exceedance Probability is defined as the probability of a particular storm event being exceeded in any one year, expressed as a percentage. A 1% AEP flood will thus have a 1% chance of occurring in any one year. Historically, and thus in many existing flood risk methodologies, storms were expressed as having a return period, which is defined as the average time period between the occurrence of flood events with the same size. A 100-year flood will, for example, occur on average once every 100 years. In the resulting maps, there is no actual difference between the two concepts; a 100-year-storm is exactly the same as storm with an AEP of 1%. There is, however, a shift towards the concept of AEPs in recent literature. Despite being a standard term in engineering applications, the concept of return period is not unique and depends on some hypotheses about data that seldom – if ever – hold true for real world records and generally underestimates the actual risk. Moreover, the concept of return period is often construed as confusing as it is for example possible – although not likely – that a 100-year flood occurs twice a year (Read & Vogel, 2015; Salvadori et al, 2016; Serinaldi, 2015). Therefore this dissertation research calculates flood risk based on AEPs instead of return periods. The relation between the two concepts is defined as $AEP = 1/R$, with R being the return period.

1.3.2 Flood risk assessments in developing regions

The flood risk tools designed for assessment in developed regions, are characterized by their dependence on large quantities of high-quality input data (Apel et al., 2009; Glas et al., 2016). Data scarcity remains a hurdle for the development of global models as well as for flood risk assessment in developing countries and SIDS, which lack the funds to acquire reliable and detailed input data (UNDRR, 2019). In such data-poor regions, mapping flood risk requires innovative and customized approaches. Remote sensing data are an important information source in many of these cases. In Cambodia, multi-temporal remote sensing data were used as only input for a flood assessment (Son et al., 2019). In another study, a rice crop damage map was created for a floodplain in Cambodia by combining remote sensing data with a Digital Elevation Model (DEM) and land use data of the region (Kwak et al., 2015). In the Kashmir Valley in India, the assessment of the flood risk was done solely based on satellite imagery (Kumar & Acharya, 2016). For study areas in Haiti, flood maps were developed based on a single historic flood event or derived from intensity-duration-frequency (IDF) curves, as more historic data were inexistent (Brandimarte et al., 2009; Heimhuber et al.,

2015). Although these studies have valuable results for their respective study areas, the implementation of these methodologies on a wider scale is hindered by the individuality of the approaches.

1.4 Research objective

The last few decades, flood risk assessments have been researched and developed extensively in many studies worldwide. However, governments and policy makers across the world still struggle to take correct measures to protect their communities and minimize disaster consequences. Especially in vulnerable developing regions, such as the SIDS, the need for adequate flood risk assessment tools becomes more apparent each day. On the International Day for Disaster Risk Reduction 2017, the United Nations Secretary-General António Guterres described this as: *“The challenge is to move from managing disasters themselves to managing disaster risk.”* (UNDRR, 2018) In several developed countries, research has led to successful flood risk tools. These tools, however, are based on large amounts of detailed, location-specific input data, making it impossible to apply these tools on data-poor regions such as the SIDS. Moreover, most flood risk assessments remain academic studies and are not or cannot be used by governments or local decision makers. **Therefore, the general research objective was to create a generic, user-friendly and low-cost toolbox to calculate flood damages and risk in the Small Island Developing States.** This objective has triggered following research questions (RQ):

RQ1: What are the limitations, constraints and possibilities of flood risk modelling in the SIDS? Is an alternative approach necessary in these developing regions?

Although flood risk assessment tools have been developed for several other study areas, the methodologies used there cannot be simply transferred to developing regions such as the SIDS. Data scarcity is an obvious, but important hurdle for the creation of adequate flood risk models in these areas. In order to create adequate flood risk maps, adequate flood hazard maps are indispensable. These maps show which areas will be flooded and what the potential water height would be. Although flood hazard mapping is not a part of this dissertation, the flood hazard maps are important input in this research as they are directly linked through the risk calculations with the quantification of the flood risk. Therefore, accurate and detailed flood hazard maps will directly lead to adequate flood risk assessment.

In order to acquire a full understanding of the constraints, as well as the possibilities, of flood risk modeling in the SIDS, two case studies are discussed in this dissertation. The first study area is the urban environment of Annotto Bay in Jamaica, while the second study area, the floodplain of the river Moustiques in Haiti, is primarily rural. Calculating flood risk for both environment types, exposes not only the limitations of flood risk modeling in the SIDS compared to existing flood risk assessment models in developed regions, but also identifies the differences between urban and rural areas. An import

research goal in these case studies was evaluating the possibility of a uniform approach for both rural and urban environments in the SIDS.

RQ2: What are the minimum data requirements to build a reliable flood risk assessment model?

In developing regions, there are very limited funds to acquire reliable and detailed data. Therefore, decision makers must be able to assess which data are worth investing in and how accurate and detailed these data need to be in order to create an adequate result. The minimum required data and the level of detail were deduced with a sensitivity analysis that tested the influence of all data on the overall result in order to determine the sensitivity of a model towards its input data.

RQ3: Are there low-cost, citizen-based acquisition methods available to collect the indispensable and location-specific flood risk input data? If yes, do these methods provide adequate results?

Detailed and accurate geographic data are expensive and often inexistent in developing regions. New data acquisition can have an even higher cost and is not always possible in remote or inaccessible areas. In these regions where collecting data through traditional acquisition methods is not possible, it is worth including the inhabitants and using their knowledge of the study area. These people have experienced past flooding and its consequences first-hand. Therefore, they can offer valuable insights on water levels and associated losses. While this crowdsourced geo-information, known as Volunteered Geographic Information (VGI) (Fast & Rinner, 2014), has been applied in several projects of which Open Streetmap is one of the most known and valued examples, the use of VGI to produce historic disaster data remains rather unexplored.

RQ4: Is it possible to develop a generic flood risk assessment tool that provides reliable results when different accuracy levels of available input data are used? How can this one tool address the needs of different types of end users?

Although several studies have valuable results for their respective study areas in developed as well as in developing regions, the implementation of these methodologies on a wider scale is hindered by the individuality of the approaches. Tools such as LATIS, created for developed countries, as well as specific studies performed in developing regions, use location-specific input data. Therefore, this dissertation focuses on the development of a flexible, low-cost flood risk mapping methodology that is based on freely available input data with global coverage but can be extended with detailed location-specific data if available. The methodology is developed into a toolbox with three modules: hazard, vulnerability and risk. The same flexibility that the toolbox allows in the input data is indispensable in the output data. Depending on the role of the end user, he or she can choose which module to use. While emergency workers will be interested in the flood hazard maps, generated in the hazard module, combined with basic land use information such as roads and buildings, governmental agencies can apply the output of the risk module to take correct mitigations and protection measures.

By allowing the end user to adapt the lay-out of the resulting flood risk maps, the toolbox enables different end users to create maps that are readable and easy-to-use in real-life applications.

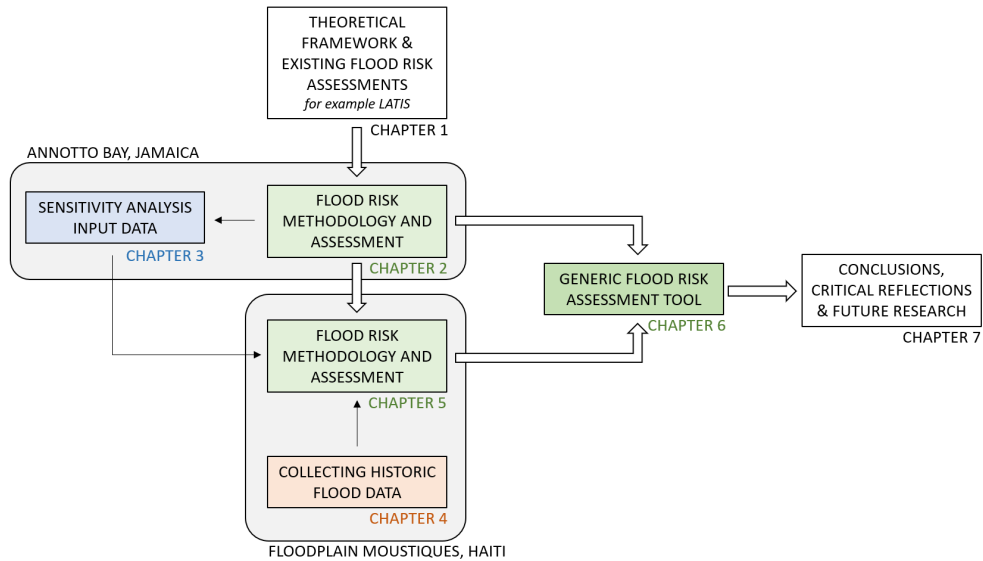


Figure 8 Positioning of the doctoral dissertation chapters in the research framework.

These four research questions are addressed in the following chapters of the proposed dissertation. Figure 8 shows the research framework and the positioning of the doctoral dissertation chapters, built around two central case studies that led to the development of a generic flood risk assessment toolbox for the SIDS.

The first case study, discussed in Chapter 2, was Annotto Bay, a coastal town in the northwest of Jamaica. The methodology of the existing flood risk assessment tool LATIS was adapted in order to fit the available input data and the urban study area characteristics. There was only flood data for one flood event obtainable, so risk maps could not be generated, but the corresponding economic and social damage map offers a clear overview of the elements most at risk during the flood of 2001.

As there is still more region-specific data available for Annotto Bay compared to other regions in the SIDS, Chapter 3 explores the importance of all input data separately by performing a sensitivity analysis for the flood risk assessment model created in Chapter 2. Twelve scenarios were used to test the sensitivity of the model towards its input data in order to delineate a minimum set of indispensable input data. This analysis offers valuable insights, not only for Annotto Bay, but for other study areas in the SIDS as well. However, due to the urban nature of the first study area, the impact of crop damage on the overall result is still largely unknown.

Therefore, a second, rural case study was performed in the floodplain of the river Moustiques in Haiti. The flood risk assessment could, however, not be executed

immediately, as the minimum input data requirements were not met. Chapter 4 describes how the missing flood data were collected through questionnaires. This technique provides region-specific damage factors for buildings, crops and livestock that were otherwise inexistent. With this collected input data, the flood risk assessment was carried out for the second case study in Chapter 5.

The methodologies of the two case studies were the base for the creation of a generic flood risk assessment toolbox, applicable worldwide. Chapter 6 focuses on the development of the toolbox and its three modules that calculate hazard, vulnerability and risk. The created toolbox runs on default, freely available, input data with global coverage that can be complemented with more region-specific data when available. The testing of this toolbox is still in the initial phase, but has shown some promising results for qualitative flood risk assessment. When fully developed and tested, this toolbox can offer an easy-to-use tool to indicate high-risk areas, applicable in all SIDS, as well as in large parts of the rest of the world.

In the final chapter, an overview is given of the findings of the previous chapters, after which the most important conclusions and opportunities are discussed. Chapter 7 also provides an answer on the research questions and offers critical reflections on the doctoral research, as well as suggestions for further research on the subject.

REFERENCES

- Akungor C., Atun F., Barquet K., Bea M., Boersma K., Coates R., Dandoulaki M., Engel, K., Frerks G., Giordano R., Jarzabek L., de Jong H., Kulakowska M., Lopez-Gunn E., Magnuszewski P., Menoni S., Pagano A., Pajak M., Regad M., Rietjens S., Solińska A., Tamas P., van Tilborg A., Warner J., & Wolbers J. (2019) *Chapter 5: Actors Response and Interaction*. In: EDUCEN Culture and Urban Disaster: A Handbook. doi: 10.18174/417184
- Apel H., Aronica G. T., Kreibich H., & Thieken A. H. (2009) Flood risk analyses-how detailed do we need to be? *Natural Hazards*, 49(1), 79-98. doi:10.1007/s11069-008-9277-8
- Apel H., Thieken A., Merz B., & Blochl G. (2004) Flood risk assessment and associated uncertainty. *Natural Hazards and Earth System Sciences*, 4(2), 295-308. doi: 10.5194/nhess-4-295-2004
- Arseni R.M., Rosu A., Calmuc M., Calmuc V.A., Iticescu C., & Georgescu L.P. (2020) Development of Flood Risk and Hazard Maps for the Lower Course of the Siret River. *Sustainability*, 12, 6588. doi: 10.3390/su12166588
- Baas S., Conforti P., Ahmed S., & Markova G. (2018) *Impact of disasters and crises on agriculture and food security, 2017*. FAO, Rome (Italy) Climate and Environment Div. <http://www.fao.org/3/i8656en/i8656EN.pdf>
- Baas S., Ramasamy S., de Pryck J., & Battista F. (2008) *Disaster Risk Management Systems Analysis: A Guide Book*. Food and Agricultural Organization of the United Nations. <http://www.fao.org/3/i0304e/i0304e.pdf>
- Brandimarte L., Brath A., Castellarin A., & Di Baldassarre G. (2009) Isla Hispaniola: A trans-boundary flood risk mitigation plan. *Physics and Chemistry of the Earth*, 34(4-5), 209-218. doi:10.1016/j.pce.2008.03.002
- Briene M., Koppert S., Koopman A., & Verkennis A. (2002) *Financiële onderbouwing kengetallen hoogwaterschade*. Netherlands Economic Institute (NEI), Rotterdam, the Netherlands. https://puc.overheid.nl/rijkswaterstaat/doc/PUC_130582_31/
- Brooks N., Adger W.N., & Kelly P.M. (2005) The determinants of vulnerability and adaptive capacity at the national level and the implications for adaptation. *Global Environmental Change – Human and Policy dimensions*, 15(2), 151-163. doi: 10.1016/j.gloenvcha.2004.12.006
- Caroleo B., Palumbo E., Osella M., Lotito A., Rizzo G., Ferro E., Attanasio A., Chiusano S., Zuccaro G., Leone M., & De Gregorio D. (2018) A Knowledge-Based Multi-Criteria Decision Support System Encompassing Cascading Effects for Disaster Management. *International Journal of Information Technology & Decision Making*, 17(5), 1469-1498. doi: 10.1142/S021962201850030X
- Celano F., & Dolsek M. (2021) Fatality risk estimation for industrialized urban areas considering multi-hazard domino effects triggered by earthquakes. *Reliability Engineering & System Safety*, 206, 107287. doi: 10.1016/j.res.2020.107287
- Clemen R.T., & Winkler R.L. (1999) Combining probability distributions from experts in risk analysis. *Risk Analysis*, 19(2), 187-203. doi: 10.1111/j.1539-6924.1999.tb00399.x
- Collymore J. (2011) Disaster management in the Caribbean: Perspectives on institutional capacity reform and development. *Environmental Hazards*, 10(1), 6-22. doi:10.3763/ehaz.2011.0002

- Curt C. (2021) Multirisk: What trends in recent works? A bibliometric analysis. *Science of the Total Environment*, 763, 142951. doi: 10.1016/j.scitotenv.2020.1429510048-9697
- Daniell D.E. (2011) Open Source Procedure for Assessment of Loss using Global Earthquake Modelling software (OPAL). *Natural Hazards and Earth System Sciences*, 11, 1885-1900. doi: 10.5194/nhess-11-1885-2011
- De Nocker L., Broekx S., Liekens I., Bulckaen D., Smets S., Gauderis J., & Dauwe W. (2004) Cost-benefit analysis to select the optimal flood protection strategy along the Scheldt. *WIT Transactions on Ecology and the Environment*, 91, 271-277. doi: 10.2495/RISK060261
- Deckers P., Kellens W., Reyns J., Vanneuville W., & De Maeyer P. (2009) A GIS for flood risk management in Flanders. In P.S. Showalter, L. Yongmei (Ed.), *Geospatial techniques in urban hazard and disaster analysis*, 51-69: Dordrecht, Springer.
- Deltares (2015) *Global flood risks mapped out*. Retrieved from <https://www.deltares.nl/en/news/global-flood-risks-mapped/>
- Dieperink C., Mees H., Priest S., Ek K., Bruzzone S., Larue C., & Matczak P. (2016) Enhancing urban flood resilience as a multi-level governance challenge: An exploration of multilevel coordination mechanisms. *Paper for the 2016 Nairobi Conference on Earth System Governance*. 26p.
- Directive 2007/60/EC of the European Parliament and of the Council of 23 October 2007 on the assessment and management of flood risks (2007).
- Dovjak M., & Kukec A. (2019) Identification of Health Risk Factors and Their Parameters. In: Dovjak M., & Kukec A. (Ed.), *Creating Healthy and Sustainable Buildings* (pp 83-120): Springer, Cham. doi: 10.1007/978-3-030-19412-3_3
- EC (2015) EU overview of methodologies used in preparation of Flood Hazard and Flood Risk Maps: Final Report. European Commission (EC). https://ec.europa.eu/environment/water/flood_risk/pdf/fhrm_reports/EU%20FHRM%20Overview%20Report.pdf
- Edmonds C., & Noy I. (2018) The economics of disaster risks and impacts in the Pacific. *Disaster Prevention and Management*, 27(5), 478-494. doi: 10.1108/DPM-02-2018-0057
- Eiser J.R., Bostrom A., Burton I., Johnston D.M., McClure J., Paton D., van der Pligt J., & White M.P. (2012) Risk interpretation and action: A conceptual framework for responses to natural hazards. *International Journal of Disaster Risk Reduction*, 1, 5-16. doi: 10.1016/j.ijdr.2012.05.002
- Fast V., & Rinner C. (2014) A systems perspective on volunteered geographic information. *ISPRS International Journal of Geo-Information*, 3(4), 1278-1292. doi: 10.3390/ijgi3041278
- FEMA (2009) *HAZUS-MH MR4 Flood Model Technical Manual*. Federal Emergency Management Agency (FEMA), Mitigation Division. https://www.fema.gov/sites/default/files/2020-09/fema_hazus_flood-model_technical-manual_2.1.pdf
- GFDRR (2014) *Understanding Risk in an Evolving World: Emerging Best Practices in Natural Disaster Risk Assessment*. Global Facility for Disaster Reduction and Recovery. https://www.gfdr.org/sites/default/files/publication/Understanding_Risk-Web_Version-rev_1.8.o.pdf
- Ghauami S.M. (2019) Multi-criteria spatial decision support system for identifying strategic roads in disaster situations. *International Journal of Critical Infrastructure Protection*, 24, 23-36. doi: 10.1016/j.ijcip.2018.10.004

- Gheuens J., Nagabhatla N., & Perera E. D. P. (2019) Disaster-Risk, Water Security Challenges and Strategies in Small Island Developing States (SIDS). *Water*, 11(4), 637. doi: 10.3390/w11040637
- Glas H., Deruyter G., De Maeyer P., Mandal A., & James-Williamson S. (2016) Analyzing the sensitivity of a flood risk assessment model towards its input data. *Natural Hazards and Earth System Sciences*, 16(12), 2529-2542. doi:10.5194/nhess-16-2529-2016
- Grigg N. S., Botham L. H., Rice L., Shoemaker W., & Tucker L. S. (1976) Urban drainage and flood control projects: economic, legal and financial aspects. *Completion report series (Colorado State University. Environmental Resources Center); no. 65*. Retrieved from <https://mountainscholar.org/handle/10217/2617>
- Hallegatte S., Rentschler J., Walsh B. (2018) *Building Back Better: Achieving resilience through stronger, faster, and more inclusive post-disaster reconstruction*. World Bank. <https://openknowledge.worldbank.org/bitstream/handle/10986/29867/127215.pdf>
- Heimhuber V., Hannemann J. C., & Rieger W. (2015) Flood Risk Management in Remote and Impoverished Areas-A Case Study of Onaville, Haiti. *Water*, 7(7), 3832-3860. doi:10.3390/w7073832
- Huizinga H. (2007) Flood damage functions for EU member states. *HKV Consultants, Implemented in the framework of the contract*, 382442-F382441SC.
- IASC (2020) *INFORM Report 2020: Shared evidence for managing crises and disasters*. Inter-Agency Standing Committee and the European Union. doi: 10.2760/953633
- ICPR (1998) *Action Plan on Flood Defence*. Retrieved from <https://www.icpdr.org/main/activities-projects/flood-action-plans>
- ICPR (2001) *Atlas of flood danger and potential damage due to extreme floods of the Rhine, International Commission for the Protection of the Rhine*. Retrieved from <https://www.iksr.org/en/public-relations/documents/archive/maps/rhine-atlas>
- IMCWorldwide Ltd (2019) *Guide to Engaging Local Actors in Disaster Recovery Frameworks*. 93p. <https://www.gfdr.org/sites/default/files/publication/Engaging%20Local%20Actors%20in%20Disaster%20Recovery%20Frameworks%20-%20Final.pdf>
- IPCC (2014) *Climate Change 2014: Synthesis Report. Contributions of Working Groups I, II and III to the Fifth Assessment Report of the Interantional Panel on Climate Change*. Switzerland. https://www.ipcc.ch/site/assets/uploads/2018/02/SYR_AR5_FINAL_full.pdf
- IPCC (2018) *Global Warming of 1.5°C. An IPCC Special Report on the Impacts of Global Warming of 1.5 C Above Pre-Industrial Levels and Related Global Greenhouse Gas Emission Pathways, in the Context of Strengthening the Global Response to the Threat of Climate Change* [Masson-Delmotte V., Zhai P., Pörtner H.-O., Roberts D., Skea J., Shukla P.R., Pirani A., Moufouma-Okia W., Péan C., Pidcock R., Connors S., Matthews J.B.R., Chen Y., Zhou X., Gomis M.I., Lonnoy E., Maycock T., Tignor M. and Waterfields T.]. <https://www.ipcc.ch/sr15/download/#full>
- ISO (2019) *Risk Management – Risk assessment techniques* (ISO Standard no. IEC 31010:2019). International Organization for Standardization (ISO). <https://www.iso.org/standard/72140.html>
- Jongman B., Kreibich H., Apel H., Barredo J., Bates P., Feyen L., & Ward P. (2012) Comparative flood damage model assessment: towards a European approach. *Natural Hazards and Earth System Sciences (NHES)*, 12(12), 3733-3752. doi: 10.5194/nhess-12-3733-2012

- Jonkman S.N. (2007). *Loss of life estimation in flood risk assessment: theory and applications*. [Doctoral dissertation, T.U. Delft] <https://library.wur.nl/ebooks/hydrotheek/1875249.pdf>
- Kappes M.S., Keiler M. von Elverfeldt K., & Glade T. (2012) Challenges of analyzing multi-hazard risk: a review. *Natural Hazards*, 64, 1925–1958. doi: 10.1007/s11069-012-0294-2
- Keating A., Mechler R., Mochizuki J., Kunreuther H., Bayer J., Hanger S., & Hochrainer-Stigler S. (2014) *Operationalizing resilience against natural disaster risk: opportunities, barriers, and a way forward*. <http://pure.iiasa.ac.at/id/eprint/11191/>
- Kellens W., Vanneuville W., Verfaillie E., Meire E., Deckers P., & De Maeyer P. (2013) Flood risk management in Flanders: past developments and future challenges. *Water Resources Management*, 27(10), 3585–3606. doi: 10.1007/s11269-013-0366-4
- Khan H., Vasilescu L.G., & Khan A. (2008) Disaster Management Cycle – A Theoretical Approach. *Journal of Management and Marketing*, 6(1), 43–50.
- Klijn F., Baan P., De Bruijn K., & Kwadijk J. (2007) *Overstromingsrisico's in Nederland in een veranderend klimaat: verwachtingen, schattingen en berekeningen voor het project Nederland Later. Q4290 voor MNP*. <https://repository.tudelft.nl/islandora/object/uuid%3A015c62a1-558d-422c-8706-efcoe4db2fc3>
- Kok M., Huizinga H. J., Vrouwenfelder A. C. W. M., & Barendregt A. (2005) *Standaard-methode 2004 – Schade en Slachtoffers als gevolg van overstromingen*. RWS Dienst Weg-en Waterbouwkunde. <https://library.wur.nl/ebooks/hydrotheek/1874298.pdf>
- Kolen B. & van Gelder P.H.A.J.M. (2018) Risk-Based Decision-Making for Evacuation in Case of Imminent Threat of Flooding. *Water*, 10, 1429. doi: 10.3390/w10101429
- Kreibich H., Seifert I., Merz B., & Thieken A. H. (2010) Development of FLEMOcs – A new model for the estimation of flood losses in companies. *Hydrological Sciences Journal*, 55, 1302–1314. doi: 10.1080/02626667.2010.529815
- Kumar R., & Acharya P. (2016) Flood hazard and risk assessment of 2014 floods in Kashmir Valley: a space-based multisensor approach. *Natural Hazards*, 84(1), 437–464. doi: 10.1007/s11069-016-2428-4
- Kwak Y., Shrestha B.B., Yorozyua A., & Sawano H. (2015) Rapid Damage Assessment of Rice Crop After Large-Scale Flood in the Cambodian Floodplain Using Temporal Spatial Data. *Ieee Journal of Selected Topics in Applied Earth Observations and Remote Sensing*, 8(7), 3700–3709. doi:10.1109/jstars.2015.2440439
- Lavell A., Oppenheimer M., Diop C., Hess J., Lempert R., Li J., & Takeuchi, K. (2012) Climate change: new dimensions in disaster risk, exposure, vulnerability, and resilience. In Field, C.B., V. Barros, T.F. Stocker, D. Qin, D.J. Dokken, K.L. Ebi, M.D. Mastrandrea, K.J. Mach, G.-K. Plattner, S.K. Allen, M. Tignor, and P.M. Midgley (Ed.), *Managing the Risks of Extreme Events and Disasters to Advance Climate Change Adaptation: Special Report of the Intergovernmental Panel on Climate Change* (pp. 25–64): Cambridge University Press.
- Lentz A. & Rackwitz R. (2004) Loss-of-Life Modelling in Risk Acceptance Criteria. *Probabilistic Safety Assessment and Management*, 1924–1929. doi: 10.1007/978-0-85729-410-4_309
- Lopez J. (2009) The Multiple Lines of Defense Strategy to Sustain Louisiana's Coast. *Journal of Coastal Research*, 54, 186–197. doi: 10.2112/SI54-020.1
- Lopez-Carresi A., Fordham M., Wisner B., Kelman I., & Gaillard J. C. (2013) *Disaster management: International lessons in risk reduction, response and recovery*. Routledge.

- Marwah N.C. (2020) Disaster Management in the Context of India's National Security: An Assessment, *Centre for Land Warfare Studies Journal*, 13(2), 115-136.
- Merz B., Kreibich H., Schwarze R., & Thieken A. (2010) Assessment of economic flood damage. *Nat. Hazards Earth Syst. Sci.*, 10(8), 1697-1724. doi: 10.5194/nhess-10-1697-2010
- Mycoo M., & Donovan M. (2017) *A Blue Urban Agenda: Adapting to Climate Change in the Coastal Cities of Caribbean and Pacific Small Island Developing States*. <https://publications.iadb.org/en/blue-urban-agenda-adapting-climate-change-coastal-cities-caribbean-and-pacific-small-island>
- Oberndorfer S., Sander P., & Fuchs S. (2020) Multi-hazard risk assessment for roads: probabilistic versus deterministic approaches. *Natural Hazards and Earth System Sciences*, 20, 3135-3160. doi: 10.5194/nhess-20-3135-2020
- ODPEM (2013) *National progress report on the implementation of the Hyogo Framework for Action (2011-2013)*. <https://www.preventionweb.net/english/hyogo/national/reports/v.php?id=33409&pid=183>
- Pescaroli G., & Kelman I. (2016) How Critical Infrastructure Orients International Relief In Cascading Disasters. *Journal of Contingencies and Crisis Management*, 25(2), 56-67. doi: 10.1111/1468-5973.12118
- Penning-Rowsell E., Johnson C., Tunstall S., Tapsell S., Morris J., Chatterton J., & Green C. (2005) *The benefits of flood and coastal risk management: a handbook of assessment techniques*. ISBN 1904750516. <https://repository.tudelft.nl/islandora/object/uuid:33f2d216-c9bf-419c-b3b1-415a6f6fd881/datastream/OBJ/download>
- Penning-Rowsell, E. C. (2015) A realistic assessment of fluvial and coastal flood risk in England and Wales. *Transactions of the Institute of British Geographers*, 40(1), 44-61. doi: 10.1111/tran.12053
- Pratzler-Wanczura S., Sapountzaki K., Ferri F., Grifoni P., Firus K., Xanthopoulos G. (2012) Linking the actors and policies throughout the disaster management cycle by 'Agreement on Objectives' – a new output-oriented management approach. *Natural Hazards and Earth System Sciences*, 12(4), 1085-1107. doi: 10.5194/nhess-12-1085-2012
- Rajendran M. (2012) Operational Risks involved in Banking Industries. *Amity Global Business Review*, 7, 50-57.
- Rozar V., Kreibich H., Schroter K., Muller M., Sairam N., Doss-Gollin J., Lall U., & Merz B. (2019) Probabilistic Models Significantly Reduce Uncertainty in Hurricane Harvey Pluvial Flood Loss Estimates. *Earth Future*, 7(4), 385-394. doi: 10.1029/2018EF001074
- Slovic P. (2000) *The perception of risk*. Earthscan Publications, Sterling, Virginia.
- Son N. T., Chen C. F., & Chen C. R. (2019) Flood assessment using multi-temporal remotely sensed data in Cambodia. *Geocarto International*, 16. doi:10.1080/10106049.2019.1633420
- Spitalar M., Brilly M., Kos D., & Zibera A. (2020) Analysis of Flood Fatalities–Slovenian Illustration. *Water*, 12(1), 64. doi: 10.3390/w12010064
- Tate E., Munoz C., & Suchan J. (2015) Uncertainty and Sensitivity Analysis of the HAZUS-MH Flood Model. *Natural Hazards Review*, 16(3), 10. doi:10.1061/(asce)nh.1527-6996.0000167
- Thieken A. H., Olschewski A., Kreibich H., Kobsch S., & Merz B. (2008) Development and evaluation of FLEMOps – a new Flood Loss Estimation MODEL for the private sector, *Flood Recovery, Innovation and Response I*, WIT Press, 315-324. doi: 10.2495/FRIAR080301

- Tsimopoulou V., Vrijling J.K., Kok M., Jonkman S.N., & Stijnen J.W. (2013) Economic implications of multi-layer safety projects for flood protection. *Paper presented on 22nd European Safety and Reliability Conference*. 7p.
- UN-OHRLLS(2011)*Small Island Developing States: Small Islands Big(ger) Stakes*. New York, USA: <http://unohrlls.org/custom-content/uploads/2013/08/SIDS-Small-Islands-Bigger-Stakes.pdf>
- UNDRR (2009) *UNISDR Terminology on Disaster Risk Reduction*. Geneva, Switzerland: Retrieved from <https://www.undrr.org/publication/2009-unisdr-terminology-disaster-risk-reduction>
- UNDRR (2015a) *Global Assessment Report on Disaster Risk Reduction 2015: Making Development Sustainable: the Future of Disaster Risk Management*. Geneva, Switzerland: United Nations Office of Disaster Risk Reduction. <https://www.undrr.org/publication/global-assessment-report-disaster-risk-reduction-2015>
- UNDRR (2015b) *Sendai Framework for Disaster Risk Reduction 2015-2030*. United Nations Office for Disaster Risk Reduction (UNDRR). https://www.preventionweb.net/files/43291_sendaiframeworkfordrren.pdf
- UNDRR (2015c) *UNISDR Working Papers on Public Investment Planning and Financing Strategy for Disaster Risk Reduction: Review of Mauritius*. Geneva, Switzerland: <https://www.undrr.org/publication/unisdr-working-papers-public-investment-planning-and-financing-strategy-disaster-risk-o>
- UNDRR (2017a) *Words into Action Guidelines: National Disaster Risk Assessment: Governance System, Methodologies, and Use of Results*. United Nations Office for Disaster Risk Reduction (UNDRR). https://www.preventionweb.net/files/52828_nationaldisasterriskassessmentwiagu.pdf
- UNDRR (2017b) *Words into Action Guidelines: National Disaster Risk Assessment: Hazard Specific Risk assessment. 4. Flood Hazard and Risk Assessment*. United Nations Office for Disaster Risk Reduction (UNDRR). https://www.preventionweb.net/files/52828_04floodhazardandriskassessment.pdf
- UNDRR (2018) *UNISDR Annual Report 2017, 2016-17 Biennium Work Programme Final Report*. Geneva, Switzerland: <https://www.undrr.org/publication/unisdr-annual-report-2017>
- UNDRR (2019) *Global Assessment Report on Disaster Risk Reduction*. Geneva, Switzerland: <https://www.undrr.org/publication/global-assessment-report-disaster-risk-reduction-2019#:~:text=The%202019%20Global%20Assessment%20Report,the%20global%20disaster%20risk%20landscape.>
- UNDRR (2020) *Funding*. Retrieved from: <https://www.undrr.org/about-undrr/funding>. Accessed on March 5th, 2021.
- University of South Carolina (2014) *Who needs loss data?* Background paper prepared for the Global Assessment Report on Disaster Risk Reduction 2015. <https://www.preventionweb.net/english/hyogo/gar/2015/en/bgdocs/University%20of%20South%20Carolina,%202014.pdf>
- Van Ackere S., Beullens J., Vanneuville W., De Wulf A., & De Maeyer P. (2019) FLIAT, An Object-Relational GIS Tool for Flood Impact Assessment in Flanders, Belgium. *Water*, 11(4), 711. doi: 10.3390/w11040711
- Vanneuville W., De Maeyer P., Maeghe K., & Mostaert F. (2003) Model the effects of a flood in the Dender catchment based on a risk methodology. *Bulletin of the Society of Cartography*, 37(2), 59-64.

- Vanneuville W., De Rouck K., Maeghe K., Deschamps M., De Maeyer P., & Mostaert F. (2005) *Spatial calculation of flood damage and risk ranking*. Paper presented at the AGILE 2005 8th conference on geographic information science.
- Visou van Eck N., Kok M., & Vrouwenvelder A. (1999) Standaardmethode Schade en Slachtoffers als gevolg van overstromingen, deel 2: Achtergronden. *HKV Lijn in water, TNO, Dienst Weg en Waterbouw*. https://puc.overheid.nl/rijkswaterstaat/doc/PUC_20427_31/
- Vlek C.A.J. (1996) A multi-level, multi-stage and multi-attribute perspective on risk assessment, decision-making and risk control, *Risk Decision and Policy*, 1(1), 9-31.
- Wallemacq P., Below R., & McLean D. (2018) *Economic losses, Poverty & Disasters (1998-2017)*. Retrieved from <https://www.undrr.org/publication/economic-losses-poverty-disasters-1998-2017>
- Warfield C. (2008) *The Disaster Management Cycle*. retrieved from: https://www.gdrc.org/uem/disasters/1-dm_cycle.html
- Wisner B., Blaikie P., Cannon T., & Davis I. (2003) *At Risk: Natural Hazards, People's Vulnerability and Disasters*. 471p. Routledge.
- WMO (2019a) *2018 Annual Report: WMO for the Twenty-first Century*. Geneva, Switzerland: https://library.wmo.int/index.php?lvl=notice_display&id=21412#.YQ9FGhKg_2x
- WMO (2019b) Greenhouse Gas Bulletin The State of Greenhouse Gases in the Atmosphere Based on Global Observations through 2018. *World Meteorological Organization*, 8. https://reliefweb.int/sites/reliefweb.int/files/resources/GHG-Bulletin-15_en.pdf
- WMO (2020) *WMO Statement on the State of the Global Climate in 2019*. <https://reliefweb.int/sites/reliefweb.int/files/resources/WMO%20Statement%20on%20the%20State%20of%20the%20Global%20Climate%20in%202019.pdf>

2

THE URBAN CASE STUDY: ANNOTTO BAY, JAMAICA

This chapter is adapted from the following journal articles:

Glas H., Jonckheere M., Mandal A., James-Williamson S., De Maeyer P., Deruyter G. (2017). A GIS-based tool for flood damage assessment and delineation of a methodology for future risk assessment: case study for Annotto Bay, Jamaica, *Natural Hazards* 88(3), 1867-1891. doi: 10.1007/s11069-017-2920-5

Glas, H., Van Ackere, S., Deruyter, G., De Maeyer, P. (2016). Flood damage assessment in a GIS : case study for Annotto Bay, Jamaica, *International Journal of Safety and Security Engineering*, 6, 508–517. Presented at the 5th International conference on Flood Risk Management and Response (FRIAR 2016). doi: 10.2495/safe-v6-n3-508-517

ABSTRACT

Flood risk assessments and damage estimations form integral parts of the disaster risk management for Jamaica, owing its vulnerability to hydro-meteorological hazards. Although island wide damage and risk assessments have been carried out for major flood events in Jamaica, few studies have been conducted for the creation of damage and risk maps for vulnerable areas. In this study, a risk-based tool was developed by transferring and adapting a proven methodology for flood risk assessment in Flanders, called LATIS, to areas with limited data resources. The town of Annotto Bay was chosen as case study due to its vulnerability to riverine flooding. The model uses input parameters such as flood data, land use, economic and social data to estimate the damage. The flooding of 2001, caused by tropical storm Michelle, was input for the model in order to estimate the damage. The produced map shows the spatial variation of the damage costs, which correlates with the flood depths. The total calculated damage cost from the flood of 2001 in the study area was estimated at USD 7.5 million. Although validation of the exact damage costs was not possible, the damage spread and number of affected elements were accurate. The model output also shows the potential number of people who would be killed as a result of the event, which was calculated at only 2 casualties. Since in reality no one died, this low estimate can be considered accurate. The results of this approach can be extended to other vulnerable areas of the island and of other Small Island Developing States (SIDS) having topographical and geographical similarities and being affected by similar hydro-meteorological events. Hence, the method allows damage assessment for data-poor regions, aiding in planning mitigation measures for flood prone communities.

Keywords: flooding, damage map, vulnerability map, risk methodology, LATIS, Jamaica

2.1 Introduction

In Jamaica, the third largest island of the Caribbean, floods are the combined effect of extreme precipitation from tropical storms and hurricanes, poor land use practices and the topography. In their compilation of flood events in Jamaica between 1900 and 2010, Taylor et al. (2014) show that there has been an average of 18 flood events per decade with a total of 103 flood events since 1990. The average number of floods per decade has thus almost tripled in the past century. The Planning Institute of Jamaica (PIOJ) reports that six severe hydro-meteorological events occurred in Jamaica during the period 2002-2007 which have resulted in massive floods and damages to infrastructures for a total loss of USD 1.02 billion (PIOJ, 2002, 2004, 2005a, 2005b, 2007, 2008, 2009, 2010, 2012). Hurricane Ivan in 2004 accounted for the highest damages and losses in the decade 2000-2009, amounting to 8% of the Gross Domestic Product (GDP) (Burgess et al., 2015). Flooding affects primarily the country's infrastructure sector, as the floodplains of Jamaica's major river systems, such as Hope River, Yallahs River, Outram River, Rio Minho, Rio Cobre and Rio Grande, are also the sites of Jamaica's major infrastructures and cities (Kingston, Montego Bay, Ocho Rios, Port Maria and Annotto Bay, for example) (Burgess et al., 2015; Ishemo, 2009; Mandal et al., 2013; Mandal & Maharaj, 2013; Mandal et al., 2016; Nandi et al., 2016; Taylor et al., 2014).

On the one hand, hydrological modelling to simulate runoff from extreme rainfall events was carried out for the Hope River watershed and the coastal town of Port Maria, both in Eastern Jamaica (Mandal et al., 2013; Mandal & Maharaj, 2013; Mandal et al., 2016), while on the other hand, other researchers have worked extensively on the physical damage assessments caused by hurricanes, such as Allen in 1980, Ivan in 2004, Dean and Felix in 2007 and Emily and Wilma in 2005 on the coastlines of Jamaica (Robinson & Khan, 2011). The studies involved generating beach profiles pre- and post-hurricane for selected beaches and coastlines across the island and analyzing impacts from storm surges generated by the above-mentioned events. The results showed a maximum run-up distance of 1000 m, which is the maximum distance the waves travelled onshore, reported for the hurricane Dean for Portland Cottage, a coastal community located in southern Jamaica. A run-up distance of 573 m was also observed for hurricane Ivan for Old Harbour Bay, a community in southern Jamaica (Robinson & Khan, 2011). Further work done by Robinson and Khan (2011) on the Negril, Annotto Bay and Mammee Bay coastline in Jamaica demonstrated that for the period from 1971 to 2003 the coastline of Negril showed a 16 cm retreat compared to the 7 cm shoreline retreat proposed by IPCC (2007).

Floodplain mapping and inundation modelling have been done for the major river systems in Jamaica, in order to create floodplain maps with a return period of 100 years. Furthermore, Burgess et al. (2015) developed a macro-scale flood risk model for Jamaica, based on 198 flood events occurring from 1678 to 2010. However, not much work has been done on detailed damage and risk assessments from flooding on a micro-scale level as well as on the creation of flood risk maps for the watersheds or for other vulnerable coastal towns and communities. Nonetheless, Koks et al. (2015) indicate the importance of a detailed flood risk assessment, taking into account the

specific characteristics of local communities and regions in the calculations, instead of using the same flood risk management measures for large areas. Since the climate and water characteristics are region-bound, the flood risk governance and risk reduction measures should also be best assessed on city-scale (Ward et al., 2013). Therefore, an adequate methodology to estimate location specific damage and risk from flood events needs to be developed for Jamaica, which can then be extended to other Small Island Developing States (SIDS). This will aid local governments and planners in identifying areas prone to increasing flood risk in order to take necessary precautions to minimize material costs and loss of lives due to future flooding events (Filatova, 2014).

Disaster risk management requires adequate data collection, related to costs and damages with regard to events and locations (Deckers et al., 2009). This is significantly lacking for developing countries, such as Jamaica and other SIDS, due to the absence of data related to location specific costs and damages (ODPEM, 2013b). In this case study, vector data, acquired by ODPEM (2013a), were used as a base for the generation of a new quantitative social and economic damage map. As Annotto Bay is a town with many informal settlements with little to no information available, it was important to use a quantitative approach based on all elements at risk present in the study area (ODPEM, 2013a). Furthermore, by taking into account the cost of the elements at risk and not only the probability of a disaster, the risk is calculated more adequately (Filatova, 2014). Although the methodology in this study also includes the creation of a risk map, this step could not be executed in the present study, due to a lack of flood data. However, the other steps of the methodology were implemented and two damage maps of one flood event in 2001 were created. This was the first of its kind being tested for Jamaica and can be extended to other test sites, as well as to other similar flood prone communities in the Caribbean, showing occurrences of similar hydro-meteorological events, as well as physiographic features.

2.2 Study Area

The island of Jamaica, covering an area of 10,990 km², is located in the Atlantic hurricane belt which makes it vulnerable to hurricanes and tropical systems (storms and atmospheric depressions). Annotto Bay is a small coastal town located in the parish of St Mary, in the north-eastern part of the island, made up of small shops, residential buildings and a few small factories. Since there is no well-known cultural heritage, the town does not accommodate tourists. Moreover, the town experiences economic challenges since the heavy decline of the sugar and particularly the banana industries. The elevations of the greater part of the area (Annotto Bay and surrounding communities) range from 200 m above sea level in the interior to 20 m above sea level near the coastline. However the urban area of Annotto Bay lies lower than 3 m above sea level (ODPEM, 2013a). The coastal town is located on an alluvial fan drained by the Annotto River, Wagwater River, Mother Ford Drain, Pencar River and the Crooked River as shown in Figure 9. All these rivers, except for the Mother Ford Drain, originate in the highlands. The Mother Ford Drain is a stream which has been channelized with concrete sides and floor to allow drainage of water in the town.

The majority of the buildings are wooden structures and lie in a linear strip bordering the coast and along the banks of Annotto River, Pencar River and Mother Ford Drain. Vegetation ranges from shrubs to mixed cultivation.

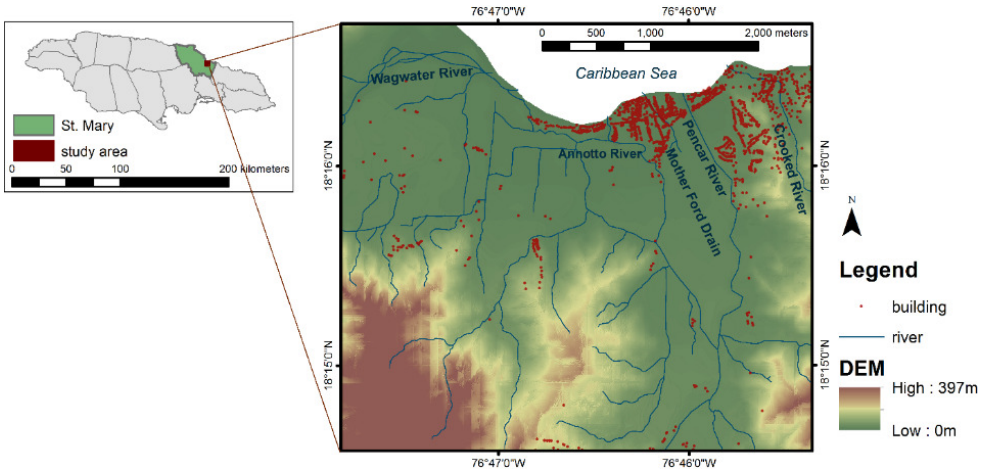


Figure 9 Situation map of Annotto Bay, St. Mary, Jamaica, with the drainage network (data source: WRA), DEM (data source: NSDMD, resolution of 6,18m), buildings and parishes (data source: ODPEM).

Annotto Bay has been affected by both riverine and coastal floods from tropical storms, hurricanes and storm surges. Aside from this, the town of Annotto Bay is home to many informal settlements, located in flood prone areas due to the lack of adequate building regulations and drainage as well as the low building costs in these areas (ODPEM, 2013a). The Community Disaster Risk Management Plan for Annotto Bay, prepared by ODPEM between 2010 and 2012, reports that most of the communities are located in areas of high susceptibility to floods due to its high drainage density and location on the low lying alluvial fan. Floods and hurricanes rank highest in the list of hazards affecting the town and its surroundings, causing damage to the roads, drains and buildings (most of which are made of wood and thus susceptible to damage). Some of the major events which have affected the town and its surroundings were hurricane Allen in 1980, which was recorded as “devastating” by ODPEM (2001), hurricane Gilbert in 1988, which caused coastal flooding and no passage of vehicular traffic for a week, heavy rainfall in October 2001, hurricanes Ivan in 2004, Emily in 2005 and Dean in 2007, and tropical storm Gustav in 2008, tropical storm Nicole in 2010, hurricane Sandy in 2012 and heavy rainfall in 2017 which all resulted in loss of lives and destruction of socio-economic goods.

Khan (2006) studied the hazard impact for Annotto Bay by using baseline data obtained by studying 40 years of coastline changes and a combination of aerial photographs, as well as GPS (Global Positioning System) based field surveys. The study involved storm surge mapping for hurricane Ivan in 2004, as well as a flood assessment from hurricane Michelle in 2001. Further studies were conducted by ODPEM with regard to preliminary flood damage assessment for Annotto Bay based on floods resulting from hurricanes

and tropical systems. Although these studies identified the extent of the hazards, a detailed in depth damage assessment was still lacking for the study area (Glas et al., 2015).

2.3 Methodology and Data

Existing flood risk assessment tools, such as LATIS, a flood risk assessment tool for Flanders, Belgium, require historical flood hazard maps, land use data and data on the costs of the potential damages. However, the study area shows certain limitations as data for only one flood event, the one of 2001, was available, and the level of detail of the available land use data was lower than the level of detail needed by these tools (Glas et al., 2015). Therefore, it was not possible to implement an existing flood risk methodology without modifications. While the general framework of the methodology used in the existing tools can remain the same, the exact calculations, input data and functions used have to differ immensely. Therefore, there was a need for an adapted methodology in this study area. The framework of this methodology is shown in Figure 10.

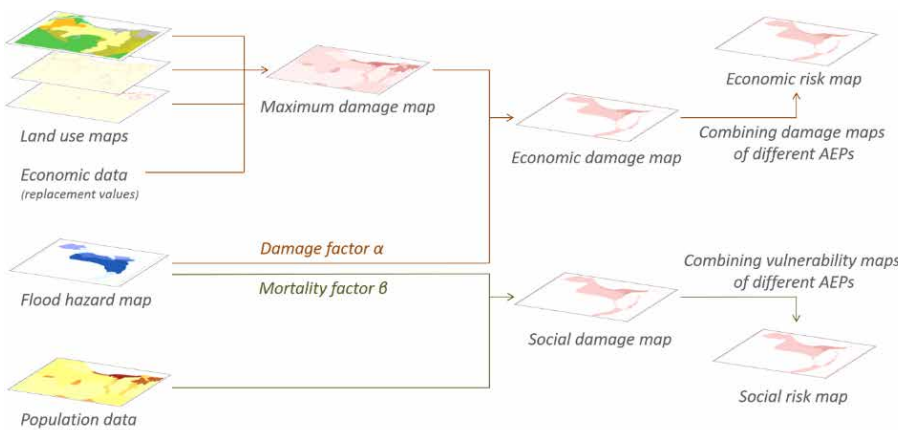


Figure 10 Risk assessment methodology flowchart used in the study of Annotto Bay, Jamaica (based on Glas et al. (2015)).

With regard to the economic damage map, only tangible damages, that have a monetary value and occur within the flood zone were taken into account. They include direct as well as indirect damages, such as production losses or clean-up costs (Deckers et al., 2009). Economic damage maps were created by combining the maximum damage map with depth-damage functions in combination with the flood extent map. To produce the maximum damage map, the replacement values, as mentioned in Figure 10, were combined with the available land use maps. Replacement values represent the total cost to replace an element at risk when it is completely destroyed. As there was no detailed information available, these replacement values were collected through average values of buildings, roads and crops for the case study of Annotto Bay. However, often flooding doesn't cause the complete destruction of an element at risk. Hence, the actual damage

cost is lower than the maximum damage cost upon total loss. Depth-damage functions represent the relationship between the water depth and the damage factor, which is a percentage of the maximum damage. This type of function is also called 'stage damage curve' and it is different for each land use category (Deckers et al., 2009; Vanneuville et al., 2002). It is crucial to use adequate depth-damage functions that are representative for the economic situation in Jamaica. The estimated damage is expressed by the following expression (Deckers et al., 2009):

$$(4) \quad D_r = \sum \alpha_i \times D_{i,max}$$

with D_r as the estimated real damage in a zone, $D_{i,max}$ as the maximum damage in a land use class i and α_i as the coefficient (damage factor) expressing the relationship between water depth and damage for land use class i . Other flood characteristics, such as flow velocity, duration and the time of occurrence are not taken into account in the standard approach to assessing economic flood damages. While there are a few individual studies on these characteristics and their impact on the damage cost, there is no uniform way in incorporating these factors in the damage calculations (Merz et al., 2010). Moreover, there is not always a clear correlation between these factors and the resulting damages. In their study, Kreibich et al. (2009) proved that the influence of flow velocity on the monetary losses to residential buildings and other infrastructure is weak or even non-existing.

Floods do not only cause material damage, but casualties as well. The social damage map is developed through a method, similar to that employed for the economic damage map, which uses population data, building density and the flood map of 2001 as input data. This social damage methodology only calculates the possible loss of life and does not take into account the number of people affected by the flood (Glas et al., 2015). Therefore, a mortality factor, based on the water levels from the flood map, was used to determine the possibility of death in a social damage map.

When flood hazard maps with different Annual Exceedance Probabilities (AEPs) are available, a risk map can be created by combining the damage maps of each AEP.

2.3.1 Input data

The damage calculations that were carried out for Annotto Bay are based on four types of input data, listed in Table 2.

Table 2 Overview of the data used in the methodology of the flood risk assessment.

DATA	TYPE	SOURCE
Land use data		
Land use	Polygon	By NLA (2001) + update based on DigitalGlobe satellite imagery (2010)
Roads	Polyline	Based on DigitalGlobe satellite imagery (2010)
Buildings	Point	By ODPEM (2013a)
Critical buildings	Point	By ODPEM (2013a)
Economic data		
Replacement values	Tables	Table 3
Flood data		
2001 flood extent	Polygon	By WRA (2001)
Depth-damage functions	Table	Table 3
Population data		
Population density	Polygon	By STATIN (2001)

The first type is the land use data, or elements at risk, which include building locations, the road network and agricultural information. Although a road dataset was available from ODPEM (2013a), the road network used in this research was extracted from satellite imagery, because the original dataset was incomplete, as many unpaved roads were not included. Even though the damage to these roads is minimal, they do provide access to buildings, making them an important visual and spatial element. The level of detail of the land use data determines after all the level of detail of the resulting economic damage map. The second type of input information is the economic data. This type comprises the replacement values for all land use. The last type of input data is the flood data. In this case, to create one economic damage map, the flood extent of the flooding caused by Tropical Storm Michelle in 2001 was used. The last input data type listed in Table 2, population data, is the main input for the social risk calculations.

The necessary information to calculate the replacement values was derived from multiple sources, listed in Table 3. Although other land use elements, such as forests, beaches, wetlands and water surfaces can be inundated as well, they are not considered to generate any economic losses and are therefore left out of the calculations. Furthermore, Table 3 shows the used depth-damage functions per element at risk.

Table 3 Sources of replacement values and depth-damage functions per damage category.

ELEMENT AT RISK	SOURCE OF REPLACEMENT VALUES	SOURCE OF DEPTH-DAMAGE FUNCTION
Building structure	By ODPEM (2011)	By Dutta et al. (2003)
Building content	By ODPEM (2011)	By Dutta et al. (2003)
Critical building	By ODPEM (2011)	By Dutta et al. (2003) (ref. buildings)
Field	By FAOSTAT (2012)	By Dutta et al. (2003)
Banana Estate	By FAOSTAT (2012)	By Jonckheere (unpublished work)
Quarry	By Vanneuville et al. (2002); MTWJ (2008); sales websites	–
Other (forest, wetland, water, beach)	–	By Dutta et al. (2003) (ref. buildings)
Road	By Collier et al. (2013)	By Vanneuville et al. (2003c)
Casualties	By ODPEM (2011); WRA (2001)	By Vanneuville et al. (2003a)

For buildings, the replacement value was calculated per building separately, depending on the material used and the number of floors. These characteristics were taken into account to determine average damage values for all types of buildings and to link a maximum damage to each building separately. No difference was made between residential and non-residential buildings. The maximum damage to buildings was divided into structural damage and content damage, where content damage is calculated as 50% of the structural damage (Cammerer et al., 2013; Davis & Skaggs, 1992; Vanneuville et al., 2003b). Critical buildings, such as hospitals, schools, churches and fire stations were also taken into account in these calculations, as the replacement values (structure and content) for these buildings were calculated precisely by ODPEM (2011).

The replacement values for crops are summarized in Table 4. The most commonly cultivated crops in Jamaica are sugar cane, citrus, melon, bean, rice, sweet potato and banana. Since there was no available parcel-level information for the different kinds of crops, an average crop value was generated for this study based on all possible crops. Yield (ton ha^{-1}) and annual producer prices ($\text{J\$ ton}^{-1}$) were assembled from the website of Food and Agriculture Organisation of the United Nations Statistics Division (FAOSTAT, 2012). Fields where crops coexist with forest were assumed not to be completely used for agriculture. Therefore, the crop value was halved for the entire sector, resulting in an estimated 50-50 ratio between forest and fields for this zone. Since the land use data did make a distinction between banana plants and other crops and the plantations take up 22% of the total study area, banana plants were treated separately. The replacement value for banana plantations was calculated in the same manner as the other crops, with data derived from FAOSTAT (2012).

Table 4 Replacement values for crops.

LAND USE CATEGORY	REPLACEMENT VALUE (USD m ⁻²)
Field	0.5547
Forest and field	0.2773
Banana plantation	0.1525

A last type of replacement value is the road infrastructure cost. The average value of a road unit in developing countries was estimated by Collier et al. (2013) at 216.30 USD m⁻¹. With an average road width of 6 m, this value was converted into 36.05 USD m⁻².

Tropical Storm Michelle induced heavy precipitation in the mountains, resulting in flash floods downstream (ODPEM, 2013a). Annotto Bay suffered from flooding up to 1.22 meters over a period of two days. A flood map, shown in Figure 11 was drawn of the maximum flood extent during these 48 hours. This map was created by measurements performed at the time of the flood. A helicopter flew over the affected area, taking photographs to determine the flood extent, linked to on site measurements of the water depth. Since this map only shows flood heights, the velocity was not taken into account in the calculations. Flood risk maps, however, should be created based on different AEPs. As only limited data on rainfall for the past extreme events were available and a rainfall-runoff model to estimate the discharges for different probabilities of exceedances was lacking, the research was restricted to the 2001 event caused by hurricane Michelle. The methodology to create the final risk map, however, was developed and is discussed here, although the map itself could not be generated due to insufficient flood data.

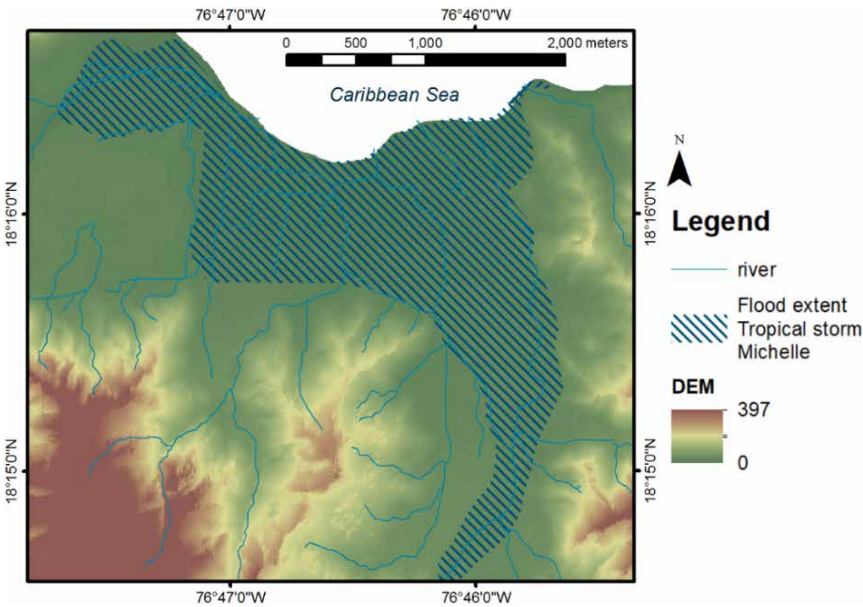


Figure 11 Measured extent of the 2001 flood caused by tropical storm Michelle (DEM source: NSDMD, resolution of 6,18 m).

2.3.2 Economic damage calculations

The economic damage assessment was carried out for the three types of damages, building, road and crop damage, separately since the input data and calculation methods for each type differ. In a final step, the total estimated economic damage is calculated by combining the damages for each of these land use categories.

2.3.2.1 Building damage

Building replacement values were calculated for each building separately. Using the point damages as such in the visualization would lead to a visual underestimation of the total damage, since the damaged points would seem very small in comparison to the entire study area. In order to generate a better visual result and facilitate the interpretation of the resulting building damage map, the building point features were aggregated per land use polygon. All replacement values of all buildings in one polygon were added up to one building replacement value per land use polygon, creating maximum damage zones.

In a second step, the maximum building damage map is combined with the flood map to create a map of the estimated building damage, corresponding to the 2001 flood event. Since most houses are somewhat elevated from ground level, the methodology adopts an average doorstep level of 0.5 m that the flood water has to overcome before a building will be inundated (Deckers et al., 2009; ODPEM, 2013a; Vanneuville et al., 2003a). Therefore, 0.5 m is deducted from the water depths for all buildings. The depth-damage functions, shown in Table 5, for building-structure and building-content originate from a model developed for Japan (Dutta et al., 2003). These functions were selected on the basis of several considerations and, in particular, (i) the structure of buildings in Japan is similar to that of Jamaican buildings, as most Japanese and Jamaican buildings are constructed with solid concrete or wooden walls and no insulating material, (ii) there is a distinction between wooden and concrete buildings, a distinction that has also been made in the database for buildings in Annotto Bay, (iii) damage factors are expressed in percentages instead of absolute values, as it is the case for many other studies; this is essential to implement the methodology in this case study as well as in other areas. The depth-damage functions were as part of a flood loss estimation model that combines a physically based distributed hydrologic model and a distributed flood loss estimation model. The depth-damage functions designed in this study are based on damage data from past floods, gathered by the Japanese Ministry of Construction since 1954 (Dutta et al., 2003).

Table 5 Flood damage factors (%) for wooden and concrete structures and their content, based on Dutta et al. (2003).

WATER DEPTH (meters)	WOODEN STRUCTURES	CONCRETE STRUCTURES	CONTENT
0.00	0	0	0
0.30	0	0	0
0.61	6	6	2
0.91	12	12	10
1.22	20	20	19
1.52	23	26	25
1.83	30	30	32
2.13	36	36	39
2.44	40	40	43
2.74	43	43	45

Since a maximum building damage value was calculated per damage zone, the two depth-damage functions for wooden and concrete structures cannot be used separately; therefore, an average value of the two functions was used. The value of the estimated damage to structures and content with the respective damage factors are defined as direct damage. In addition to direct damage, indirect damage, which involves for example clean-up costs, was also calculated for buildings. This value is expressed as a percentage of the direct damage, varying from 1% to 15%, dependent on the damage degree of the structure (Vanneuville et al., 2002). When the flood level is relatively low, but the water has entered the building, the total damage will be low as well, but the indirect clean-up costs will be substantial compared to the overall damage. However, when the damages are higher, due to high flood levels, the clean-up cost will not increase at the same rate. Therefore, the indirect damage percentage is calculated using following empirical equation:

$$(5) \text{ Indirect damage (\%)} = 1 + \left(1 - \frac{2 * \alpha_{stru} + \alpha_{con}}{3}\right) \times (15 - 1)$$

With α_{stru} as the damage factor for structure and α_{con} as the damage factor for content. The total estimated damage to buildings is the sum of direct damage and indirect damage.

Every building must be accessible from a road. This assumption was applied in this assessment by creating two buffers around the road network, at 25 meters and at 60 meters. Samples in the study area showed that 90 percent of all buildings are located in the 25 meters buffer zone and 99 percent in the 60 meters buffer zone. These buffers are added to the calculations as extra polygons. Since the resulting damage maps show the damage per m², large polygons will cause the damage to be spread evenly over a large surface and visually seem low. The extra polygons, that contain the largest part of the buildings, and thus the largest building damages, will aid in a better allocation of the damage, as this same damage will be spread over a smaller polygon. The visual result of this adaptation is illustrated in Figure 12.

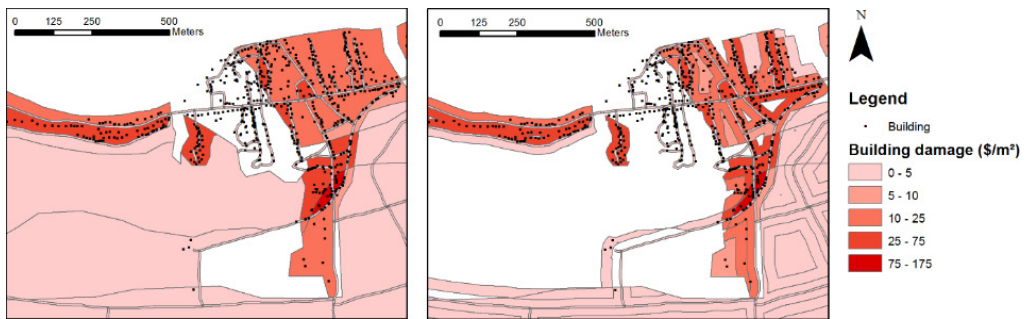


Figure 12 Visual comparison between building damage calculations without buffers (left) and with buffers (right).

The spatial distribution of building damage is more accurate and high risk areas are distinctly indicated, but there is no difference in the total damage cost calculations. Especially large land use polygons without any damage except building damage, for example in the wetland area, benefit immensely from these buffers.

2.3.2.2 Crop damage

The depth-damage functions for crops in Table 6 originate from the Japanese model developed by Dutta et al. (2003) as well. In this model, there is a detailed distinction between types of crops, similar to the ones that are most cultivated in Jamaica. In contrary to the depth-damage functions for buildings by Dutta et al. (2003) that only take water depth into consideration, the depth-damage functions for crops take into account both water depth and flood duration. In this case, the flood lasted for two days (ODPEM, 2013a). Since the exact crops cultivated in Annotto Bay are unknown, an average damage factor was calculated based on the damage values as described by Dutta et al. (2003). Indirect damage, which primarily involves production losses, was set at 10% of the direct damage (Vanneuville et al., 2002). These two values are summed up to obtain the total estimated damage for crops.

Table 6 Flood damage factors for crops for a two-day flood, based on Dutta et al. (2003).

WATER DEPTH (meters)	BEANS	CHINESE CABBAGE	DRY CROPS	MELON
0.00	0	0	0	0
0.30	30	58	30	30
0.61	30	58	30	30
0.91	40	66	43	39
WATER DEPTH (meters)	PADDY	VEGETABLE WITH ROOT	SWEET POTATO	GREEN LEAVE VEGETABLES
0.00	0	0	0	0
0.30	24	43	26	24
0.61	24	43	26	24
0.91	38	74	40	44

An adequate depth-damage function for banana plants was not found in literature. Therefore, a new function, based on the characteristics of the banana plant, was drafted. These plants can only survive water saturation conditions up to 48 hours because of the fragile roots (Rajamannan, 2004). Consequently, the depth-damage function is a linear function that reaches 100% damage after 48 hours of inundation. The water depth was not taken into account as this parameter was not important. The indirect damage is 10% of the direct damage.

2.3.2.3 Road damage

A road dataset of the area was available for this research, giving a class and corresponding width to each road (ODPEM, 2013a). Although this information allowed a more precise damage calculation, a comparison with satellite imagery showed big disparities between the available dataset and the reality. Many unpaved roads were missing and the simplification of the data, due to its larger scale, caused the location of other roads to differ from reality. Additionally, damage to roads showed to be significantly smaller than building damage. Therefore, the priority was given to adding all unpaved roads, losing the class information, in order to enhance the accuracy of the building damage spread.

Most roads and bridges in Jamaica are not elevated. Consequently, they suffer considerable damage during a flood. The depth-damage function for roads is the same as in LATIS because roads are constructed in the same manner in both regions and will thus suffer the same proportion of damage. The damage factor for roads is expressed by the following function (Vanneuville et al., 2003c):

$$(6) \quad f = \min(0.28 \times d; 0.18 \times d + 0.1; 1)$$

where d represents the water depth in meters.

2.3.3 Social damage calculations

The methodology used to calculate the number of people killed is very similar to the one used to calculate the economic damage. Small statistical sectors were drawn based on similar characteristics such as building density and land use; inhabitants were assumed to be spread homogeneously across the number of houses. As such, the number of inhabitants per sector was calculated based on the number of houses per statistical sector (ODPEM, 2011) and the number of people per household in 2001, which was an average of 3 for St. Mary (WRA, 2002). The spread of the inhabitants per statistical sector based on the number of houses per sector was statistically tested and has proven to be significant with a significance level of 5%. The number of casualties is expressed by Equation (2) from Chapter 1 (Vrisou van Eck et al., 1999). Since there was no available rise velocity information for the flood event of 2001, the drown factor based on the rise velocity was set at 100%, which corresponds to a rise velocity higher than 3 m per hour. This is the safest presumption, but could lead to an overestimation of the number of casualties.

The drown factor based on flood depth is expressed by the following equation:

$$(7) \quad f_d = \exp(1.16 \times d - 7.3)$$

where d represents the water depth in meters (Vrisou van Eck et al., 1999). People are assumed to be inside their homes during the flood. Therefore, the doorstep level of 0.5 m has to be overcome before the house is considered as inundated (Deckers et al., 2009; ODPEM, 2013a; Vanneuville et al., 2003a).

2.3.4 Risk calculations

For the case study of Annotto Bay, a social and an economic damage map were created based on a flood map of 2001 and not on a flood hazard map with a certain AEP. Therefore, the corresponding flood risk maps could not be created in this study. In the future, however, a rainfall-runoff model could be created for the study area and flood hazard maps with AEPs could be generated. For each flood hazard map with a specific AEP, a damage map can be created using the same methodology, visualized in Figure 10. All damage maps can then be combined in order to generate one flood risk map, showing the risk of damage per year. The risk can be calculated by using the following equation (Deckers et al., 2009):

$$(8) \quad R = \sum_{i=1} \frac{1}{i} (D_i - D_{i-1})$$

with R as the risk, D_i as the damages related to a flood with an AEP of i .

Since the creation and validation of flood hazard maps with AEPs is time-consuming, in practice only a few would be created. The flood damage between two AEPs will be linearly interpolated in order to simplify the equation (Vanneuville et al., 2003a). This simplification is done based on the choice of AEPs after the creation of the rainfall-runoff models.

2.4 Results

2.4.1 Economic damage map

Before generating the final economic damage map for Annotto Bay, the three types of damage are visualized separately in Figure 13. The cost of each type of damage and the damaged area is given in Table 7. It is immediately clear that the building damage cost is substantially higher than the cost of the other two types, while the crop damage has the largest spread. The total damaged area is not equal to the sum of the areas per damage type, as some polygons contain more than one type. For example, rural areas with housing will have building damage as well as crop damage.

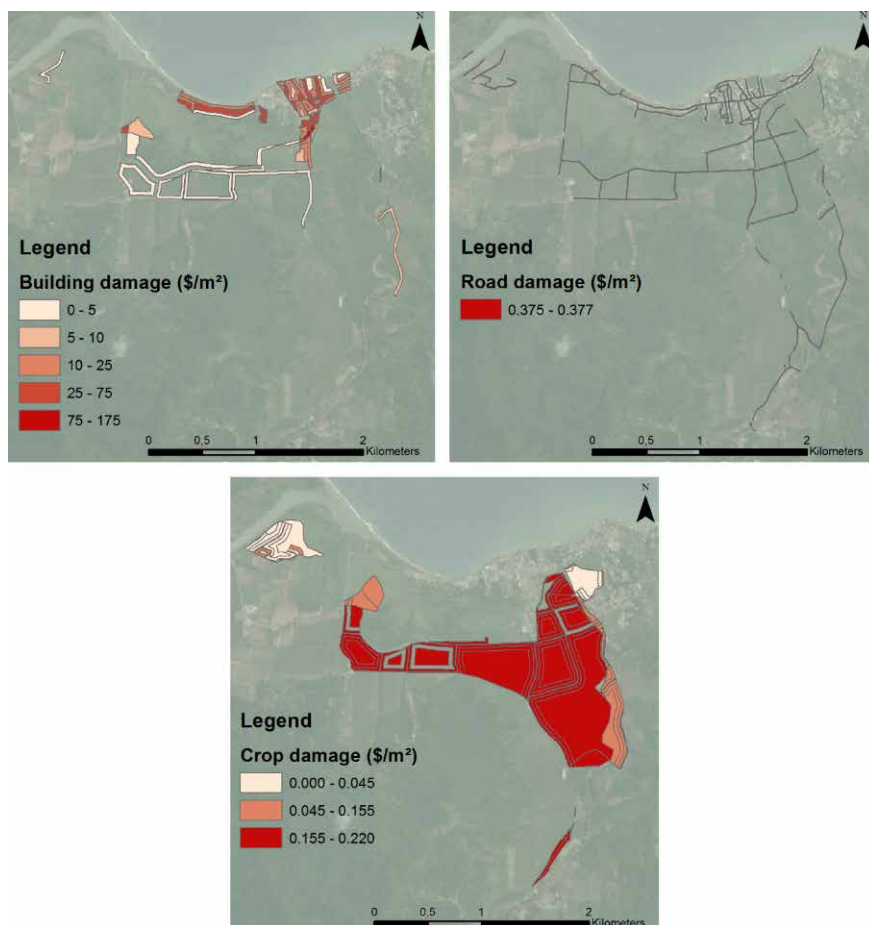


Figure 13 Economic damage maps for the 2001 flood in Annotto Bay, Jamaica, per damage type (top left: building damage, to right: road damage, bottom: crop damage).

Table 7 Overview of the damage cost and damaged area per damage type.

	DAMAGE COST (USD)	DAMAGED AREA (m ²)
Building damage	7 080 000	520 000
Road damage	50 000	140 000
Crop damage	370 000	2 050 000
TOTAL DAMAGE	7 500 000	2 460 000

As a result of the use of the two buffers for building locations, the total damaged building area is limited. Without buffers, the damaged area for buildings would be 1 860 000 m². However, when only looking at the average building area of the houses that were damaged, the building area of the damaged houses is only 130 000 m². Hence, the buffers still cause an overestimation of the damaged building area, but the result is much closer to the reality.

In a next step, the final economic damage map was generated, by adding up the three separate damage types. This map is shown in Figure 14. Due to the high damage values of buildings, the distinction in crop damage has disappeared. However, it is clear the high risk areas are located in the low-lying urban areas and along the main road, parallel to the coastline. The wetlands do not have any damage, except for the buffers along the roads, since a few houses are located there.

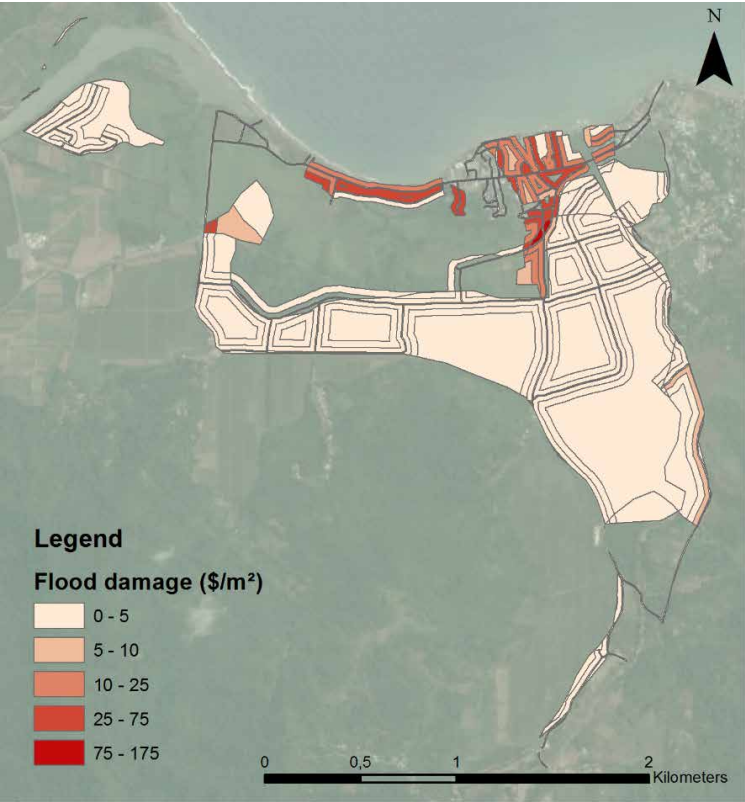


Figure 14 Economic damage map for the 2001 flood in Annotto Bay.

With a maximum damage cost of 175 USD m⁻², this flooding has not completely destroyed any houses, due to the low flow velocity of the water (< 3 m s⁻¹) (ODPEM, 2013a). Considering that the replacement value of buildings is on average 836 USD m⁻², the estimated damage is almost five times lower than the value for complete destruction.

2.4.2 Social damage map

The number of calculated casualties per km² is displayed in Figure 15. The number is considerably higher in the built-up area, because of the higher population density in this area. In Table 8, an overview is given of the absolute and relative estimated numbers. The total number of people killed during the flood is extremely low, almost zero.

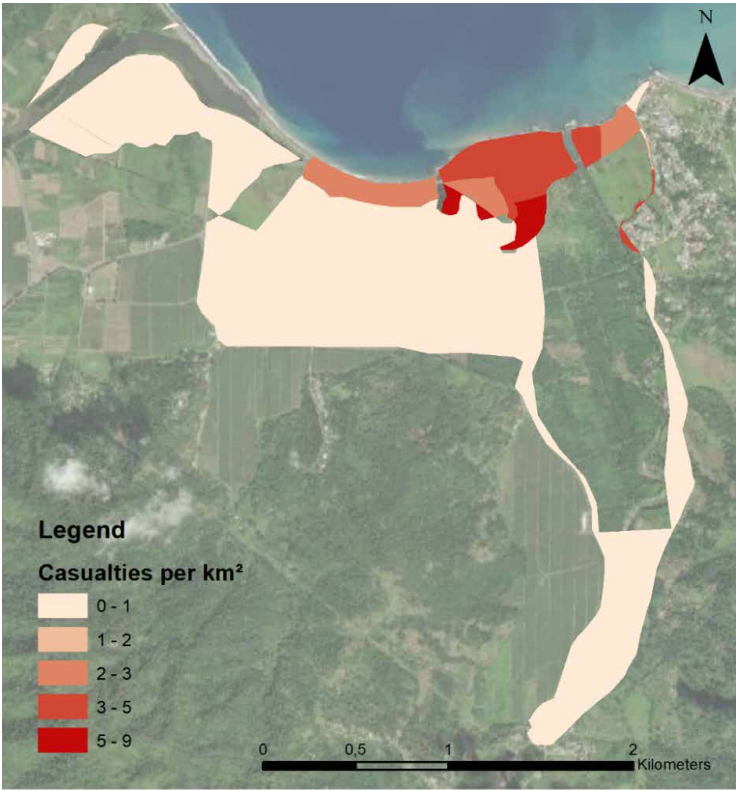


Figure 15 Social damage maps for Annotto Bay, Jamaica.

Table 8 Overview of the estimated number of casualties for Annotto Bay, Jamaica.

	ESTIMATED VALUES
Total number of casualties	1.74
Average number of casualties per km ²	0.03
Maximum number of casualties per km ²	0.34

2.5 Discussion

Although several cost and damage assessments have been done for the entire island, a damage assessment based on flood levels and replacement values was not yet developed. Hence, this research serves as a test case to extend this risk-based methodology to other areas of the island and helps in a better understanding of flood risk and its spatial extent, as well as the impact on infrastructures in Jamaica.

The main goal was to visualize the high risk areas and give an adequate estimation of the damage cost and damage location. Therefore, the preference was given to

a road dataset based on satellite imagery, rather than using the available road data with classes. This new dataset has lend the opportunity to add buffers that localize the buildings more precisely. Given that the building damage cost is the biggest share in the overall cost, this approach offers a better visual result. The buffers around the road network can help to better allocate building damage, even in study areas where the land use data are less detailed.

Verifying and validating the results and the accuracy of the methodology is not a sinecure. There is not much information available on the exact damage costs caused by the 2001 flood. The only available source that describes the damage of the event is a report by ODPEM (2013a). In this report, some general numbers for building, crop and road damages caused by tropical storm Michelle, are listed. These numbers are compared with the results of this study per damage type.

Exact building damage values were not available for the historic flood. However, the ODPEM report concerning the 2001 flood states that 749 of the 1632 buildings, included in the report, were exposed to inundations at that time (ODPEM, 2013a). Since the borders of the study area in this study are not identical to the borders in the ODPEM report, the number of houses taken into account in this study is 1415, of which 799 were assessed as affected by the flood. The number of exposed buildings is slightly higher, due to the fact that rural buildings were also assessed in this study, as opposed to the ODPEM report where the buildings in rural areas were not taken into account, leading to an addition of 41 affected buildings.

When looking at road damage, the ODPEM report states that 3.5 km of the main roads were damaged during the 2001 flood (ODPEM, 2013a). This number is impossible to compare with the results of the road damage assessment, since the road dataset that was used does not make a distinction between main roads, secondary roads and unpaved roads. According to the flood tool, 22.7 km of roads were affected by the inundations. Since the total road damage cost is a very small share of the total damage cost, the accuracy of this result and the importance of these calculations can be questioned, but roads do give access to buildings and serve as evacuation routes during disasters. One could argue that the road damage cost can be neglected in urban areas, where building damage takes up a much larger part of the total damage. In rural areas, however, the road damage cost could be within a larger order of magnitude. Hence, further research should focus on the importance of the road damage calculations in these rural areas to determine if future flood damage analysis should only take into account the accessibility of roads, rather than the accurate damage cost.

In total, 74 ha cultivated land was inundated during tropical storm Michelle in 2001 (ODPEM, 2013a). The banana plantations were damaged the worst; in fact 11 ha of the total area were completely destroyed. In this study, through the methodology, a total area of banana plantations, affected by floods, was calculated to be equal to 161 ha and the area of other affected crops was equal to 44 ha. This apparent overestimation is due to the simplification of the depth-damage function of banana plants and not taking into account the period of the year and the cultivation cycle. As bananas are harvested at the end of summer, after which the plants are cut at the soil line, and new plants are

planted again in spring, it is very likely that there were not much plants on the fields at the time of the flooding (Stover & Simmonds, 1987). Furthermore, this study did not make a distinction between plants that were affected and plants that were destroyed. Wind was an additional factor that also caused a lot of damage to all crops (ODPEM, 2013a) and could not be taken into account in this study. Furthermore, due to the very small part of crop damage cost in the total damage value, it is impossible to assess the accuracy of the crop damage calculations in this urban study area.

The coastal location of Annotto Bay and its vulnerability lead to a high flood risk. The squatted communities with informal houses raise the biggest concern, as these buildings occupy 35% of all those present in the town center (ODPEM, 2013a). Moreover, some are located at the watermark, as a consequence of the coastal erosion which equals 4 m in 7 years. It can also be stated that the roads had a significant impact on the flood extent in 2001. The construction of the highway without drainage structures in 2000 hindered infiltration and has caused more severe floods. Furthermore, as roads become impassable when flooded, possible evacuation is hindered (ODPEM, 2013a).

Casualties are expressed in human lives, not in monetary value. Hence, the result could not be added to the economic damage map and a separate social damage map, showing the possible casualties, was generated. According to ODPEM (2013a), 2740 of the 5422 inhabitants of Annotto Bay were exposed to the flood of 2001. In this study, 2693 of the 4811 inhabitants were taken into account. However, the social damage map shows only the possible casualties, which were calculated at only 1.7 people for the entire study area. This low number is still an overestimation, as in reality, no one died as a result of the event, and can be explained by the fact that people flee in case of flooding and relocate to nearby shelters to stay safe, while the methodology presumes that all inhabitants stay in their houses.

2.6 Conclusions

Although several mitigation measures, such as early warning systems, dikes and drainage structures have already been taken in Annotto Bay (ODPEM, 2013a), these measures would be more effective if they were based on an adequate risk assessment methodology, as presented in this study. The methodology assists decision makers in identifying the high risk areas in need of mitigation measurements to reduce damages and decrease the flood risk of the region. The flood water can, for example, be led to areas with little to no risk, using these areas as water storage without increasing the potential damages. Other mitigation measures are building codes for areas at risk, for example elevated structures, or even permanent relocation.

The cost of building damage in the ODPEM study is limited to the damage to critical buildings (ODPEM, 2013a). In this study, this damage is complemented with the damage to all buildings, by using GPS input data, average replacement values and representative depth-damage functions (Dutta et al., 2003). This has improved the accuracy of the damage estimations.

The depth-damage functions for buildings and crops need to be tested thoroughly for different regions in the SIDS and adequate average replacement values need to be calculated. Further steps in the research will include collecting more economic, social and land use data of categories which are not taken into account in the current model. More rural areas will provide the opportunity to test the crop damage calculations while information on different flood events will provide the option to re-evaluate the depth-damage functions.

This methodology provides the possibility of performing a risk assessment in data-poor regions with a high vulnerability to flood hazards on micro-scale level, helping local communities in better allocation of their funds. Although this study is only a first step in creating an accurate quantitative flood risk assessment for all SIDS, the first results are promising. Informal settlements, located close to the shoreline or next to a wetland, are indicated by the model to be prone to damage. This corresponds to the reality, where these buildings experience more damage of flooding and their inhabitants are more vulnerable. Due to the coastal location of Annotto Bay and the presence of the Annotto River and the Pencar River, the town is highly vulnerable to flooding and it can be concluded that this is correctly indicated in this study.

ACKNOWLEDGMENTS

The authors acknowledge the Water Resources Authority, the Meteorological Service of Jamaica, the Office of Disaster Preparedness and Emergency Management, Jamaica and National Spatial Data Management Division, Jamaica for the data provided.

REFERENCES

- Burgess, C. P., Taylor, M. A., Stephenson, T., Mandal, A., & Powell, L. (2015). A macro-scale flood risk model for Jamaica with impact of climate variability. *Natural Hazards*, 78(1), 231-256. doi: 10.1007/s11069-015-1712-z
- Cammerer, H., Thieken, A. H., & Lammel, J. (2013). Adaptability and transferability of flood loss functions in residential areas. *Natural Hazards and Earth System Sciences*, 13(11), 3063. doi: 10.5194/nhess-13-3063-2013
- Collier, P., Kirchberger, M., & Söderbom, M. (2013). The cost of road infrastructure in developing countries. *Centre for the Study of African Economies*. Retrieved from: http://www.soderbom.net/13_05_02_Unit%20cost%20paper.pdf
- Davis, S. A., & Skaggs, L. L. (1992). *Catalog of residential depth-damage functions used by the army corps of engineers in flood damage estimation*. Retrieved from <https://apps.dtic.mil/dtic/tr/fulltext/u2/a255462.pdf>
- Deckers, P., Kellens, W., Reyns, J., Vanneuville, W., & De Maeyer, P. (2009). A GIS for flood risk management in Flanders. In P.S. Showalter, L. Yongmei (Ed.), *Geospatial techniques in urban hazard and disaster analysis* (pp. 51-69): Dordrecht, Springer.
- Dutta, D., Herath, S., & Musiake, K. (2003). A mathematical model for flood loss estimation. *Journal of hydrology*, 277(1-2), 24-49. doi: 10.1016/S0022-1694(03)00084-2
- FAOSTAT (2012). *Crops*. Retrieved from: <http://faostat3.fao.org/download/Q/QC/E>

- Filatova, T. (2014). Market-based instruments for flood risk management: a review of theory, practice and perspectives for climate adaptation policy. *Environmental science & policy*, 37, 227-242. doi: 10.1016/j.envsci.2013.09.005
- Glas, H., Jonckheere, M., De Maeyer, P., & Deruyter, G. (2015). A GIS-based flood risk tool for Jamaica: the first step towards a multi-hazard risk assessment in the Caribbean. *International multidisciplinary scientific GeoConference SGEM*, 15(2.2), 643-650. doi: 10.5593/SGEM2015/B22/S11.080
- IPCC (2007). *Climate Change 2007: Synthesis Report. Contributions of Working Groups I, II and III to the Fourth Assessment Report of the Intergovernmental Panel on Climate Change [Core Writing Team; R.K. Pachauri and L.A. Meyers (eds.)]*. Geneva, Switzerland: <https://www.ipcc.ch/report/ar4/syr/>
- Ishemo, A. (2009). Vulnerability of coastal urban settlements in Jamaica. *Management of Environmental Quality: An International Journal*, 20(4), 451-459. doi: 10.1108/14777830910963771
- Khan, S. (2006). Impact of storms on coastal communities: Annotto Bay, Jamaica. *Real Risk*, 63-64. Tudor Rose.
- Koks, E. E., Jongman, B., Husby, T. G., & Botzen, W. J. (2015). Combining hazard, exposure and social vulnerability to provide lessons for flood risk management. *Environmental science & policy*, 47, 42-52. doi: 10.1016/j.envsci.2014.10.013
- Kreibich, H., Piroth, K., Seifert, I., Maiwald, H., Kunert, U., Schwarz, J., ... Thieken, A. (2009). Is flow velocity a significant parameter in flood damage modelling? *Natural Hazards and Earth System Sciences*, 9(5), 1679-1692. doi: 10.5194/nhess-9-1679-2009
- Mandal, A., Barrett, L., & Smith, D. (2013). *Hydrological modelling for simulation of flooding from extreme events in Jamaica: case study of the Hope River Watershed*. Paper presented at the International Conference on Flood Resilience: Experiences in Asia and Europe, University of Exeter, UK.
- Mandal, A., & Maharaj, A. (2013). Flooding in Jamaica with assessment of riverine inundation of Port Maria, St Mary. *Bulletin de la Société Géologique de France*, 184(1-2), 165-170. doi: 10.2113/gssgfbull.184.1-2.165
- Mandal, A., Stephenson, T. S., Brown, A. A., Campbell, J. D., Taylor, M. A., & Lumsden, T. L. (2016). Rainfall-runoff simulations using the CARIWIG Simple Model for Advection of Storms and Hurricanes and HEC-HMS: Implications of Hurricane Ivan over the Jamaica Hope River watershed. *Natural Hazards*, 83(3), 1635-1659. doi: 10.1007/s11069-016-2380-3
- Merz, B., Kreibich, H., Schwarze, R., & Thieken, A. (2010). Assessment of economic flood damage. *Nat. Hazards Earth Syst. Sci.*, 10(8), 1697-1724. doi: 10.5194/nhess-10-1697-2010
- MTWJ (2008). *Annual Transport Statistics Report: Jamaica in Figures 2005-2006*. Kingston, Jamaica: <https://www.mtw.gov.jm/images/Reports/TransportStatistics-Report2005-2006.pdf>
- Nandi, A., Mandal, A., Wilson, M., & Smith, D. (2016). Flood hazard mapping in Jamaica using principal component analysis and logistic regression. *Environmental Earth Sciences*, 75(6), 465. doi: 10.1007/s12665-016-5323-0
- NLA (2001). *Land use data of Jamaica*.
- ODPEM (2001). *Damage Assessment Report*. Kingston, Jamaica: https://www.odpem.org.jm/wp-content/uploads/2019/08/National_Damage_Assessment_Plan_for_Jamaica.pdf

- ODPEM (2011). *Building Inventory*.
- ODPEM (2013a). *Multi Hazard Risk Assessment Annotto Bay, St Mary*. Kingston, Jamaica: <https://www.mona.uwi.edu/cardin/annotto-bay-multi-hazard-risk-assessment>
- ODPEM (2013b). *National progress report on the implementation of the Hyogo Framework for Action (2011-2013)*. <https://www.preventionweb.net/english/hyogo/national/reports/v.php?id=33409&pid:183>
- PIOJ (2002). *Jamaica: Macro-socio-economic Assessment of Damage done by the Flood Rains and Landslides May 2002*. Kingston, Jamaica: http://pioj.gov.jm/Portals/o/Sustainable_Development/MAY%202002%20Flood%20Rains.pdf
- PIOJ (2004). *Jamaica: Macro-socio-economic and Environmental Assessment of the Damage done by Hurricane Ivan Sept 10-12, 2004*. Kingston, Jamaica: http://pioj.gov.jm/Portals/o/Sustainable_Development/Hurricane%20Ivan.pdf
- PIOJ (2005a). *Assessment of the Socio-economic and Environmental Impact of Hurricane Wilma on Jamaica*. Kingston, Jamaica: http://pioj.gov.jm/Portals/o/Sustainable_Development/Hurricane%20Wilma.pdf
- PIOJ (2005b). *Assessment of the Socio-economic and Environmental Impact of Hurricanes Dennis and Emily on Jamaica*. Kingston, Jamaica: http://pioj.gov.jm/Portals/o/Sustainable_Development/Dennis%20Emily%20Report.pdf
- PIOJ (2007). *Assessment of the Socio-economic and Environmental Impact of Hurricane Dean on Jamaica*. Kingston, Jamaica: http://pioj.gov.jm/Portals/o/Sustainable_Development/Hurricane%20Dean.pdf
- PIOJ (2008). *Assessment of the Socio-economic and Environmental Impact of Tropical Storm Gustav on Jamaica*. Kingston, Jamaica: http://pioj.gov.jm/Portals/o/Sustainable_Development/Tropical%20Storm%20Gustav.pdf
- PIOJ (2009). *Vision 2030 Jamaica – National Development Plan*. Kingston, Jamaica: <http://www.vision2030.gov.jm/>
- PIOJ (2010). *Jamaica Macro Socio-economic and Environmental Assessment of the Damage and Loss caused by Tropical Depression No. 16/Tropical Storm Nicole*. Kingston, Jamaica: http://pioj.gov.jm/Portals/o/Sustainable_Development/Tropical%20Storm%20Nicole_Impact%20Assessment_Final.pdf
- PIOJ (2012). *Jamaica Macro Socio-economic and Environmental Assessment of the Damage and Loss caused by Hurricane Sandy*. Kingston, Jamaica: <http://pioj.gov.jm/ResearchandData/tabid/82/Default.aspx>
- Rajamannan, A. H. (2004). Flood Protection for banana and plantain plants. Retrieved from: <https://patentimages.storage.googleapis.com/ad/01/c2/0e544a282959f6/US20040242418A1.pdf>
- Read, L.K., & Vogel, R.M. (2015). Reliability, return periods, and risk under nonstationary. *Water Resources Research*, 51(8), 6381-6398. doi: 10.1002/2015WR017089
- Robinson, E., & Khan, S. (2011). *Physical impacts by some recent hurricanes on the coast of Jamaica*. Marine Geology Unit, UWI. <http://45.33.1.181:88/cgi-bin/koha/opac-detail.pl?biblionumber=7202>
- Salvadori, G., Durante, F., De Michele, C., Bernardi, M., & Petrella, L. (2016). A multivariate copula-based framework for dealing with hazard scenarios and failure probabilities. *Water Resources Research*, 52(5), 3701-3721. doi: 10.1002/2015WR017225
- Serinaldi, F. (2015). Dismissing return periods! *Stochastic environmental research and risk assessment*, 29(4), 1179-1189. doi: 10.1007/s00477-014-0916-1

- STATIN (2001). *Census of Population and Housing Jamaica*. Retrieved from <https://statinja.gov.jm/Popcensus.aspx>
- Stover, R. H., & Simmonds, N. W. (1987). *Bananas*, Longman Scientific & Technical.
- Taylor, M. A., Mandal, A., Burgess, C., & Stephenson, T. (2014). Flooding in Jamaica: Causes and Controls. In D. Dave (Ed.), *Flooding and Climate Change: Sectorial Impacts and Adaptation Strategies for the Caribbean Region* (pp. 163-187). New York: Nova Science Publishers Inc.
- Vanneuville, W., De Maeyer, P., Maeghe, K., & Mostaert, F. (2003a). Model the effects of a flood in the Dender catchment based on a risk methodology. *Bulletin of the Society of Cartography*, 37(2), 59-64.
- Vanneuville, W., Maeghe, K., De Maeyer, P., & Mostaert, F. (2003b). Risicobenadering bij waterbeheersingsplannen, Methodologie en case study Denderbekken, aanvulling 1: Slachtoffers. Ghent, Belgium: <http://documentatiecentrum.watlab.be/owa/imis.php?module=ref&refid=141991>
- Vanneuville, W., Maeghe, K., De Maeyer, P., & Mostaert, F. (2003c). Risicobenadering bij waterbeheersingsplannen, Methodologie en case study Denderbekken, aanvulling 2: Lijninfrastructuur. Ghent, Belgium: <http://www.marinespecies.org/imis.php?module=ref&refid=141993&basketaction=add>
- Vanneuville, W., Maeghe, K., De Maeyer, P., Mostaert, F., & Bogaert, P. (2002). Risicobenadering bij waterbeheersingsplannen, Methodologie en case study Denderbekken, basisrapport. Ghent, Belgium: <http://www.compendiumkustenzee.be/en/imis-mog?module=ref&refid=141990>
- Vrisou van Eck, N., Kok, M., & Vrouwenvelder, A. (1999). Standaardmethode Schade en Slachtoffers als gevolg van overstromingen, deel 2: Achtergronden. *HKV Lijn in water, TNO, Dienst Weg en Waterbouw*. https://puc.overheid.nl/rijkswaterstaat/doc/PUC_20427_31/
- Ward, P. J., Pauw, W., Van Buuren, M., & Marfai, M. A. (2013). Governance of flood risk management in a time of climate change: the cases of Jakarta and Rotterdam. *Environmental Politics*, 22(3), 518-536. doi: 10.1080/09644016.2012.683155
- WRA (2001). 2001 flood extent.
- WRA (2002). Rapid Impact Assessment of Communities in Portland and St. Mary Affected by the October and November 2001 Flood Rains. Kingston, Jamaica, WRA.

3

ANALYZING THE SENSITIVITY OF THE FLOOD RISK ASSESSMENT MODEL TOWARDS ITS INPUT DATA

This chapter is adapted from the following journal article:

Glas H., Deruyter G., De Maeyer P., Mandal A., James-Williamson S. (2016).
Analyzing the sensitivity of a flood risk assessment model towards its input data,
Natural Hazards and Earth System Sciences, 16(12), 2529-2542. doi: 10.5194/
nhess-16-2529-2016

ABSTRACT

The Small Island Developing States (SIDS) are characterized by an unstable economy and low-lying, densely populated cities, resulting in a high vulnerability to natural hazards. Flooding affects more people than any other hazard. To limit the consequences of these hazards, adequate risk assessments are indispensable. Satisfactory input data for these assessments are hard to acquire, especially in developing countries. Therefore, in this study, a methodology was developed and evaluated to test the sensitivity of a flood risk assessment model towards its input data in order to determine a minimum set of indispensable data. In a first step, a benchmark economic damage map was created for the case study of Annotto Bay, Jamaica, based on the flood extent map of the 2001 inundations caused by Tropical Storm Michelle. Three damages were taken into account: building, road and crop damage. Eleven other scenarios were generated, each with a different combination of input data, testing one of the three damage calculations for its sensitivity. One main conclusion was that population density, in combination with an average number of people per household, is a good parameter in determining the building damage when exact building locations are unknown. Furthermore, the importance of roads for an accurate visual result was demonstrated.

Keywords: flooding, risk assessment, damage map, sensitivity analysis, SIDS

3.1 Introduction

While, in many developed countries, a risk-based flood tool has already been developed (Apel et al., 2009; Kok et al., 2005; Tate et al., 2015; Vanneuville et al., 2005), the use of such risk assessment models has been limited, due to questions about the uncertainty and reliability of the results (Merz et al., 2010). Since these methodologies are built on input data that each have their own accuracy and uncertainty, the output of the methodology has an uncertainty that is very difficult to quantify (Yu et al., 2013). Furthermore, an increase of the input data accuracy doesn't automatically imply a decrease of the output's uncertainty (Apel et al., 2009).

In developing countries, the limited data availability forces researchers to find other types of input data for flood damage and risk assessments. Kumar and Acharya (2016), for example, have performed a flood risk assessment in Kashmir Valley, India, using satellite imagery as input. Kwak et al. (2015) created a rice crop damage map for the Cambodian floodplain using satellite imagery combined with a DEM and land use data. Other studies have attempted to provide adequate damage and risk results by using vector data, for example the risk assessment for Annotto Bay, performed by ODPEM (2013b).

Since the necessary input data are hard to find in developing countries, a thorough assessment of the data needed should be done. What are the minimum data requirements to build a reliable model? What is the sensibility of the model to the different datasets? These are the questions that need to be answered whilst keeping in mind that a certain degree of uncertainty is inherent to the methodology.

This paper investigates the different types of data used in a flood risk assessment for Annotto Bay, Jamaica, and their influence on the overall result by performing a sensitivity analysis on the risk assessment model with different combinations of input data. The output of every combination is tested on its accuracy based on the estimated total material loss and affected area and the geographic positions of high- and low-risk areas, compared to the benchmark output that uses all available data.

3.1.1 Sensitivity analysis

Data and methodology uncertainties are inherent to every risk assessment model (Carrington & Bolger, 1998). Since they can influence decision-making, these uncertainties have been quantified in several previous studies (Apel et al., 2008; Apel et al., 2004; Weichel et al., 2007; Yu et al., 2013). More and more exact data does not always translate in a decrease of the uncertainty, since the influence on the final result differs for each input data set (Apel et al., 2008).

In many Small Island Developing States (SIDS), geographic and statistical data availability is a major issue. Moreover, the data available has a questionable accuracy (Glas et al., 2015). Therefore, it is important to define the importance and influence of

every input dataset. With a sensitivity analysis, the influence of all input data on the overall result and its degree of detail is determined. When the sensitivity of a model towards its input is known, the minimum required data and the level of detail in order to get a result with an acceptable level of accuracy, can be deduced. Although uncertainty analyses are frequently performed in the literature, sensitivity analyses to determine the necessity of the input data are rare. Nonetheless, this information is useful in setting up an uncertainty analysis. The impact of an input dataset on the final result can serve as an indication of the impact of the uncertainty of this dataset on the overall result and its uncertainty.

In this study, the input of a flood risk assessment performed for Annotto Bay, Jamaica (Glas et al., 2015), was used as case study for the sensitivity analysis, because in 2012 a lot of accurate data were collected for this town in the framework of another research program (ODPEM, 2013b). Since hydraulic and rainfall data are scarce in this region, and return periods of floods are unknown, this quantitative risk assessment focuses on material damage due to inundations caused by the Tropical Storm Michelle, in 2001 (WRA, 2002).

3.1.2 Study area

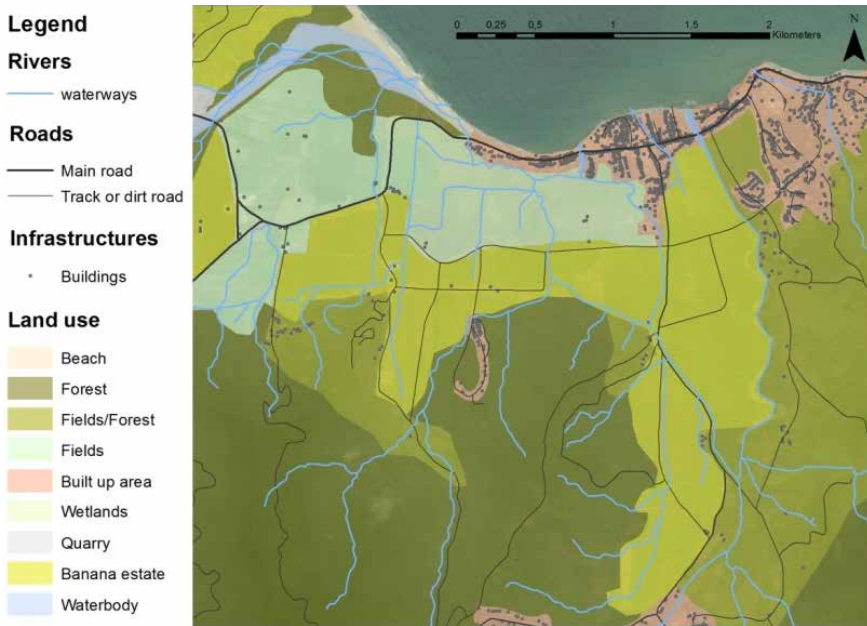


Figure 16 Situation map Annotto Bay (Glas et al., 2015).

Annotto Bay is a small coastal town in the northeast of Jamaica. The town is vulnerable to several natural hazards, of which storm surges and riverine flooding are the most severe (ODPEM, 2013b). This is due to the high-risk location of the community. Not only is the town situated close to the coastline, but it is also enclosed by the Blue Mountains. This

topography, together with the presence of four rivers traversing Annotto Bay, causes the rapid flooding of the community whenever precipitation occurs in the mountains (WRA, 2002). Since the highest point of the town is only three meters above Mean Sea Level, Annotto Bay suffers severely from storm surges as well. There are about 5,500 inhabitants in the area, living mainly in concrete and wooden buildings (STATIN, 2001). The land use in the study area and the locations of the rivers, roads and buildings is shown in Figure 16.

All damage calculations made in this study were based on the flood map of the inundations on both the 28th and the 29th of October, 2001, caused by Tropical Storm Michelle. The city of Annotto Bay was largely flooded for two days (Figure 17). Houses, infrastructure and crops were damaged. However, since the flow velocity was less than 0.3 m s^{-1} , there was only little severe structural damage (ODPEM, 2013b).

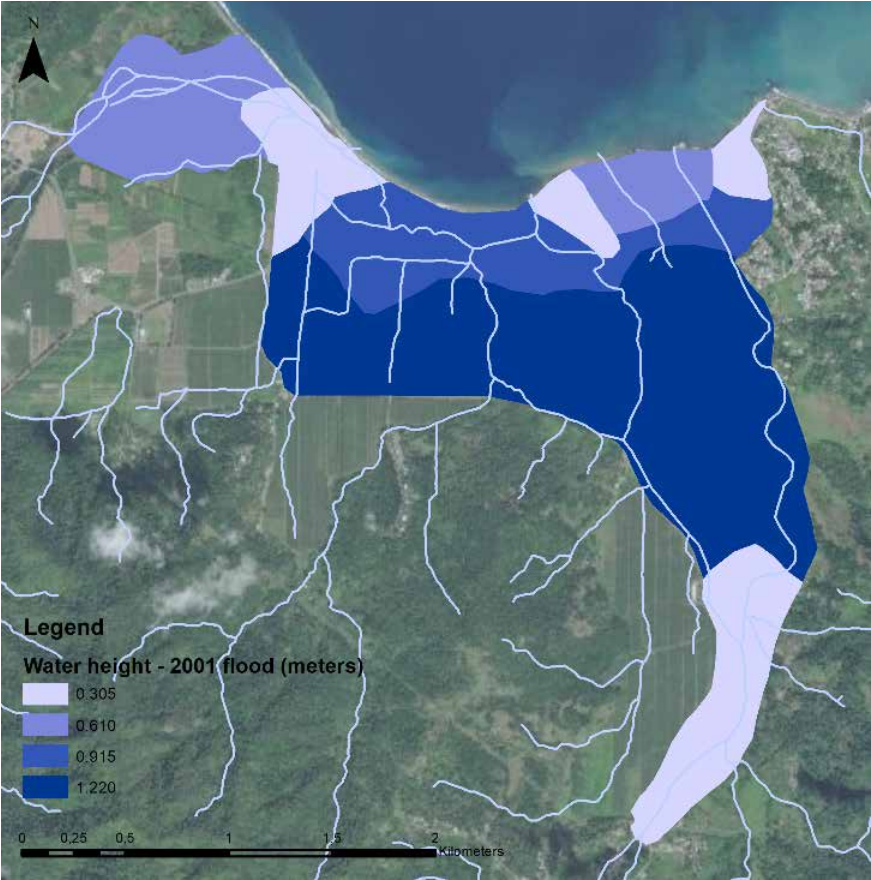


Figure 17 Flood extent of 2001 inundations caused by Tropical Storm Michelle in Annotto Bay, Jamaica (Glas et al., 2015).

3.2 Methods and results

In a first step, a benchmark flood risk assessment model was determined. This model was created using all available data and was based on the Flemish LATIS methodology (Deckers et al., 2009) and on a risk assessment performed by ODPEM (2013b). In the benchmark risk assessment, geographic information was combined with the replacement values of the elements at risk and with the damage factors. Replacement values represent the cost to rebuild an element when it is totally destroyed, while the damage factors are an estimate of the degree of destruction based on the flood level, in meters, at the location of the element at risk. Hence, the damage factor will be a number between 0 and 1, with 0 being no damage at all and 1 being complete destruction. The three types of elements at risk that suffered most damage according to ODPEM (2013b) were buildings, crops and roads. Due to limited information on other types and the impact of the flooding on these elements at risk, only the damage costs for buildings, crops and roads were calculated by multiplication of the replacement value by the damage factor to generate an economic damage map, indicating the total damage cost per square meter for the study area.

This first assessment, the benchmark, is called Scenario 1 (S1). Eleven other scenarios, each with less, or less detailed, input data than S1, were tested and compared to this first one. Table 9 shows an overview of all scenarios and Table 10 provides a matrix showing which data were used in each scenario. The scenarios are discussed per sensitivity type. Four types were tested: building damage sensitivity, road damage sensitivity, crops damage sensitivity and data type sensitivity. In each section, the methods are discussed first, followed by the results.

Table 9 Overview of investigated scenarios in the sensitivity analysis.

SCENARIO	DESCRIPTION	USED INPUT DATA
S1	Detailed approach	Land use data Roads (classes) – line 2001 flood data Building locations + materials + number of floors
S2	Building materials and number of floors unknown	building locations average material values average number of floors
S3	Building locations, materials and number of floors unknown	number of buildings known presumed to be equally spread in the urban area
S4	Building density is calculated based on population density (3 people per building)	Population density is used to determine number of buildings in statistical sectors
S5	Building density is calculated based on number of people in study area (3 per building)	Number of people in the study area is used to determine number of buildings
S6	Road classes are unknown	Average values for the width and the cost of the roads are used

SCENARIO	DESCRIPTION	USED INPUT DATA
S7	All roads are unknown and not taken into account No road data are used	
S8	All roads are unknown but taken into account as a percentage of land use (5% in urban areas, 2% in rural areas) No road data are used, but the damage is calculated based on a percentage of land use	
S9	Roads are only used to divide land use polygons – no road damage Roads are used as a division tool, not to calculate damage	
S10	Difference between banana plants and other crops is unknown In the damage calculations, the same damage factors and maximum costs are used to determine the cost of the crops and the banana plants	
S11	Raster approach (10mx10m) based on population density All input data (vector) are converted to raster data with a resolution of 10 meters	
S12	Raster approach (30mx30m) based on population density All input data (vector) are converted to raster data with a resolution of 30 meters	

Table 10 Overview of the input data used per scenario.

	S1	S2	S3	S4	S5	S6	S7	S8	S9	S10	S11	S12
Building locations												
Number of floors												
Building material												
Average building values												
Critical buildings												
Number of buildings												
Population density												
Number of people												
Roads												
Road classes												
Average road values												
Land use data												
Banana plants – crops												
Average crop values												
2001 Flood extent												
Depth-damage functions												

For each scenario, four elements were compared: the spatial difference, the visual output, the total damage cost and the total damaged area. To test the first element, all damage maps were converted into raster maps with a resolution of 5 meters. Then, the value of every pixel was compared to the values of its neighbors. The spatial difference is defined in Equation (9) as the probability that a pixel has a different value than its neighbor:

$$(9) \quad SD = \frac{\sum_1^n \frac{P_{sd}}{P_s}}{n}$$

where SD is the spatial difference, P_s the number of neighboring pixels, P_{sd} the number of neighboring pixels with a different value and n the total number of pixels. The concept of spatial difference is also demonstrated in Figure 18. The value of the spatial difference is thus a tool to describe the level of detail of a damage map. Since the resulting damages were assigned to classes in the final maps, this level of detail would be difficult to deduct from only the visual mode of representation. Together with the total damage cost, which is the sum of the calculated building, road and crops damages, and the total damaged area, the visual result and the spatial difference determine the influence of each type of data on the overall result.

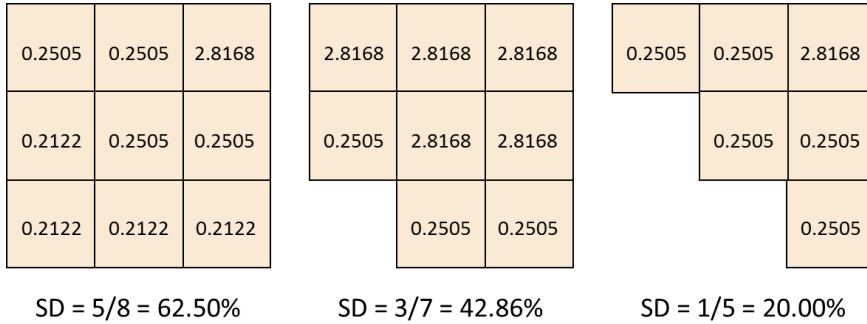


Figure 18 Calculation of the spatial difference (SD) of three center pixels with $SD = \text{number of neighboring pixels with different value} / \text{number of neighboring pixels}$.

All scenarios were modelled in ArcGIS 10.2 using Python. The methodology of the risk assessment was automated through a script written in the ArcPy module. Although small differences exist between the scenarios, caused by the use of different or less input data, the overall methodology remains the same.

3.2.1 Benchmark map

3.2.1.1 Method

To generate the benchmark map, three types of damages were assessed. Building damage calculations were based on the exact GPS position of all of the buildings in Annotto Bay, as well as their building materials and the number of floors (ODPEM, 2013b). By using average Jamaican market values, calculated by ODPEM (2013b) for the material cost and the building surface area, a maximum damage value was determined per building. Subsequently, the real damages were calculated by multiplying these maximum damage values with a damage factor based on the water levels. The damage factor were transferred from Japanese depth-damage functions, as retrieved from Dutta et al. (2003), and the water levels were retrieved from the 2001 flood map (WRA, 2001). The Japanese depth-damage functions could be transferred to Jamaica due to the similarities in geography and building engineering procedures. Most Japanese and Jamaican buildings are constructed in a similar manner with solid concrete or wooden walls. The distinction between these two building types is made in the depth-damage functions as well as in the building database of Annotto Bay. The calculated real

damages were then summed up per land use polygon, in order to generate a clear view of the building damage.

The damage to roads was calculated using the road network dataset (ODPEM, 2013b). This dataset divides the roads into four classes, each with their own properties, for example the width of the road. The line dataset was converted into polygons, based on the different widths. Using an average maximum road damage, calculated by Collier et al. (2013) for developing countries, and combining this with damage factors from the Flemish LATIS flood risk assessment tool (Deckers et al., 2009), the real damage was then calculated for all roads.

Finally, the crop damage map was generated. A difference was made between banana plants and other crops, due to the different reaction to inundations and the different average cost of the crops. As banana plants can only survive water saturated conditions up to 48 hours because of their fragile roots (Rajamannan, 2004), the duration of the flood is especially important for these plants, since a two-day flood, as this was the case in 2001, causes 100 percent destruction of the plants. For the damage calculations of the other crops, an average was used of the damage factors of eight crop types defined by Dutta et al. (2003). These crops are commonly cultivated in Japan as well as in Jamaica. Therefore, the crop depth-damage functions could also be transferred. The maximum crop damage value was based on information from FAOSTAT (2012) and was multiplied with this damage factor to determine the crop damage cost. Since the damage factor for the banana plants was 1, their real damage value was equal to the maximum damage value.

Since there is only very limited information on the exact consequences of the 2001 flood, the benchmark model could not be validated. However, the small amount of information that was available, could serve as an indication. The number of affected houses, for example, was 749 (ODPEM, 2013b), while the benchmark model calculated this at 799. The overestimation can be explained by the fact that rural buildings were also assessed in this study, as opposed to the ODPEM report where the buildings in rural areas were not taken into account, leading to an addition of 41 affected buildings. There was no comparable data for road and crop damage.

The lack of validation increased the uncertainty of the model. However, this research did not take into account the uncertainties of the input data or the model, since the aim of this research was to investigate the sensitivity of the model towards its input data. Hence, to identify the influence of each type of input data, S1 was an acceptable benchmark.

3.2.1.2 Results

The benchmark damage map visualizes the output of the flood risk assessment model for Annotto Bay, as shown in Figure 19. Table 11 contains the three numeric elements on which the comparison of the scenarios is based: the total damage, the total damaged area and the spatial difference, as calculated for S1. The total damage cost is calculated at 7.49 million USD, of which 7.08 million USD, or 94.6% is damage to buildings.

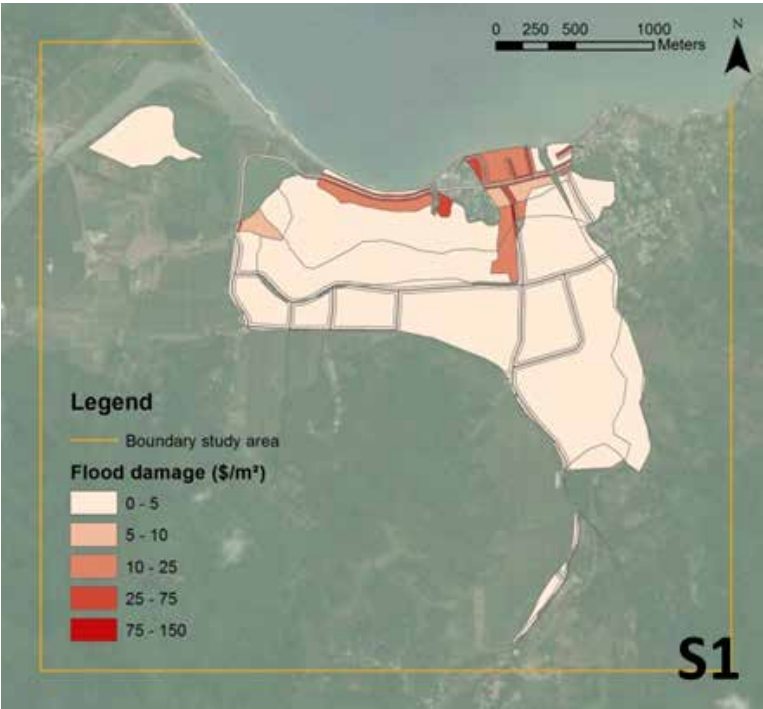


Figure 19 Scenario 1 (S1): Benchmark damage map of Annotto Bay, using all available input data.

Table 11 Calculated total damage, total damaged area and spatial difference for S1.

	TOTAL DAMAGE (USD)	TOTAL DAMAGED AREA (m²)	SPATIAL DIFFERENCE
S1	7 490 000	3 182 000	0.048

3.2.2 Building damage sensitivity

3.2.2.1 Methods

In the next four scenarios, the sensitivity of the flood risk assessment model towards the data used to calculate building damage was investigated. In S2, the information concerning materials and the number of floors was removed and replaced by average values for all buildings in Annotto Bay. In S3, the location of the buildings was also eliminated, leaving only the number of buildings in the total study area as information. In this scenario, after testing the available data in and around the study area, including the exact building locations and the land use data, 90% of the buildings was presumed to be in urban areas and the other 10% in rural areas. In S4 and S5, population information was used to determine the building damage, based on the average number of 3 people per building (WRA, 2002). In S4, the population density per statistical sector was used to calculate the number of buildings. In S5, however, only the total number of people in the study area was known. Here, the same assumption was made as in S3 about the division of buildings between rural and urban areas.

3.2.2.2 Results

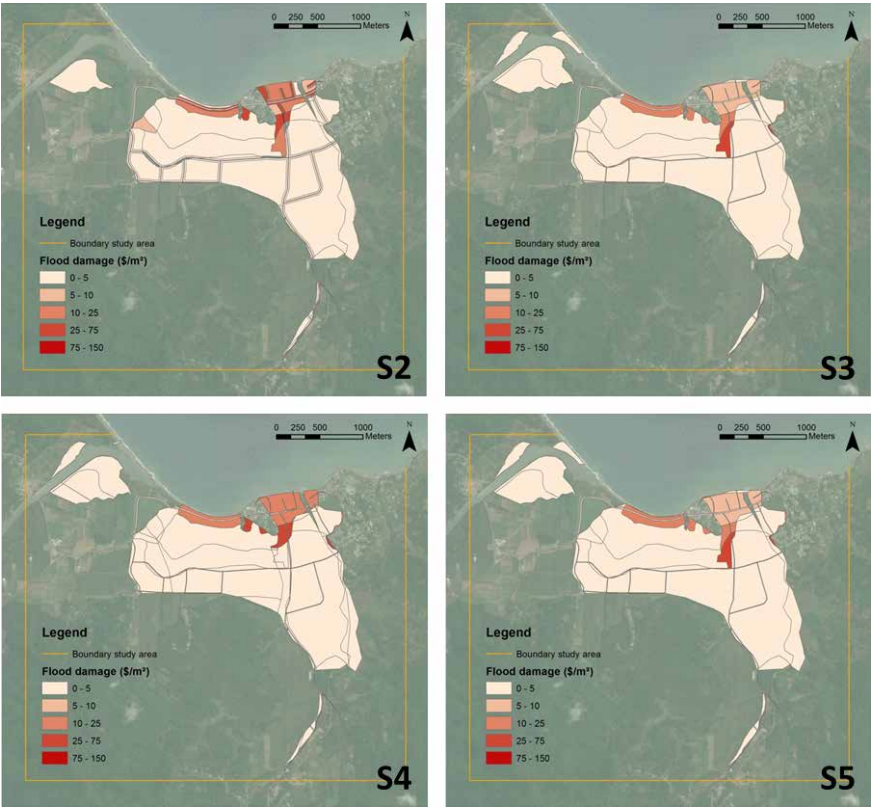


Figure 20 Damage maps for Annotto Bay for S2, S3, S4 and S5. (Top left: (S2) Building materials and number of floors unknown, Top right: (S3) Building locations, materials and number of floors unknown, Bottom left: (S4) Building density is calculated based on population density, Bottom right: (S5) Building density is calculated based on number of people in study area.)

Figure 20 shows the visual result of the four scenarios, while Table 12 shows the calculated damage, the damaged area and the spatial difference in comparison to the benchmark results of S1. Visually, no big changes can be observed in the indication of the high-risk areas. The slightly lower spatial difference in S3 and S5 does indicate a decrease in the level of detail. While S2 gives the result that is most similar to the result of S1, the table clearly shows an important difference of 19.75% in the calculation of the total damage cost. This percentage rises to 20.88% when only taking into account the building damage. Although the visual result of S4 is less detailed than the benchmark, the spatial difference of 0.045 indicates a similar level of detail as in S1. Moreover, this scenario gives the best result towards the calculation of the total damage. The calculated building damage of S4 is 6.59 million USD, which is 6.96% lower than the calculated building damage in S1.

Table 12 Calculated total damage, total damaged area and spatial difference for S2, S3, S4 and S5 in comparison to S1.

	TOTAL DAMAGE (USD)		TOTAL DAMAGED AREA (m ²)		SPATIAL DIFFERENCE	
S1	7 490 000		3 182 000		0.048	
S2	8 969 000	+19.75%	3 182 000	+0.00%	0.048	+0.00%
S3	5 412 000	-27.74%	3 441 000	+8.14%	0.041	-14.20%
S4	6 997 000	-6.58%	3 401 000	+6.88%	0.045	-5.64%
S5	5 412 000	-27.24%	3 441 000	+8.14%	0.041	-14.20%

3.2.3 Road damage sensitivity

3.2.3.1 Methods

Scenarios 6, 7, 8 and 9 were used to assess the sensitivity of the risk assessment towards the road data. In S6, the road classes were presumed to be unknown, giving all roads the same average width. S7 did not take the roads into account. In S8, the location of the roads was eliminated and therefore, they were calculated as a percentage of the land use. After analyzing the available data in and around the study area, the percentages were set at 5% roads in urban areas and 2% in rural areas. S9 only used the road network to divide the land use polygons, but did not take them into account in the damage calculations.

3.2.3.2 Results

The road cost is only a small share of the total calculated damage. This is clear when comparing the total damage of the four scenarios to the damage of the benchmark in Table 13. S6, for example, generates almost identical numbers as S1. Visually, these scenarios are almost identical. However, when assessing only the road damage, S6 generates a damage cost of 41 thousand USD, which is 20.59% higher than the calculated damage cost of 34 thousand USD in S1.

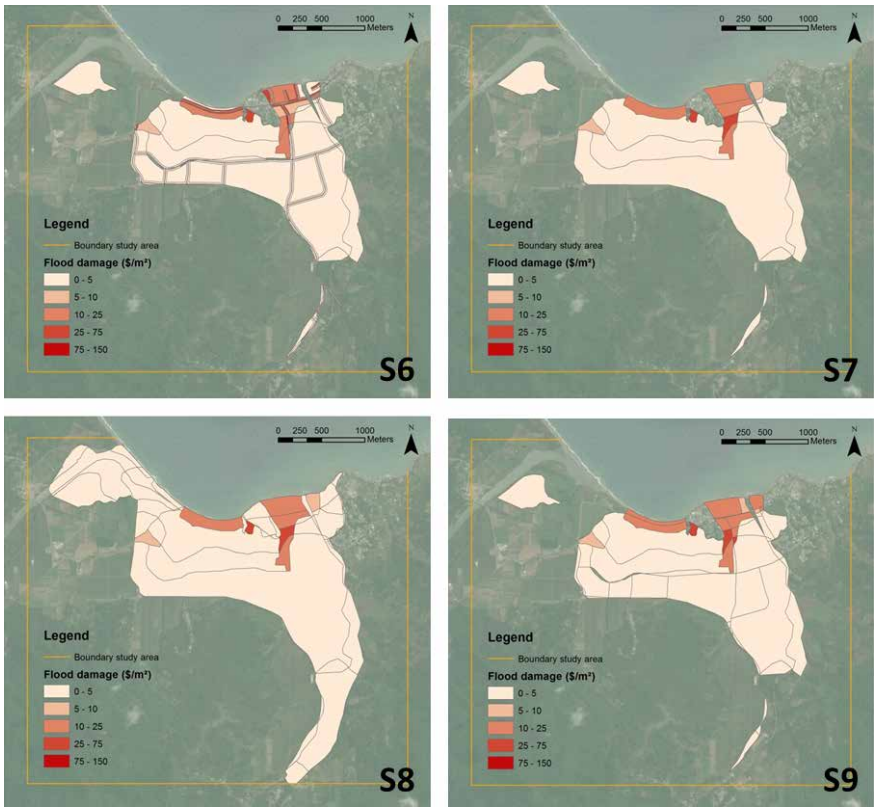


Figure 21 Damage maps for Annotto Bay for S6, S7, S8 and S9. (Top left: (S6) Road classes are unknown, Top right: (S7) All roads are unknown and not taken into account, Bottom left: (S8) All roads are unknown but taken into account as a percentage of land use, Bottom right: (S9) Roads are only used to divide land use polygons – no road damage.)

Table 13 Calculated total damage, total damaged area and spatial difference for S6, S7, S8 and S9 in comparison to S1.

	TOTAL DAMAGE (USD)		TOTAL DAMAGED AREA (m²)		SPATIAL DIFFERENCE	
S1	7 490 000		3 182 000		0.048	
S6	7 496 000	+0.08%	3 180 000	−0.06%	0.048	+0.00%
S7	7 459 000	−0.41%	3 171 000	−0.35%	0.016	−66.18%
S8	7 490 000	+0.00%	4 347 000	+36.61%	0.018	−63.47%
S9	7 459 000	−0.41%	3 159 000	−0.72%	0.022	−54.91%

There is a significant difference in damaged area between S1 and S8. Since the threshold value for road damage is 0.00 meters and the road damage is spread over the entire study area in S8, all flooded areas have damage. Moreover, visually, S8 shows a different, less accurate, result than the other scenarios, as shown in Figure 21.

The scenario has a low spatial difference of 0.018. The total road damage cost of 32 thousand USD, however, is only 5.88% lower than the damage cost in S1.

Although S7 clearly has a better visual result than S8, indicating the areas without any damage more accurately, the spatial difference of this scenario is lower. Due to a larger damaged area in S8, more pixels are taken into account in the spatial difference calculations, increasing the possibility of having neighboring pixels with a different value. The level of detail is thus higher in S8, but the visual result shows large deviations from S1. The removal of the roads in S7 and S9 only has a small effect on the total damage and damaged area, but it does have an important influence on the level of detail, as proven by the spatial differences. The ninth scenario, nonetheless, does have a more accurate visual result than the other road scenarios, due to the use of the road network to divide the land use polygons.

3.2.4 Crops damage sensitivity

3.2.4.1 *Methods*

S10 tested the sensitivity of the model by assuming the difference between banana plants and other crops was unknown. An average maximum damage value was calculated from the values for banana plants and other crops, grown in Jamaica. The damage factor used was also an average, but only of the damage factors of other crops, since the damage factor for banana plants was 100% for every water depth, due to the duration of the flood.

3.2.4.2 *Results*

Since the real damage value of the crops is rather small in comparison to building damage values, S10 only has a small effect on the result. Therefore, the visual view of the map is almost identical to the benchmark damage map. This can be seen in Figure 22. Furthermore, Table 14 demonstrates that the calculated total damage and damaged area differ only little from the values that were generated by the model used for S1. However, the crop damage cost of 154 thousand USD in S10 is 58.60% lower than the crop damage cost of 372 thousand USD in S1.

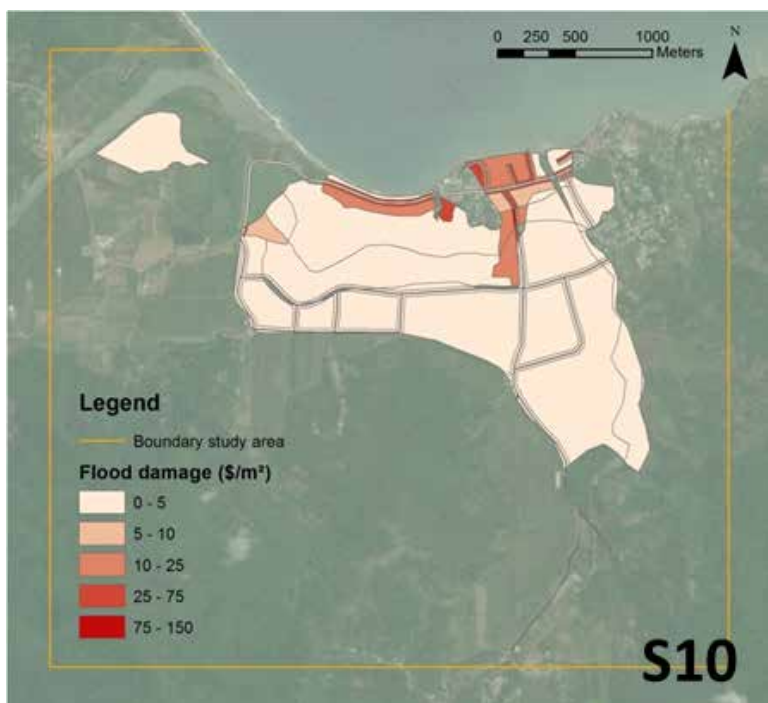


Figure 22 Damage map for Annotto Bay for S10. (Difference between banana plants and other crops is unknown.)

Table 14 Calculated total damage, total damaged area and spatial difference for S10 in comparison to S1.

	TOTAL DAMAGE (USD)		TOTAL DAMAGED AREA (m²)		SPATIAL DIFFERENCE	
S1	7 490 000		3 182 000		0.048	
S10	7 272 000	−2.91%	3 110 000	−2.26%	0.048	−0.21%

3.2.5 Data type sensitivity

3.2.5.1 Methods

The last two scenarios looked into the sensitivity of the model towards the input data type. In the benchmark model, all input data were vector data. In areas with little data available, however, a lot of information will have to be gathered from satellite imagery. Therefore, all input data in S11 and S12 were converted to raster data with a resolution of 10mx10m for S11 and 30mx30m for S12 to simulate satellite data. The former resolution was chosen since several commercial high-resolution satellite systems, e.g. SPOT, provide images with a world coverage with this resolution. The Landsat program uses the latter resolution and provides free images through an online service. The calculations for the building damage were based on population data, in the same way as in S4.

3.2.5.2 Results

Although the two damage maps, as shown in Figure 23, visually do not differ a lot from the maps of S1 and S4, Table 15 shows that the total damage cost is substantially higher than the cost in S1 and S4. All three separate damage costs show a large overestimation compared to S1 and S4. The road damage cost, especially, is 27 times larger in S11 and even 78 times larger in S12 than in S1. This is due to the fact that road damage is calculated per pixel, and the pixels in both scenarios have a resolution larger than the width of the roads. Hence, the area assigned to roads is overestimated.

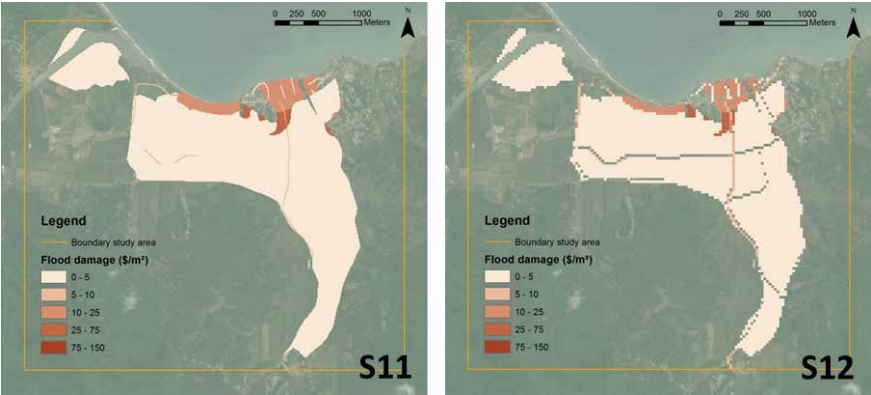


Figure 23 Damage maps for Annotto Bay for S11 and S12. (Left: (S11) Raster approach (10x10) based on population density, Right: (S12) Raster approach (30x30) based on population density.)

The total damaged area is also slightly larger, due to the conversion of the polygon flood map to a raster map. Since the input of the scenarios was raster data, every pixel has been calculated separately. Therefore, the level of detail, and thus the spatial difference, is higher than in S7, S8 and S9. When comparing the results of S11 and S12, it can be stated that the spatial difference shows a growing decrease of accuracy as the resolution of the raster data increases. Moreover, the visual result is less detailed and gaps arise in the final map.

Table 15 Calculated total damage, total damaged area and spatial difference for S11 and S12 in comparison to S1.

	TOTAL DAMAGE (USD)		TOTAL DAMAGED AREA (m²)		SPATIAL DIFFERENCE	
S1	7 490 000		3 182 000		0.048	
S4	6 997 000	−6.58%	3 401 000	+6.88%	0.045	−5.64%
S11	9 692 000	+29.40%	3 807 000	+19.64%	0.047	−1.67%
S12	8 425 000	+12.48%	3 613 000	+13.54%	0.032	−33.61%

3.3 Discussion

In all scenarios, more than 90% of the total flood damage consists of building damages. Consequently, scenarios that test the models sensibility for building data show the largest deviations in the total damage. Figure 24 shows the deviation for every scenario from the total cost of S1.

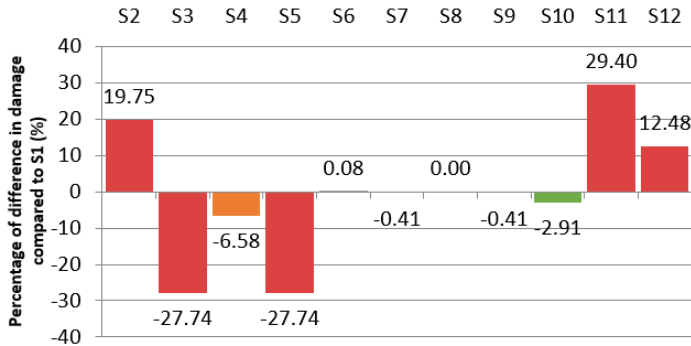


Figure 24 Deviation of total damage of all scenarios in relation to S1 (=0).

When looking at the scenarios focusing on building damage, S4 has the best result, with a deviation of 6.58% in relation to the result of S1. This scenario has calculated the damage cost based on population density per statistical sector. In the case study of Annotto Bay, the benchmark study made use of the exact GPS locations of all buildings in the region. In many other areas in the SIDS, this detailed information is not available. Population data, however, exist for most regions free of charge (STATIN, 2001; Steele et al., 2018). Since the model gives a good result, visually as well as in the total damage cost, this scenario must definitely be investigated further. The importance of an accurate average number of people per household was proven by running the same model with an average of 2 and an average of 4 people per household instead of the average of 3, as given by WRA (2002). When testing the former, the total damage cost of 4.83 million USD is 35.55% lower than S1, while the latter gives a resulting cost that is 21.75% higher than the resulting damage cost of S1. Other recent flood exposure studies have proven the close link between population data and building locations with accurate results (Smith et al., 2019; Zhu et al., 2020).

When only relying on Figure 24, it could be stated that the model is not sensitive to road data at all. However, not only the total damage must be taken into account, but also the spatial impact and the total damaged area have to be included. In Figure 25, the last factor is given. It is clear that S8, the scenario where roads are taken into account as a percentage of the land use, is not a good simplification. Since buildings have a threshold value to be marked as 'inundated' of 0,5 meters, but roads are marked immediately as flooded, the total damaged area in S8 is a big overestimation of the reality. This is affirmed by the visual result, showing a lot of damaged area with a low cost per square meter.

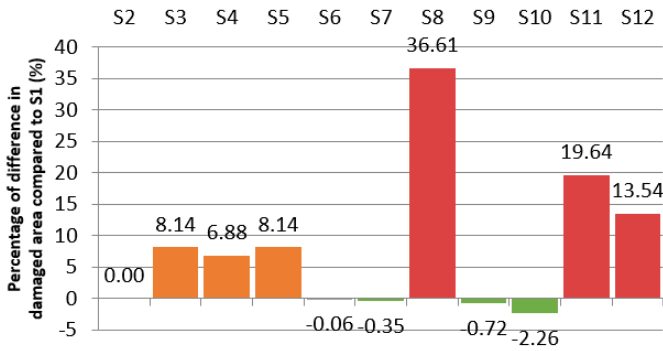


Figure 25 Deviation of total damaged area of all scenarios in relation to S1 (=0).

Although S7 scores very well for the total damage as well as for the total damaged area, the result is a lot less accurate than the benchmark map. This becomes clear when looking at Figure 26, that visualizes the deviation of the spatial difference of all scenarios in relation to S1. In this figure, three scenarios that test the influence of road data have the highest deviation and thus show significantly less detail in their damage map. Although the roads are negligible for the total damage and the damaged area, they are, nonetheless, an indispensable part in creating a visually accurate map.

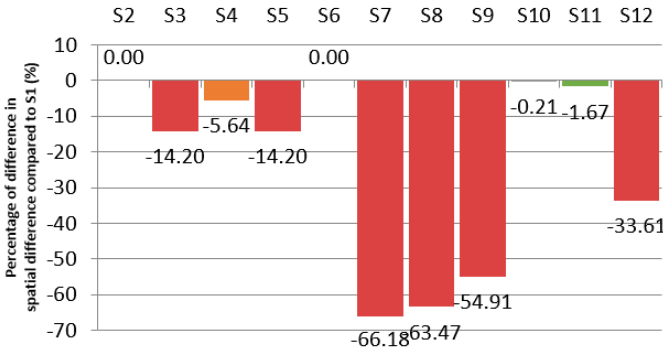


Figure 26 Deviation of spatial difference of all scenarios in relation to S1 (=0).

Visually, as well as in total damage and damaged area, the difference between crops and banana plants has a small effect on the results, as shown in Figure 26. It must be stated that this is the case for this case study of Annotto Bay, where building damage is the major type of damage. When looking into other regions, where agriculture plays a more important role, the difference between crops can be a lot more significant for the results. This has to be further investigated.

Finally, S11 and S12 have shown the sensitivity of the flood risk assessment model towards the input data type. In this case, all input data were converted to raster data with common open source resolutions (Deruyter et al., 2018; Feyisa et al., 2014). Although the visual result was similar to the benchmark, there was a clear difference in the total damage and the damaged area, as both scenarios show an overestimation of both

elements. Due to the low resolution of S12, the final map shows a significant amount of gaps that do not have any damage value and are not included in the damaged area. Therefore, a lower overestimation is observed in S12 compared to S11. The visual result, however, is the least detailed of all scenarios, with important information missing. Therefore, vector data have the preference when working in a relatively small study area. When some input data are vector and other raster data, it should be considered to vectorize the last type in order to avoid losing detail. This methodology will give the most accurate result. In larger-scale studies, remote sensing data are a popular input data type for flood risk mapping in a data-poor context, and has provided accurate results (Kumar & Acharya, 2016; Kwak et al., 2015; Rabby et al.; Son et al., 2019).

3.4 Conclusion

In several industrialized countries, risk-based flood tools were developed to predict and estimate the damages caused by inundations. Such tools are constantly being optimized and are adopted for urban and rural planning in order to prevent damages from future inundations caused for instance by climate change or high degrees of urbanization. Although a lot of detailed data are fed as input for these models, a certain degree of uncertainty is inherent and can never be fully eliminated.

In developing countries the detailed data needed by these models is not available. Therefore, to determine if the methodology used in the developed countries can be transferred to developing countries, it is necessary to know what the sensibility of the models is towards the input data. For this research, a risk-based model for the case study of Annotto Bay was used (Glas et al., 2015). The results show that it is indeed possible to reduce the level of detail substantially, without adding significantly to the model uncertainties.

Since the 2001 flood especially hit the urban areas of Annotto Bay, the building data were the most significant type of data in this study. The scenario that uses the population density and the average number of people per household to calculate the number of buildings as a simplification for the exact location of the buildings produced the best results. The deviation of the total damage cost was only 7% in comparison to the benchmark. As population data have a global availability, in many cases for free, this is an important finding that can be transferred to case studies in other urban areas. It must be stated, however, that an accurate number of people per household is indispensable in this scenario.

Another finding of this study is the importance of road data. Although roads have a small effect on the overall cost, they do have a role in the visual end result. An accurate road dataset helps to divide the land use, and to determine the building damage more precisely. In this light, the possibility of using remote sensing images to create road datasets must be investigated, since many available datasets do not include all roads. When using satellite imagery, the road classes cannot be taken into account, but this has been proven to have little impact on the result. Furthermore, a complete dataset can

definitely help in defining building damage, since every building must have access to a road and will thus most likely be located close to this road. Combining this information with population data should be investigated further.

No conclusions could be made from the sensitivity analysis towards crop data, because, in this case study, the impact was too small. The results showed little difference between the benchmark scenario, where crops and banana plants were treated separately, and the scenario where an average cost was used. To further investigate the impact of crop data, a more rural area should be investigated. However, it can already be concluded that the difference between crops and banana plants can be eliminated in study areas where urban areas are most affected by flooding.

Finally, the data type plays an important role in the accuracy of the final result of a risk assessment on this micro-scale. Using raster data, from satellite imagery for example, causes an overestimation of the total damage and the damaged area, due to the resolution, which causes loss of information detail. Therefore, vector data are preferred as input data in the risk methodology in case of a micro-scale study area. When only raster data are available for certain indispensable input data, this raster data should be vectorized instead of rasterizing the available vector input data. In further research, more types of raster data with different resolutions should be tested, as well as combinations of raster and vector data, for study areas on different scales.

This sensitivity analysis of the Annotto Bay flood risk assessment model is a first and important step in determining which data are indispensable and which data can be adapted, replaced or ignored in a risk assessment. Although the road damage has a small impact on the overall damage cost, this data type is indispensable for an accurate visual result. Furthermore, it is shown that population density data, in combination with an average number of people in a household, is an adequate replacement of the exact housing locations as input data for building damage. Nonetheless, more research should be done in other regions to validate the results of the sensitivity analysis and to investigate the impact to the damage types in different situations.

REFERENCES

- Apel, H., Aronica, G. T., Kreibich, H., & Thielen, A. H. (2009). Flood risk analyses-how detailed do we need to be? *Natural Hazards*, 49(1), 79-98. doi:10.1007/s11069-008-9277-8
- Apel, H., Merz, B., & Thielen, A. H. (2008). Quantification of uncertainties in flood risk assessments. *International Journal of River Basin Management*, 6(2), 149-162. doi: 10.1080/15715124.2008.9635344
- Apel, H., Thielen, A. H., Merz, B., & Blöschl, G. (2004). Flood risk assessment and associated uncertainty. *Natural Hazards and Earth System Sciences*, 4(2), 295-308. doi: 10.5194/nhess-4-295-2004
- Carrington, C. D., & Bolger, P. M. (1998). Uncertainty and risk assessment. *Human and Ecological Risk Assessment: An International Journal*, 4(2), 253-257. doi: 10.1080/10807039891284325
- Collier, P., Kirchberger, M., & Söderbom, M. (2013). The cost of road infrastructure in developing countries. *Centre for the Study of African Economies*. Retrieved from: http://www.soderbom.net/13_05_02_Unit%20cost%20paper.pdf
- Deckers, P., Kellens, W., Reyns, J., Vanneuville, W., & De Maeyer, P. (2009). A GIS for flood risk management in Flanders. In P.S. Showalter, L. Yongmei (Ed.), *Geospatial techniques in urban hazard and disaster analysis* (pp. 51-69): Dordrecht, Springer.
- Deruyter, G., Glas, H., & Piette, T. (2018). Semi-automatic flood detection using historic satellite imagery. *International Multidisciplinary Scientific GeoConference: SGEM*, 18(2.3), 551-558. doi: 10.5593/sgem2018/2.3/S11.070
- Dutta, D., Herath, S., & Musiake, K. (2003). A mathematical model for flood loss estimation. *Journal of hydrology*, 277(1-2), 24-49. doi: 10.1016/S0022-1694(03)00084-2
- FAOSTAT (2012). Crops. Retrieved from: <http://faostat3.fao.org/download/Q/QC/E>
- Feyisa, G. L., Meilby, H., Fensholt, R., & Proud, S. R. (2014). Automated Water Extraction Index: A new technique for surface water mapping using Landsat imagery. *Remote Sensing of Environment*, 140, 23-35. doi: 10.1016/j.rse.2013.08.029
- Glas, H., Jonckheere, M., De Maeyer, P., & Deruyter, G. (2015). A GIS-based flood risk tool for Jamaica: the first step towards a multi-hazard risk assessment in the Caribbean. *International multidisciplinary scientific GeoConference SGEM*, 15(2.2), 643-650. doi: 10.5593/SGEM2015/B22/S11.080
- Kok, M., Huizinga, H. J., Vrouwenvelder, A. C. W. M., & Barendregt, A. (2005). Standaard-methode 2004 - Schade en Slachtoffers als gevolg van overstromingen. Retrieved from <https://library.wur.nl/ebooks/hydrotheek/1874298.pdf>
- Kumar, R., & Acharya, P. (2016). Flood hazard and risk assessment of 2014 floods in Kashmir Valley: a space-based multisensor approach. *Natural Hazards*, 84(1), 437-464. doi: 10.1007/s11069-016-2428-4
- Kwak, Y., Shrestha, B. B., Yorozya, A., & Sawano, H. (2015). Rapid Damage Assessment of Rice Crop After Large-Scale Flood in the Cambodian Floodplain Using Temporal Spatial Data. *Ieee Journal of Selected Topics in Applied Earth Observations and Remote Sensing*, 8(7), 3700-3709. doi:10.1109/jstars.2015.2440439
- Merz, B., Kreibich, H., Schwarze, R., & Thielen, A. (2010). Assessment of economic flood damage. *Nat. Hazards Earth Syst. Sci.*, 10(8), 1697-1724. doi: 10.5194/nhess-10-1697-2010

- ODPEM (2013). *National progress report on the implementation of the Hyogo Framework for Action (2011-2013)*. <https://www.preventionweb.net/english/hyogo/national/reports/v.php?id=33409&pid:183>
- Rabby, M. F., Haque, D. M. E., & Selim, M. Flood Inundated Agricultural Damage and Loss Assessment Using Earth Observation. *International Journal of Excellence Innovation and Development*, 1(1), 60-69.
- Rajamannan, A. H. (2004). Flood Protection for banana and plantain plants. Retrieved from: <https://patentimages.storage.googleapis.com/ad/01/c2/0e544a282959f6/US20040242418A1.pdf>
- Smith, A., Bates, P. D., Wing, O., Sampson, C., Quinn, N., & Neal, J. (2019). New estimates of flood exposure in developing countries using high-resolution population data. *Nature communications*, 10(1), 1-7. doi: 10.1038/s41467-019-09282-y
- Son, N. T., Chen, C. F., & Chen, C. R. (2019). Flood assessment using multi-temporal remotely sensed data in Cambodia. *Geocarto International*, 16. doi:10.1080/10106049.2019.1633420
- STATIN (2001). *Census of Population and Housing Jamaica*. Retrieved from <https://statinja.gov.jm/Popcensus.aspx>
- Steele, J. E., Nieves, J., Tatem, A. J., Forget, Y., Shimoni, M., Linard, C., & Ieee. (2018). Worldpop – Fusion of Earth and Big Data for Intraurban Population Mapping. *Igarss 2018 – 2018 IEEE International Geoscience and Remote Sensing Symposium, 2070-2071*. doi: 10.1109/IGARSS.2018.8518181
- Tate, E., Munoz, C., & Suchan, J. (2015). Uncertainty and Sensitivity Analysis of the HAZUS-MH Flood Model. *Natural Hazards Review*, 16(3), 10. doi:10.1061/(asce)nh.1527-6996.0000167
- Vanneuville, W., De Rouck, K., Maeghe, K., Deschamps, M., De Maeyer, P., & Mostaert, F. (2005). *Spatial calculation of flood damage and risk ranking*. Paper presented at the AGILE 2005 8th conference on geographic information science.
- Weichel, T., Pappenberger, F., & Schulz, K. (2007). Sensitivity and uncertainty in flood inundation modelling? Concept of an analysis framework. *Advances in Geosciences*, 11, 31-36. doi: 10.5194/adgeo-11-31-2007
- WRA (2001). 2001 flood extent.
- WRA (2002). Rapid Impact Assessment of Communities in Portland and St. Mary Affected by the October and November 2001 Flood Rains. Kingston, Jamaica, WRA.
- Yu, J., Qin, X., & Larsen, O. (2013). Joint Monte Carlo and possibilistic simulation for flood damage assessment. *Stochastic environmental research and risk assessment*, 27(3), 725-735. doi: 10.1007/s00477-012-0635-4
- Zhu, S., Dai, Q., Zhao, B., & Shao, J. (2020). Assessment of Population Exposure to Urban Flood at the Building Scale. *Water*, 12(11), 3253. doi: 10.3390/w12113253

4

COLLECTING HISTORIC FLOOD DATA IN DATA-POOR REGIONS – A CITIZEN APPROACH

This chapter is adapted from the following conference paper and book chapter:

Glas H., Deruyter G., De Maeyer P. (2018). Flood risk assessment in data sparse regions: the use of questionnaires to collect historic flood data – a case study for the river Moustiques in Haiti, *International Multidisciplinary Scientific GeoConference SGEM*, 18(2.3), 377-384. doi: 10.5593/sgem2018/2.3/S11.048
(Won the Award for Best Presentation at the 18th International Multidisciplinary Scientific GeoConference SGEM 2018)

Glas H., Deruyter G. (2020). Collecting historic flood data in data-sparse areas – a citizen approach. In B. Boonstra, P. Davids & A. Staessen (Eds.), *Opening up the Planning Landscape: 15 years of Actor-relational Approaches to Spatial Planning in Flanders, the Netherlands and Beyond*, 103-111. doi: 10.17418/B.2020.9789491937446

ABSTRACT

Flooding caused by storm surges, tropical storms and hurricanes causes severe damages in Haiti every year. When these inundations occur, the affected areas become inaccessible, preventing field work to register the flood water height and extent. High-resolution satellite imagery and aerial photography, on the other hand, are too expensive for a developing country like Haiti. The lack of this data results in a lack of adequate flood maps and models, making it impossible to predict the cost of the damages and take the right measures to minimize them. The information necessary to generate flood maps can, however, also be found in the knowledge of the inhabitants of the affected areas. These people remember if their house was flooded and if their properties were damaged due to flooding. Therefore, a questionnaire was drawn up and 294 households in the study area, the floodplain of the river Moustiques in the Northwest of Haiti, were questioned about the most recent and the most severe flood in their memory. In total, 19 different historic flood events were described in 347 answered questionnaires. This research aims to create flood maps by combining the coordinates of the house of each questioned person with the flood height they remembered. Furthermore, flood damage factors were generated from the questionnaires, in which the inhabitants indicated how much damage was caused by each inundation to their houses, crops, livestock and vehicles. The average damage percentages for houses show an increase when the flood height increases. For crops, livestock and vehicles, however, this increase is not visible. This can be due to the fact that these elements are not located in the same area as the houses of which the coordinates and flood height are used. The collected data cannot be taken too literally, as the memory of people is not always correct. However, by combining this information with other geographic data of the study area, it is possible to create flood maps and damage factors in order to establish a flood risk assessment of a data-poor region against a low cost.

Keywords: flood risk, questionnaires, damage factors, Haiti

4.1 Introduction

Flood risk assessments lead to more effective risk management and strengthen the resilience of a community (UNDRR, 2019). While several adequate flood risk assessment tools are available for developed regions, these remain inexistent for most developing countries due to the lack of funds to acquire the necessary reliable input data. Especially the lack of accurate and detailed flood data, in particular flood damage factors, hinders an adequate assessment. Depth-damage functions from existing tools are designed specifically for their area of application. Transferring these functions can lead to uncertainty and inaccuracy in the flood risk calculations (Merz et al., 2010; Scorzini & Frank, 2017). Therefore, Huizinga et al. (2017) have developed global flood depth-damage functions per continent. For smaller case studies, however, these continental depth-damage functions are often too generic and not region-specific enough. Other studies have focused on the creation of functions applicable on a smaller site, based on a probabilistic approach (McGrath et al., 2019; Wu et al., 2021) or based on damage data from one flood event (Nascimento et al., 2006; Scorzini & Frank, 2017). For the latter group, traditionally, this location-specific flood data can be acquired by field work, registering water heights and extents and corresponding damages during the flood event, or can be derived from high-resolution satellite imagery or aerial photography. Both methods, however, have important disadvantages. While the former technique is often not applicable, since the affected areas are inaccessible during a flood, the latter is too expensive for a developing country. Therefore, this research focuses on a third method to gather the necessary historic flood data: questioning the inhabitants.

Involving citizens to collect geographic data, is not a new concept. Volunteered Geographic Information (VGI) is defined as crowdsourced geo-information, provided by a wide range of participants with varying levels of education, knowledge and skills that produces novel, and often valuable, geographical content (Fast & Rinner, 2014). One of the most known and valued examples of VGI is OpenStreetmap. While citizen-led movements producing scientific hazard data during disasters as well as environmental monitoring projects that can act as a warning system for emergency response and for longitudinal scientific studies on hazards, are increasingly common (Bird, 2009; Hultquist & Cervone, 2018; Sprake & Rogers, 2014; Thieken et al., 2017), the use of VGI to gather historic disaster data remains rather unexplored. Nonetheless, people living in flood-prone areas can offer valuable insights on water levels and associated losses of past flooding, as they experienced the inundation and its consequences first-hand.

4.2 Study area

Due to its turbulent history, characterized by a constant political instability that hindered the economic and human development, Haiti is presently the poorest country of the Northern Hemisphere (Rossilon, 2016). Deforested plains encircled by steep mountains characterize the island state's landscape, as 63 percent of the

country's surface has a slope of 20 percent or more (Dolisca et al., 2007; Rossilon, 2016). This topography and land cover also define the 222 km² large catchment of the river Moustiques, one of the only almost permanent waterways in the rural northwest department, where the climate is typically arid (PROTOS, 2011). Nonetheless, in the hurricane season from August through October, the 20 km² large floodplain of the catchment (Figure 27) can receive as much as 600mm precipitation per day, frequently causing flash floods with devastating economic and human consequences, including damages to infrastructures and crops, livestock losses, human injuries and even casualties (Government of Haiti, 2010).

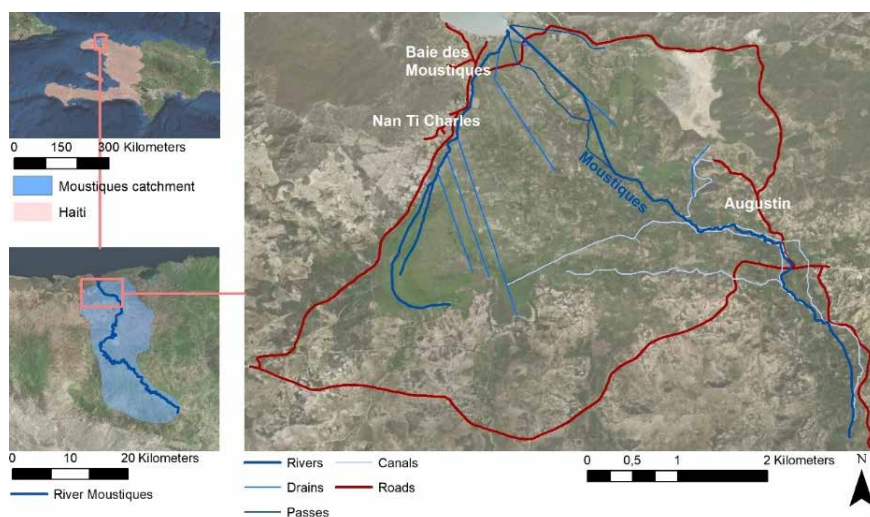


Figure 27 Overview of the floodplain of the catchment of the river Moustiques, located in the northwest of Haiti.

With the use of questionnaires, the almost 2000 inhabitants of the floodplain were questioned on historic flood events and the corresponding damages to their own properties. In January 2018, trained pollsters conducted the survey among all households of the three villages in the floodplain; Baie des Moustiques, situated at the coastline, the neighboring village of Nan Ti Charles, and Augustin, located on the opposite side of the floodplain. The photographs in Figure 28 show the villages and inhabitants of the study area. The results of this survey were then processed into detailed, location-specific input data for a flood risk assessment.

4.3 Methodology

The research can be divided into three phases: the preparation, the field work and the post processing. During the first phase, the questionnaire was drawn up in French, and then translated by the local partners in Haitian Creole (see Appendix for the French version). In January 2018, the second phase took place. During 6 days, 6 local inhabitants conducted the surveys of 294 households. Finally, the results of these questionnaires were digitalized and analyzed.



Figure 28 Aerial photo of Ti Charles and Baie des Moustiques (left) and residents of a fishermen dwelling in Baie des Moustiques (right). (Photographs taken during the fieldwork in 2018).

The questionnaire that was drawn up in the first phase was divided into six sections. In the first section, general information was gathered on the questioned and his or her residence. Then, in the second part, information on the household, number of people and their age was collected. Section 3 dealt with the possession of vehicles and section 4 with the agricultural activities of the household. Possession of livestock and possession of farmland were questioned here. The final two parts of the questionnaire concerned the knowledge on historic flood events. In section 5, the height and duration of the most recent flooding in the memory of the questioned was gathered, as well as the corresponding damages to houses, vehicles, livestock and farmland. Section 6 contained the same questions regarding the most severe flooding in the knowledge of the questioned (Glas & Deruyter, 2018).

In January 2018, 6 trained pollsters conducted the surveys during 6 days. All 294 households in the three villages were questioned. 71 of them were located in Nan Ti Charles, 164 in Baie des Moustiques and the remaining 59 in Augustin. While all 294 questioned inhabitants answered section 5 on the most recent flood event, only 53 of them also recollected a more severe flood event, which led to 321 descriptions of 18 different historic inundations and 26 descriptions of flood events without a date, shown in Table 16. During this stage, GPS measurements and data collection using a drone were carried out as well for later analysis.

Table 16 Overview of the number of descriptions given per historic inundation by the respondents of the questionnaire in the floodplain of the river Moustiques, Haiti (Glas & Deruyter, 2018).

DATE FLOOD EVENT	NUMBER OF DESCRIPTIONS
October 1954	2
November 1986	2
October 2005	5
September 2008	2
October 2008	4
January 2010	1
October 2015	1
August 2016	1
September 2016	2
October 2016	5
November 2016	2
December 2016	1
January 2017	3
March 2017	1
September 2017	29
November 2017	8
January 2018	250
No date given	26

Many people in the study area do not have the necessary education to adequately determine water heights in metrical units. Furthermore, some of the flood events they described were a long time ago, which complicates a correct recollection of the water height as an exact height measurement. However, people often recall the flood level vividly relative to their own body height. Even in developed countries, people are more inclined to say the water is knee-deep than the water level is for example 46 cm. Therefore, the questionnaire respondents were asked to indicate the water level as they experienced it in their homes by using a figure of a person, which made it easy to indicate the water height as reaching to their ankles, knees, thigh, navel, armpits, shoulders or head (Figure 29). Other options were no water in the house or a water level higher than the head. By using the average body measures for men and women, the indicated water levels were then translated into metrical units. To indicate the degree of damage to their house, the respondents could choose four options: no damage, small damages, large damages or complete destruction of the building.

In the analysis phase, the water heights derived from the questionnaires were linked to the degree of damage to their house, as indicated in the questionnaires. With this information, a percentage of damage to residential buildings was calculated for every flood height. For the calculation of damage factors for vehicles, farmland and livestock, two situations were compared. First, the number of vehicles and livestock, as well as the area of farmland, owned by the questioned, was calculated for a non-flooded situation, based on the information given in the general information sections. Then, these numbers were combined with the number of animals that have died, vehicles that were damaged and the degree of damage to crops for every flood event described. These results were used to draft flood damage factors for crops, livestock and vehicles.

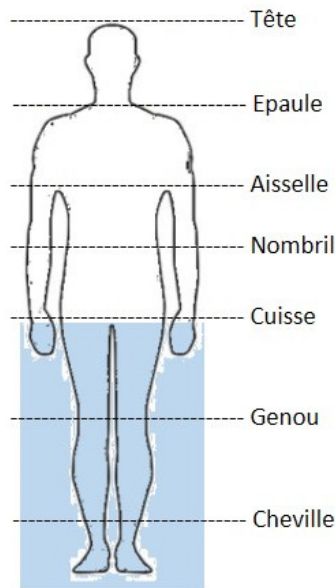


Figure 29 Figure from questionnaire to indicate flood height with an example water level reaching to the thigh (Glas & Deruyter, 2018).

In the last phase of the research, the collected data were digitalized and organized in a database. Using the GPS coordinates of the houses, acquired while conducting the surveys, a shapefile of the buildings in the villages was generated. All other data from the questionnaire were joined with this geographic data.

Finally, for every described flood event, the height of the inundation was linked to the location of the house, where the survey was conducted. These water heights are to be combined with a DEM (digital elevation model) of the area to create historic flood maps. As existing open source DEMs have a spatial resolution of 30m, which is too low to generate an adequate historic flood map (Santillan & Makinano-Santillan, 2016), aerial photography, performed during the field work in January 2018, was used to create a high-resolution model of the study area. This process is still ongoing, and, thus, the historic flood maps have not yet been created.

4.4 Results

In a first step of the analysis, the general household information was processed. In total, 1,868 people live in the study area, of which 945 men and 923 woman. Baie des Moustiques is the largest village in the floodplain, with 1040 inhabitants and an average of 6.34 people per household. Augustin has the highest average of people per household, 7.11 to be specific, and a total population of 420. Finally, Nan Ti Charles has 408 inhabitants and an average of 5.75 people per household. In Table 17, an overview of the number of people per household is given per sex and age for each of the villages.

Table 17 Overview of the number of people in the floodplain of the river Moustiques, Haiti, for the villages Nan Ti Charles, Baie des Moustiques and Augustin (Glas & Deruyter, 2018).

	NAN TI CHARLES		BAIE DES MOUSTIQUES		AUGUSTIN	
	MALE	FEMALE	MALE	FEMALE	MALE	FEMALE
CHILDREN (<15y)	85	74	230	201	91	71
ADULTS (15y-64y)	117	117	290	293	104	137
SENIORS (>64y)	9	6	13	13	6	11
TOTAL	211	197	533	507	201	219

Then, the GPS locations, gathered in the questionnaires, were used to create a shapefile of the residential buildings in the study area. Figure 30 shows a map of the 294 buildings, per village. All other acquired data are linked to this geographic data. Each point on the map contains the information of that household, as well as the flood height of one or two historic flood events and the corresponding damages.

In Figure 31, the damage factors for buildings, based on the water levels and corresponding damage degrees gathered during the surveys, are visualized. The graph shows an overall upward trend, indicating a linear relationship between the degree of damage to a residential building and the water level. However, there are a few small

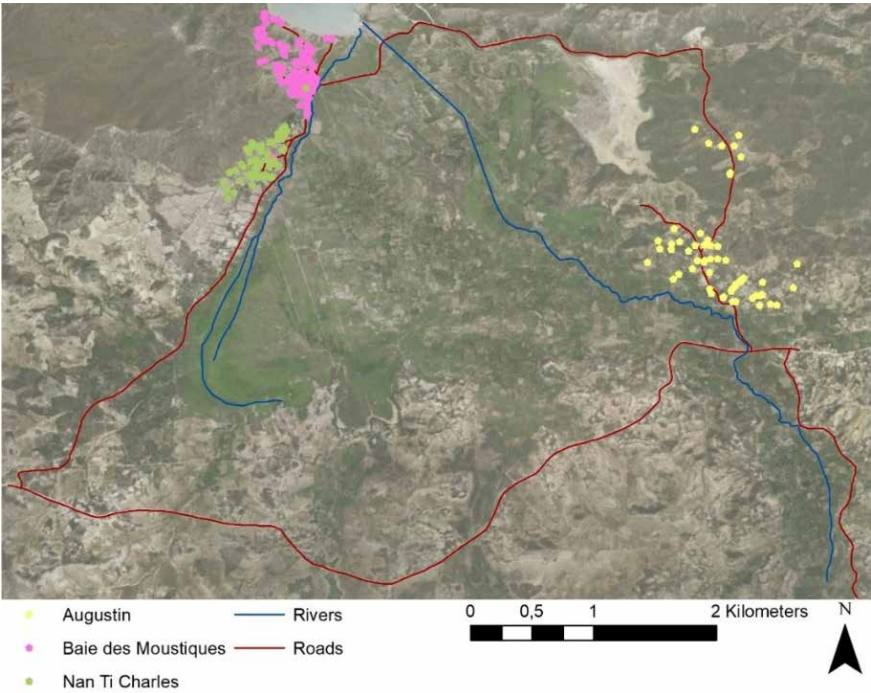


Figure 30 Location of residential buildings in the floodplain of the catchment of the river Moustiques, Haiti, based on the coordinates acquired by questionnaires, conducted in January 2018 (Glas & Deruyter, 2018).

Damage function for residential buildings

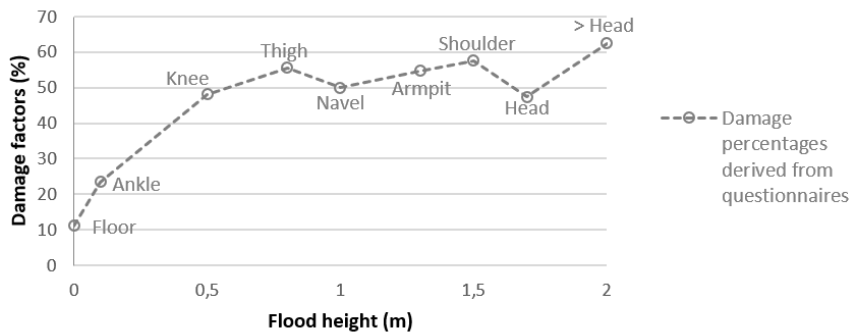


Figure 31 Depth-damage function for residential buildings in the floodplain of the catchment of the river Moustiques, Haiti. The vertical axis shows the degree of damage to the building, while the horizontal axis displays the water level.

peaks visible on the graph. These can be explained by the uneven distribution of the number of flood events per water height. While 201 questioned people described a flood with a water level 'head', there were only 9 described inundations with a water level 'knee' and 9 with a water level 'thigh'. The damage factor for the 'head' water level will thus be a lot more averaged than the factor for the other water levels.

For the other elements at risk, the drafted depth-damage functions did not show any trend. For vehicles, this can be explained by the very low number of households that possess a vehicle. Only 1 household in the study area owned a car, 17 owned a motorcycle and 4 owned a boat. Furthermore, 58 households possessed one or more horses that they use for transport, 109 animals in total. In the most recent flooding, in January 2018, the car was not damaged, but 4 motorcycles and 2 boats were. Of the 109 horses, 19 did not survive the inundation. While these numbers include all vehicles in the entire study area, and are thus representative, they are too low to create adequate damage factors per water level.

Although there was sufficient information on crops and livestock, the drafted depth-damage functions did not have the expected result as there was no trend visible. All data on flood damages are linked to the GPS locations of the questionnaires. The acquired flood heights are thus the water levels as observed in the houses. However, the farmlands are located in the center of the floodplain. The animals are also kept in these fertile grass areas, and not near the villages. Therefore, there is no relationship between the water level and the damages to farmland and livestock, as these are not in the same location. Nonetheless, the analysis of the damages to these agricultural activities has shown that these elements are highly affected by flooding. 227 people of the 294 questioned had livestock. Only 22 of these households did not lose any animals during the flooding of January 2018. On the other hand, 62 of them have lost all livestock. In total, 58% of all animals in the study area have died during this inundation. An overview of the damages to the crops can be seen in Table 18.

Table 18 Overview of the damage percentages for the crops in the floodplain of the river Moustiques, Haiti, after the flooding in January 2018. The second column shows the number of households that own farmland with this type of crop (Glas & Deruyter, 2018).

CROP	NUMBER OF HOUSEHOLDS	DAMAGE PERCENTAGE (%)
Corn	178	67.69
Beans	168	62.24
Plantain	156	78.00
Shallot	129	85.93
Banana	59	36.95
Millet	52	42.01
Sweet potato	41	48.67
Manioc	32	35.19
Others	9	25.00
TOTAL		72.25

In total, the damage percentage for crops was 72.25% for the flooding of January 2018. Shallot and plantain are the most vulnerable for inundation, with the highest damage factors, followed by corn and beans. These four crops are not only the least resilient to flooding, but are also the most cultivated in the study area. Banana and manioc have a much lower damage factor, but are also less cultivated. These damage percentages, for farmland as well as for livestock, clearly show the high impact of flooding in the rural study area. Therefore, a flood map will be created for the entire floodplain. Then, the generated water levels in the center of the floodplain can be linked to the acquired damage degrees and adequate depth-damage functions can be drafted.

4.5 Discussion and conclusions

The acquisition of flood data forms a major challenge in developing regions. In these areas, conducting questionnaires offers new possibilities, as it is a low-cost, fast and targeted acquisition method that can provide information on historic floods that is otherwise inexistent. As the information can be gathered at any time, the need to perform real-time measurements during a disaster is eliminated. Several studies have shown that this form of ‘citizen science’ is valuable, certainly in areas where other historic data are inexistent (Fast & Rinner, 2014; Hultquist & Cervone, 2018). However, the data are subjective, as the memory of a person is not always an accurate and objective recollection of the event. Extreme events such as flooding can have a traumatic effect on people, causing their memory of the event to be unreliable. This subjectivity is inherent to the used technique, as Babbie (2013) defined the basic objective of a questionnaire as to obtain not only facts, but also opinions about a phenomenon from people who are informed on a specific issue. Furthermore, the composition of the questions is extremely important as unclear questions can cause confusion and unusable answers. While some of these concerns can be addressed, for example by briefing the pollsters and providing background information, there is still a risk of systematic bias. Results

should thus be always critically analyzed, keeping the subjectivity of the respondents in mind. Previous studies using questionnaires to gather recent flood data, where validation was possible, have proven the accuracy of this data acquisition technique (Suriya et al., 2012; Thieken et al., 2017). The first test was performed in the floodplain of the river Moustiques, only a few days after a severe flood event. The answers show that the inhabitants have a clear and complete recollection of that recent flood, while the answers given on older flood events were often incomplete and even inconsistent.

This first test, where questionnaires were used to develop location-specific depth-damage functions, clearly shows the potential of this type of citizen science. The generated depth-damage function for buildings can be implemented in a qualitative risk assessment, where different degrees of damage are linked to a certain water level, rather than the specific percentages. The first analysis of the questionnaires clearly indicated the high impact of flooding on other damage types, such as the agricultural activities in the rural study area. 58% of the livestock was killed by the flooding of January 2018 and 72.25% of the crops were damaged during that same inundation. In order to create depth-damage functions for these damage types, however, the questionnaire should be adapted, with a more direct link between the indicated water level and the land use type where that level was observed.

Future research should focus on techniques to create a more even distribution in the descriptions per flood height. This will lead to better averaged and more representative damage factors for each water level. In this case study, 294 people of the total population of 1,848 were questioned. Increasing this number is a first step, but the setup of the questionnaire should also be evaluated to optimize the line of questioning. Adapting the questionnaire will lead to an increase in the valuable data that can be derived from the answers.

While this data acquisition technique offers indispensable input for developing countries, developed regions such as Flanders, Belgium, already rely on a large amount of detailed and accurate input data to perform a flood risk assessment. However, the use of questionnaires can benefit these regions as well. Firstly, these degrees can be used to develop location-specific depth-damage functions for crops, buildings and roads, since the functions used in current flood risk assessment are derived from literature and are not always representative for the study area. Another benefit of this acquisition method is the active involvement of citizens. The questionnaire raises awareness of flood risk among the respondents and offers them a means to share their concerns on the subject. This leads to an empowering effect on the residents of the area at risk. This low-cost method thus provides a whole range of new possibilities to generate and validate flood risk maps, as well as to communicate flood risk with the population.

ACKNOWLEDGMENTS

The authors would like to thank Join for Water, our Belgian partners as well as the local Haitian employees, for facilitating our field work and sharing their knowledge and data on the study area. Furthermore, we would like to thank everyone at ODRINO for assisting us on the field and aiding in any way possible during our stay in Moustiques. Finally a word of gratitude to the Research Foundation – Flanders (FWO) for funding the field work.

REFERENCES

- Babbie, E. R. (2013). *The basics of social research*, Cengage learning.
- Bird, D. K. (2009). The use of questionnaires for acquiring information on public perception of natural hazards and risk mitigation—a review of current knowledge and practice. *Natural Hazards and Earth System Sciences*, 9(4), 1307-1325. doi: 10.5194/nhess-9-1307-2009
- Dolisca, F., McDaniel, J. M., Teeter, L. D., & Jolly, C. M. (2007). Land tenure, population pressure, and deforestation in Haiti: The case of Foret des Pins Reserve. *Journal of Forest Economics*, 13(4), 277-289. doi:10.1016/j.jfe.2007.02.006
- Fast, V., & Rinner, C. (2014). A systems perspective on volunteered geographic information. *ISPRS International Journal of Geo-Information*, 3(4), 1278-1292. doi: 10.3390/ijgi3041278
- Glas, H., & Deruyter, G. (2018). *Questionnaires sur l'impact des inondations dans le bassin versant de la rivière Moustiques, Haïti*.
- Government of Haiti (2010). *Analysis of Multiple Natural Hazards in Haiti (NATHAT)*. Retrieved from <https://reliefweb.int/report/haiti/analysis-multiple-natural-hazards-haiti-nathat>
- Huizinga, J., De Moel, H., & Szewczyk, W. (2017). *Global flood depth-damage functions: Methodology and the database with guidelines*. Retrieved from https://publications.jrc.ec.europa.eu/repository/bitstream/JRC105688/global_flood_depth-damage_functions__10042017.pdf
- Hultquist, C., & Cervone, G. (2018). Citizen monitoring during hazards: Validation of Fukushima radiation measurements. *GeoJournal*, 83(2), 189-206. doi: 10.1007/s10708-017-9767-x
- McGrath, H., El Ezz, A. A., & Nasteve, M. (2019). Probabilistic depth–damage curves for assessment of flood-induced building losses. *Natural Hazards*, 97(1), 1-14. doi: 10.1007/s11069-019-03622-3
- Merz, B., Kreibich, H., Schwarze, R., & Thieken, A. (2010). Assessment of economic flood damage. *Nat. Hazards Earth Syst. Sci.*, 10(8), 1697-1724. doi: 10.5194/nhess-10-1697-2010
- Nascimento, N., Baptista, M., Silva, A., Léa Machado, M., de Lima, J. C., Gonçalves, M., ... Machado, É. (2006). Flood-damage curves: Methodological development for the Brazilian context. *Water Practice and Technology*, 1(1). doi: 10.2166/wpt.2006.022
- PROTOS (2011). Évaluation transversale 2010 – Mise en œuvre de la stratégie GIRE et intégration de la problématique changement climatique – Etude de cas – Haïti. Retrieved from https://www.joinforwater.ngo/sites/default/files/publications/files/2.evaluation_gire_et_cc_haiti_version_finale.pdf

- Rossillon, F. (2016). *Face à la détresse humaine et environnementale, Gestion Intégrée de l'Eau et Ecosanté, leviers de développement pour une Haïti nouvelle*. In L'eau dans les pays en développement – Retour d'expériences de gestion intégrée et participative avec les auteurs locaux (pp. 313-366). Belgium.
- Santillan, J., & Makinano-Santillan, M. (2016). Vertical Accuracy Assessment of 30-M Resolution ALOS, ASTER, and SRTM Global DEMs over Northeastern Mindanao, Philippines. *International Archives of the Photogrammetry, Remote Sensing & Spatial Information Sciences*, 41, 149-156. doi: 10.5194/isprsarchives-XLI-B4-149-2016
- Scorzini, A., & Frank, E. (2017). Flood damage curves: new insights from the 2010 flood in Veneto, Italy. *Journal of Flood Risk Management*, 10(3), 381-392. doi: 10.1111/jfr3.12163
- Sprake, J., & Rogers, P. (2014). Crowds, citizens and sensors: process and practice for mobilising learning. *Personal and ubiquitous computing*, 18(3), 753-764. doi: 10.1007/s00779-013-0715-6
- Suriya, S., Mudgal, B., & Nelliya, P. (2012). Flood damage assessment of an urban area in Chennai, India, part I: methodology. *Natural Hazards*, 62(2), 149-167. doi: 10.1007/s11069-011-9985-3
- Thieken, A., Kreibich, H., Müller, M., & Lamond, J. (2017). *Data collection for a better understanding of what causes flood damage—experiences with telephone surveys*. In Flood damage survey and assessment: new insights from research and practice, 95-106. doi: 10.1002/9781119217930.ch7
- UNDRR (2019). *Global Assessment Report on Disaster Risk Reduction*. Geneva, Switzerland: <https://www.undrr.org/publication/global-assessment-report-disaster-risk-reduction-2019#:~:text=The%202019%20Global%20Assessment%20Report,the%20global%20disaster%20risk%20landscape>.
- Wu, Z., Lv, H., Meng, Y., Guan, X., & Zang, Y. (2021). The determination of flood damage curve in areas lacking disaster data based on the optimization principle of variation coefficient and beta distribution. *Science of The Total Environment*, 750, 142277. doi: 10.1016/j.scitotenv.2020.142277

5

THE RURAL CASE STUDY: THE FLOODPLAIN OF THE RIVER MOUSTIQUES, HAITI

This chapter is adapted from the following journal article:

Glas H., De Maeyer P., Merisier S., Deruyter G. (2020). Development of a low-cost methodology for data acquisition and flood risk assessment in the floodplain of the river Moustiques in Haiti, *Journal of Flood Risk Management*, 13(2), 17p.
doi: 10.1111/jfr3.12608

ABSTRACT

Over the past two decades, Haiti was struck by 30 storm events and 40 floods, affecting over 3.5 million people. Being the poorest country in the Northern hemisphere, it is unable to allocate funds to risk assessment and management. Therefore, this research developed a low-cost methodology to analyze flood risk in data-poor regions. The floodplain of the river Moustiques was chosen as study area. First, a methodology was developed and input data were gathered from existing data, literature, field data, and open source data. Then, a flood risk assessment was performed for the area. The resulting economic risk map and social risk map indicate that the region is at risk for nearly 2 million USD and has potentially 60 casualties per year. Although the assessment was performed as a quantitative analysis, the resulting maps should be interpreted qualitatively, as the values could not be validated. Nonetheless, the results clearly indicate the high-risk areas where measures should be taken. Furthermore, this research shows the potential of citizen science, in the form of a questionnaire survey conducted in the floodplain. This low-cost and fast acquisition method provided many different input data for flood risk assessment, from population data to damage factors and validation information on historic flooding.

Keywords: flooding, risk methodology, citizen science, data-poor regions, Haiti

5.1 Introduction

Since its independence in 1804, the republic of Haiti is plagued by political instability, war and revolution. Due to its turbulent history that hindered the economic and human development, there is an extremely limited availability of basic services such as water supply, sanitation, health care and education (Kijewski-Correa et al., 2018). As a result, the island state is currently the poorest country in the northern hemisphere (Rossilon, 2016). Based on the household survey of 2012, conducted by the International Household Survey Network (IHSN), the World Bank concludes that over 6 million Haitians, equal to 59% of the total population, live below the national poverty line of 2.41 USD per day. Furthermore, over 2.5 million, or 24%, inhabitants fall below the national extreme poverty line of 1.23 USD per day. (World Bank, 2018) Moreover, year by year, Haiti is ranked lower in the Human Development Index. This index of the United Nations Development Programme (UNDP) represents the wellbeing of the population in reference to the life expectancy, the degree of education and the Gross National Income (GNI) of a country. In the most recent ranking of 2017, Haiti is ranked 168th of 189 countries with a score of merely 0.498 on a scale of 0 to 1, losing 19 places in comparison to the Human Development Index of 2009 (UNDP, 2011, 2018).

Haiti is located on the island Hispaniola, sharing its eastern border with the Dominican Republic, in the Greater Antilles archipelago of the Caribbean Sea. The islands topography is defined by high and steep mountains, as 63% of the countries surface has a slope of 20% or more (Rossilon, 2016). With a mere 3% forest cover, Haiti is one of the most deforested states worldwide (Dolisca et al., 2007). Furthermore, the country is located in the Hurricane Belt, the area with the highest occurrence rate of hurricanes and tropical storms worldwide (Wallemacq et al., 2018). All these elements led to an extreme vulnerability towards natural hazards, in specific hydro-meteorological disasters such as storm surges and flooding.

According to the EM-DAT database, Haiti has suffered through 30 storm events and 40 floods in the past two decades, leading to a total of 7,680 deaths and more than 3.5 million people affected (CRED, 2018). In May 2004, extreme and intense precipitation, originated by a tropical depression, led to flash floods of the river Soliette, destroying 1,698 houses and damaging another 1,687. Furthermore, the flood event killed 1,059 and injured 153 Haitians (Brandimarte et al., 2009). Only a few months later, in September 2004, Tropical Storm Jeanne struck the country, causing widespread flooding and killing approximately 2,800 people (Colindres et al., 2007). The island state is not only vulnerable to flood events, but also suffers regularly from seismic activity. In January 2010, a 7.0 magnitude earthquake struck the capital Port-au-Prince. This disaster caused over 220,000 deaths and displaced more than 2.3 million Haitians (OCHA, 2010). The affected area barely had time to recover, as two years later Hurricane Isaac crossed the southern peninsula of Haiti. The associated flooding affected 70,000 people, living in 180 still remaining earthquake refugee camps (Heimhuber et al., 2015; OCHA, 2012). On the 4th of October 2016, the passage of Category 4 Hurricane Matthew over the same peninsula caused major floods across the country, severely damaging roads and houses. The impact on the residential infrastructures was similar to the

2010 earthquake (Kijewski-Correa et al., 2018). In the arrondissement Les Cayes, 80% of all residential buildings was destroyed (OCHA, 2016). Even more than the severity of these disaster events on their own, their high frequency and the repeated impacts on the population and infrastructure, form a major challenge for Haiti and hinder its development. This is proven by the island state's second place on the Global Long-Term Climate Risk Index ranking (Eckstein et al., 2018).

Hazard risk assessments attempt to minimize the impact of disasters by identifying and localizing the high-risk areas and by estimating the cost of material and human losses associated with natural hazards. HAZUS-MH, for example, is a multi-hazard risk assessment tool developed by the US Federal Emergency Management Agency (FEMA) (Tate et al., 2015). Although specifically designed for the United States, HAZUS-MH is for many researchers worldwide the standard in damage and loss estimation and thus widely used for earthquake, hurricane and flood risk analyses (Bendito et al., 2014; Levi et al., 2015; Park et al., 2016). The available statistical and quantitative information of this tool, however, is not representative for each study area (Jongman et al., 2012). A number of other GIS-based tools provide a more region-specific approach to flood risk mapping specifically, such as the HISS-SSM model for the Netherlands, the LATIS model for Flanders, Belgium, and the FLEMO model for Germany (Apel et al., 2009; Kok et al., 2005; Vanneuville et al., 2005). These tools all use the same methodology, that has provided adequate results in areas where extensive and detailed input data are available. In many developing countries, however, models with this methodology and high input-needs do not offer adequate results, due to the lack of detailed data. In these data-poor regions, such as Haiti, flood risk mapping is limited to innovative approaches for specific case study areas. Brandimarte et al. (2009) developed a flood risk mitigation plan for the catchment of the river Soliette, based on a numerical model of one historic flood event. Domeneghetti et al. (2015) implemented topographical surveys and hydraulic analyses to further plan flood mitigation measures in the region. However, for most Haitian rivers, historic flood data, as well as topographic and bathymetric data, are completely inexistent. Therefore, Joseph et al. (2018) reconstructed the riverbed and floodplain of the Cavaillon River using differential GPS and a UAV. Heimhuber et al. (2015) created a flood risk assessment for Onaville in Haiti, based on design floods derived from intensity-duration-frequency (IDF) curves in absence of historic flood information. The topography of the risk area and the river channel geometry were reconstructed using a combination of LIDAR, drone-photogrammetry and Satellite (TanDEM-X) DEMs. While these projects produced valuable results for their respective study areas, the individuality of the different approaches and data needs hinder the implementation of these methodologies in other areas or on a wider scale. Therefore, in this research a low-cost methodology was developed for data acquisition and flood risk analysis, applicable in all data-poor regions and on different scale levels. Furthermore, this paper focuses on the applied data acquisition methods and their possible implementation on a wider scale.

5.2 Flood risk methodology

The generic flood risk assessment methodology developed for Annotto Bay, Jamaica by Glas et al. (2017) was enhanced to ensure a generic approach. This methodology focuses on two types of risk: economic and social risk. The former implies the potential direct damage to elements at risk, such as buildings, roads and crops, and is expressed in USD m⁻² per year, while the latter is calculated in number of casualties per m² per year (Glas et al., 2017).

The economic risk map is based on land use information, such as the location of roads, buildings and farmlands. The associated vulnerability is calculated by combining this land use data with the replacement values per land use type, which are the costs to replace these elements at risk in case of total destruction. This calculation leads to a maximum damage map, showing the vulnerability of the region, expressed in USD m⁻². In a next step, the damage for one hazard event with a specific Annual Exceedance Probability (AEP) is calculated by combining the maximum damage map with a flood hazard map that shows the flood depths. The relation between hazard and vulnerability is determined by the damage factor α , the percentage of damage for each specific element at risk for a certain flood height. The calculations for social risk follow the same workflow. However, instead of land use data, population data are required as input and combined with the flood hazard map using a mortality factor β that defines the percentage of casualties for each flood depth. In a final step, the economic and social risk maps are created by combining the damage or vulnerability maps for the different AEPs.

Glas et al. (2016) analyzed the sensitivity of this risk assessment methodology to its input data in order to define a minimum set of input data, indispensable for an adequate assessment. A main conclusion was the importance of the availability of accurate and detailed road network data. Furthermore, the possibility to use population information was proven useful for economic risk calculations in the absence of detailed building information. These findings were the base of the fieldwork and research presented here.

5.3 Study area

The northwest of the island state Haiti is characterized by an overall extremely dry climate, and the 46 km long river Moustiques is one of the rare permanent waterways in this region. Its catchment covers an area of 222 km² and has 40,000 inhabitants (Rossilon, 2016). The river rises from the mountain range Massif de Terre Neuve at a height of 697 m and flows into the sea canal Canal de la Tortue between the mainland and the island Île de la Tortue at the Baie de Moustiques.

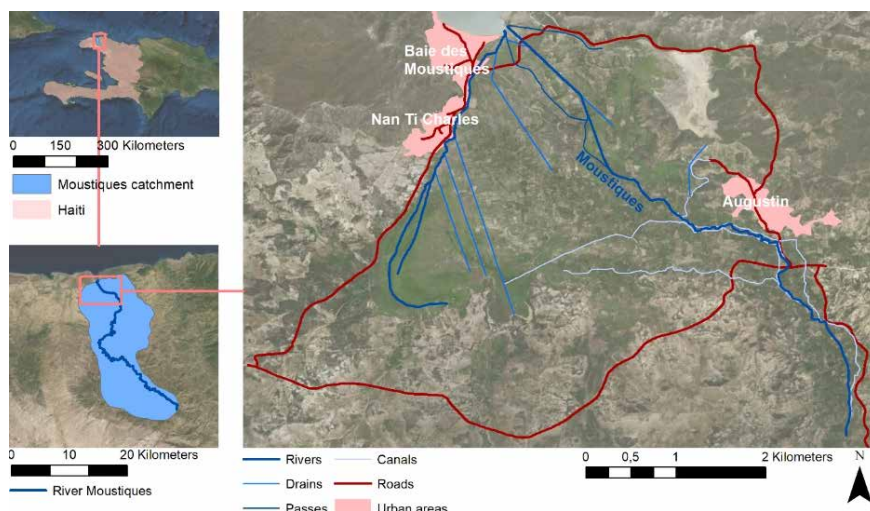


Figure 32 Study area: floodplain of the river Moustiques in the northwest of Haiti (based on Glas et al. (2018)).

Although the climate in the area is arid, the catchment receives a considerable amount of rain that varies between 500 mm and 1,200 mm per year (PROTOS, 2011). In 2010, the Haitian government distributed a nationwide flood hazard map, in which the floodplain of the Moustiques was classified as vulnerable to exceptional hazards, which are defined as cyclones, storms and hurricanes that produce as much as 600 mm precipitation in 24 hours (Government of Haiti, 2010). Several canals irrigate the agricultural lands (Figure 32) that take up the largest part of the floodplain. The drains were constructed to quickly discharge an excess of water during a flood event. For that same purpose, two tributaries of the Moustiques, called Passes in the region, were dug manually. The roads surrounding the floodplain are unpaved streets with a width of approximately 6 meters thus allowing car traffic in the region. The many smaller tracks for pedestrians are not shown on the map.

The floodplain of the river Moustiques with a total area of 20 km² and a population of 1,868 people was chosen as study area (Figure 32). Three villages are included in the study: Baie des Moustiques, located at the coastline of the bay, the neighboring village of Nan Ti Charles, and Augustin, situated on the eastern side of the floodplain.

5.4 Input data

The necessary input data can be divided into four categories: land use data, economic data, flood hazard maps and population data. The input in each of these categories can be subdivided into spatial or numeric data. While land use information, flood data and population densities are classified as spatial data, the replacement values and damage factors in the economic data category are numeric data. Table 19 presents an overview of the input data and their source of acquisition.

Table 19 Overview data types and sources for the flood risk assessment of the floodplain of the river Moustiques, Haiti.

SPATIAL DATA		
Data type	Acquisition source type	Exact source
Buildings	Open source data	OSM (OpenStreetMap)
Roads	New data + Open source data	Field work 2018 (Chapter 4) + OSM
Crops	Existing data	Join For Water GIS data
Population density	New data	Field work 2018 (Chapter 4)
Flood hazard map	New data	Antea Group
NUMERIC DATA		
Data type	Acquisition source type	Exact source
Replacement values for		
- Buildings	Literature	UCLBP (2016) + IHSI (2003)
- Roads	Literature	Collier et al. (2015) + MTPTC (2001)
- Crops	Open source data	(FAOSTAT, 2017)
Damage factors for		
- Buildings	New data	Field work 2018 (Chapter 4)
- Roads	Literature	Vanneuville et al. (2003)
- Crops	New data	Field work 2018 (Chapter 4)
Mortality factor	Literature	Vanneuville et al. (2003)

5.4.1 Land use data

The land use categories taken into account in this research were the location of buildings, agricultural lands, and the road network. Other land use types that occur in the study area, such as wetlands and natural vegetation zones, were not included in the analysis since their economic replacement value in case of flooding is considered to be negligible and is therefore set to 0.00 USD m⁻² (Vanneuville et al., 2003). The building data are a polygon shapefile downloaded from OSM.

Volunteers drew the buildings as part of a mapping action from HOT (Humanitarian OpenStreetMap Team) after the passage of Hurricane Matthew in Haiti, in October 2016. High resolution aerial imagery, donated by Digital Globe, was used as base map (HOT, 2016). For this research, the accuracy of the OSM building dataset was validated with differential GPS coordinates of a small set of buildings, acquired during fieldwork in January 2018. Furthermore, manually re-mapping all buildings in Baie des Moustiques and Nan Ti Charles, present in the Digital Globe imagery of January 2017, validated the completeness of the OSM buildings.

During the field campaign of 2018 also a large part of the road network was measured by means of differential GPS. This newly created dataset was then complemented with data from the same HOT project.

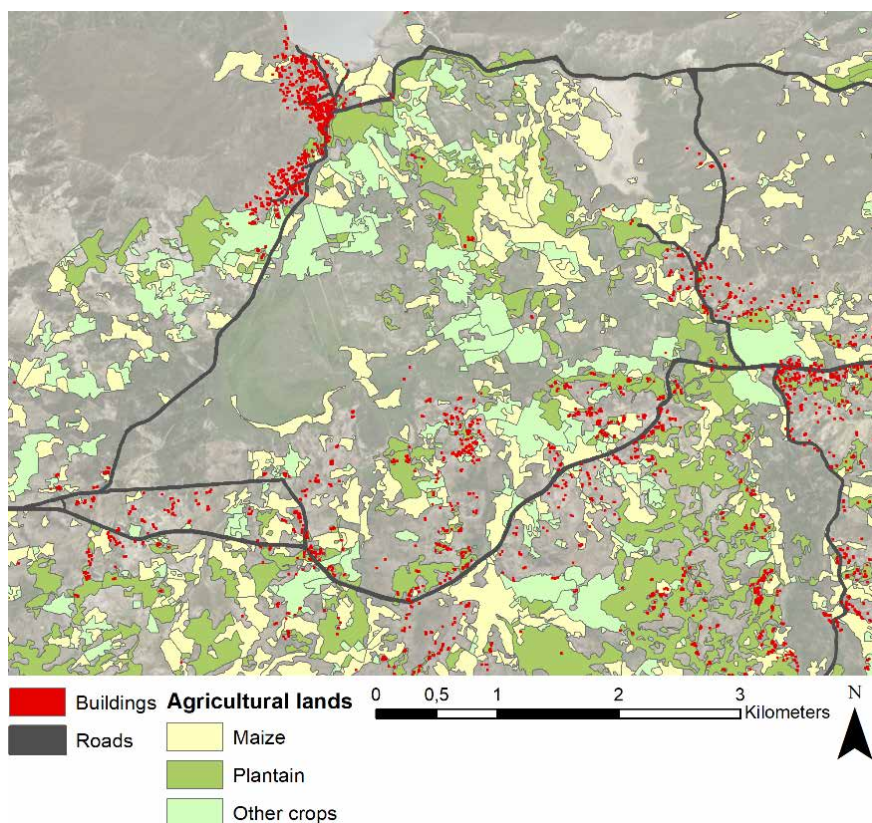


Figure 33 Land use map showing the land use taken into account in the economic flood risk assessment of the floodplain of the river Moustiques, Haiti (data source: OpenStreetMap, Join For Water and own data).

The land use type agricultural lands was extracted from an existing polygon land use dataset, acquired by the Belgian NGO Join For Water. This dataset contains three types of land use: plantain, maize, and other crops. Although the data have a high level of detail, the metadata is missing and thus, the data and method of data acquisition is unknown. Therefore, an assessment and a validation of the completeness and correctness of the crop data was done during the fieldwork GPS measurements. Figure 33 shows the land use map used for the study area, combining building, road and crop data.

5.4.2 Economic data

Each element at risk, as determined in the land use maps, is linked to a replacement value, expressed in USD m⁻². For all building types, the same average value was used, because Glas et al. (2016) proved in the sensitivity analysis of input data for flood risk assessments that using one average replacement value provides accurate flood risk results. The average value for buildings used for this case study is shown in Table 20 and was drafted based on two literature sources. The first was a report from

the UCLBP describing the damages to civil constructions after the passage of Hurricane Matthew (UCLBP, 2016). This report describes five types of residential housing and their cost per square meter, as well as the average surface: precarious housing (tents, structures made from construction waste or clay), taudis (slum housing), ajoupas (wooden structures), one-level housing and apartments. Based on this information, an average replacement value per housing type was calculated. The second source is a national questionnaire survey on the living conditions in Haiti, executed by the IHSI in 2003 (IHSI, 2003). In the results, distribution percentages of the housing types are given for each department. Other housing types, that is not included in the five types of residential housing as defined in the report of UCLBP (2016), are linked to an average replacement value of the other types as more exact information was not available. The spatial building data from OSM do not differentiate in types of housing, but the results from the questionnaires do show large differences in occurrence for each housing type. Therefore, the distribution percentages for the department Nord-Ouest were used as weights to calculate a weighted average replacement value for buildings in the study area.

Table 20 Distribution percentages and replacement values for buildings in the catchment of the river Moustiques, Haiti, based on reports from the UCLBP (2016) and the IHSI (2003).

Housing type	Distribution percentage (%)	Replacement value (USD m ²)
Precarious housing	34.10	10.00
Taudis	8.85	20.00
Ajoupas	8.85	65.00
One-level housing	38.80	52.00
Apartments	1.30	52.00
Other types	8.10	39.80
Average		35.01

All roads in the study area are unpaved roads with an average reconstruction value of 150,000 USD km-1 in Haiti (MTPTC, 2001). According to the ROCKS (Roads Cost Knowledge System) database, which includes eight different Haitian road projects, Haitian roads have an average width of 6 meters (Collier et al., 2015). This was confirmed for the study area by random checks during the fieldwork in 2018. Combining the two literature sources, a replacement value for roads of 25.00 USD m-2 was calculated. Since there is no classification in the spatial road dataset, this value was set for every road in the study area.

Finally, the replacement values for crops were calculated based on open source data from the Food and Agriculture Organization of the United Nations (FAOSTAT). For 15 crop types that are cultivated in the study area, the total cultivated surface and the gross production value for Haiti in 2017 were listed (Table 21). Then, the values of all crops – except for maize and plantain – were averaged to determine the replacement value. As maize and plantain are specified separately in the spatial data, these types require a separate replacement value.

Table 21 Replacement values for crops in the catchment of the river Moustiques, Haiti, based on data from FAOSTAT (2017).

Crop type	Replacement value (USD m ⁻²)
Bananas	0.14
Beans	0.04
Cassava	0.05
Coconuts	0.03
Eggplants	0.24
Fruits, fresh	0.19
Mangoes	0.46
Onions	0.11
Pumpkins	0.21
Sweet potatoes	0.04
Tomatoes	0.57
Vegetables, fresh	0.09
Yams	0.20
Average other crops	0.18
Maize	0.01
Plantains	0.14

5.4.3 Population data

During the fieldwork in January 2018, a survey was conducted among all 294 households residing in the three villages located in the study area, indicated in Figure 32. In the general household information section of the questionnaire, data on the composition of, and the number of people in the households, were registered (Glas et al., 2018). Each questionnaire was linked to a GPS location. For the visualization of the number of inhabitants, this point data were aggregated in a raster with a 30mx30m resolution. Then, the total population numbers were processed into a population density map (Figure 34).

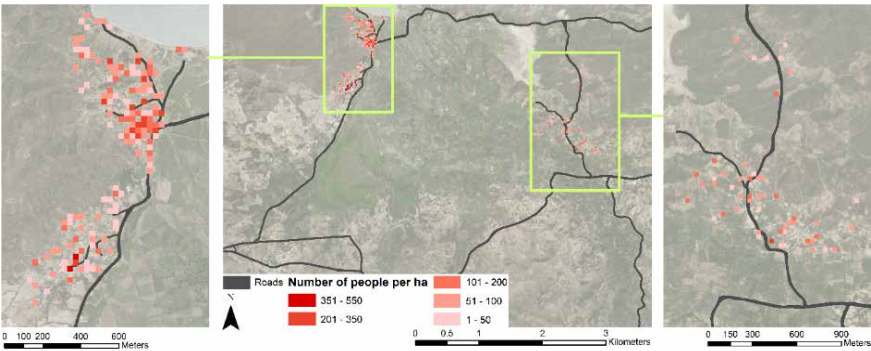


Figure 34 Population density map for the floodplain of the river Moustiques, Haiti.

5.4.4 Flood hazard maps

For the whole catchment of the Moustiques, Antea Group created three flood hazard maps in raster format (30mx30m) for respective AEPs of 50%, 10% and 2%. Flood hazard was mapped in terms of flood heights using openLISEM, a spatial hydrological model that simulates runoff, sediment dynamics and shallow floods (De Roo et al., 1994). Land cover input was derived from Globcover (300mx300m) using a compilation of parameters based on various experimental studies as proposed by Liu and De Smedt (2004). Soil mapping units from the FAO-UNESCO Soil Map of the World were converted into likely USDA soil texture classes, that served as base for associated hydrological parameters (Saxton & Rawls, 2006). The SRTM DEM was used as elevation input data. However, as the 30m resolution is insufficient to describe the morphology of the river network accurately, the catchment river network was extracted as vector data from OSM and added to the model. The statistical component of flood hazard, the AEP, was incorporated based on an Intensity-Duration-Frequency (IDF) curve for West-Puerto-Rico (NOAA) as there was no curve available for the study area. However, the curve was compared to Cuban and Bahamian studies and was proven consistent for the Caribbean area. The results of the flood mapping methodology in openLISEM were verified by Antea Group against a similar analysis carried out for Papua New Guinea, which was validated using existing flood hazard maps in that region (De Sutter et al., 2018). Figure 35 visualizes the flood extent and water heights in the floodplain of the river for each AEP.

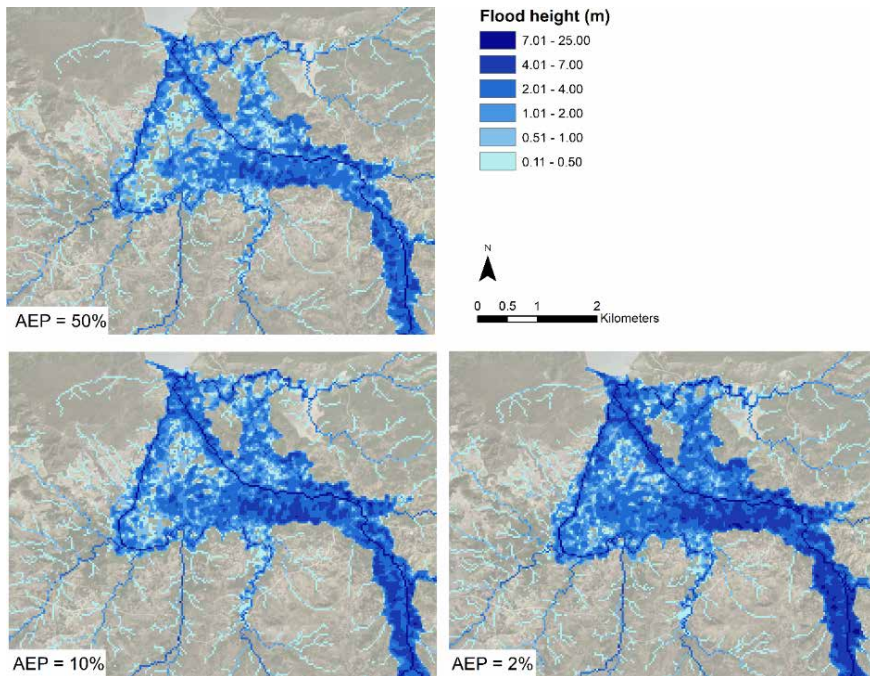


Figure 35 Flood hazard maps with AEP of 50% (top), AEP of 10% (bottom left) and AEP of 2% (bottom right) for the floodplain of the river Moustiques, Haiti (based on Antea Group 2018).

5.4.5 Damage and mortality factors

The damage factors for the economic risk calculations were derived from different sources. For buildings, they were based on the questionnaires from 2018 in which the inhabitants were questioned about their knowledge of historic flooding and the corresponding damages to their house ('no damage', 'limited damages', 'large damages' or 'complete destruction'). In total, 19 different flood events were described in 347 responses (Glas et al., 2018). The derived flood damage factors are visualized in Figure 36. Although these percentages do not show a linear increase, the assumption was made that a higher flood level will always result in a damage percentage equal to, or higher than, the previous factor. The in this way adapted damage factors are shown as the depth-damage function for residential buildings in Figure 36 and were used as such as input in this risk assessment. Figure 37 visualizes the functions for all land use types up to a water height of 2 meters. As most buildings in the study area are one-level buildings, the flood water is able to damage the roof of the building when surpassing the height of 2 meters. This extra roof damage is visible in the function in the form of an upward kink at 2 meters.

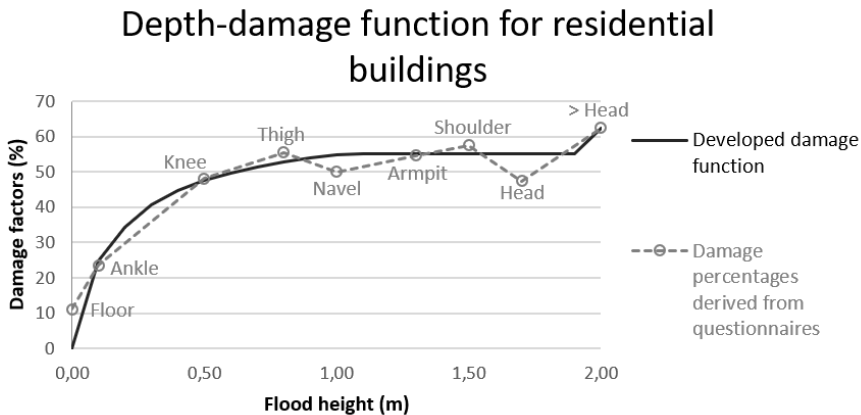


Figure 36 Depth-damage function for residential buildings in the floodplain the river Moustiques, Haiti. The vertical axis shows the degree of damage to the building in percentages; the horizontal axis displays the water level (Glas et al., 2018).

The damage factors for roads are based on the function that was drafted by Vanneuville et al. (2003) for roads and railroads:

$$(10) \quad f = \min(0.28 \times d; 0.18 \times d + 0.1; 1)$$

In Equation (10), f is the damage factor and d is the water height in meter.

Damage to crops is not only determined by the water height, but also by the duration of the flood and the time of the year that the flood occurs (Dutta et al., 2003). However, the flood hazard map only provides information on the water height for a certain AEP. As

there are no adequate depth-damage functions available in literature that are based on only the water height for the crops cultivated in the study area, only one damage factor was taken into account per crop type. These factors were derived from data on historic flood events gathered in the questionnaires from 2018 (Glas et al., 2018). In Figure 37, the depth-damage functions for all elements at risk are shown separately.

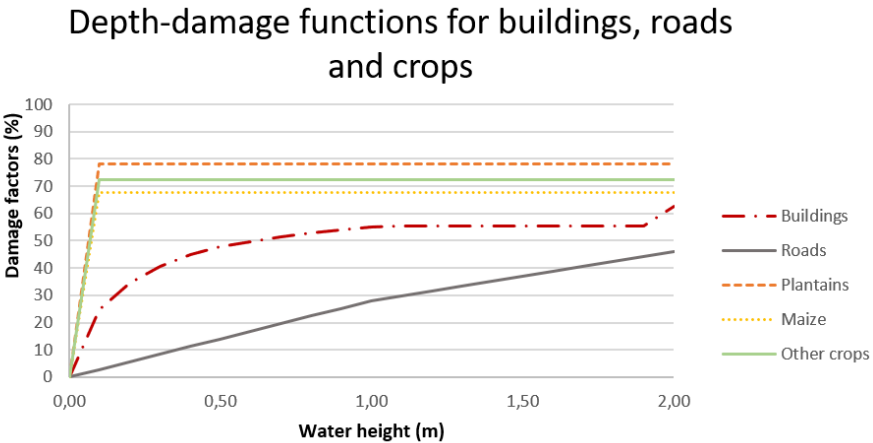


Figure 37 Depth-damage functions for buildings, roads and crops in percentages for water heights from 0.00m up to 2.00m for the floodplain of the river Moustiques, Haiti, based on Glas et al. (2018) and Vanneville et al. (2003).

To calculate the social risk, a depth-mortality function is used to define the relation between the number of people living in an area and the flood height in that same area. The number of casualties is expressed with following depth-mortality function, based on Vrisou van Eck et al. (1999):

$$(11) \quad N = \exp(1.16 \times d - 7.3) \times P$$

In Equation (11), N is the number of casualties, d is the water height and P is the total population. The mortality factor only accounts for the potential number of people killed by flooding, not for affected or wounded people.

5.5 Results

5.5.1 Economic risk calculations

In the first step of the methodology, a maximum damage map (Figure 38) was created by combining the land use data with the replacement values for each land use type. This map visualizes the damage costs for the study area if all elements would be completely destroyed.

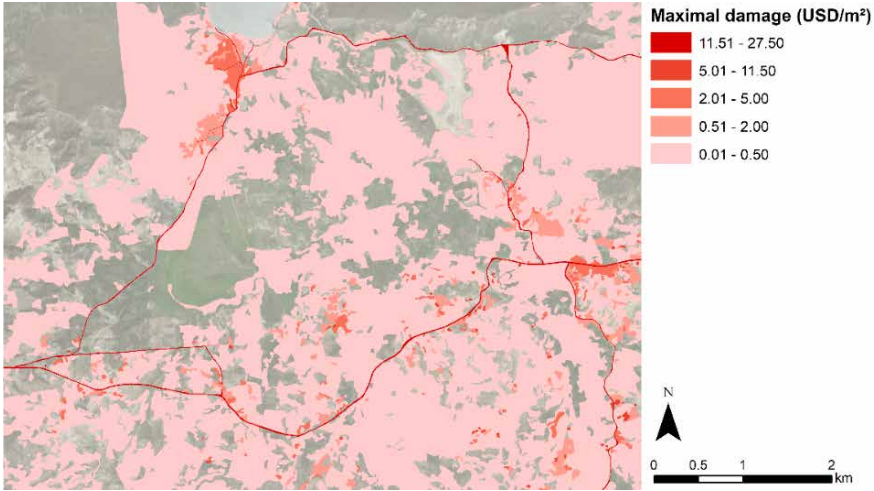


Figure 38 Maximum damage map for the floodplain of the river Moustiques, Haiti.

The agricultural fields take up the largest area in the floodplain. However, due to the low replacement value, the total maximum damage for crops is less than half the damage for buildings (Table 22). The highest maximum damage value, nearly 8 million USD, belongs to the road network. In total, a value of over 13 million USD is at risk in the floodplain of the river.

Table 22 Overview of the maximum damage values for the floodplain of the river Moustiques, Haiti.

	Total maximum damage (USD)
Buildings	3,823,250
Crops	1,598,100
Roads	7,790,900
Total	13,212,250

By combining the maximum damage values with the water heights in the flood hazard maps using the acquired damage factors, three economic damage maps were created with respective AEPs of 50%, 10% and 2%. (Figure 39). Table 23 shows the calculated damage values for each of these three scenarios. Although visually, virtually no difference is noticeable between the economic damage maps, the total damage values in Table 23 show significant deviations, e.g. the total damage cost of the 2% AEP flood exceeds the one of the 50% AEP flood with 15%. It is clear that the road damage cost is the determining factor for this difference.

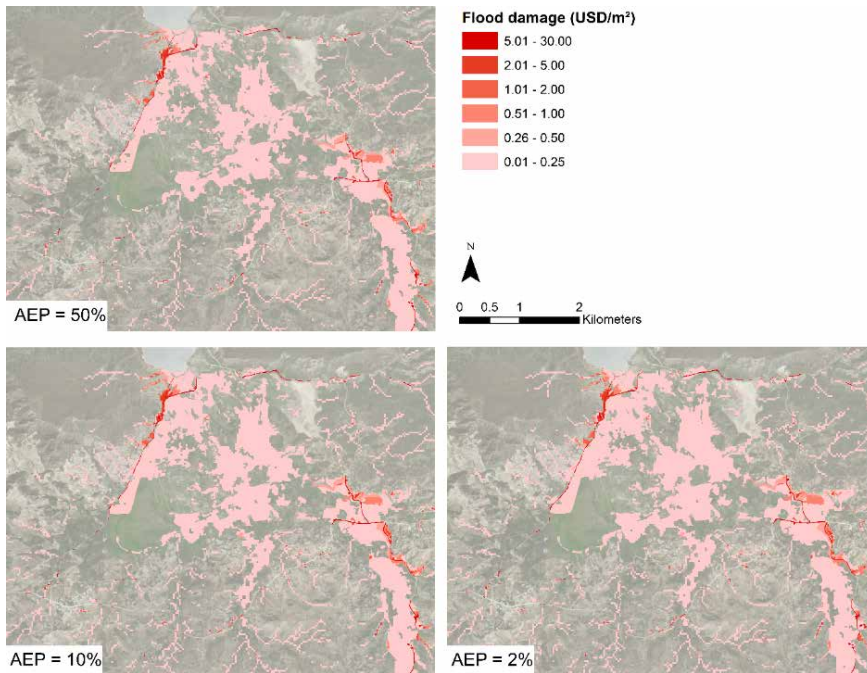


Figure 39 Economic damage maps for floods with AEP of 50% (top), AEP of 10% (bottom left) and AEP of 2% (bottom right) for the floodplain of the river Moustiques, Haiti.

Table 23 Overview of the estimated damage values for a 50% AEP flood, a 10% AEP flood and a 2% AEP flood for the floodplain of the river Moustiques, Haiti.

	AEP = 50%	AEP = 10%	AEP = 2%
Building damage (USD)	1,282,000	1,334,000	1,390,000
Crop damage (USD)	1,176,000	1,176,000	1,176,000
Road damage (USD)	1,368,500	1,616,000	1,862,250
Total damage (USD)	3,826,500	4,126,000	4,428,250
Total damaged area (m²)	7,047,500	7,576,750	8,052,750
Average damage (USD m⁻²)	0.54	0.58	0.62
Maximum damage (USD m⁻²)	27.49	27.49	27.49

The final step of the economic risk calculations consists of combining the three economic damage maps into one economic risk map showing the risk in USD m⁻² per year. This operation is defined as (Thieken et al., 2006):

$$(12) \quad R = \sum_{i=1}^k \frac{1}{i} \times D_i$$

In Equation (12), R is the risk, D_i is the damage that corresponds with an AEP of $1/i$ and k is the number of different flood hazard maps available. However, this expression overestimates the damage, as the same damages that occur to an element at risk in different flood scenarios are counted separately and then summed up. For example, if a

house is completely destroyed by a flood with an AEP of 50%, as well as by a flood with a 10% AEP, this damage will be counted double using Equation (12). Therefore, in this research, risk was expressed as a composed summation of the damages of a flood with an AEP of 100% and the extra damages of floods with lower AEPs, that do not happen when a flood with a higher AEP is passing by. This is expressed mathematically with Equation (8) (Chapter 2) designed by Vanneuville et al. (2003). This equation implies an unlimited availability of all possible flood hazard maps, while in reality, only a limited number of flood hazard scenarios is calculated. In this study, three maps were available and Equation (8) was thus interpolated accordingly. As the flood hazard map with an AEP of 100% was not created, the map with 50% AEP was used as base, resulting in:

(13)
$$R = 50\% * D_{50\%} + \left(\frac{\frac{1}{3} + \frac{1}{4} + \dots + \frac{1}{10}}{10-2}\right) (D_{10\%} - D_{50\%}) + \left(\frac{\frac{1}{11} + \frac{1}{12} + \dots + \frac{1}{50}}{50-10}\right) (D_{2\%} - D_{10\%})$$

The result of this calculation is the economic flood risk map (Figure 40).

Table 24 lists the corresponding risk values. The calculated total risk in the study area is nearly 2 million USD per year, which corresponds with 15% of the maximum damage value. The road risk takes up the largest part, 37%, followed by the building risk with 33% and the crop risk with 30%.

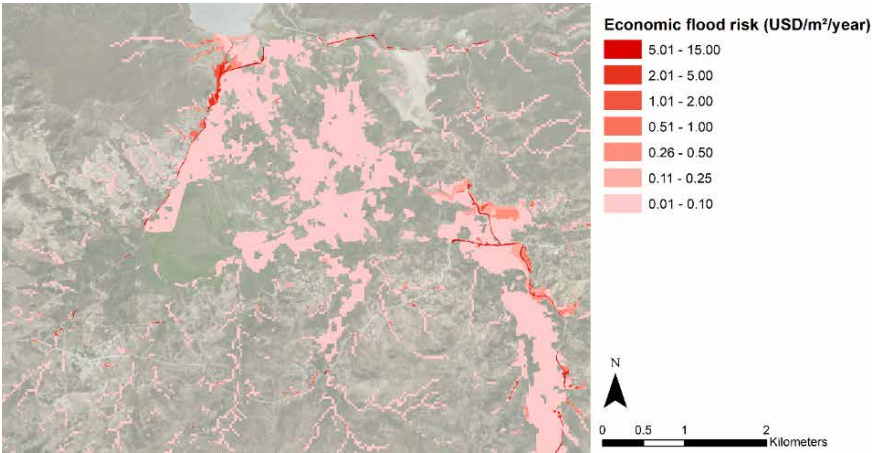


Figure 40 Economic flood risk map for the floodplain of the river Moustiques, Haiti.

Table 24 Overview of the total risk values for the floodplain of the river Moustiques, Haiti.

	Total risk (USD per year)
Buildings	652,500
Crops	587,000
Roads	740,750
Total	1,980,250

5.5.2 Social risk calculations

For each AEP, the flood heights of the flood hazard map were combined with the population number in that same area using the corresponding mortality factor. These calculations led to a vulnerability map per AEP, showing the potential number of casualties for each of the three scenarios. Figure 41 shows the vulnerability maps for the villages of Baie des Moustiques and Nan Ti Charles, while Figure 42 visualizes the maps for Augustin.

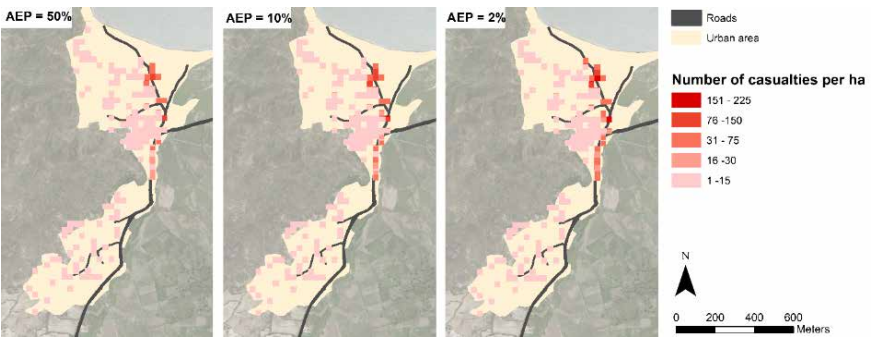


Figure 41 Vulnerability maps for a 50% AEP flood (left), 10% AEP flood (middle) and 2% AEP flood (right) for the villages of Baie des Moustiques and Nan Ti Charles, Haiti.

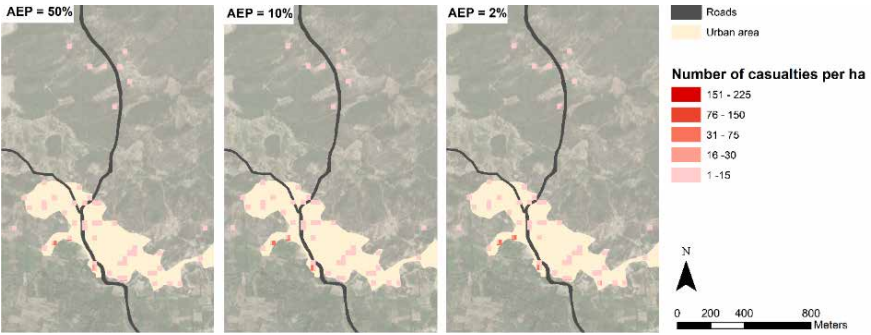


Figure 42 Vulnerability maps for a 50% AEP flood (left), 10% AEP flood (middle) and 2% AEP flood (right) for the village of Augustin, Haiti.

While visually, there is little difference between the three AEP scenarios, the total number of potential casualties is 22% higher for the 10% AEP flood and even 53% higher for the 2% AEP flood in comparison to the 50% AEP flood, as listed in Table 25. The low-lying village of Baie des Moustiques has the highest potential for casualties in all three scenarios, since it is located at the mouth of the small river Ti Charles.

Table 25 Overview of the potential casualties for a 50% AEP flood, a 10% AEP flood and a 2% AEP flood for the villages in the floodplain of the river Moustiques, Haiti.

	AEP = 50%	AEP = 10%	AEP = 2%
Baie des Moustiques	79.92	100.78	127.70
Nan Ti Charles	11.99	12.19	12.36
Augustin	17.38	20.27	26.75
Total number of casualties	109.29	133.24	166.81

The vulnerability maps for the three AEPs are combined into one social risk map using the same Equation (13) as in the economic risk map calculations. The result is visible in Figure 43.

Table 26 lists the total number of potential casualties per village. Baie des Moustiques has the highest risk of casualties, as almost 75% of the potential casualties in the study area are inhabitants of the low-lying village.

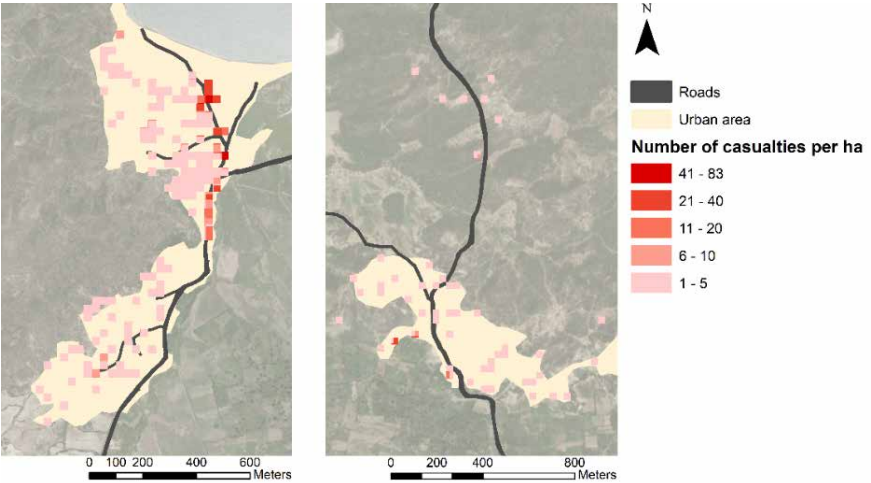


Figure 43 Social risk map for the villages Baie des Moustiques and Nan Ti Charles (left), and for the village Augustin (right) in the floodplain of the river Moustiques, Haiti.

Table 26 Overview of the total number of potential casualties per year for the floodplain of the river Moustiques, Haiti.

	Number of potential casualties per year
Baie des Moustiques	44.74
Nan Ti Charles	6.04
Augustin	9.46
Total	60.24

5.6 Discussion

As the main reason for the lack of adequate flood risk assessment in the study area is the absence of adequate input data, this paper presents a flood risk assessment methodology based on a new, low-cost data acquisition method in the form of a questionnaire survey. As this methodology is new, it is important to evaluate and validate the outcome.

The risk assessment in this research estimates that yearly 23% of the buildings in the study area are at risk of flood damages. However, in the survey of the population of the three villages in the study area (Glas & Deruyter, 2018), 72% of the respondents indicated their home as damaged by the described flood event. The first reason for this discrepancy is that they described the most severe flood in their memory. Hence, the AEP of this flood will most likely be low. Secondly, homes in the department of Nord-Ouest consist on average of 2.5 buildings (IHSL, 2003). Therefore, if only one of the buildings was damaged, the entire home was indicated as damaged in the questionnaire, which leads to an overestimation.

The damage factors for buildings and crops were drafted based on the survey of Glas et al. (2018). The derived damage factors are region-specific and based on a large distribution of answers. Several other studies have proven that this form of citizen science, where data are generated purely from input from citizens, is valuable, especially in areas where other historic data are inexistent (Fast & Rinner, 2014; Hultquist & Cervone, 2018). 250 of the 297 surveyed households described the flooding of January 2018 that occurred only a few days earlier. Although the answers were based on fresh memories, which could increase the accuracy and reliability, it is important to take into account the raw emotions of people after a disaster, which may lead to spurious answers. Ideally, the surveys should have been conducted after the questioned people were recovered from the emotions.

For roads, the depth-damage function drafted by Vanneuville et al. (2003) for Flanders, Belgium was used. However, road construction and maintenance in Europe is difficult to compare with the Haitian context. Therefore, further research should focus on the development of a region-specific depth-damage function for roads. The necessary input for such a function could be gathered through a questionnaire survey.

The risk assessment methodology presented in this paper is based on widely spread risk concepts and methods, described in various research. These concepts were adapted for region-specific circumstances. While the added value of this approach lies in the applicability and suitability of the methods and results for this specific area and its inhabitants, a shortcoming of this methodology is that only direct economic damages were calculated. In other studies, indirect damages such as production losses and cleaning costs are included as a fraction of the direct damages (Grigg et al., 1976; Vanneuville et al., 2005). However, calculating these indirect damages accurately is problematic, especially in data-poor regions (Penning-Rowsell et al., 2005). Therefore, indirect damage calculations were not included in the presented methodology. This,

however, does not imply that these losses cannot be significant, especially in rural areas where the livelihoods of many inhabitants depend on agriculture.

In the social risk map, casualties are expressed in loss of human lives. The map visualizes the number of potential deadly victims, but does not show the number of people affected by the flooding. While the total number of potential casualties is calculated at 60.24 per year or less than 4% of the total population in the area, the results of the survey conducted by Glas et al. (2018) indicate that approximately 40% of the inhabitants are affected by a flood event. Furthermore, the overall vulnerability of the people is extremely high due to a high degree of reduced mobility: 40.26% of the population is younger than 15, 3.10% is older than 65 (Glas et al., 2018), and 11.30% of the inhabitants between the ages of 15 and 65 years old suffer from a long-term illness or are disabled. A second reason for the high number of people affected is the poor state of the limited road infrastructure, which impedes a timely evacuation. Finally, the only way of warning and informing the population in the study area before and during a flood event is through church services and word-to-mouth, in contrast to other regions in Haiti where hurricane and flood emergency warning services provide the necessary information on time.

The final step in the risk calculations is the generation of the risk maps by combining the damage maps for different AEPs. In this research, a flood map with an AEP of 100% was not available and could thus not be used as base for the risk formula. Therefore, the 50% AEP flood was used as base by multiplying the damages with the AEP. This implies that the damages that correspond with a 50% AEP flood are twice the damages of a 100% AEP flood. However, in reality, there is no linear relationship between two flood scenarios as shown in Table 23 and Table 25. Furthermore, due to the topography of the floodplain, a large flat area surrounded by steep mountains, the flood extent of a flood with a 100% AEP would not be significantly different from the extent of the 50% AEP flood, the 10% AEP flood and the 2% AEP flood. Moreover, corresponding damages would not be half of the damages of the 50% AEP flood, as is presumed in the risk formula used now. It is thus most likely that the total risk is an underestimation of the real risk, as the base of the formula is now only half of the 50% AEP flood damages, but would be higher in reality.

5.7 Conclusions

Many flood risk assessments have shown adequate and promising results in developed regions and on large scales. In many developing countries, however, the lack of detailed data has hindered the production of usable results, especially on a micro-scale. Therefore, this research has focused on developing a low-cost methodology for data acquisition and flood risk analysis for the floodplain of the river Moustiques in Haiti. In a first step, the risk methodology was defined, based on state-of-the art practices as well as on the region-specific conditions and restrictions. Then, the necessary input data were listed and a low-cost data acquisition methodology was presented to gather the missing information.

Conducting a survey of the population by questionnaires is a fast and targeted acquisition method. Furthermore, it provides region-specific data, allowing an assessment on micro-scale. Questionnaires can provide information on historic floods that is otherwise inexistent. Finally, this information can be gathered at any time, eliminating the need to perform measurements at the time of a disaster. This is a big advantage, as this study area, like many others, is often inaccessible during a flood. However, the method has a few important disadvantages that require care and caution in the processing, such as unclear questioning or an unreliable memory of the event, caused by the traumatic impact of the disaster. This form of citizen science is a great added value in flood risk assessment in data-poor areas, but needs more research and validation based on other, more objective, data sources. Another data source that needs further research is satellite imagery, for example the radar satellite from Sentinel 1 that can provide observations through cloud cover and, as open source data, can provide objective region-specific input for flood risk analysis.

Every flood risk assessment is based on certain assumptions, generalizations and aggregated data in order to evaluate the risk and potential damages of future flooding. Therefore, it is always difficult to validate the results of the assessment and evaluate the accuracy of the methodology. In this research, as well as in other data-poor study areas, this validation procedure is extra complicated due to inexistent historic flood data. While the results could not be validated, the input data and methodology could. Based on the results of the sensitivity analysis performed by Glas et al. (2016), the determining input data were gathered and the accuracy and completeness of this data were tested and validated. While the quantitative results are too uncertain to be used as a decision factor, a qualitative approach of the risk map, that shows the high-risk areas and indicates where measures should be taken, does provide decision makers with an adequate tool to allocate the available funds. The locations of these high-risk areas are confirmed by the results of the questionnaire survey.

The floodplain of the river Moustiques is a rural area where agricultural lands take up the lion's share of the land use. The potential risk to these crops per square meter is only a fraction of the potential risk to buildings and roads. This leads to a risk map where the high-risk areas are concentrated around the built-up areas. The difference in risk between the different crops is invisible in such a map, as all agricultural lands are indicated as low-risk, compared to the buildings and roads. Furthermore, the methodology only takes into account direct losses, while many of the households in the study area depend on the crop harvest for their livelihood. Crop damages will thus have a large indirect impact on the community. Therefore, future research should explore incorporating indirect losses in the risk methodology. Moreover, other visualization methods could allow a better interpretation of the risks per land use type. Urban zones need other mitigation and adaptation measures than rural zones. By providing the risk information on direct and indirect damages per land use type, decision makers will be better equipped to allocate the correct measures to the correct zones.

ACKNOWLEDGMENTS

The authors would like to thank Join For Water, our Belgian partners as well as the local Haitian employees, for facilitating our field work and sharing their knowledge and data on the study area. Furthermore, we would like to thank Bruce Robinson and everyone at ODRINO for assisting us on the field and aiding in any way possible during our stay in Moustiques. A word of gratitude goes to the Research Foundation – Flanders (FWO) for partially funding the field work. Finally, we would like to thank Edith Maroy and Ivan Rocabado from Antea Group for their work in creating adequate flood hazard maps for the study area.

REFERENCES

- Apel, H., Aronica, G. T., Kreibich, H., & Thielen, A. H. (2009). Flood risk analyses-how detailed do we need to be? *Natural Hazards*, 49(1), 79-98. doi:10.1007/s11069-008-9277-8
- Bendito, A., Rozelle, J., & Bausch, D. (2014). Assessing Potential Earthquake Loss in Merida State, Venezuela Using Hazus. *International Journal of Disaster Risk Science*, 5(3), 176-191. doi:10.1007/s13753-014-0027-0
- Brandimarte, L., Brath, A., Castellarin, A., & Di Baldassarre, G. (2009). Isla Hispaniola: A trans-boundary flood risk mitigation plan. *Physics and Chemistry of the Earth*, 34(4-5), 209-218. doi:10.1016/j.pce.2008.03.002
- Colindres, R. E., Jain, S., Bowen, A., Domond, P., & Mintz, E. (2007). After the flood: an evaluation of in-home drinking water treatment with combined flocculent-disinfectant following Tropical Storm Jeanne - Gonaïves, Haiti, 2004. *Journal of Water and Health*, 5(3), 367-374. doi:10.2166/wh.2007.032
- Collier, P., Kirchberger, M., & Söderbom, M. (2015). *The Cost of Road Infrastructure in Low and Middle Income Countries*. Retrieved from <https://documents.worldbank.org/en/publication/documents-reports/documentdetail/124841468185354669/the-cost-of-road-infrastructure-in-low-and-middle-income-countries>
- CRED (2018). *EM-DAT Database*. Retrieved from https://www.emdat.be/emdat_db/
- De Roo, A., Wesseling, C., Cremers, N., Offermans, R., Ritsema, C., & Van Oostindie, K. (1994). LISEM: a new physically-based hydrological and soil erosion model in a GIS-environment, theory and implementation. *IAHS Publications-Series of Proceedings and Reports-Intern Assoc Hydrological Sciences*, 224, 439-448.
- De Sutter, R., Rocabado, I., D'Heayer, T., Deleu, J., Maroy, E., Salazar, D., . . . Pirola, E. (2018). *Climate hazard, vulnerability and risk assessment for East Sepik Province in Papua New Guinea, Final report*. Retrieved from https://info.undp.org/docs/pdc/Documents/PNG/Report_Climate%20Risk%20Vulnerability%20Assessment_East%20Sepik.pdf
- Dolisca, F., McDaniel, J. M., Teeter, L. D., & Jolly, C. M. (2007). Land tenure, population pressure, and deforestation in Haiti: The case of Forêt des Pins Reserve. *Journal of Forest Economics*, 13(4), 277-289. doi:10.1016/j.jfe.2007.02.006

- Domeneghetti, A., Gandolfi, S., Castellarin, A., Brandimarte, L., Di Baldassarre, G., Barbarella, M., & Brath, A. (2015). Flood risk mitigation in developing countries: deriving accurate topographic data for remote areas under severe time and economic constraints. *Journal of Flood Risk Management*, 8(4), 301-314. doi:10.1111/jfr3.12095
- Dutta, D., Herath, S., & Musiake, K. (2003). A mathematical model for flood loss estimation. *Journal of hydrology*, 277(1-2), 24-49. doi: 10.1016/S0022-1694(03)00084-2
- Eckstein, D., Künzel, V., & Schäfer, L. (2018). *Global Climate Risk Index 2018 - Who suffers most from extreme weather events? Weather-related loss events in 2016 and 1997 to 2016*. Berlin, Germany: <https://reliefweb.int/report/haiti/global-climate-risk-index-2018-who-suffers-most-extreme-weather-events-weather-related>
- FAOSTAT (2017). *Crops*. Retrieved from <http://www.fao.org/faostat/en/#data/QC>
- Fast, V., & Rinner, C. (2014). A systems perspective on volunteered geographic information. *ISPRS International Journal of Geo-Information*, 3(4), 1278-1292. doi: 10.3390/ijgi3041278
- Glas, H., & Deruyter, G. (2018). *Questionnaires sur l'impact des inondations dans le bassin versant de la rivière Moustiques, Haïti*.
- Glas, H., Deruyter, G., & De Maeyer, P. (2018). Flood risk assessment in data sparse regions: the use of questionnaires to collect historic flood data-a case study for the river moustiques in Haiti. *International Multidisciplinary Scientific Geoconference SGEM*, (18, 2.3), 377-384. doi: 10.5593/sgem2018/2.3/S11.048
- Glas, H., Deruyter, G., De Maeyer, P., Mandal, A., & James-Williamson, S. (2016). Analyzing the sensitivity of a flood risk assessment model towards its input data. *Natural Hazards and Earth System Sciences*, 16(12), 2529-2542. doi:10.5194/nhess-16-2529-2016
- Glas, H., Jonckheere, M., Mandal, A., James-Williamson, S., De Maeyer, P., & Deruyter, G. (2017). A GIS-based tool for flood damage assessment and delineation of a methodology for future risk assessment: case study for Annotto Bay, Jamaica. *Natural Hazards*, 88(3), 1867-1891. doi:10.1007/s11069-017-2920-5
- Government of Haiti (2010). *Analysis of Multiple Natural Hazards in Haiti (NATHAT)*. Retrieved from <https://reliefweb.int/report/haiti/analysis-multiple-natural-hazards-haiti-nathat>
- Grigg, N. S., Botham, L. H., Rice, L., Shoemaker, W., & Tucker, L. S. (1976). Urban drainage and flood control projects: economic, legal and financial aspects. *Completion report series (Colorado State University. Environmental Resources Center)*; no. 65. Retrieved from <https://mountainscholar.org/handle/10217/2617>
- Heimhuber, V., Hannemann, J. C., & Rieger, W. (2015). Flood Risk Management in Remote and Impoverished Areas-A Case Study of Onaville, Haiti. *Water*, 7(7), 3832-3860. doi:10.3390/w7073832
- HOT (2016). *Hurricane Matthew Update*. Retrieved from https://www.hotosm.org/updates/2016-10-08_hurricane_matthew_update
- Hultquist, C., & Cervone, G. (2018). Citizen monitoring during hazards: Validation of Fukushima radiation measurements. *GeoJournal*, 83(2), 189-206. doi: 10.1007/s10708-017-9767-x
- IHSI (2003). *Enquête sur les conditions de vie en Haïti*. Retrieved from <https://publications.iadb.org/fr/enquete-sur-les-conditions-de-vie-et-developpement-social-en-haiti-du-nord-lcsds>. doi: 10.18235/0002472

- Jongman, B., Kreibich, H., Apel, H., Barredo, J., Bates, P., Feyen, L., . . . Ward, P. (2012). Comparative flood damage model assessment: towards a European approach. *Natural Hazards and Earth System Sciences (NHESS)*, 12(12), 3733-3752. doi: 10.5194/nheiss-12-3733-2012
- Joseph, A., Gonomy, N., Zech, Y., & Soares-Fraza, S. (2018). Modelling and analysis of the flood risk at Cavaillon City, Haiti. *Houille Blanche-Revue Internationale De L Eau*(2), 68-75. doi:10.1051/lhb/2018020
- Kijewski-Correa, T. L., Kennedy, A. B., Taflanidis, A. A., & Prevatt, D. O. (2018). Field reconnaissance and overview of the impact of Hurricane Matthew on Haiti's Tiburon Peninsula. *Natural Hazards*, 94(2), 627-653. doi:10.1007/s11069-018-3410-0
- Kok, M., Huizinga, H. J., Vrouwenvelder, A. C. W. M., & Barendregt, A. (2005). Standaard-methode 2004 - Schade en Slachtoffers als gevolg van overstromingen. Retrieved from <https://library.wur.nl/ebooks/hydrotheek/1874298.pdf>
- Levi, T., Bausch, D., Katz, O., Rozelle, J., & Salamon, A. (2015). Insights from Hazus loss estimations in Israel for Dead Sea Transform earthquakes. *Natural Hazards*, 75(1), 365-388. doi:10.1007/s11069-014-1325-y
- Liu, Y., & De Smedt, F. (2004). WetSpa extension, a GIS-based hydrologic model for flood prediction and watershed management. *Vrije Universiteit Brussel, Belgium*, 1, e108. https://www.vub.be/WetSpa/downloads/WetSpa_manual.pdf
- MTPTC (2001). *Pour un développement durable des infrastructures routières – Document de formulation de Stratégie*. Retrieved from <https://www.mtptc.gouv.ht/media/upload/doc/publications/strategieMTPTC.pdf>
- OCHA (2010). *Haiti Earthquake – Situation Report #23 – 22 February 2010*. Retrieved from <https://reliefweb.int/report/haiti/haiti-earthquake-situation-report-23>
- OCHA (2012). *Haiti: Damage, Needs and Responses (as of 27 August 2012)*. Retrieved from <https://reliefweb.int/map/haiti/haiti-damage-needs-and-responses-27-august-2012>
- OCHA (2016). *Haiti one month after the storm – Humanitarian response in Haiti in the aftermath of Hurricane Matthew*. Retrieved from <https://reliefweb.int/report/haiti/haiti-one-month-after-storm>
- Park, J. H., Shin, M., & Cho, G. H. (2016). A dynamic estimation of casualties from an earthquake based on a time-use survey: applying HAZUS-MH software to Ulsan, Korea. *Natural Hazards*, 81(1), 289-306. doi:10.1007/s11069-015-2079-x
- Penning-Rowsell, E., Johnson, C., Tunstall, S., Tapsell, S., Morris, J., Chatterton, J., & Green, C. (2005). *The benefits of flood and coastal risk management: a handbook of assessment techniques*. ISBN 1904750516. <https://repository.tudelft.nl/islandora/object/uuid:33f2d216-c9bf-419c-b3b1-415a6f6fd881/datastream/OBJ/download>
- PROTOS (2011). Évaluation transversale 2010 – Mise en œuvre de la stratégie GIRE et intégration de la problématique changement climatique – Etude de cas – Haïti. Retrieved from https://www.joinforwater.ngo/sites/default/files/publications/files/2.evaluation_gire_et_cc_haiti_version_finale.pdf
- Rossillon, F. (2016). *Face à la détresse humaine et environnementale, Gestion Intégrée de l'Eau et Ecosanté, leviers de développement pour une Haïti nouvelle*. In *L'eau dans les pays en développement - Retour d'expériences de gestion intégrée et participative avec les auteurs locaux* (pp. 313-366). Belgium.

- Saxton, K. E., & Rawls, W. J. (2006). Soil water characteristic estimates by texture and organic matter for hydrologic solutions. *Soil science society of America Journal*, 70(5), 1569-1578. doi: 10.2136/sssaj2005.0117
- Tate, E., Munoz, C., & Suchan, J. (2015). Uncertainty and Sensitivity Analysis of the HAZUS-MH Flood Model. *Natural Hazards Review*, 16(3), 10. doi:10.1061/(asce)nh.1527-6996.0000167
- Thieken, A., Merz, B., Kreibich, H., & Apel, H. (2006). *Methods for flood risk assessment: Concepts and challenges*. Paper presented at the International workshop on flash floods in urban areas 2006, Sultanate of Oman. 12p.
- UCLBP (2016). *Evaluation des besoins post cyclone Mathieu dans le secteur logement*. Retrieved from <https://www.undp.org/content/dam/haiti/docs/rapport/UNDP-HT-Rapport-sectoriel-Logement-sm.pdf?download>
- UNDP (2011). *Human Development Report 2011: Sustainability and Equity: A Better Future for All*. New York, USA: <http://hdr.undp.org/en/content/human-development-report-2011>
- UNDP (2018). *Human Development Indices and Indicators – 2018 Statistical Update*. New York, USA: <http://hdr.undp.org/en/content/human-development-indices-indicators-2018-statistical-update#:~:text=Human%20Development%20Indices%20and%20Indicators%3A%202018%20Statistical%20update%20is%20being,trends%20in%20human%20development%20indicators>.
- Vanneuville, W., De Maeyer, P., Maeghe, K., & Mostaert, F. (2003). Model the effects of a flood in the Dender catchment based on a risk methodology. *Bulletin of the Society of Cartography*, 37(2), 59-64.
- Vanneuville, W., De Rouck, K., Maeghe, K., Deschamps, M., De Maeyer, P., & Mostaert, F. (2005). *Spatial calculation of flood damage and risk ranking*. Paper presented at the AGILE 2005 8th conference on geographic information science.
- Vrisou van Eck, N., Kok, M., & Vrouwenvelder, A. (1999). Standaardmethode Schade en Slachtoffers als gevolg van overstromingen, deel 2: Achtergronden. *HKV Lijn in water, TNO, Dienst Weg en Waterbouw*. https://puc.overheid.nl/rijkswaterstaat/doc/PUC_20427_31/
- Wallemacq, P., Below, R., & McLean, D. (2018). *Economic losses, Poverty & Disasters (1998-2017)*. Retrieved from <https://www.undrr.org/publication/economic-losses-poverty-disasters-1998-2017>
- World Bank (2018). *The World Bank in Haiti: overview*. Retrieved from <http://www.worldbank.org/en/country/haiti/overview>

6

FLOOD RISK MAPPING WORLDWIDE – A FLEXIBLE METHODOLOGY AND TOOLBOX

This chapter was adapted from the following journal article:

Glas H., Rocabado I., Huysentruyt S., Maroy E., Salazar Cortez D., Coorevits K., De Maeyer P., Deruyter G. (2019). Flood risk mapping worldwide – a flexible methodology and toolbox, *Water*, 11(11), 2371. doi: 10.3390/w11112371

The research presented in this chapter was a cooperation with a team from Antea Group, led by Ivan Rocabado. The developed toolbox is built around three modules that run independently from each other. The first, the hazard module, was researched, developed and tested by Antea Group. The following two modules, the vulnerability and the risk module, were developed by the author based on the research presented in the previous chapters of this dissertation. The raster calculations were also developed and tested by the author. Flood hazard maps are required input for the risk module, and, therefore, the hazard module is a valuable addition to the flood risk assessment toolbox. However, the creation of these maps is not an inherent part of the risk methodology presented in the proposed dissertation.

The methodology and development of the hazard module are thus only briefly explained. For a more detailed breakdown of the hazard module, the author refers to the original journal article or one of the co-authors of Antea Group, who created the module (Ivan Rocabado, Danitza Salazar Cortez and Edith Maroy).

ABSTRACT

Flood risk assessments predict the potential consequences of flooding, leading to more effective risk management and strengthening resilience. However, adequate assessments rely on large quantities of high-quality input data. Developing regions lack reliable data or funds to acquire them. Therefore, this research has developed a flexible, low-cost methodology for mapping flood hazard, vulnerability and risk. A generic methodology was developed and customized for freely available data with global coverage, enabling risk assessment worldwide. The default workflow can be enriched with region-specific information when available. The practical application is assured by a modular toolbox developed on GDAL and PCRASTER. This toolbox was tested for the catchment of the river Moustiques, Haiti, for which several flood hazard maps were developed. Then, the toolbox was used to create social, economic and physical vulnerability maps. These were combined with the hazard maps to create the three corresponding flood risk maps. After creating these with the default data, more detailed information, gathered during field work, was added to verify the results of the basic workflow. These first tests of the developed toolbox show promising results. The toolbox will allow policy makers in developing countries to perform reliable flood risk assessments and generate the necessary maps.

Keywords: flood hazard map, vulnerability, flood risk, open source, Haiti

6.1 Introduction

While over the past years, many researchers have worked on computing accurate local flood risk assessment models, with promising results, data scarcity remains a hurdle for the development of global models as well as for flood risk assessment in developing countries, which lack the funds to acquire reliable and detailed input data (UNDRR, 2019). In data-poor regions, this has led to innovative and customized approaches for mapping flood risk (Brandimarte et al., 2009; Heimhuber et al., 2015; Kumar & Acharya, 2016; Kwak et al., 2015; Son et al., 2019). Although these studies have valuable results for their respective study areas, the implementation of these methodologies on a wider scale is hindered by the individuality of the approaches.

Therefore, this research has developed a flexible, low-cost methodology for mapping flood hazard, vulnerability and risk in data-poor regions. As the risk mapping is based on freely available input data with global coverage, the methodology is applicable worldwide. A modular framework for the risk calculations was developed, which allows the default workflow to be extended and enriched with optional modules that make use of region-specific, detailed information when available. The practical application is designed as a modular toolbox developed on GDAL and PCRASTER. Hence, the framework and toolbox provide a generic set of algorithms and spatiotemporal calculations for mapping flood hazard, vulnerability and risk that can be enhanced to account for local specificities. A user-interface allows access to the toolbox and modification of the algorithms without any programming experience.

6.1.1 Definitions

The United Nations Office of Disaster Risk Reduction (UNDRR) defines risk as the combination of the probability of a hazardous event and its negative consequences which result from interactions between natural or man-made hazard(s), vulnerability, exposure and capacity (UNDRR, 2009). Capacity is described as the combination of all the strengths, attributes and resources available within the system to manage and reduce disaster risks and strengthen resilience. While incorporating capacity can offer valuable and interesting insights, quantifying this correctly requires a large amount of location-specific input data. As this is contradictory with the research aim, the proposed method leaves aside capacity and follows the conventional notation of risk: **Risk = Hazard × Vulnerability**. As such, three main modules were defined in the workflow: Hazard, vulnerability and risk.

Hazard is a broad term, that is described as a process, phenomenon or human activity that may cause loss of life, injury or other health impacts, property damage, social and economic disruption or environmental degradation (UNDRR, 2009). In this research, the hazard module is limited to flooding as a single event. The probability of flooding in the study area is determined through statistical analysis (Deckers et al., 2009). The resulting flood hazard maps depict the water extents and flood heights for specific Annual Exceedance Probabilities (AEPs), expected probabilities of a particular water level and discharge that may occur in any year.

Vulnerability is defined by the UNDRR as a set of conditions and processes resulting from physical, social and economic factors, which increase the susceptibility of a community to the impact of the hazard (UNDRR, 2009). This research takes into account three types of vulnerability caused by flooding: Social, physical and economic vulnerability. Social vulnerability is defined by the number of people vulnerable to a potential flood; physical vulnerability is determined by the potential material damages to infrastructure (buildings, roads,...); and economic vulnerability comprises the potential economic damages, including damages to infrastructure as well as crop damages.

In this research, risk is calculated by combining the vulnerability maps with the flood hazard data for different AEPs. Social risk is defined as the potential number of casualties due to flooding each year. The risk level for material damages is described in physical risk, while economic risk determines the risk level for economic damages. Both are initially calculated in USD m⁻² per year and then classified in five risk levels.

6.2 Materials and methods

6.2.1 Methodology workflow

The total workflow is visualized in Figure 44 and can be divided in three large modules. The hazard and vulnerability modules run independently from one another, while the risk module depends on input data from the first two.

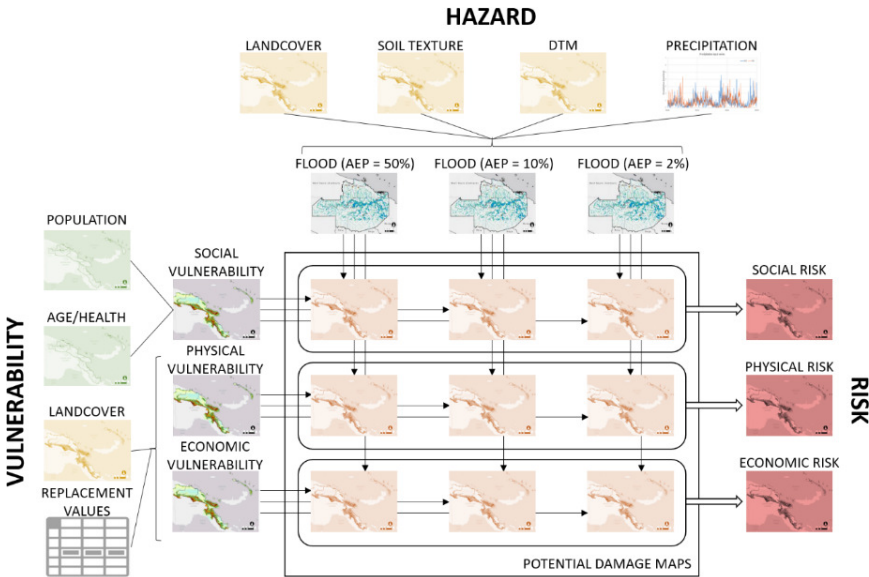


Figure 44 Workflow of flood risk mapping, as followed in the developed toolbox.

6.2.1.1 Hazard Module

Table 27 Parameter maps used in the hydrological model openLISEM.

DATA	DERIVED PARAMETER MAP	SYMBOL/UNIT
Rainfall series	Rainfall depth	(mm hr ⁻¹)
DEM	Local Drain Direction (LLD)	
	Outlet	
	Gradient	S (mm ⁻¹)
	Catchment delineation (optional)	
Soil texture	Hydraulic conductivity	Ksat (mm h ⁻¹)
	Average suction at wetting front	Ψ (cm)
	Porosity	Θs
	Initial moisture	Θi
Land use/Land cover	Surface random roughness	RR (cm)
	Cover fraction	Cover (-)
	Manning's roughness coefficient	n (-)
	Leaf area index of the plant cover in a gridcell	LAI (m ² /m ²)
	Crop height	(m)
Channel	LDD channel	
	Channel width	(m)
	Channel depth	(m)
	Side angle	(-)
	Gradient	(-)

Flood hazard is mapped in terms of flood heights and extent using the modelling framework proposed by De Roo and Jetten at the Univerity of Twente: openLISEM (De Roo et al., 1996; De Roo et al., 1994). openLISEM is a publicly available spatial hydrological model that can simulate runoff, sediment dynamics and shallow floods. Only the components modelling rainfall-runoff and hydrodynamic flows were used for calculating flood hazard. The equations describing these processes are parameterized with spatially-distributed parameters associated with land cover, soil, relief and channel characteristics. The required maps are listed in Table 27. The workflow of pre-processing and modelling steps is represented in Figure 45.

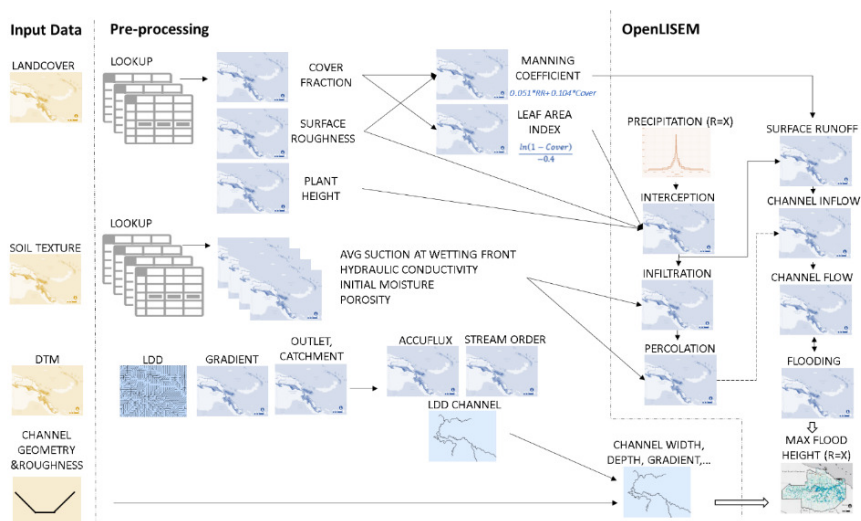


Figure 45 Workflow of the hazard module for floods as followed in the developed toolbox (preprocessing steps) and the OpenLISEM model.

In data-poor contexts, reasonable assumptions make it possible to generate the many input parameter maps based on soil texture, land cover classes and the digital terrain model alone. This can be done with predefined lookup tables based on the literature and automatized with an algorithm in PCRaster (Karssenberget al., 2010). Parameters were derived from GlobCover land cover classes (300 m × 300 m) using a compilation of parameters based on various experimental studies as proposed by Liu & De Smedt (2004) for the 17 IGBP vegetation type classes (Eidenshink & Faundeen, 1994). For soil types, soil mapping units described in the FAO-UNESCO Soil Map of the World were first converted into likely USDA soil texture classes based on the fraction of fine, medium and coarse material. Hydrological parameters associated with USDA texture classes were then taken from Saxton and Rawls (2006). Elevation data are available globally at 30 m horizontal resolution (SRTM) but this is generally insufficient to describe accurately the morphology of the river network. Therefore, it is helpful to make use of more detailed information on hydrography, channel shape, depth and width, bed roughness, and location of outlets. Vector data of river networks are available in datasets such as HydroSHEDS or OpenStreetMap or can be digitalized based on remote sensing and satellite images. River channels are rasterized and variables of length, width and depth are associated to each pixel. With limited knowledge about the geometry of the channel, width and depth are interpolated based on the distance to the outlet. Available information on roads and possible barriers can also be integrated into the model.

The notion of risk should combine a spectrum of different types of events, mild frequent ones as well as rare extreme ones. Therefore, hazard must be known for a number of AEPs. This statistical component is derived from rainfall Intensity-Duration-Frequency (IDF) curves. These curves are calculated by meteorological services across the world based on historical rainfall records and geostatistical methods. For each probability of occurrence, or AEP, all the most likely storms are plotted according to their duration

and intensity. For the US and the Caribbean, IDF curves are made available online by the National Oceanic and Atmospheric Administration NOAA (OWP, 2018). Alternatively, they can be computed based on rainfall intensity time series derived from microwave and radar data provided by satellites such as TRMM & GPM (NASA) or the GSMaP project (JAXA). The openLISEM model simulates flow and flood areas based on a specific rainfall event however, rather than IDF curves. In order to associate a probability to each flood hazard map, composite storms are designed as to generate the highest possible runoff concentration for a certain probability of rain. “Composite” design storms are proposed by Berlamont (1999), who combines all critical storm durations into one single event. They are determined by setting out the rainfall volumes from the IDF-relationship symmetrically around the center of the storm.

The results of openLISEM and the proposed flood mapping strategy were verified against a similar analysis carried out for Papua New Guinea (De Sutter et al., 2018) which was validated using existing flood hazard maps for that region.

6.2.1.2 Vulnerability module

Three types of vulnerability are mapped: social, physical and economic vulnerability. Figure 46 visualizes the module default workflow, as well as the optional data that can be added.

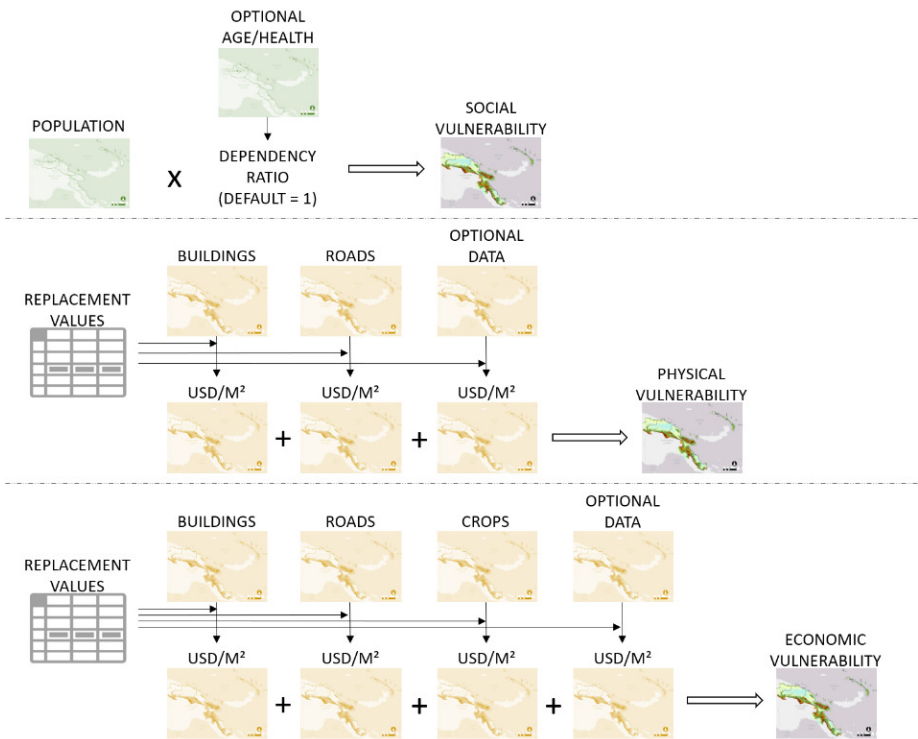


Figure 46 Workflow of the vulnerability module for social vulnerability (top), physical vulnerability (middle) and economic vulnerability (bottom), as followed in the developed toolbox.

In the default workflow, social vulnerability is defined by the population density, which is the only indispensable input data for this module. The default data in the workflow are the freely available WorldPop data. WorldPop distributes census population data based on land cover information, such as location of settlements, roads and rivers (Steele et al., 2018), resulting in maps with a 100 m × 100 m resolution. However, when more detailed population distribution data are available this default data can be replaced with it. Furthermore, when age or health information is available, the workflow can be extended, adding a dependency ratio to the module. This factor is then multiplied with the number of people in an area to calculate the potential vulnerability of the area. The dependency ratio is defined as:

$$(14) \quad DR = \frac{Y+S+LTS}{W}$$

In Equation (14), *DR* stands for Dependency Ratio, *Y* represents the number of children younger than 15, *S* the number of seniors older than 64, *LTS* the number of working people (aged 15–64) with a long-term sickness and *W* the number of people at a working age (15–64). A large number of senior citizens, children and sick people will result into a factor higher than 1 that will be multiplied with the total number of inhabitants. On the other hand, a small amount of seniors, children and workers with a long-term sickness will result in a factor lower than 1. In the final step, five vulnerability classes are defined, and the social vulnerability map is generated.

Physical vulnerability only takes into account material damages to buildings and roads, while economic vulnerability also takes into account the economic damages to farmlands. Both physical and economic vulnerabilities are expressed in USD m² and are based on freely available land cover data, combined with more detailed information on buildings, crops and roads. The default global land cover map used is GlobCover from ESA and has a spatial resolution of 300 m × 300 m (Bicheron et al., 2008). In a first step, these data are supplemented with detailed building and road data, available from OpenStreetMap. Combining these default datasets, creates the land cover map that is used as input for the economic and physical vulnerability calculations. However, it is also possible to add extra land cover data if available. In the next step, the land cover data are linked to a list with replacement values. These values represent the cost to rebuild an element at risk in case of complete destruction. The default replacement values were gathered from literature and reports. The crop costs were derived from data from the Food and Agricultural Organization of the United Nations (FAOSTAT) (FAOSTAT, 2017), Road cost was based on the unit cost data from the Roads Cost Knowledge System (ROCKS) developed by the World Bank's Transport Unit (World Bank, 2018). Both crop and road costs were calculated per country. Building replacement costs, on the other hand, were averaged per region in the world, based on reports from real estate consultancy businesses such as Turner & Townsend and Compass International, Inc. (Compass International Inc., 2018; Turner & Townsend, 2018). It is also possible to add location-specific replacement values if available. Combining these values with the land cover map, and assigning each value to one of the five vulnerability classes, leads to the two vulnerability maps.

6.2.1.3 Risk module

The vulnerability and flood hazard maps generated in the previous modules form the main input data for the risk calculations. Figure 47 shows how the risk module combines both the resulting risk maps.

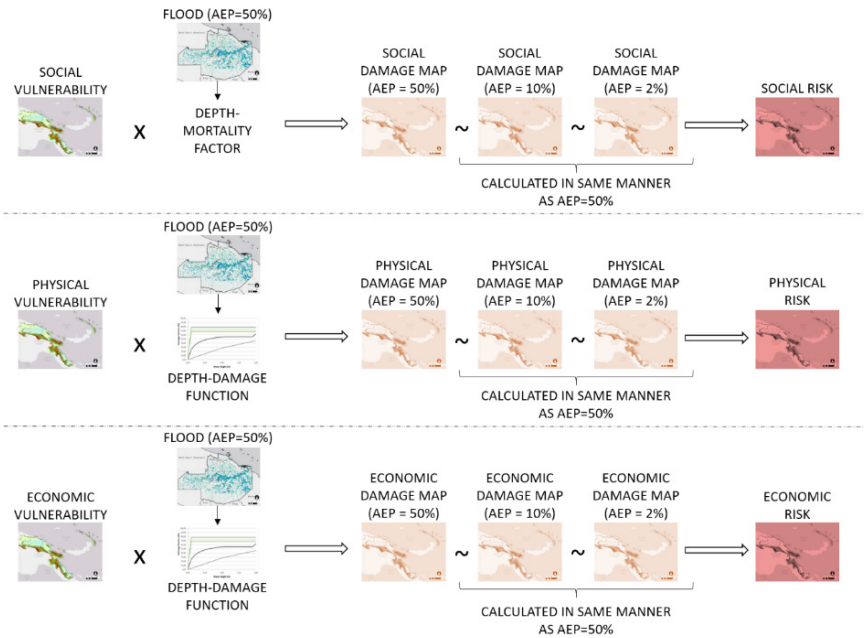


Figure 47 Workflow of the risk module for social risk (top), physical risk (middle) and economic risk (bottom), as followed in the developed toolbox.

The physical and economic vulnerability maps are combined with the flood hazard maps using depth-damage functions, which are gathered from literature and are added as default tables in the toolbox. Table 28 gives an overview of the default depth-damage functions available and their application scale and area.

Dependent on the location, scale and land cover of the study area, a different depth-damage function can be chosen. It is also possible to add another, more specific, function for a specific case study. The result is a series of potential economic damage maps, each corresponding to a potential flood event with a specific AEP. These maps are combined using Equation (8), presented in Chapter 2. The result is a physical and economic risk map showing the risk in USD m⁻² per year. In a final step, these risk damages are classified into five categories, resulting in a qualitative risk map.

To calculate the social risk, a depth-mortality function is used that defines the relation between hazard and vulnerability, expressed in Equation (7) in Chapter 2. The number of casualties becomes a proxy for potential social damage; the resulting social damage maps are combined in an identical manner as physical and economic risk, using Equation (8) in Chapter 2. The final result is a social risk map that visualizes the number of casualties, divided in five risk classes.

Table 28 Overview of default depth-damage functions available in the toolbox.

DEPTH-DAMAGE FUNCTION	DEVELOPED BY	DEVELOPING METHOD	APPLICATION SCALE	APPLICATION AREA
HAZUS Model	Federal Insurance Administration (FIA) & US Army Corps of Engineers (USACE)	Expert judgment	Local State Regional	USA
Rhine Atlas Model	International Commission for the Protection of the Rhine (ICRP)	Empirical information	Catchment	Rhine Area/ Germany
LATIS	Flemish Environment Agency (FEA)	Expert judgment	Regional National	Flanders/ Belgium
Damage scanner Model	Rijkswaterstaat Water, Verkeer en Leefomgeving	Expert judgment	Regional National	The Netherlands
Joint Research Centre Model	Directorate General Joint Research Centre (DG JRC)	Average of all assessed depth-damage functions	Continent	Worldwide
Multi-Colored Manal Model	Flood Hazard Research Centre (FHRC) Middlesex University	Expert judgment	Local Regional	UK
FLEMO	German Research Centre for Geosciences	Empirical information	Local Regional National	Germany
Japan	Dutta et al. (2003)	Expert judgment	Local Region- al National	Japan/ tropical island states

6.2.2 Toolbox

The flood risk mapping toolbox is a set of modules written in Python 3.6 relying on PCRaster 4.2 (Karssenberg et al., 2010), GDAL, GeoPandas, Rasterio and Shapely as main libraries (Figure 48). In order to improve processing performance while using high resolution and/or wide extend maps, the toolbox takes advantage of the parallel computing module from PCRaster.

The toolbox user interface (UI) will hold a set of input files in csv format describing the project metadata, information data folders, look up tables and files. The advanced syntax of these input files allows describing the workflow commands and complex functional relationships in a flexible manner.

The toolbox contains a built-in ‘default’ workflow, which consists of basic modules to create flood hazard, vulnerability and risk maps using open source and globally available data. Several depth-damage functions, each applicable for a specific geographic region, are available in the toolbox, Furthermore, the toolbox contains default replacement values that the user can apply when no location-specific economic data are available.

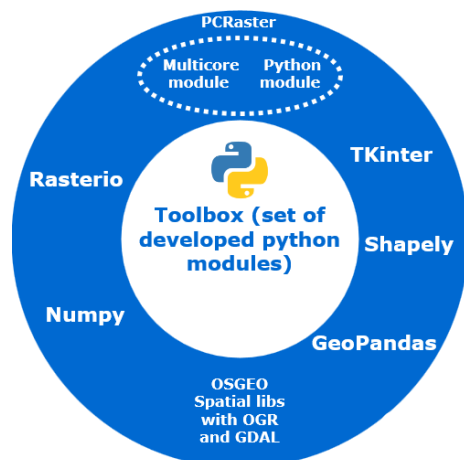


Figure 48 Flood risk mapping toolbox software schema.

While this default input is provided for users with a limited mapping knowledge, as listed in Table 29, the toolbox allows a mapping expert to customize the input files and workflow commands to better match each particular case study and particular methodology. The toolbox also enables splitting the main workflow to process separately either vulnerability or risk maps. Furthermore, the input can be customized to different locations and scales without any modification in the source code.

Table 29 Overview of the input data for the three modules.

DATA TYPE	MANDATORY	SOURCE USED FOR DEFAULT METHODOLOGY
HAZARD MODULE		
Digital Terrain Model (DTM)	Y	SRTM DEM (30 × 30 m resolution)
Landcover data	Y	Globcover (300 × 300 m resolution)
Soil texture data	Y	FAO-UNESCO Digital Soil Map of the World (vector)
Precipitation data	Y	IDF curves (national weather agencies, NOAA) or rainfall intensity time series derived from TRMM & GPM (NASA) or GSMaP (JAXA).
Channels/river network	N	OpenStreetMap (vector)
VULNERABILITY MODULE		
Population density data	Y	WorldPop (100 × 100 m resolution)
Landcover data	Y	Globcover (300 × 300 m resolution)
	Y	OpenStreetMap (vector)
Replacement values	Y	Crops – FAOSTAT (2017)
	Y	Buildings – Turner & Townsend (2018) and Compass International Inc. (2018)
	Y	Roads-ROCKS (World Bank, 2018)
RISK MODULE		
Flood hazard maps	Y	Created in hazard module
Vulnerability maps	Y	Created in vulnerability module
Depth-damage functions	Y	see Table 28
Depth-mortality function	Y	Visou van Eck et al. (1999)

6.2.3 Study Area

The developed toolbox was tested for the catchment of the river Moustiques, situated in the northwest of the island state Haiti. The catchment has 40,000 inhabitants and a total area of 222 km² (Rossilon, 2016). The 46 km long river is one of the only almost permanent waterways in this region characterized by an overall extremely dry climate. It rises from the mountain range Massif de Terre Neuve at a height of 697 m and flows into the Baie de Moustiques, a bay at the sea canal Canal de la Tortue between the mainland and the island Île de la Tortue. The hurricane season that runs from August through October is characterized by torrential rains and flash floods, leading up to 1200 mm measured precipitation per year (PROTOS, 2011). Moreover, the Haitian government classified the floodplain of the Moustiques as vulnerable to exceptional hazards, such as cyclones, storms and hurricanes that produce as much as 600 mm precipitation in 24 h (Government of Haiti, 2010).

The study area lacks a hydro-meteorological gauging network; therefore, no reliable information regarding gauged rainfall nor flood discharges could be identified. Historical flood events were not documented and they remain only in the mind of the residents.

6.3 Results

In a first step, hazard, vulnerability and risk maps were derived following the basic algorithm: using the default, freely available input data only. In a subsequent step, more detailed information on the study area, gathered during a field mission, was introduced to improve the input data. This step enabled testing some of the optional modules, by providing extra in-depth information, but also testing alternative algorithms in the toolbox. Moreover, the results of the basic workflow were verified with this new set of more detailed vulnerability and risk maps.

6.3.1 Results Default Modules

Using the hazard workflow, three flood hazard maps were created. The first has an AEP of 50%, the second one of 10% and the last one has a 2% AEP. The default input data were complemented with an Intensity Duration Frequency (IDF) curve of West Puerto Rico (NOAA), as there was no IDF curve available for Haiti. However, the curve was compared to Cuban and Bahamian studies and was proven to be consistent for the Caribbean area. Three composite storms, presented in Figure 49, were designed based on the IDF curve to produce the flood hazard maps, shown in Figure 50.

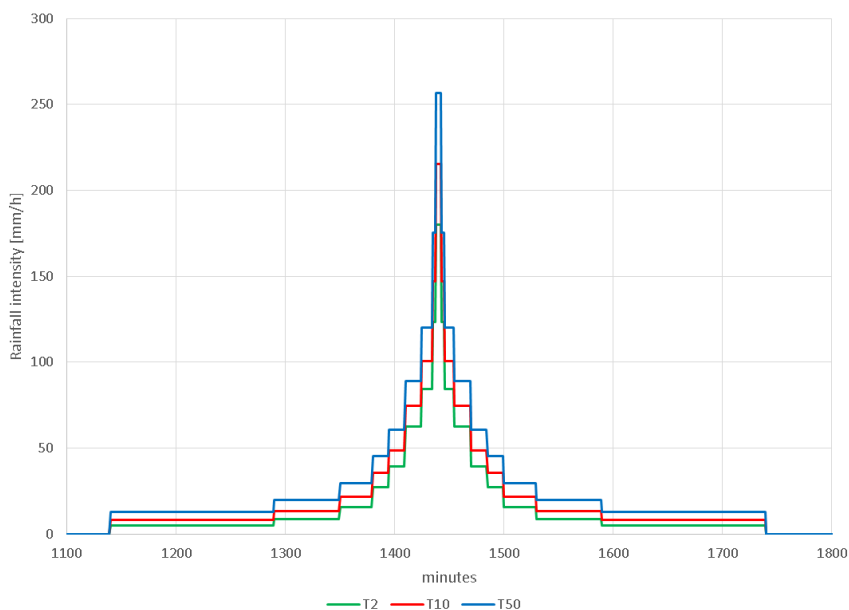


Figure 49 Composite storms for AEPs of 50% (T2), 10% (T10) and 2% (T50) according to IDF-relationships in West Puerto Rico (NOAA).

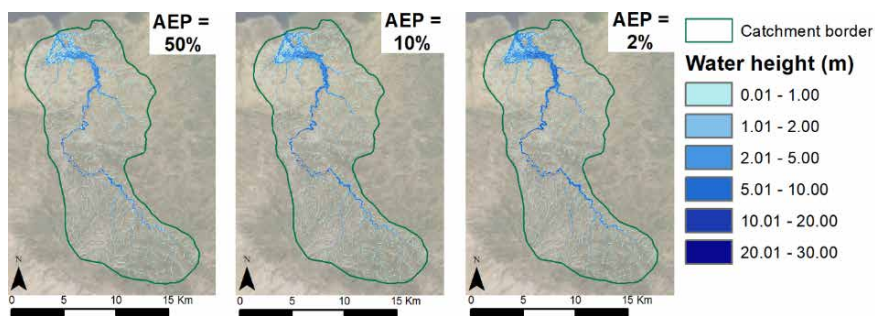


Figure 50 Flood hazard maps for three AEPs of the catchment of the river Moustiques, Haiti, as created by the toolbox.

Due to the scale of the maps, they seem to show little to no difference. Therefore, a numerical comparison was made and depicted in Table 30. Here, it becomes clear that the 2% AEP has 2.16% more affected area than the 50% AEP and 1.07% more flooded area than the 10% AEP. Furthermore, especially the higher flood levels (more than 5 m) occur more often during a 2% AEP flood. The limited vertical accuracy of SRTM is at the basis of the apparent poor sensitivity.

Table 30 Flooded area and numerical comparison for the three AEPs in the catchment of the river Moustiques, Haiti.

FLOOD HEIGHT (m)	AEP = 50%		AEP = 10%		AEP = 2%	
	AFFECTED AREA (m ²)	% OF TOTAL AREA	AFFECTED AREA (m ²)	% OF TOTAL AREA	AFFECTED AREA (m ²)	% OF TOTAL AREA
0.01–1.00	16,324,500	7.38	16,796,500	7.59	17,346,000	7.84
1.01–2.00	4,797,500	2.17	4,887,000	2.21	4,694,000	2.12
2.01–5.00	6,347,000	2.87	7,397,500	3.34	8,114,000	3.67
5.01–10.00	1,364,000	0.62	1,928,500	0.87	2,974,000	1.34
10.01–20.00	111,000	0.05	346,500	0.16	590,000	0.27
20.01–30.00	0	0.00	12,000	0.00	15,500	0.00
TOTAL	28,944,000	13.08	31,368,000	14.17	33,733,500	15.24

In the vulnerability module, three maps were created representing the social, economic and physical vulnerability of the catchment. Figure 51 shows these maps with the vulnerability classified in five vulnerability levels.

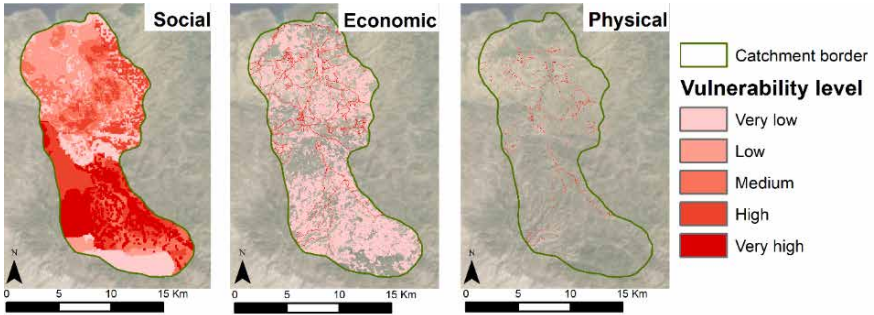


Figure 51 Social, Economic and physical vulnerability map of the catchment of the river Moustiques, Haiti, as created by the toolbox.

Table 31 lists the exact vulnerability values linked to each level. These class values were chosen in order to create a clear visual result that highlights the high-risk areas in the catchment. The exact class values are based on the average population density and replacement values of the elements taken into account in the study area. Specific numerical information on the vulnerabilities is listed in Table 32. As the data from WorldPop aggregate the population data over the country surface, the population density is never zero. Therefore, the entire catchment appears to have a social vulnerability. The economic vulnerability is widespread as well, as more than 56% of the area is economically vulnerable. However, most of this vulnerable area only has a very low vulnerability level. These are mostly farmlands. The physical vulnerability

looks much more limited in extend, as it takes into account land cover elements, namely buildings and roads which require a stronger zoom in the map to actually appreciate them in full.

Table 31 Minimum and maximum values of vulnerability levels for social, economic and physical vulnerability in the catchment of the river Moustiques, Haiti.

VULNERABILITY LEVEL	SOCIAL (People ha ⁻¹)		ECONOMIC (USD m ⁻²)		PHYSICAL (USD m ⁻²)	
	MIN VALUE	MAX VALUE	MIN VALUE	MAX VALUE	MIN VALUE	MAX VALUE
Very low	0.01	0.50	0.01	0.50	0.01	0.50
Low	0.51	1.00	0.51	2.00	0.51	2.00
Medium	1.01	1.50	2.01	3.50	2.01	3.50
High	1.51	2.00	3.51	5.00	3.51	5.00
Very high	2.01	>2.01	5.01	>5.01	5.01	>5.01

Table 32 Vulnerable area and numerical information on social, economic and physical vulnerability in the catchment of the river Moustiques, Haiti.

VULNERABILITY LEVEL	SOCIAL		ECONOMIC		PHYSICAL	
	VULNERABLE AREA (m ²)	% OF TOTAL AREA	VULNERABLE AREA (m ²)	% OF TOTAL AREA	VULNERABLE AREA (m ²)	% OF TOTAL AREA
Very low	36,482,500	16.48	109,837,000	49.63	1,878,000	0.85
Low	51,328,500	23.19	3,938,500	1.78	1,452,000	0.66
Medium	44,797,500	20.24	3,431,500	1.55	1,490,000	0.67
High	47,055,500	21.26	2,228,000	1.01	1,419,500	0.64
Very high	41,652,500	18.82	4,954,500	2.24	1,439,000	0.65
TOTAL	221,316,500	100.00	124,389,500	56.20	7,678,500	3.47

The last module combines the created flood and vulnerability maps into three risk maps depicting the yearly social, economic and physical risk. These maps are presented in Figure 52, while the case-study-specific risk level values are presented in

Table 33. The numerical information is summarized in Table 34. The social risk map clearly shows a higher risk upstream the river. This is due to the higher population density, and thus the higher social vulnerability in that area. 15.88% of the population, which is disseminated within 13.13% of the catchment area, is yearly at risk due to flooding. Economically, the elements in 14.22% of the catchment area are at risk, which is more than 25% of all vulnerable elements. The physical risk is limited to 0.81% of the total catchment area, but this is still more than 23% of the total physical vulnerable elements.

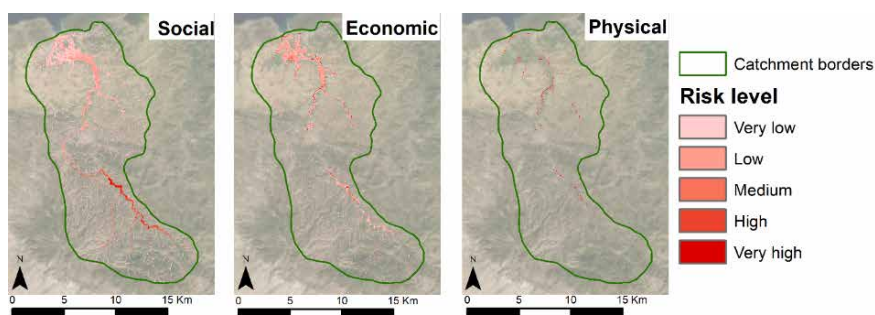


Figure 52 Social, Economic and physical risk map of the catchment of the river Moustiques, Haiti, as created by the toolbox.

Table 33 Minimum and maximum values of risk levels for social, economic and physical risk in the catchment of the river Moustiques, Haiti.

RISK LEVEL	SOCIAL (People ha ⁻¹)		ECONOMIC (USD m ⁻²)		PHYSICAL (USD m ⁻²)	
	MIN VALUE	MAX VALUE	MIN VALUE	MAX VALUE	MIN VALUE	MAX VALUE
Very low	0.01	0.25	0.01	0.10	0.01	0.10
Low	0.26	1.00	0.11	0.20	0.11	0.20
Medium	1.01	2.50	0.21	0.50	0.21	0.50
High	2.51	5.00	0.51	1.00	0.51	1.00
Very high	5.01	>5.01	1.01	>1.01	1.01	>1.01

Table 34 Area at risk area and numerical information on social, economic and physical risk in the catchment of the river Moustiques, Haiti.

RISK LEVEL	SOCIAL		ECONOMIC		PHYSICAL	
	AREA AT RISK (m ²)	% OF TOTAL AREA	AREA AT RISK (m ²)	% OF TOTAL AREA	AREA AT RISK (m ²)	% OF TOTAL AREA
Very low	19,541,500	8.83	21,199,500	9.58	333,000	0.15
Low	7,136,000	3.22	9,033,000	4.08	345,500	0.16
Medium	1,055,500	0.48	437,000	0.20	371,500	0.17
High	972,500	0.44	424,000	0.19	354,000	0.16
Very high	348,000	0.16	388,000	0.18	398,500	0.18
TOTAL	29,053,500	13.13	31,481,500	14.22	1,802,500	0.81

6.3.2 Comparison with Results Obtained with Optional Data

In order to verify the results of the toolbox, the default risk maps were compared to the results of the workflow using more detailed input data. In order to calculate the social risk, detailed population information, on building level, was acquired. These data

were gathered during fieldwork in 2018 (Glas et al., 2018). The results of both scenarios are shown in Figure 53. While only 172,000 m², or 0.42% of the total floodplain area, is classified as at risk using the detailed population data, the default workflow classifies 11,056,000 m² or 27.22% of the total area as at risk.

Even more interesting is comparing the number of people vulnerable and at yearly risk in the two scenarios. 1846 people live in the floodplain according to the detailed population data. The WoldPop data, on the other hand, estimate the total number of inhabitants at 3143, an overestimation of more than 70%. When comparing the number of people at risk, however, the default data classify barely half of the people as calculated with the detailed data as at risk, as 939 people are at risk according to the default method, while 1798 inhabitants are at risk using the detailed data.

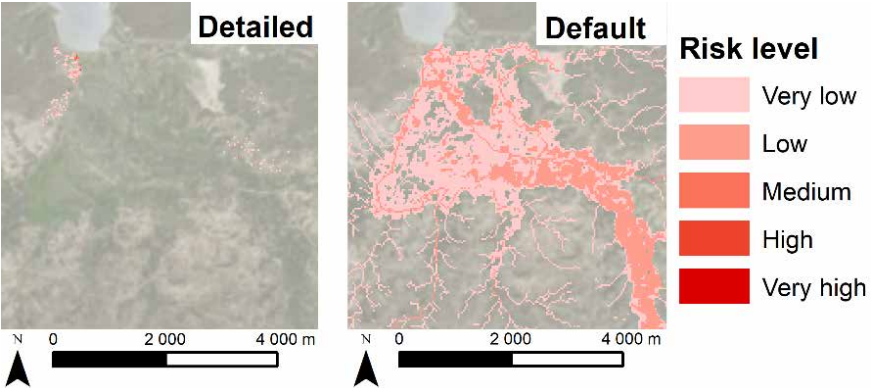


Figure 53 Comparison of the social risk map that was created using detailed input data and the optional modules (left) and the social risk map created using the default modules of the toolbox (right) for the floodplain of the catchment of the river Moustiques, Haiti.

The economic risk was calculated for the default data as well as for optional modules, including more detailed data on the farmlands, the crop types that are cultivated and the corresponding replacement values. This detailed information was only available for the floodplain of the catchment, so this was the only area taken into account in this comparison. Both resulting risk maps are shown in Figure 54.

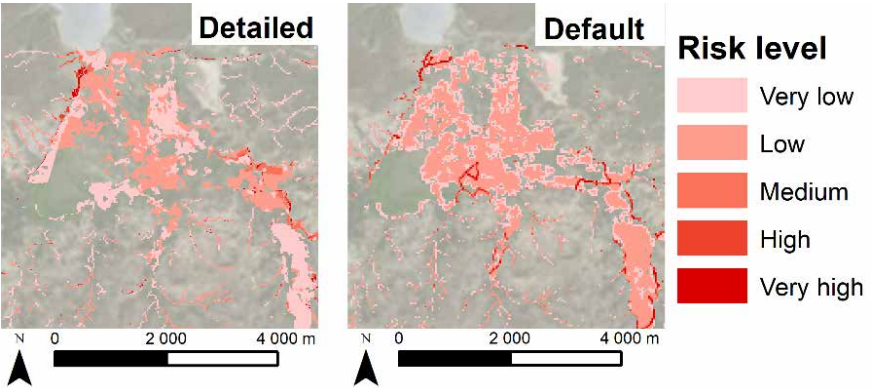


Figure 54 Comparison of the economic risk map that was created using detailed input data and the optional modules (left) and the economic risk map created using the default modules of the toolbox (right) for the floodplain of the catchment of the river Moustiques, Haiti.

Visually, it is clear that the risk computed with the default data is overestimated compared to the risk computed with more detailed data in the center of the floodplain. This is confirmed by the numerical analysis in Table 35. The default workflow calculates 12.6% more risk in the floodplain than the detailed information. The overestimation is mainly located in the low risk level.

Table 35 Area at risk and numerical information on the economic risk calculated by the optional modules using detailed input and the toolbox using the default modules and default input data for the floodplain of the catchment of the river Moustiques, Haiti.

RISK LEVEL (m)	DETAILED		DEFAULT	
	AREA AT RISK (m²)	% OF TOTAL AREA	AREA AT RISK (m²)	% OF TOTAL AREA
Very low	3,305,000	8.14	2,835,500	6.98
Low	3,258,000	8.02	4,464,000	10.99
Medium	242,000	0.60	203,000	0.50
High	85,500	0.21	214,500	0.53
Very high	104,000	0.26	160,500	0.40
TOTAL	6,994,500	17.22	7,877,500	19.40

The physical risk was not included in this comparison, as there were no alternative input data available with a higher level of detail for buildings or roads than the default OpenStreetMap data.

6.4 Discussion

The generated flood hazard maps show the large impact of flooding on the study area. Even the 50% AEP flood affects 13.08% of the total catchment area. The extent of the floods with AEPs of 10% and 2% are only slightly larger than this 50% AEP flood extent. This can be attributed to the regions topography. As the floodplain of the river is low-lying and flat, this area will inundate completely whenever a flood occurs, independent from the AEP of this flood. Therefore, it is most likely that a computed 100% AEP flood would have an extent only slightly smaller than the one of the 50% AEP flood. However, no flood map was generated for an AEP of 100%, as the 30 × 30 SRTM DEM was too coarse to see any difference from the 50% AEP flood map. When there are funds available for the acquisition of detailed data, the toolbox user should focus on acquiring a high-resolution DTM.

A detailed validation of the flood hazard maps for the study area is not feasible due to lack of adequate measurements. Nevertheless, expert judgement indicates that the simulated floods were realistic enough for the purposes of the risk mapping, as the same methodology showed adequate and validated results in Papua New Guinea (De Sutter et al., 2018).

Figure 51 and Figure 52 present the resulting social, economic and physical vulnerability and risk maps for the catchment. These maps are an important visual tool for decision makers to comprehend the distribution of vulnerability and risk in the area. Both results were classified in five levels. The class values were determined to create an optimal visual result based on the average population density in the study area for social vulnerability and risk, and on the location-specific replacement values for economic and physical vulnerability and risk. In other case studies, the user can choose the number of vulnerability and risk classes, that will then be calculated by the toolbox based on the population density and replacement values of that specific location, in order to generate a clear visual result.

The social vulnerability and risk were based on WorldPop data as input data. As Worldpop distributes the population numbers using land use data, the population density is nowhere equal to zero. However, this study area is a predominantly rural region, with most inhabitants living concentrated in small villages. Although the total population number for the catchment is correct using WorldPop data, the distribution overestimates the population in the rural areas and underestimates it in the villages. This explains the large overestimation of the number of people living in the floodplain. Moreover, due to the even distribution of the inhabitants, there is a large error in the social risk map of the floodplain, as the area at risk using the default WorldPop data is 64 times larger than the area at risk using the detailed population data. When evaluating the number of people at risk, however, the WorldPop data underestimate this drastically, as only 939 inhabitants are situated in the area at risk, while the detailed data lead to 1798 people at risk. This is due to the fact that almost all inhabitants live in the villages, which are located in the flood zone. Therefore, 97.40% of all inhabitants of the floodplain are classified as at risk. The WorldPop data, on the other hand, distribute the number of people evenly across the floodplain, and as such, more people are situated outside the flood zone, as only 29.88% of the total population in the floodplain is at risk using the default methodology. The WorldPop shows thus clear shortcomings in this rural area. Moreover, WorldPop is not available for every country in the world. This is a major disadvantage of WorldPop as default data in the toolbox, as global coverage is an important condition for the input data.

The validation of the economic risk was done using more detailed farmland input data. These data replaced the GlobCover default data with a resolution of only 300 m × 300 m. For buildings and roads, OpenStreetMap was used as this is the most detailed information available for this study area. When comparing the results, the detailed crop data lead to a lower risk, specifically 2.18% less than the default data. As this is a rural area, the crop data have a significant effect on the result. However, as the damage cost of agricultural lands is substantially lower than the cost of roads and buildings, this effect is only visible within the lower risk levels. While the GlobCover data do lead to a small overestimation, mainly due to its low resolution and lack of detail, this overestimation remains limited and the result remains a valuable overview of the risk and its distribution within the area.

The default input data for physical vulnerability and risk are building and road information from OpenStreetMap. The building data show the building footprints and

the road data show the axes of all roads. These data are the most detailed available and, therefore, no validation could be made with other input.

6.5 Conclusions

When the UI is fully developed, the methodology and toolbox will allow experts in developing countries and data-poor regions to perform reliable flood risk assessments and generate the necessary hazard, vulnerability and risk maps. The generic workflow is a robust and customizable algorithm that can be applied to any study area; it can be based on 'default data', which is freely available from different sources, but it can also be enriched with data surveyed within the study area. However, complete global coverage remains one of the most difficult conditions for the default input data. Although all data used are available in most parts of the world, it is impossible to ensure that the toolbox will provide results for every study area worldwide. The exact restrictions in geographic distribution are being mapped and listed and will be added to the toolbox manual.

The first case study for the catchment of the river Moustiques shows promising results. Despite the lack of historical hydro-meteorological data, the use of a physically-based distributed flood model using open remote sensing data provides a scientific base to flood mapping in this data-poor region. With no perspective on ever acquiring on-site hydrological data, the flood model should however be validated in the future using aerial photos of flooded areas or local reporting on disasters when they become available. Also, the WorldPop data have proven to be inaccurate for rural areas. More test cases should be carried out in urban and semi-urban areas to determine the accuracy of WorldPop data in these regions. Furthermore, due to the lack of WorldPop data for some countries, another methodology is that links population numbers based on census data to buffers around roads or to building locations from OpenStreetMap is tested to replace the WorldPop data as input, since this methodology has proven to provide accurate results in previous research.

The economic risk map based on default data shows a good representation of the risk, although it depicts a small overestimation compared to the risk map based on detailed data. This is caused by the large presence of farmlands, that cover the lion part of the catchment. Furthermore, the resolution of GlobCover data is too coarse for a small study area as the catchment of the river Moustiques.

Further development of the toolbox will include additional test cases, chosen based on their land use distribution and their scale. As such, the impact and the accuracy of GlobCover data will be further examined. Also, more case studies in other countries, developed as well as developing, will be used to validate the available replacement values, depth-damage functions and depth-mortality functions. Finally, additional natural hazards will be incorporated in the mapping methodology to develop a multi-hazard risk assessment toolbox, applicable worldwide that provides clear and practical risk maps. After this validation and testing phase, the toolbox can be made publicly and open source available.

REFERENCES

- Berlamont, J. (1999). *The influence of rainfall and model simplification on combined sewer system design*. Katholieke Universiteit Leuven, Leuven.
- Bicheron, P., Defourny, P., Brockmann, C., Schouten, L., Vancutsem, C., Huc, M., . . . Arino, O. (2008). *GLOBCOVER: products description and validation report*. <https://ec.europa.eu/jrc/en/publication/books/globcover-products-description-and-validation-report>
- Brandimarte, L., Brath, A., Castellarin, A., & Di Baldassarre, G. (2009). Isla Hispaniola: A trans-boundary flood risk mitigation plan. *Physics and Chemistry of the Earth*, 34(4-5), 209-218. doi:10.1016/j.pce.2008.03.002
- Compass International Inc. (2018). *Global Construction Costs Yearbook 18th Edition*. Retrieved from <https://www.compassinternational.net/wp-content/uploads/2017/01/Global-Construction-Sample.pdf>
- De Roo, A., Offermans, R., & Cremers, N. (1996). LISEM: A single-event, physically based hydrological and soil erosion model for drainage basins. II: Sensitivity analysis, validation and application. *Hydrological processes*, 10(8), 1119-1126.
- De Roo, A., Wesseling, C., Cremers, N., Offermans, R., Ritsema, C., & Van Oostindie, K. (1994). LISEM: a new physically-based hydrological and soil erosion model in a GIS-environment, theory and implementation. *IAHS Publications-Series of Proceedings and Reports-Intern Assoc Hydrological Sciences*, 224, 439-448.
- De Sutter, R., Rocabado, I., D'Heayer, T., Deleu, J., Maroy, E., Salazar, D., . . . Pirola, E. (2018). *Climate hazard, vulnerability and risk assessment for East Sepik Province in Papua New Guinea, Final report*. Retrieved from https://info.undp.org/docs/pdc/Documents/PNG/Report_Climate%20Risk%20Vulnerability%20Assessment_East%20Sepik.pdf
- Deckers, P., Kellens, W., Reyns, J., Vanneuville, W., & De Maeyer, P. (2009). A GIS for flood risk management in Flanders. In P.S. Showalter, L. Yongmei (Ed.), *Geospatial techniques in urban hazard and disaster analysis* (pp. 51-69): Dordrecht, Springer.
- Dutta, D., Herath, S., & Musiake, K. (2003). A mathematical model for flood loss estimation. *Journal of hydrology*, 277(1-2), 24-49. doi: 10.1016/S0022-1694(03)00084-2
- Eidenshink, J. C., & Faundeen, J. L. (1994). The 1 km AVHRR global land data set: first stages in implementation. *International Journal of Remote Sensing*, 15(17), 3443-3462. Doi: 10.1080/01431169408954339
- FAOSTAT. (2017). Crops. Retrieved from <http://www.fao.org/faostat/en/#data/QC>
- Glas, H., Deruyter, G., & De Maeyer, P. (2018). Flood risk assessment in data sparse regions: the use of questionnaires to collect historic flood data-a case study for the river moustiques in Haiti. *International Multidisciplinary Scientific Geoconference SGEM*, (18, 2.3), 377-384. doi: 10.5593/sgem2018/2.3/S11.048
- Government of Haiti (2010). *Analysis of Multiple Natural Hazards in Haiti (NATHAT)*. Retrieved from <https://reliefweb.int/report/haiti/analysis-multiple-natural-hazards-haiti-nathat>
- Heimhuber, V., Hannemann, J. C., & Rieger, W. (2015). Flood Risk Management in Remote and Impoverished Areas-A Case Study of Onaville, Haiti. *Water*, 7(7), 3832-3860. doi:10.3390/w7073832

- Karssenbergh, D., Schmitz, O., Salamon, P., de Jong, K., & Bierkens, M. F. (2010). A software framework for construction of process-based stochastic spatio-temporal models and data assimilation. *Environmental Modelling & Software*, 25(4), 489-502. doi: 10.1016/j.envsoft.2009.10.004
- Kumar, R., & Acharya, P. (2016). Flood hazard and risk assessment of 2014 floods in Kashmir Valley: a space-based multisensor approach. *Natural Hazards*, 84(1), 437-464. doi: 10.1007/s11069-016-2428-4
- Kwak, Y., Shrestha, B. B., Yorozya, A., & Sawano, H. (2015). Rapid Damage Assessment of Rice Crop After Large-Scale Flood in the Cambodian Floodplain Using Temporal Spatial Data. *Ieee Journal of Selected Topics in Applied Earth Observations and Remote Sensing*, 8(7), 3700-3709. doi:10.1109/jstars.2015.2440439
- OWP (2018). *Precipitation Frequency Data Server*. Retrieved from: <https://hdsc.nws.noaa.gov/hdsc/pfds/index.html>
- PROTOS (2011). Évaluation transversale 2010 – Mise en œuvre de la stratégie GIRE et intégration de la problématique changement climatique – Etude de cas – Haïti. Retrieved from https://www.joinforwater.ngo/sites/default/files/publications/files/2.evaluation_gire_et_cc_haiti_version_finale.pdf
- Rossillon, F. (2016). *Face à la détresse humaine et environnementale, Gestion Intégrée de l'Eau et Ecosanté, leviers de développement pour une Haïti nouvelle*. In L'eau dans les pays en développement - Retour d'expériences de gestion intégrée et participative avec les auteurs locaux (pp. 313-366). Belgium.
- Saxton, K. E., & Rawls, W. J. (2006). Soil water characteristic estimates by texture and organic matter for hydrologic solutions. *Soil science society of America Journal*, 70(5), 1569-1578. doi: 10.2136/sssaj2005.0117
- Son, N. T., Chen, C. F., & Chen, C. R. (2019). Flood assessment using multi-temporal remotely sensed data in Cambodia. *Geocarto International*, 16. doi:10.1080/10106049.2019.1633420
- Steele, J. E., Nieves, J., Tatem, A. J., Forget, Y., Shimoni, M., Linard, C., & Ieee. (2018). Worldpop - Fusion of Earth and Big Data for Intraurban Population Mapping. *Igarss 2018 - 2018 Ieee International Geoscience and Remote Sensing Symposium*, 2070-2071. doi: 10.1109/IGARSS.2018.8518181
- Turner&Townsend. (2018). *International construction markets survey 2018*. Retrieved from <https://www.turnerandtowntsend.com/en/perspectives/international-construction-market-survey-2018/>
- UNDRR (2009). *UNISDR Terminology on Disaster Risk Reduction*. Geneva, Switzerland: Retrieved from <https://www.undrr.org/publication/2009-unisdr-terminology-disaster-risk-reduction>
- UNDRR (2019). *Global Assessment Report on Disaster Risk Reduction*. Geneva, Switzerland: <https://www.undrr.org/publication/global-assessment-report-disaster-risk-reduction-2019#:~:text=The%202019%20Global%20Assessment%20Report,the%20global%20disaster%20risk%20landscape>.
- Vrisou van Eck, N., Kok, M., & Vrouwenvelder, A. (1999). Standaardmethode Schade en Slachtoffers als gevolg van overstromingen, deel 2: Achtergronden. *HKV Lijn in water, TNO, Dienst Weg en Waterbouw*. https://puc.overheid.nl/rijkswaterstaat/doc/PUC_20427_31/
- World Bank (2018). *The World Bank in Haiti: overview*. Retrieved from <http://www.worldbank.org/en/country/haiti/overview>

7

DISCUSSION AND CONCLUSION

7.1 General discussion

7.1.1 Research overview

This dissertation outlines the realization of a generic flood risk assessment methodology and toolbox for developing regions such as the SIDS. Existing assessment techniques for developed countries cannot simply be transferred to the SIDS, as the latter do not have the same resources and data available as the former regions. Furthermore, the land use and infrastructure in these island states is completely different. Therefore, existing assessment techniques were adapted and further developed to deal with these challenges hindering flood risk assessment in developing regions, and the SIDS in particular.

In the first step of the doctoral research – the case study of Annotto Bay (Chapter 2) – the focus was on determining the best input data and methodology for every step of the flood risk calculations. The case study provided valuable insights on how to transfer and adapt the methodology from LATIS and other existing methodologies to benefit a study area with limited data availability in the SIDS. Some of the LATIS concepts were incorporated in the methodology for the Annotto Bay flood risk assessment. These calculations are based on literature from Europe and the USA (Cammerer et al., 2013; Davis & Skaggs, 1992; Vanneuville et al., 2003), the regions with the most flood risk expertise and research in the world. There was no region-specific and adequate literature on flood risk assessment found for Jamaica or other SIDS. Some of the damage factors were used from a study performed in Japan (Dutta et al., 2003), an island with similar building characteristics as Jamaica. While in Japan, wooden buildings are most common (56%), followed by 34% concrete and steel structures (Ministry of Internal Affairs and Communications, 2013), the latter is the most common construction material in Jamaica, used in 74% of all buildings (PIOJ, 2017). As Dutta et al. (2003) differentiates between the two materials, resulting in two separate depth-damage functions, and the same classification in building material was applied in the building dataset for Annotto, the functions could be transferred and adequately applied in the Jamaican case study. An important conclusion of this first research step was the importance of the availability of adequate, region-specific data to create an adequate assessment. Therefore, in a later stage in the doctoral research, during the case study of the floodplain of the Moustiques (Chapter 5), most literature references and calculations from Europe and the USA were replaced by region-specific data, acquired through questionnaires (Glas & Deruyter, 2018), enabling a more detailed and accurate assessment.

Although, the lack of flood hazard maps for Annotto Bay hindered the creation of the risk maps in this stage of the research, and as such, did not lead to an actual end result at this point, this first case study was an important step towards the development of the flood risk mapping methodology and toolbox. Included in this toolbox is the hazard module, which enables flood hazard mapping for study areas worldwide, and thus for Annotto Bay as well. With these flood hazard maps as input, adequate flood risk maps for the study area can be generated in the future.

Although this first case study was carried out with a lot less data than most existing flood risk tools, there was still more region-specific data available compared to other regions in the SIDS. Therefore, the importance and necessity of all input data needed to be determined and fast and low-cost methods to acquire missing, but indispensable region-specific information had to be tested and investigated. This led to a sensitivity analysis of the newly developed flood risk methodology for Annotto Bay towards its input data (Chapter 3). In this analysis, twelve scenarios were generated, each with a different combination and level of detail of input data. The first scenario, the benchmark, was created with all available and most detailed data. It is worth noticing that the benchmark map as presented in Chapter 3 is not identical to the economic damage map as created in Chapter 2. For this first flood damage assessment performed in Annotto Bay (Chapter 2), two buffers – at 25 meters and at 60 meters – were added around the road network, because in the study area 90 percent of all buildings are located in the 25 meters buffer and 99 percent in the 60 meters buffer. These buffer limits are specific for the Annotto Bay study area, and should thus be redefined when assessing other regions in the SIDS. The calculations in Chapter 2 estimated a total damaged area of 2 460 000 m². For the benchmark scenario of the sensitivity analysis (Chapter 3), the second buffer of 60 meters was removed from the calculations, which led to a total damaged area of 3 182 000 m², or almost 30% more than the result of Chapter 2. If the two buffers would have been kept for the benchmark scenario, the results of most of the other scenarios would have differed significantly from the benchmark, for visual output as well as for total damaged area. As these buffers were specific to the Annotto Bay study area, this approach was chosen to allow a more honest and generic comparison of the different scenarios to the benchmark. The removal of the 60 meters buffer only influenced the visual result and the total damaged area, but there was no difference between the resulting estimated total damage cost as calculated in Chapter 2 and the result of the benchmark of the sensitivity analysis.

The conclusion of the sensitivity analysis showed that population data, which is generally available, even for data-poor regions (Steele et al., 2018), in combination with an average number of people per household are a good parameter in determining the building damage in case exact building locations are unknown. Due to recent VGI initiatives such as OpenStreetMap (HOT, 2016), however, the location of buildings is available as vector data for many areas in the world. Recent studies have shown that the close link between these building locations and population data, as proven in the sensitivity analysis, can be turned around and deployed to better allocate social damages and risk in the future (Smith et al., 2019; Zhu et al., 2020). Furthermore, the importance of a complete road dataset for an accurate visual result was proven. For crop damage calculations, however, no conclusions could be made since Annotto Bay is a primarily urban community and crop damage had an extremely low impact on the overall result.

An apparent need for more research, data and information on rural areas has led to a second case study in the floodplain of the river Moustiques, in the northwest of Haiti. As there was less data available for this rural region than the minimum requirements for an adequate flood risk assessment as defined in Chapter 3, new input data needed to be acquired. Especially historic flood data for which existing acquisition methods were

inaccessible or too expensive, were lacking. Therefore, a new method was developed, generating flood damage factors based on the knowledge of the inhabitants of the area (Chapter 4). This information was gathered through questionnaires. Based on the answers given by the respondents on questions about the most recent and most severe flood in their memory, damage factors for buildings and crops were determined. The building damage factors were calculated by combining the flood level indicated by the respondent and the degree of damage to the house. As such, a region-specific depth-damage function for buildings was created. For crops, however, there was no information on the flood levels in the agricultural fields. Therefore, only an overall crop damage degree for the entire study area could be calculated. While previous studies have used questionnaires to gather recent information on flooding (Bird, 2009; Suriya et al., 2012; Thieken et al., 2017), this research was the first of its kind to create damage factors based on the questionnaire results. Although the data gathered in such way have a certain degree of subjectivity (Babbie, 2013), as the memory of a person is not always an accurate recollection of the event, this low-cost and fast acquisition method provided information on past floods that is otherwise inexistent. Furthermore, Thieken et al. (2017) proved with adequate validation data that this technique provides accurate results. By critically analyzing the results, the risk of systematic bias was minimized.

The results of the questionnaires were then complemented with existing data, literature, field data and open source data, and used as input to the flood risk assessment for the floodplain of the river Moustiques (Chapter 5). The resulting risk map clearly indicated the high-risk areas. Although the assessment was performed as a quantitative analysis, the results should be interpreted qualitatively, as the exact values could not be validated. While for the case study of Annotto Bay, building damage takes up the lion share of the total damage, in this rural case study, the different damage types are in the same order of magnitude. The calculated crop damage risk was 587,000 USD/year, or 30% of the total risk, while the building damage risk was 652,000 USD/year or 33% of the total risk. While in urban case studies the influence of crop damage is negligible, this is definitely not the case in this rural case study.

In a final step, the methodologies for both case studies were adapted to create a generic and flexible methodology for flood risk mapping in study areas worldwide (Chapter 6). Workflows for mapping flood hazard, vulnerability and risk were created and customized for freely available data with global coverage, ensuring possible assessments worldwide. If available, region-specific data can be added. The practical application is assured by a modular toolbox, that was tested for the catchment of the river Moustiques, based on the available default data as well as on more detailed information. The first test results showed that the generic workflow is a robust algorithm that can be applied to any area worldwide.

7.1.2 Addressing the research questions

The general research objective of this dissertation was to create a generic, user-friendly and low-cost methodology and toolbox to calculate flood damages and risk in the Small Island Developing States. The two case studies discussed in this

dissertation have directly led to addressing this research objective in Chapter 6. However, the development of this toolbox was not straightforward, as there were many hurdles that needed to be overcome during the research. Encountered problems and the corresponding solutions, as well as important detours necessary to understand flood risk in the SIDS fully and obtain valuable results, are addressed in the research questions.

RQ1: What are the limitations, constraints and possibilities of flood risk modelling in the SIDS? Is an alternative approach necessary in these developing regions?

Two case studies were performed to assess flood risk in the SIDS. The first was located in the urban environment of Annotto Bay, Jamaica, and the second in the rural floodplain of the river Moustiques in Haiti. In both studies, existing risk assessment methodologies could not be transferred and an alternative methodology was delineated. The most obvious and important constraint is data scarcity as the extensiveness and level of detail required for input data of existing flood risk tools for developed countries cannot be met in the study areas. While building locations and population and road data are often available, even open source, other data such as flood maps, numeric data and validation data are much harder to come by.

Multiple flood hazard maps with different Annual Exceedance Probabilities (AEPs) are indispensable for an accurate risk assessment, but require a lot of region-specific and detailed input such as landcover, soil texture, a high-resolution DTM and channel geometry and roughness. For study areas in the SIDS, this information is mostly inexistent or not accurate or detailed enough. At best, the water heights and extent of a certain historic flood were measured and available in a flood map for that one flood event, allowing the computation of a damage map for that specific inundation, as was the case for Annotto Bay.

Numeric input data for flood risk assessment consist of replacement values on the one hand and damage and mortality factors on the other hand. It is possible to find this data on global, continental and sometimes even state level, but this is often not specific enough to create an accurate assessment on micro-scale. In the case of Annotto Bay, for example, building damage factors were used that were developed for Japan. These were chosen as the topography and building techniques in both cases are similar and are thus a good option. However, an adequate depth-damage function for the specific study area would be preferable and offer more reliable results, in particular in the case of a quantitative assessment. Therefore, region-specific damage factors, based on the input given by the residents of the study area, were used in the case of the floodplain of the river Moustiques.

A third data limitation is the lack of validation data in both case studies. The developed methodology itself can be tested, evaluated and validated based on other research and similar methodologies and their results. However, the quantitative results in both studies could not be validated and, therefore, the results should be used qualitatively, for example by introducing risk classes.

Although these constraints complicate flood risk assessment in the SIDS, the methodology proposed in this dissertation offers possibilities as well. While in previous studies in developing regions, there was a clear focus on strategic locations and buildings, the proposed methodology provides information on all infrastructure in the study area, offering a more complete overview of the potential damage and risk. Furthermore, the use of vector data in these micro-scale study areas provides more detailed risk allocation and a more understandable visualization of the risk distribution. This can lead to a better understanding of flood risk by the local governments and decision makers, and thus a more adequate allocation of their limited funds and resources. Moreover, the resulting flood risk map can raise awareness among the inhabitants of the study area and offer clear insights on the risks they face.

RQ2: What are the minimum data requirements to build a reliable flood risk assessment model?

The flood risk methodology delineated in this dissertation takes into account three damage types: building damage, crop damage and road damage. For each damage type, data requirements and recommendations were determined by analyzing the sensitivity of the risk methodology towards the input data.

Differentiating between building materials by using different replacement values has shown a low impact on the overall result of the building damage calculations. Even exact building locations can be left aside, provided that population density data is available. Combined with an accurate number of people per household, this indispensable population data have proven to be an adequate replacement for building locations when these are not available. This opens up possibilities for flood risk mapping worldwide, as population data are available, open source or for a low cost, for large parts of the world. Furthermore, as population data can be used as vector data as well as raster data, without loss of detail, it can easily be deployed in larger, macro-scale study areas.

Although road damage has a very low impact on the overall cost in both case studies performed in this dissertation, accurate road data as input are indispensable for a clear visual result. Moreover, when using population data instead of the exact building locations, the building damage is located in buffers around the road network, as every building must have access to a road. Therefore, the focus for road input data needs to be on using a complete dataset, including unpaved roads and tracks, instead of on having different road classes or widths as input.

The final damage type, crop damage, can be calculated based on land use data that identifies the agriculture lands, and average replacement values for crops. The former can be found open source as a raster file, but using a higher resolution or vector data increases the accuracy of the risk assessment drastically. The latter can be derived from freely available statistics gathered by FAOSTAT for each country every year. As crop damage has a low impact on the overall result, even in rural areas, differentiating between crop types has little to no effect on the accuracy of the resulting flood risk map.

RQ3: Are there low-cost, citizen-based acquisition methods available to collect the indispensable and location-specific flood risk input data? If yes, do these methods provide adequate results?

Collecting spatial information, such as land use data, through citizen involvement has been successfully applied in many projects. The most known and valued example is OpenStreetMap. This open source map offers adequate spatial information on building locations, water and road networks and has a global coverage.

Volunteered Geographic Information (VGI) methods were not applied to gather historic flood data before. Therefore, this dissertation has investigated the possibility of involving the inhabitants of a study area to collect the indispensable flood data by using questionnaires. The respondents provided information on previous flooding and the corresponding damages to their homes, vehicles, crops and livestock. The results of the questionnaires were processed into location-specific damage factors, directly applicable in a flood risk assessment of the area. This low-cost, fast and targeted method can be applied in remote and data-poor regions. Moreover, it allows an active involvement of the inhabitants, raising flood risk awareness among the population. However, people's memories of extreme events can be affected by the traumatizing effect of the event. Therefore, an inherent constraint of this data acquisition technique is a certain degree of subjectivity. Hence, the formulation of the questions must be clear and the pollsters must be briefed thoroughly to minimize the possibility of unreliable results. When these prerequisites are fulfilled, the questionnaires provide adequate location-specific input data.

RQ4: Is it possible to develop a generic flood risk assessment tool that provides reliable results when different accuracy levels of available input data are used? How can this one tool address the needs of different types of end users?

In this dissertation, a flexible and low-cost methodology for mapping hazard, vulnerability and risk was developed and applied in a toolbox developed on GDAL and PCRASTER. This methodology was not developed for a specific case study, but is built as a generic framework that can be applied to case studies of different sizes and with different characteristics. The core of this modular framework is built as a default workflow that runs on freely available input data with global coverage to ensure the practical application of the toolbox in study areas worldwide. Several depth-damage functions for specific geographic regions are available in the toolbox, as well as default replacement values. The default workflow can be extended with optional modules that run on region-specific data when these are available. As these data often have a different accuracy and application level than the default data, the region-specific data are converted to raster data by calculating the occupancy percentage of each data type in the resulting raster pixels. This minimizes accuracy loss during the conversion to a lower resolution.

In most countries, governments are responsible for the choice and implementation of the flood risk management framework and the corresponding flood measures.

Therefore, these authorities are the largest group of potential end users of the toolbox. While flood risk assessment as part of an integrated flood risk management is often researched on a national or regional level, many of the possible flood measures perform best on a smaller scale. In developing countries, however, many local authorities on municipality, city or even regional level lack the means and budget to take these measures and develop a resilient flood risk strategy. In these areas, local non-governmental organizations often fill in this gap by raising the necessary funds and setting up projects to protect and help the local community. These NGO's form a second group of end users. Both authorities and non-governmental organizations can use the toolbox to create flood risk maps that show the potential risk to the inhabitants of their area and the elements at risk. These maps can then be used in the mitigation and prevention phase as a tool to help determine which flood measures should be applied in each region. As the flood risk assessment toolbox is designed as a modular framework that does not only allow the creation of flood risk maps, but also of hazard and vulnerability maps, the toolbox can be deployed in other phases of the disaster framework as well. Emergency responders for example, that are active in the response phase after a flood, can combine the information from the hazard module with for example the road network, to determine an evacuation plan suitable for the area. While together with governments and NGO's, emergency responders form the primary end users, the toolbox will be made open source available, allowing other actors in the flood risk assessment framework to create valuable output that can aid in further research or the decision making and planning towards a flood resilient future. While the default workflow can be followed by users with limited mapping knowledge, the toolbox allows a mapping expert to adapt the input and workflow commands to better match each particular case study. This flexibility allows all types of users to visualize hazard, vulnerability and risk and create corresponding maps, that fit the purpose of the assessment.

7.1.3 Discussion

In this dissertation, the urban environment of Annotto Bay in Jamaica and the rural floodplain of the river Moustiques in Haiti were subject to a flood risk assessment. There are significant differences in the output and the impact and importance of each element of the risk calculations of the two areas. However, the aim of these case studies was not to deliver flood damage and risk maps representative for all SIDS, but to delineate a risk methodology that proves to be robust and accurate for these study areas and that can be applied in other regions in the SIDS. Although these areas differ from one another in environmental, topographic and land use properties, the used methodology remains unchanged and is thus characteristic for both case studies, and by extension for all SIDS, and is therefore generic. In the methodology, the situational aspect is handled by the use of region-specific replacement values and depth-damage functions, allowing a generic approach that provides accurate and valuable output, representative for the chosen study area, applicable in all SIDS as well as in other data-poor regions in the world.

A flood can have a widespread impact, not only – direct and indirect – in the areas that were inundated, but indirectly in other communities as well (GFDRR, 2014). Direct

damages can include injuries and fatalities, property damages, ecological loss and destruction of culturally significant sites, while indirect damages can contain loss of education, displacement of families, power outages, loss of income and interrupted businesses and supply chains (University of South Carolina, 2014). Some of these potential losses are tangible and can be expressed in a monetary value or a number of losses, while other intangible losses cannot be quantified that easily. As the losses and their size depend on many factors, of which the actual flood event is just one, it is extremely difficult to anticipate and quantify the potential of indirect losses, despite their size, even relative to other – direct – losses (GFDRR, 2014). Therefore the flood risk methodology and toolbox as proposed in this dissertation only takes into account direct economic and social losses. Social losses are defined in the methodology as casualties, while economic losses are calculated based on building, road and crop damage. In an urban area, for example Annotto Bay in Jamaica, the building damages take up the largest part of these economic losses. However, when a rural area is taken under consideration, the three damage costs are from a similar size. For the floodplain of Moustiques, road damage was the largest cost, closely followed by building and crop damage. As the proportions of each damage can vary depending on the study area characteristics, it is important that the generic methodology takes into account all three damage types.

As other direct losses, such as ecological or cultural heritage damage, are more complicated to quantify and require other – less common – data, these were not incorporated in the existing methodology. In other regions, where more data are available, flood risk researchers have investigated the value of nature and its ecosystems and developed ways to calculate ecological flood risk (Bwambale et al., 2018; Scheuer et al., 2011; Van Ackere et al., 2019). In each of these studies, the intangible ecological flood risk was calculated separately from economic and social risk, and was not quantified in the same manner. Several studies focused on flood risk in cultural heritage sites use a similar approach, using multi-criteria assessments and indices to evaluate the risk instead of monetary values (Dassanayake et al., 2015; Figueiredo et al., 2020; Holicky & Sykora, 2010). As these intangible losses are commonly not calculated as monetary values, further expansion of the risk toolbox for the SIDS should focus on the creation of an extra module that incorporates the value of nature and the corresponding ecological risk and a module focused on flood risk in cultural heritage sites rather than attempting to add these potential damages to the existing modules.

Many existing tools that calculate damages and risk caused by riverine flooding focus on inundation depth as the main determinant for flood damage. This implies a slowly rising riverine flood, with a low flow velocity as prototype (Kreibich et al., 2009). In many of the SIDS, however, flash floods are the most common type of flooding and cause the most damages. Not only are flash floods, due to their higher flow velocity, expected to cause greater structural damage, the evacuation time is limited as well. Moreover, flash floods typically have a high debris flow, solids in the flood water, which can cause additional damages to structures located in the flood path (Garrote et al., 2016). While studies have shown the limited impact of flow velocity on the monetary losses for past flooding in Europe (Karagiorgos et al., 2016; Kreibich et al., 2009; Merz et al., 2010), little research has been done on this subject in the SIDS. More historic

information, not only on water depth, velocities and possible debris in the water, but also on corresponding damages, should be gathered to be able to assess the impact of each flood factor and create adequate flood damage factors that can be used in an economic flood risk assessment.

An indispensable step in the creation of an adequate flood risk assessment toolbox is validation. While validating the resulting risk maps, that show the annual potential losses, is complicated due to the fact that these do not represent the real consequences of one event, but show an average estimate of the annual cost of flooding. Therefore, adequate data that validates these risk maps should consist of years of detailed flood and corresponding damage data. These high data requirements are difficult to meet, due to time and budget as well as privacy legislation that often prohibits the acquisition of losses and damages on building or person level. Although the validation of the output risk maps is complicated, it is possible to validate the methodology and input data. The methodology as presented in this doctoral research is adapted from several existing methodologies that have proven their worth and were thoroughly validated in their own study area (Jongman et al., 2012). While these existing methodologies rely on large amounts of detailed input data, the aim of this research was to create an adequate methodology with limited input data. In the sensitivity analysis performed in Chapter 3, the more detailed data were simplified, adapted or generalized to mimic the freely available data that could serve as input data. As such, a minimum set of input data was delineated that still provides accurate results compared to the output of the methodology with more detailed input data. It is important to note that the flood hazard maps were not a part of this sensitivity analysis, although their accuracy will have a significant impact on the accuracy of the flood risk maps. Further validation research should therefore take these maps and their impact on the overall methodology into account.

For the case study of the floodplain of the river Moustiques in Haiti, a field work mission to acquire detailed and accurate validation input data was planned within the doctoral research. Unfortunately, due to the unstable political situation in Haiti, the first field work mission, necessary to acquire input data for the flood risk assessment, was postponed a year, after which hurricane Irma caused a second delay in the planning. Eventually, this first mission took place 18 months after it was initially planned. In 2019, the validation field work mission was scheduled and budgeted for, but due to political unrest that led to violence aimed at foreigners at first and the COVID-19 pandemic after that, this mission could not yet take place and validation input data for this case study were not yet acquired.

The flood risk assessment toolbox is not a stand-alone tool, but should be incorporated and embedded into a larger framework that focuses on flood risk management and the water system of a region as a whole. Water is a resource before being a treat, and vicinity to water is an important advantage for many human activities, for example urban development, transport and energy production (UNDRR, 2017). As such, areas with a high flood vulnerability such as coastal and floodplain areas are often valuable assets as well. Therefore, flood risk assessment should be an integral part of an integrated flood management, where the goal is to maximize the net benefit from the

use of the area rather than try to fully control floods (WMO, 2009). Integrated flood risk management is often based on a combination of measures that address risk reduction, retention and transfer through a strategic mix of structural and non-structural measures for preparedness, response and recovery. These measures range from structural interventions that reduce flooding itself, for example building dams, dikes and levees or making channel improvements as part of the catchment management, to measures that reduce the risk of damage, for example introducing flood warning systems and building codes, adapting land use planning by not locating new assets in flood-prone high risk zones or flood proofing of existing structures (UNDRR, 2017; WMO, 2009). The output of the proposed flood risk assessment toolbox – the hazard, vulnerability and risk maps – play an important role in guiding decision makers in the composition of a set of flood measures, specifically and optimal for their community.

7.2 Critical reflections and future developments

Although flood risk has been extensively researched the past few decades, there is still an apparent need for adequate flood risk assessment in data-poor, developing regions such as the SIDS. An overview of the reasons for this research gap and the limitations and constraints of flood risk mapping in developing regions has been provided in this dissertation. Furthermore, solutions in the form of new input data acquisition techniques are given, as well as a flexible methodology and toolbox, based on freely available default data, that allows flood risk mapping in study areas worldwide. However, in order to achieve the same level of knowledge and expertise on flood risk in developing countries – which often have a high flood vulnerability – as in developed countries, three important hurdles still need to be overcome: the input data, the case study choice and the climate change consequences. In the next sections, reflections and recommendations, as well as possible future developments to overcome these hurdles are put forward.

7.2.1 The input data

The lack of adequate input data is the main restriction for mapping flood risk in developing regions. Throughout this research, however, it has become apparent that there are often more data available for a given area than initially anticipated. Especially land use data and replacement values are often already existent. However, these existing data are scattered across various institutions such as public authorities, NGOs or research institutions and was gathered for projects with a completely different purpose than flood risk assessment. Moreover, while the results of projects and research are eagerly shared through publications, there is still a lot of hesitation among researchers and project leaders to share the input data as well. Especially in developing countries such as the SIDS, where funds and resources to collect new data are limited, this protective mentality complicates and slows down ongoing research. Sharing data and knowledge has to be encouraged more in order to create an open research climate that will not only benefit flood risk assessment in developing countries, but other research projects as well.

The data acquisition technique proposed in this dissertation, gathering input data through questionnaires, offers a low-cost solution to collect the data that remain otherwise inexistent. This technique was used to generate location-specific damage factors for buildings and crops. By adapting the questionnaire setup, it is possible to collect other, hard to come by, data as well. The addition of a section on road damages and accessibility would aid in the development of region-specific depth-damage functions for roads, eliminating the need to use the Flemish depth-damage functions in other regions of the world. Furthermore, a section can be added on social risk. By registering the number of people that were hurt during a historic flood, as well as the number of people displaced, the social vulnerability of that specific study area can be calculated more adequately. When the number of casualties caused by that same flooding is known, location-specific mortality factors can be drafted.

A final reflection on input data deals with the chosen data type. In both case studies presented in this dissertation, vector data were used to generate an adequate flood risk map. However, the proposed flood risk toolbox runs on raster data, as most default data are already in raster format. For micro-scale study areas, using vector data is an added value, as this increases the level of detail in the calculations as well as in the visual result. For macro-scale study areas, however, vector data are harder to come by and processing large vector data requires more computer resources than raster calculations. Furthermore, there is little to no uniformity in how vector data are structured for study areas across the world, which complicates the generic, global usability the flood risk toolbox pursues. Therefore, raster data were chosen as input data type. The input vector data, such as buildings and roads, are converted to raster by taking into account the percentage each of the vector elements takes up in one pixel. Further calculations then use this percentage. This methodology preserves the level of detail of the vector data and allows an easy combination with the less accurate raster input data. More testing should be performed in order to thoroughly assess the influence of the input data type in several case studies. Then, recommendations for future studies can be delineated, based on the scale of the study area as well as on the available input data, in order to make a weighted decision on the input data type.

7.2.2 The case study choice

During the first tests of the developed flood risk methodology and toolbox, some drawbacks of the default input data were encountered. In order to better map the usage restrictions and performance accuracy of the data, the toolbox needs to be tested further in other countries, developed as well as developing. The questionnaire is a fast and targeted method to collect location-specific data and thus an excellent technique to create validation data for the flood risk toolbox. By conducting the questionnaires in a series of diverse case studies, the accuracy of the toolbox, and of the default data, can be better evaluated.

It is, however, not easy to find suitable new case study areas. The protective mindset of researchers towards their own gathered data and information is not the only factor complicating the acquisition of new input and case studies. On the one hand, the

characteristics of a study area used to check and validate the methodology must be well known to the researchers, and should be based on both available data as on field work to allow the detection and analysis of faulty calculations or results. Organizing a field work mission demands, however, time and resources and is therefore not always possible. On the other hand, new study areas must be carefully chosen, as it needs to be possible to test all modules and workflows of the toolbox. Therefore, each chosen study area must have different characteristics that test the data and methodology in a different way. While the first case study of the toolbox was mainly rural and on micro-scale, new tests should focus on urban areas, as well as areas on the fringe and on larger scale study areas.

When the toolbox is tested thoroughly and perfected for flood risk calculations, additional natural hazards can be incorporated in the mapping methodology. Testing the expanded toolbox implies new case studies, situated in areas where these other hazard types have impact. This dissertation has focused on Caribbean SIDS, where flooding is the most common and destructive disaster type (Collymore, 2011). In African SIDS, however, the largest damages are caused by droughts, while storms, earthquakes and tsunamis are the main disasters in Pacific SIDS (Baas et al., 2018). In order to create an adequate multi-hazard risk assessment toolbox, these natural hazard types must definitely be incorporated in the risk methodology. This namely implies an extension of the hazard module, while the vulnerability and risk module can maintain their workflow and methodology as these modules are not dependent on the hazard type.

7.2.3 The climate change consequences

The flood risk methodology as presented in this dissertation focuses on calculating the potential damages and present risk, providing decision makers with clear information and allowing them to adequately allocate their resources and thus minimize the risk. However, in order to take adequate future-proof measures, decision makers should not only take into account current hazards and their consequences, but also the effects of climate change and its interaction with the social, ecological and economic systems. This concept is described in literature as *climate proofing*, and offers the tools to reach a climate resilient solution (Colls et al., 2009). While many climate prediction models describe the potential scenarios of the future climate on different scales, there is a lack of practical applications offering tools to adapt the climate policies and offer climate resilient solutions to decision makers, in developing as well as in developed regions (IPCC, 2014). This is partly due to the high complexity of climate change, its effects and the relation with the current environment. Moreover, the data necessary to correctly identify and quantify these aspects are in many areas non-existent (Donovan et al., 2019).

Although governments, project developers and other actors in developing areas are aware of the climate challenges and are willing to take adaptation measures in order to enhance the climate resilience, it is often unclear what the effects of these measures will be and to which extent they will be sufficient. Therefore, a tool to evaluate the climate resilience of the study area as well as of new urban development projects

is indispensable and must contain an integrated multi-disciplinary approach that combines the knowledge of experts from different disciplines with spatial data in order to adequately evaluate the climate resilience and identify the opportunities and risks of the study area and new projects.

7.2.3.1 Identifying areas at future risk

The author took a first step in the development of such a climate resilience test, by delineating a straight-forward, clear and easy-to-use methodology to identify the areas at future risk (Glas et al., 2019). As the effects of climate change are extremely complex and diverse, a simplification is necessary to create a comprehensive tool methodology. Sea level rise, possible drought and flooding are the most imminent threats to many developing countries and their infrastructures, and should thus definitely be taken into account (IPCC, 2014).

According to the IPCC, global sea level rise has been observed since the 1970s. It is very likely that the sea level will keep rising during the 21st century, at a faster rate. The predicted rise is in the range of 0.26 to 0.82m globally by 2100 (IPCC, 2014). However, the sea level rise will not be uniform across regions. For example, due to its proximity to the equator, sea level rise in the Caribbean region will be more pronounced than elsewhere (Simpson et al., 2010). Therefore, sea level rise in these regions should be calculated with the upper limit of the range, 0.82m. In Figure 55, the first results of the climate resilience testing for the two study areas discussed in this dissertation, Annotto Bay, Jamaica, and the floodplain of the river Moustiques in Haiti, are shown. A potential sea level rise of one meter was tested. This value was chosen as the DEM used, ASTER GDEM (a product of METI and NASA), has a vertical precision of 1m. Most of the plain of the river Moustiques will be inundated with this sea level rise. This would affect 157 of the 3285 buildings and approximately 5km of the road network. In Annotto Bay, the sea level rise would largely inundate the main highway that runs close to the coastline, as well as 136 of the 233 buildings in the study area. The buildings in the Haitian case study are situated on the mountain side and, therefore, only a mere 5 percent of the houses are affected by the rise. In Annotto Bay, the houses are mainly built in the low-lying areas at risk, and thus 58 percent of them would be inundated. Even though both study areas are affected by sea level rise, Annotto Bay has a much higher risk of building damages and is thus less climate resilient.

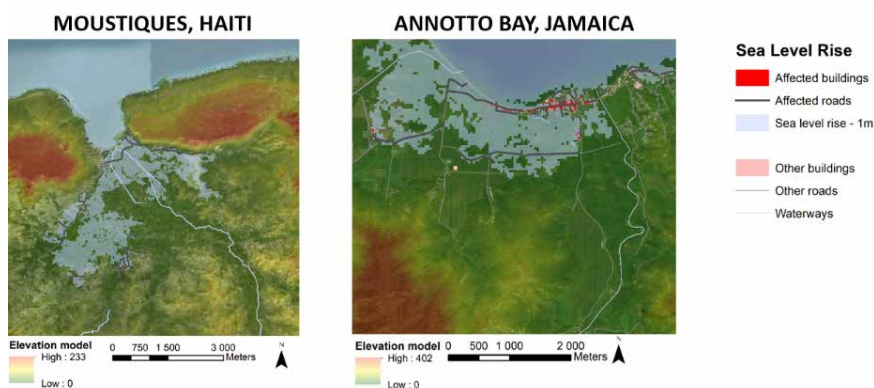


Figure 55 Risk of a potential sea level rise of 1m by 2100 for the floodplain of the river Moustiques in Haiti (left) and Annotto Bay in Jamaica (right) (Glas et al., 2019).

Drought is defined as a period of abnormally dry weather long enough to cause a serious hydrological imbalance. Drought is a relative term, dependent on the normal precipitation-related activity in the area that is under discussion (IPCC, 2014). For example, precipitation shortage during the growing season will impinge on crop production. Therefore, regions should invest in crop types that are adapted to climate change, especially in areas at risk for drought. Figure 56 is a visualization of how resilient each study area is in case of long drought periods. Two buffers were generated around the main waterways, one of 50 meters and one of 100 meters. These buffers visualize the areas that will benefit from the water in the stream by irrigation, and will thus be fertile ground for agricultural activities, even in dry periods. Furthermore, the crop types are linked to a list of climate resilience scores. Crop types that can grow under limited precipitation receive a high score, while plants that need a lot of water to grow get a lower score. Both case study areas have a large amount of banana and plantain lands. These plants have a low resilience to drought, especially in the growing stage. Maize, present in the floodplain of the river Moustiques, is classified in the lowest class of drought resilience, as it is a plant in need of a lot of water. Both study areas have agricultural lands where the crop type is not specified. These are classified in the medium risk class.

An increase in precipitation as well as the sea level rise will cause more regular and severe flooding, especially in low-lying coastal areas. Flood events that have a theoretical AEP of for example 2% in the present will be more common in the future, and will thus have a higher AEP (Lavell et al., 2012). The increased flood risk is directly related to the expected increase in precipitation in the equatorial area. It is likely that there will be up to 34.2 percent more rainfall by 2100 in the Caribbean (IPCC, 2014). The tool testing the climate resilience should take into account this extra amount of precipitation to create new flood hazard maps, and recalculate the AEPs. However, due to the complex nature of flood hazard mapping, these maps were not yet created in this preliminary research.

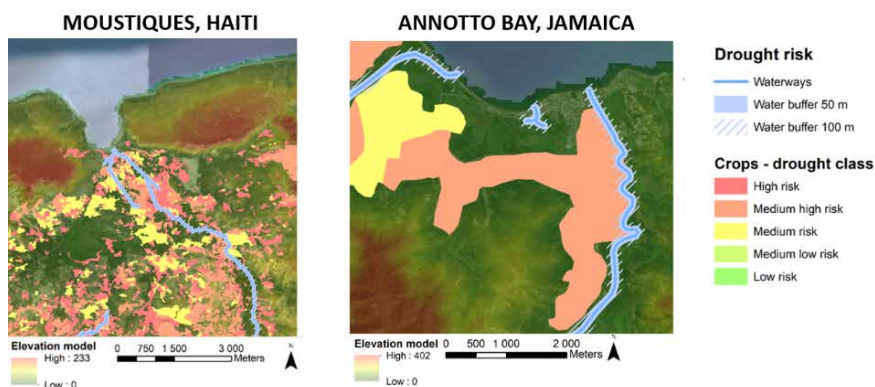


Figure 56 Drought risk for the floodplain of the river Moustiques in Haiti (left) and Annotto Bay in Jamaica (right) (Glas et al., 2019).

7.2.3.2 Future development

A climate resilience test needs input from experts from different disciplines to adequately assess the results of the first risk assessments and identify opportunities and risks for the region or for a specific urban development project. This information could for example be gathered using a questionnaire which would inquire into non-spatial information of the region or project, as well as evaluate the results of the first step. The experts should be able to draw on the created maps, identifying areas of interest or pinpointing concerns, adding comments and extra information to aid in a final climate resilience assessment. This methodology would allow the evaluation of a study area or project on its climate resilience without the need of an extensive climate change knowledge. As such, this test is not only closely linked to the research objective of this dissertation, but also an indispensable future development for a correct assessment of the risks, current and future, that communities worldwide face.

REFERENCES

- Baas S., Conforti P., Ahmed S., & Markova G. (2018) *Impact of disasters and crises on agriculture and food security, 2017*. FAO, Rome (Italy) Climate and Environment Div. <http://www.fao.org/3/i8656en/i8656EN.pdf>
- Babbie E. R. (2013) *The basics of social research*, Cengage learning.
- Bird D. K. (2009) The use of questionnaires for acquiring information on public perception of natural hazards and risk mitigation—a review of current knowledge and practice. *Natural Hazards and Earth System Sciences*, 9(4), 1307-1325. doi: 10.5194/nhess-9-1307-2009
- Bwambale B., Muhumuza M., & Nyeko M. (2018) Traditional ecological knowledge and flood risk management: A preliminary case study of the Rwenzori. *Jâmbá: Journal of Disaster Risk Studies*, 10(1), 1-10. doi: 10.4102/jamba.v10i1.536
- Cammerer H., Thieken A. H., & Lammel J. (2013) Adaptability and transferability of flood loss functions in residential areas. *Natural Hazards and Earth System Sciences*, 13(11), 3063. doi: 10.5194/nhess-13-3063-2013
- Colls A., Ash N., & Ikkala N. (2009) *Ecosystem-based Adaptation: a natural response to climate change* (Vol. 21): Iucn Gland. <https://www.iucn.org/content/ecosystem-based-adaptation-a-natural-response-climate-change>
- Collymore J. (2011) Disaster management in the Caribbean: Perspectives on institutional capacity reform and development. *Environmental Hazards*, 10(1), 6-22. doi:10.3763/ehaz.2011.0002
- Dassanayake D., Burzel A., & Oumeraci H. (2015) Methods for the Evaluation of Intangible Flood Losses and Their Integration in Flood Risk Analysis. *Coastal Engineering Journal*, 57(1). doi: 10.1142/S0578563415400070
- Davis S. A. & Skaggs L. L. (1992) *Catalog of residential depth-damage functions used by the army corps of engineers in flood damage estimation*. Retrieved from <https://apps.dtic.mil/dtic/tr/fulltext/u2/a255462.pdf>
- Donovan J., Gutierrez S. J. A., & Tan M. (2019) *Global Environment Outlook 6, Chapter 3: The Current State of our Data and Knowledge*. Cambridge, UK: <https://www.unenvironment.org/resources/global-environment-outlook-6>
- Dutta D., Herath S., & Musiak K. (2003) A mathematical model for flood loss estimation. *Journal of hydrology*, 277(1-2), 24-49. doi: 10.1016/S0022-1694(03)00084-2
- Figueiredo R., Romao X., & Pauperio E. (2020) Flood risk assessment of cultural heritage at large spatial scales: Framework and application to mainland Portugal. *Journal of cultural heritage*, 43, 163-174. doi: 10.1016/j.culher.2019.11.007
- Garrote J., Alvarenga F., & Díez-Herrero A. (2016) Quantification of flash flood economic risk using ultra-detailed stage–damage functions and 2-D hydraulic models. *Journal of hydrology*, 541, 611-625. doi: 10.1016/j.jhydrol.2016.02.006
- GFDRR (2014) *Understanding Risk in an Evolving World: Emerging Best Practices in Natural Disaster Risk Assessment*. Global Facility for Disaster Reduction and Recovery. https://www.gfdr.org/sites/default/files/publication/Understanding_Risk-Web_Version-rev_1.8.o.pdf
- Glas H., & Deruyter G. (2018) *Questionnaires sur l'impact des inondations dans le bassin versant de la rivière Moustiques, Haïti*.
- Glas H., Deruyter G., & De Maeyer P. (2019) Evaluating the climate resilience in data-sparse regions – an automated GIS-based toolbar. *International Multidisciplinary Scientific GeoConference: SGEM*, 19(2.2), 815-822. doi: 10.5593/sgem2019/2.2/S11.100

- Holicky M. & Sykora M. (2010) Assessment of Flooding Risk to Cultural Heritage in Historic Sites. *Journal of Performance of Constructed Facilities*, 24(5), 432-438. doi: 10.1061/(ASCE)CF.1943-5509.0000053
- HOT (2016) Hurricane Matthew Update. Retrieved from https://www.hotosm.org/updates/2016-10-08_hurricane_mattew_update
- IPCC (2014) *Climate Change 2014: Synthesis Report. Contributions of Working Groups I, II and III to the Fifth Assessment Report of the Interantional Panel on Climate Change*. Switzerland. https://www.ipcc.ch/site/assets/uploads/2018/02/SYR_AR5_FINAL_full.pdf
- Jongman B., Kreibich H., Apel H., Barredo J., Bates P., Feyen L., & Ward P. (2012) Comparative flood damage model assessment: towards a European approach. *Natural Hazards and Earth System Sciences (NHES)*, 12(12), 3733-3752. doi: 10.5194/nhess-12-3733-2012
- Karagiorgos K., Thaler T., Hübl J., Maris F., & Fuchs S. (2016) Multi-vulnerability analysis for flash flood risk management. *Natural Hazards*, 82(1), 63-87. doi: 10.1007/s11069-016-2296-y
- Kreibich H., Piroth K., Seifert I., Maiwald H., Kunert U., Schwarz J., . . . Thieken A. (2009) Is flow velocity a significant parameter in flood damage modelling? *Natural Hazards and Earth System Sciences*, 9(5), 1679-1692. doi: 10.5194/nhess-9-1679-2009
- Lavell A., Oppenheimer M., Diop C., Hess J., Lempert R., Li J., . . . Takeuchi K. (2012) Climate change: new dimensions in disaster risk, exposure, vulnerability, and resilience. In Field C.B., V. Barros, T.F. Stocker, D. Qin, D.J. Dokken, K.L. Ebi, M.D. Mastrandrea, K.J. Mach, G.-K. Plattner, S.K. Allen, M. Tignor, and P.M. Midgley (Ed.), *Managing the Risks of Extreme Events and Disasters to Advance Climate Change Adaptation: Special Report of the Intergovernmental Panel on Climate Change* (pp. 25-64): Cambridge University Press.
- Merz B., Kreibich H., Schwarze R., & Thieken A. (2010) Assessment of economic flood damage. *Nat. Hazards Earth Syst. Sci.*, 10(8), 1697-1724. doi: 10.5194/nhess-10-1697-2010
- Ministry of Internal Affairs and Communications (2013) *Housing and Land Survey. Dwellings by Type of Dwelling (2 Groups), Construction Material (5 Groups) and Year of Construction (14 Groups) – Japan*. Retrieved from: https://www.e-stat.go.jp/en/stat-search/files?page=1&layout=datalist&toukei=00200522&tstat=000001063455&cycle=0&tclass1=000001063456&tclass2=000001063457&stat_infid=000028504306&tclass3val=0
- PIOJ (2017) *Jamaica Survey of Living Conditions (JSLC) 2017: Executive Summary*. Planning Institute of Jamaica (PIOJ). Retrieved from: <https://www.pioj.gov.jm/product/jamaica-survey-of-living-conditions-jslc-2017-executive-summary/>
- Scheuer S., Haase D., & Meyer V. (2011) Exploring multicriteria flood vulnerability by integrating economic, social and ecological dimensions of flood risk and coping capacity: from a starting point view towards an end point view of vulnerability. *Natural Hazards*, 58(2), 731-751. doi: 10.1007/s11069-010-9666-7
- Simpson M. C., Scott D., Harrison M., Sim R., Silver N., O'Keeffe E., . . . McSharry P. (2010) *Quantification and Magnitude of Losses and Damages Resulting from the Impacts of Climate Change: Modelling the Transformational Impacts and Costs of Sea Level Rise in the Caribbean (Full Document)*. Barbados, West Indies: <https://www.preventionweb.net/publications/view/16915>

- Smith A., Bates P. D., Wing O., Sampson C., Quinn N., & Neal J. (2019) New estimates of flood exposure in developing countries using high-resolution population data. *Nature communications*, 10(1), 1-7. doi: 10.1038/s41467-019-09282-y
- Steele J. E., Nieves J., Tatem A. J., Forget Y., Shimoni M., Linard C., & Ilee. (2018) Worldpop – Fusion of Earth and Big Data for Intraurban Population Mapping. *Igarss 2018 – 2018 IEEE International Geoscience and Remote Sensing Symposium*, 2070-2071. doi: 10.1109/IGARSS.2018.8518181
- Suriya S., Mudgal B., & Nelliyat P. (2012) Flood damage assessment of an urban area in Chennai, India, part I: methodology. *Natural Hazards*, 62(2), 149-167. doi: 10.1007/s11069-011-9985-3
- Thieken A., Kreibich H., Müller M., & Lamond J. (2017) *Data collection for a better understanding of what causes flood damage—experiences with telephone surveys*. In Flood damage survey and assessment: new insights from research and practice, 95-106. doi: 10.1002/9781119217930.ch7
- UNDRR (2017) *Words into Action Guidelines: National Disaster Risk Assessment: Hazard Specific Risk assessment. 4. Flood Hazard and Risk Assessment*. United Nations Office for Disaster Risk Reduction (UNDRR). https://www.preventionweb.net/files/52828_04floodhazardandriskassessment.pdf
- University of South Carolina (2014) *Who needs loss data?* Background paper prepared for the Global Assessment Report on Disaster Risk Reduction 2015. <https://www.preventionweb.net/english/hyogo/gar/2015/en/bgdocs/University%20of%20South%20Carolina,%202014.pdf>
- Van Ackere S., Beullens J., Vanneuville W., De Wulf A., & De Maeyer P. (2019) FLIAT, An Object-Relational GIS Tool for Flood Impact Assessment in Flanders, Belgium. *Water*, 11(4), 711. doi: 10.3390/w11040711
- Vanneuville W., Maeghe K., De Maeyer P., & Mostaert F. (2003) Risicobenadering bij waterbeheersingsplannen, Methodologie en case study Denderbekken, aanvulling 2: Lijninfrastructuur. Ghent, Belgium: <http://www.marinespecies.org/imis.php?module=ref&refid=141993&basketaction=add>
- WMO (2009) *Integrated Flood Management: concept paper*. World Meteorological Organization (WMO). https://www.floodmanagement.info/publications//concept_paper_e.pdf
- Zhu S., Dai Q., Zhao B., & Shao J. (2020) Assessment of Population Exposure to Urban Flood at the Building Scale. *Water*, 12(11), 3253. doi: 10.3390/w12113253

8

APPENDIX

This appendix contains the French version of the questionnaire as distributed in the floodplain of the river Moustiques, Haiti, in January 2018. The questionnaire is set up in French, but was translated to Haitian Creole before the survey was conducted. After consultation with our local partners, the decision was made to delete questions 21, 27, 46, 52 from the questionnaire, as these questions may have given the respondents a wrong idea of the purpose of the questionnaire.

QUESTIONNAIRE SUR L'IMPACT DES INONDATIONS DANS LE BASSIN VERSANT DE LA RIVIERE MOUSTIQUES, HAITI

Nous faisons subir ce questionnaire sur l'impact des inondations dans la région. Nous voulons vous poser quelques questions au sujet de votre ménage et des inondations historiques. Les résultats de ce questionnaire seront utilisés pour optimiser les mesures de protection et pour diffuser de l'information correcte sur les risques d'inondation auprès de la population locale. Vos données seront traitées avec confidentialité et ne seront pas transmises au tiers. Ce questionnaire est volontaire et vous êtes libres de ne pas répondre à quelques ou à toutes les questions. Cependant, nous espérons que vous voulez collaborer, parce que votre connaissance est d'une très grande valeur pour nous.

SECTION 1: DONNEES PERSONELLES

Date de l'interview	Jour: <input type="text"/> Mois: <input type="text"/> Année: <input type="text"/> .
Nom du participant	<input type="text"/> .
Sexe	<input type="checkbox"/> Homme <input type="checkbox"/> Femme
Age	<input type="text"/> ans
Village	<input type="text"/> .
Code de maison	<input type="text"/> .
Commentaires	<input type="text"/> .
	<input type="text"/> .
	<input type="text"/> .
	<input type="text"/> .
	<input type="text"/> .

SECTION 2: COMPOSITION DU MENAGE

Cette section concerne la composition de votre ménage. On vous demande seulement au sujet des personnes qui cohabitent avec vous dans la même maison.

- 1 Quel est le sexe du chef de famille?
☐ Homme
☐ Femme
- 2 Quel âge a le chef de famille?
 Ans
- 3 Le ménage se compose de combien de personnes?
 Personnes

- 4 Mettez le nombre des membres du ménage dans le tableau ci-dessous pour chaque classe d'âge et chaque sexe.

Classe d'âge	Homme	Femme
Les enfants âgés de moins de 5 ans.		
Les enfants âgés de 5 à 14 ans.		
Les personnes âgées de 15 à 64 ans.		
Les personnes âgées de plus de 64 ans.		

- 5 Combien de femmes sont enceinte dans le ménage?

Femmes

- 6 Combien de personnes âgées de 15 à 64 ans ont été malades ou incapables de travailler pendant au moins 3 mois dans la dernière année ?

Personnes

SECTION 3: LA POSSESSION DE MOYENS DE DEPLACEMENT

Cette section concerne votre possession de moyens de déplacement. Si vous n'avez pas des moyens de déplacement, vous ne devez pas répondre les questions dans cette section.

- 7 Quels moyens de déplacement sont en votre possession? Donnez aussi le nombre des moyens de déplacement.

- ☐ Pas de moyen de déplacement
- ☐ Vélo Nombre:
- ☐ Cyclomoteur Nombre:
- ☐ Moto Nombre:
- ☐ Voiture particulière Nombre:
- ☐ Camionnette / SUV Nombre:
- ☐ Tracteur Nombre:
- ☐ Camion Nombre:
- ☐ Animaux (équins) Nombre:
- ☐ Autres: Nombre:

Possibilité de réponses multiples.

SECTION 4: ACTIVITES AGRICOLES

Cette section concerne vos activités agricoles. On vous demande au sujet des terres agricoles que vous cultivez, même si vous n'êtes pas le propriétaire de ces terres. On vous demande aussi au sujet des animaux en votre possession.

- 8 Travaillez-vous des terres agricoles?

- ☐ Oui
- ☐ Non (à la question 10)

9 Quels végétaux sont cultivés par le ménage? Si possible, donnez aussi la dimension de la surface.

- | | |
|--|--|
| <input type="checkbox"/> Bananes | Surface: <input type="text"/> |
| <input type="checkbox"/> Bananes plantains | Surface: <input type="text"/> |
| <input type="checkbox"/> Mangue | Surface: <input type="text"/> |
| <input type="checkbox"/> Riz | Surface: <input type="text"/> |
| <input type="checkbox"/> Haricots | Surface: <input type="text"/> |
| <input type="checkbox"/> Maïs | Surface: <input type="text"/> |
| <input type="checkbox"/> Patates douces | Surface: <input type="text"/> |
| <input type="checkbox"/> Manioc | Surface: <input type="text"/> |
| <input type="checkbox"/> Yam | Surface: <input type="text"/> |
| <input type="checkbox"/> Autres: | <input type="text"/> Surface: <input type="text"/> |

Possibilité de réponses multiples.

10 Avez-vous des animaux?

- ☐ Oui
- ☐ Non (à la question 12)

11 Quels animaux sont en votre possession? Donnez aussi le nombre des animaux.

- | | |
|----------------------------------|---|
| <input type="checkbox"/> Moutons | Nombre: <input type="text"/> |
| <input type="checkbox"/> Chèvres | Nombre: <input type="text"/> |
| <input type="checkbox"/> Vaches | Nombre: <input type="text"/> |
| <input type="checkbox"/> Chevaux | Nombre: <input type="text"/> |
| <input type="checkbox"/> ânes | Nombre: <input type="text"/> |
| <input type="checkbox"/> Mules | Nombre: <input type="text"/> |
| <input type="checkbox"/> Porcs | Nombre: <input type="text"/> |
| <input type="checkbox"/> Poulets | Nombre: <input type="text"/> |
| <input type="checkbox"/> Autres: | <input type="text"/> Nombre: <input type="text"/> |

Possibilité de réponses multiples.

SECTION 5: L'INONDATION LA PLUS RECENTE

Cette section concerne l'inondation la plus récente dans votre mémoire. Si vous ne savez pas une réponse à une question, vous pouvez passer cette question.

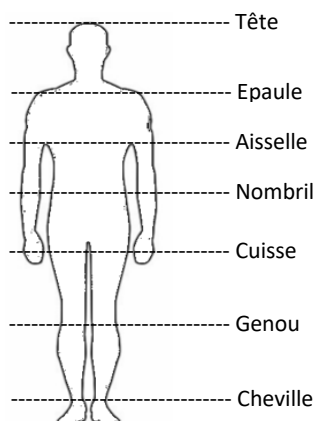
12 A quelle date a eu lieu l'inondation la plus récente?

Jour: Mois: Année:

13 Quelle était la durée de l'inondation?

Jours

- 14 Quel était le niveau de l'eau maximal dans les environs pendant l'inondation la plus récente?
Coloriez la figure jusqu'au niveau de l'eau pour vous-même.



-
- 15 Le ménage, a-t-il déménagé à cause de l'inondation la plus récente?
- ☐ Oui
 - ☐ Non (à la question 19)
-

- 16 Vers où a le ménage déménagé?
- ☐ Nouvelle maison permanente (à la question 18)
 - ☐ Maison temporaire / tente
 - ☐ abri / école / église
 - ☐ chez les voisins
 - ☐ En famille
 - ☐ En plein air
 - ☐ Autres:
-

- 17 Quelle était la durée du déménagement à cause de l'inondation la plus récente?
- ☐ Moins d'une semaine
 - ☐ Entre 1 et 3 semaines
 - ☐ Entre 3 et 6 semaines
 - ☐ Plus de 6 semaines
-

- 18 Quelle était la raison du déménagement?
- ☐ Maison détruite ou endommagée
 - ☐ Besoin de traitement médicale
 - ☐ S'occuper de famille touchée
 - ☐ Autres:

Possibilité de réponses multiples.

19 Votre maison, a-t-elle été détruite ou endommagée par l'inondation la plus récente?

- ☐ Oui, la maison a été peu endommagée
 - ☐ Oui, la maison a été très endommagée
 - ☐ Oui, la maison était complètement détruite
 - ☐ Non (à la question 24)
-

20 Avez-vous réparé votre maison après l'inondation la plus récente?

- ☐ Oui
 - ☐ Non (à la question 23)
-

21 Quels étaient les coûts estimés pour réparer votre maison?

Gourde

22 Les réparations à votre maison, quand sont-elles effectuées?

- ☐ Moins d'un mois après l'inondation (à la question 24)
 - ☐ Entre 1 et 3 mois après l'inondation (à la question 24)
 - ☐ Entre 3 et 6 mois après l'inondation (à la question 24)
 - ☐ Plus de 6 mois après l'inondation (à la question 24)
-

23 Si la maison n'était pas réparée, quelle est la raison?

- ☐ Les réparations ne sont pas urgentes
- ☐ Les réparations ne sont pas nécessaires
- ☐ Les réparations sont trop chères
- ☐ Autres:

Possibilité de réponses multiples.

24 Vos moyens de déplacement, ont-ils été détruits ou endommagés par l'inondation la plus récente?

- ☐ Oui, des moyens de déplacement ont été endommagés
 - ☐ Non (à la question 30)
-

25 Quels moyens de déplacement ont été détruits ou endommagés? Donnez aussi le nombre des moyens de déplacement endommagés.

☐ Vélo Nombre:

☐ Cyclomoteur Nombre:

☐ Moto Nombre:

☐ Voiture particulière Nombre:

☐ Camionnette / SUV Nombre:

☐ Tracteur Nombre:

☐ Camion Nombre:

☐ Animaux (équins) Nombre:

☐ Autres: Nombre:

Possibilité de réponses multiples.

26 Avez-vous réparé ou remplacé les moyens de déplacement après l'inondation la plus récente?

☐ Oui

☐ Non (à la question 29)

27 Quels étaient les coûts estimés pour réparer ou remplacer vos moyens de déplacement?

☐ Lourde

28 Les réparations à vos moyens de déplacement, quand sont-elles effectuées?

☐ Moins d'un mois après l'inondation (à la question 30)

☐ Entre 1 et 3 mois après l'inondation (à la question 30)

☐ Entre 3 et 6 mois après l'inondation (à la question 30)

☐ Plus de 6 mois après l'inondation (à la question 30)

29 Si les moyens de déplacement n'étaient pas réparés, quelle est la raison?

☐ Les réparations ne sont pas urgentes

☐ Les réparations ne sont pas nécessaires

☐ Les réparations sont trop chères

☐ Autres:

Possibilité de réponses multiples.

30 Vos végétaux, ont-ils été complètement ou partiellement détruits par l'inondation la plus récente?

☐ Oui

☐ Non (à la question 33)

31 Quels végétaux ont été détruits ou endommagés? Donnez aussi le degré d'endommagement.

- | | | | |
|--|------------------------------|-------------------------------|---|
| <input type="checkbox"/> Bananes | <input type="checkbox"/> Peu | <input type="checkbox"/> Très | <input type="checkbox"/> Complètement détruit |
| <input type="checkbox"/> Bananes plantains | <input type="checkbox"/> Peu | <input type="checkbox"/> Très | <input type="checkbox"/> Complètement détruit |
| <input type="checkbox"/> Mangue | <input type="checkbox"/> Peu | <input type="checkbox"/> Très | <input type="checkbox"/> Complètement détruit |
| <input type="checkbox"/> Riz | <input type="checkbox"/> Peu | <input type="checkbox"/> Très | <input type="checkbox"/> Complètement détruit |
| <input type="checkbox"/> Haricots | <input type="checkbox"/> Peu | <input type="checkbox"/> Très | <input type="checkbox"/> Complètement détruit |
| <input type="checkbox"/> Maïs | <input type="checkbox"/> Peu | <input type="checkbox"/> Très | <input type="checkbox"/> Complètement détruit |
| <input type="checkbox"/> Patates douces | <input type="checkbox"/> Peu | <input type="checkbox"/> Très | <input type="checkbox"/> Complètement détruit |
| <input type="checkbox"/> Manioc | <input type="checkbox"/> Peu | <input type="checkbox"/> Très | <input type="checkbox"/> Complètement détruit |
| <input type="checkbox"/> Yam | <input type="checkbox"/> Peu | <input type="checkbox"/> Très | <input type="checkbox"/> Complètement détruit |
| <input type="checkbox"/> Autres: | <input type="text"/> | | |
| | <input type="checkbox"/> Peu | <input type="checkbox"/> Très | <input type="checkbox"/> Complètement détruit |
-

32 Combien de végétaux avez-vous vendu après l'inondation la plus récente par rapport à les végétaux vendus dans des autres années?

- ☐ Moins que les autres années
- ☐ Plus au moins la même quantité
- ☐ Plus que les autres années
-

33 Quels animaux ont été morts à cause de l'inondation la plus récente? Donnez aussi le nombre des animaux morts.

- ☐ Pas d'animaux morts (à la question 37)
- ☐ Moutons Nombre:
- ☐ Chèvres Nombre:
- ☐ Vaches Nombre:
- ☐ Chevaux Nombre:
- ☐ ânes Nombre:
- ☐ Mules Nombre:
- ☐ Porcs Nombre:
- ☐ Poulets Nombre:
- ☐ Autres: Nombre:

Possibilité de réponses multiples.

34 Avez-vous remplacé les animaux tués après l'inondation la plus récente?

- ☐ Oui
- ☐ Non (à la question 36)
-

- 35 Quand avez-vous remplacé les animaux tués?
- ☐ Moins d'un mois après l'inondation (à la question 37)
 - ☐ Entre 1 et 3 mois après l'inondation (à la question 37)
 - ☐ Entre 3 et 6 mois après l'inondation (à la question 37)
 - ☐ Plus de 6 mois après l'inondation (à la question 37)
-

- 36 Si les animaux n'étaient pas remplacés, quelle est la raison?

- ☐ Ce n'était pas urgent
- ☐ Ce n'était pas nécessaire
- ☐ C'était trop cher
- ☐ Autres:

Possibilité de réponses multiples.

SECTION 6: L'INONDATION LA PLUS VIOLENTE DANS VOTRE MEMOIRE

Cette section concerne l'inondation la plus violente dans votre mémoire. Si l'inondation la plus violente est la même inondation que l'inondation la plus récente, vous ne devez pas répondre à les questions dans cette section. Si vous ne savez pas une réponse à une question, vous pouvez passer cette question.

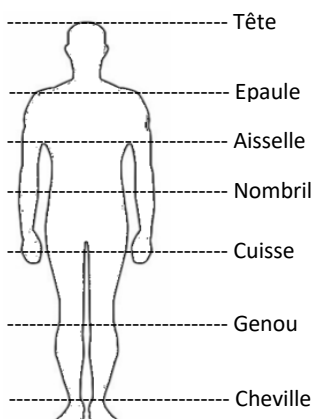
- 37 A quelle date a eu lieu l'inondation la plus violente? Vous pouvez donner une date approximative.

Jour: Mois: Année:

- 38 Quelle était la durée de l'inondation?

Jours

- 39 Quel était le niveau de l'eau maximal dans les environs pendant l'inondation la plus violente? Coloriez la figure jusqu'au niveau de l'eau pour vous-même.



40 Le ménage, a-t-il déménagé à cause de l'inondation la plus violente?

- ☐ Oui
☐ Non (à la question 44)
-

41 Vers où a le ménage déménagé?

- ☐ Nouvelle maison permanente (à la question 43)
☐ Maison temporaire / tente
☐ abri / école / église
☐ chez les voisins
☐ En famille
☐ En plein air
☐ Autres:
-

42 Quelle était la durée du déménagement à cause de l'inondation la plus violente?

- ☐ Moins d'une semaine
☐ Entre 1 et 3 semaines
☐ Entre 3 et 6 semaines
☐ Plus de 6 semaines
-

43 Quelle était la raison du déménagement?

- ☐ Maison détruite ou endommagée
☐ Besoin de traitement médicale
☐ S'occuper de famille touchée
☐ Autres:
-

Possibilité de réponses multiples.

44 Votre maison, a-t-elle été détruite ou endommagée par l'inondation la plus violente?

- ☐ Oui, la maison a été peu endommagée
☐ Oui, la maison a été très endommagée
☐ Oui, la maison était complètement détruite
☐ Non (à la question 49)
-

45 Avez-vous réparé votre maison après l'inondation la plus violente?

- ☐ Oui
☐ Non (à la question 50)
-

46 Quels étaient les coûts estimés pour réparer votre maison?

Gourde

- 47 Les réparations à votre maison, quand sont-elles effectuées?
- ☐ Moins d'un mois après l'inondation (à la question 49)
 - ☐ Entre 1 et 3 mois après l'inondation (à la question 49)
 - ☐ Entre 3 et 6 mois après l'inondation (à la question 49)
 - ☐ Plus de 6 mois après l'inondation (à la question 49)
-

- 48 Si la maison n'était pas réparée, quelle est la raison?

- ☐ Les réparations ne sont pas urgentes
- ☐ Les réparations ne sont pas nécessaires
- ☐ Les réparations sont trop chères
- ☐ Autres:

Possibilité de réponses multiples.

- 49 Vos moyens de déplacement, ont-ils été détruits ou endommagés par l'inondation la plus violente?

- ☐ Oui, des moyens de déplacement ont été endommagés
 - ☐ Non (à la question 55)
-

- 50 Quels moyens de déplacement ont été détruits ou endommagés? Donnez aussi le nombre des moyens de déplacement endommagés.

- | | |
|---|------------------------------|
| <input type="checkbox"/> Vélo | Nombre: <input type="text"/> |
| <input type="checkbox"/> Cyclomoteur | Nombre: <input type="text"/> |
| <input type="checkbox"/> Moto | Nombre: <input type="text"/> |
| <input type="checkbox"/> Voiture particulière | Nombre: <input type="text"/> |
| <input type="checkbox"/> Camionnette / SUV | Nombre: <input type="text"/> |
| <input type="checkbox"/> Tracteur | Nombre: <input type="text"/> |
| <input type="checkbox"/> Camion | Nombre: <input type="text"/> |
| <input type="checkbox"/> Animaux (équins) | Nombre: <input type="text"/> |

☐ Autres: . Nombre: .

Possibilité de réponses multiples.

- 51 Avez-vous réparé ou remplacé les moyens de déplacement après l'inondation la plus violente?

- ☐ Oui
 - ☐ Non (à la question 54)
-

- 52 Quels étaient les coûts estimés pour réparer ou remplacer vos moyens de déplacement?

☐ Gourde

53 Les réparations à vos moyens de déplacement, quand sont-elles effectuées?

- ☐ Moins d'un mois après l'inondation (à la question 55)
 - ☐ Entre 1 et 3 mois après l'inondation (à la question 55)
 - ☐ Entre 3 et 6 mois après l'inondation (à la question 55)
 - ☐ Plus de 6 mois après l'inondation (à la question 55)
-

54 Si les moyens de déplacement n'étaient pas réparés, quelle est la raison?

- ☐ Les réparations ne sont pas urgentes
- ☐ Les réparations ne sont pas nécessaires
- ☐ Les réparations sont trop chères
- ☐ Autres:

Possibilité de réponses multiples.

55 Vos végétaux, ont-ils été complètement ou partiellement détruits par l'inondation la plus violente?

- ☐ Oui
 - ☐ Non (à la question 58)
-

56 Quels végétaux ont été détruits ou endommagés? Donnez aussi le degré d'endommagement.

- | | | | |
|---|------------------------------|-------------------------------|---|
| <input type="checkbox"/> Bananes | <input type="checkbox"/> Peu | <input type="checkbox"/> Très | <input type="checkbox"/> Complètement détruit |
| <input type="checkbox"/> Bananes plantains | <input type="checkbox"/> Peu | <input type="checkbox"/> Très | <input type="checkbox"/> Complètement détruit |
| <input type="checkbox"/> Mangue | <input type="checkbox"/> Peu | <input type="checkbox"/> Très | <input type="checkbox"/> Complètement détruit |
| <input type="checkbox"/> Riz | <input type="checkbox"/> Peu | <input type="checkbox"/> Très | <input type="checkbox"/> Complètement détruit |
| <input type="checkbox"/> Haricots | <input type="checkbox"/> Peu | <input type="checkbox"/> Très | <input type="checkbox"/> Complètement détruit |
| <input type="checkbox"/> Maïs | <input type="checkbox"/> Peu | <input type="checkbox"/> Très | <input type="checkbox"/> Complètement détruit |
| <input type="checkbox"/> Patates douces | <input type="checkbox"/> Peu | <input type="checkbox"/> Très | <input type="checkbox"/> Complètement détruit |
| <input type="checkbox"/> Manioc | <input type="checkbox"/> Peu | <input type="checkbox"/> Très | <input type="checkbox"/> Complètement détruit |
| <input type="checkbox"/> Yam | <input type="checkbox"/> Peu | <input type="checkbox"/> Très | <input type="checkbox"/> Complètement détruit |
| <input type="checkbox"/> Autres: <input type="text"/> | | | |
| | <input type="checkbox"/> Peu | <input type="checkbox"/> Très | <input type="checkbox"/> Complètement détruit |
-

57 Combien de végétaux avez-vous vendu après l'inondation la plus violente par rapport à les végétaux vendus dans des autres années?

- ☐ Moins que les autres années
 - ☐ Plus au moins la même quantité
 - ☐ Plus que les autres années
-

58 Quels animaux ont été morts à cause de l'inondation la plus violente? Donnez aussi le nombre des animaux morts.

☐ Pas d'animaux morts (à la fin du questionnaire)

☐ Moutons Nombre:

☐ Chèvres Nombre:

☐ Vaches Nombre:

☐ Chevaux Nombre:

☐ ânes Nombre:

☐ Mules Nombre:

☐ Porcs Nombre:

☐ Poulets Nombre:

☐ Autres: Nombre:

Possibilité de réponses multiples.

59 Avez-vous remplacé les animaux tués après l'inondation la plus violente?

☐ Oui

☐ Non (à la question 61)

60 Quand avez-vous remplacé les animaux tués?

☐ Moins d'un mois après l'inondation (à la fin du questionnaire)

☐ Entre 1 et 3 mois après l'inondation (à la fin du questionnaire)

☐ Entre 3 et 6 mois après l'inondation (à la fin du questionnaire)

☐ Plus de 6 mois après l'inondation (à la fin du questionnaire)

61 Si les animaux n'étaient pas remplacés, quelle est la raison?

☐ Ce n'était pas urgent

☐ Ce n'était pas nécessaire

☐ C'était trop cher

☐ Autres:

FIN DU QUESTIONNAIRE

Nous vous remercions de votre collaboration.

© Hanne Glas, Ghent University, 2021.

ISBN

978-94-6355-487-9

Cover design

Roger Van Hecke and

Charlotte Alice Dossche

Interior design and production

André Diepgrond / In Ontwerp, Assen

Digital access

Jan-Kees van Loon, New Ink

Communicatie, Groningen

This work is intellectual property and subject to copyright. All rights reserved, whether the whole or part of the material is concerned. Duplication of this publication or parts thereof is permitted only under the provisions of the 'Auteurswet' (Copyright Law) of the 23th of September 1912, in its current version, and permission for use must always be obtained from InPlanning. Violations are liable to prosecution under Dutch Law.

PhD Series InPlanning

// IN //
PLAN //
/ NING

Published by InPlanning

Oude Kijk in 't Jatstraat 6,

9712 EG Groningen, The Netherlands

info@inplanning.eu

www.inplanning.eu

The InPlanning PhD Series supports the publication and distribution of PhD theses produced within Schools of Planning. The InPlanning PhD Series is part of the InPlanning portfolio of books, journals, posters, videos, documentaries and other information carriers. The InPlanning PhD Series is available via

www.inplanning.eu



"Eau Dlo" - interpretation of a Haitian landscape by Charlotte Alice Dossche.